Universitat Ramon Llull

DOCTORAL THESIS

Title

The DosRST two-component system of *Mycobacterium tuberculosis*: Characterizing the activation mechanism of DosR response regulator as a potential target for novel antimycobacterial drugs

Presented by

Marta Anna Marszałek

Centre

IQS School of Engineering

Department

Bioengineering

Directed by

Dra. Maria Teresa Pellicer Moya
Dr. Antoni Planas Sauter

C. Claravall, 1-3
08022 Barcelona
Tel. 936 022 200
Fax 936 022 249
E-mail: urlsc@sec.url.es
www.url.es

ABSTRACT

Tuberculosis, the infectious disease caused by *Mycobacterium tuberculosis*, is a global health problem with approximately two million deaths annually. One-third of the world population is chronically infected with *Mycobacterium tuberculosis* but do not show clinical symptoms although there is a 10% risk to development active disease, representing an uncontrollable reservoir of tuberculosis. In this asymptomatic condition, referred to as latent tuberculosis, *Mycobacterium tuberculosis* is located within granulomatous lesions in the host and is resistant to currently available antimycobacterial drugs.

Two-component regulatory systems in bacteria are a major class of signal transduction proteins involved in adaptation to environmental changes. Typical system contains a membrane-bound histidine kinase that plays a crucial role in sensing environmental stimuli, and a cytosolic response regulator. This pair of proteins functions as a molecular switch that controls diverse adaptive environmental responses. *Mycobacterium tuberculosis* has eleven complete two-component systems. The DosRST system, composed of a response regulator, DosR, and two histidine kinases, DosS and DosT, plays a key role in *Mycobacterium tuberculosis* adaptation to latent tuberculosis. DosS and DosT autophosphorylate at conserved histidine residues and both proteins transfer this phosphor moiety to aspartic acid residue 54 of DosR. The phosphorylation of Asp54 serves as a switch to activate DosR and to increase the affinity for its cognate DNA promoters. Threonines 198 and 205 of DosR play a crucial role in DosR dimerization and DNA binding. The molecular dynamics with wild type and mutant version of DosR show different stability in the formation of the active DosR dimer. They also show the reduction or the abolishment of protein-DNA interactions because of the repulsions generated by negatively charged mutated residues. Moreover, substitutions in threonines 198 and 205 of DosR have a relevant effect on the chemical and enzymatic phosphorylation of DosR and on its DosS-catalysed dephosphorylation.

The DosRST two-component system is a good target for the development of novel antimycobacterial drugs against dormant forms of *M. tuberculosis.* A structure-based discovery programme of inhibitors of DosR response regulator has been initiated with commercially available compounds showing a certain degree of similarity with a phenylcoumarin derivative previously described as DosR-DNA interfering molecule.

Resum

La tuberculosi, la malaltia infecciosa causada per *Mycobacterium tuberculosis*, es un problema de salut global que provoca aproximadament 2 milions de morts anuals. Un terç de la població mundial es troba crònicament infectada amb *Mycobacterium tuberculosis* però no mostra símptomes clínics encara que té un risc d'un 10% de desenvolupar la malaltia, la qual cosa representa un reservori incontrolable de tuberculosi. En aquesta condició asimptomàtica, coneguda com a tuberculosi latent, *Mycobacterium tuberculosis* es localitza en lesions granulomatoses a l'hoste i és resistent als medicaments antimicobacterians existents en l'actualitat.

En bacteris, els sistemes reguladors de dos components son un conjunt de proteïnes implicades en l'adaptació a canvis en l'entorn del microorganisme. Un sistema de dos components típic consta d'una histidina quinasa unida a membrana que té un paper essencial com a sensor dels canvis ambientals i un regulador transcripcional citosòlic que exerceix la seva funció controlant l'expressió de gens diana. Aquest parell de proteïnes funciona com un interruptor molecular que controla diferents respostes adaptatives a canvis a l'ambient cel·lular. *Mycobacterium tuberculosis* té 11 sistemes de dos components complets. El sistema DosRST, composat per un regulador transcripcional, DosR, i dues histidines quinases, DosS i DosT, té un paper estel·lar en l'adaptació de *Mycobacterium tuberculosis* a la tuberculosi latent. DosS i DosT s'autofosforilen en residus conservats d'histidina i ambdues proteïnes transfereixen aquesta un unitat de fosfat al residu d'àcid aspàrtic en posició 54 del regulador DosR. La fosforilació d'Asp54 és un interruptor que activa DosR i incrementa la seva afinitat per als promotors dels gens que regula. Les treonines 198 i 205 de DosR tenen un paper crucial en la dimerització de DosR i en la seva unió al DNA. Les dinàmiques moleculars realitzades amb la proteïna salvatge DosR i amb versions mutants mostren diferències notables en la formació del dímer actiu. També mostren una reducció o abolició completa de les interaccions proteïna-DNA a causa de les repulsions generades pels residus mutants carregats negativament. Encara més, les substitucions en Thr198 i Thr205 tenen un important efecte en la fosforilació química i enzimàtica de DosR així com també en la seva defosforilació catalitzada per DosS.

El sistema de dos components DosRST és una bona diana per al desenvolupament de nous compostos amb activitat antimicobacteriana contra formes dorments de *Mycobacterium tuberculosis.* S'ha iniciat un programa de recerca dirigit al desenvolupament d'inhibidors específics de la proteïna reguladors DosR, usant com a punt de partida compostos comercials estructuralment relacionats amb un derivat fenilcumarínic que ha estat descrit com a molècula que interfereix en la interacció DosR-DNA.

Resumen

La tuberculosis, la enfermedad infecciosa causada por *Mycobacterium tuberculosis*, es un problema de salud global que provoca aproximadamente 2 millones de muertes anuales. Un tercio de la población mundial se encuentra crónicamente infectada con *Mycobacterium tuberculosis* pero no muestra síntomas clínicos aunque tiene un riesgo de un 10% de desarrollar la enfermedad, lo que representa un reservorio incontrolable de tuberculosis. En esta condición asintomática, conocida como tuberculosis latente, *Mycobacterium tuberculosis* se localiza en lesiones granulomatosas en el huésped y es resistente a los medicamentos antimicobacterianos existentes en la actualidad.

En bacterias, los sistemas regulatorios de dos componentes son un conjunto de proteínas implicadas en la adaptación a cambios en el entorno del microorganismo. Un sistema de dos componentes típico consta de una histidina quinasa unida a membrana que tiene un papel esencial como sensor de los cambios ambientales y un regulador transcripcional citosólico que ejerce su función controlando la expresión de genes diana. Este par de proteínas funciona como un interruptor molecular que controla distintas respuestas adaptativas a cambios en el ambiente celular. *Mycobacterium tuberculosis* tiene 11 sistemas de dos componentes completos. El sistema DosRST, compuesto por un regulador transcripcional, DosR, y dos histidinas quinasas, DosS y DosT, juega un papel estelar en la adaptación de *Mycobacterium tuberculosis* a la tuberculosis latente. DosS y DosT se autofosforilan en residuos conservados de histidina y ambas proteínas transfieren esta unidad de fosfato al residuo de ácido aspártico en posición 54 del regulador DosR. La fosforilación de Asp54 es un interruptor que activa a DosR e incrementa su afinidad por los promotores de los genes que regula. Las treoninas 198 y 205 de DosR juegan un papel crucial en la dimerización de DosR y en su unión al DNA. Las dinámicas moleculares realizadas con la proteína salvaje DosR y con versiones mutantes muestran diferencias notables en la formación del dímero activo. También muestran una reducción o abolición completa de las interacciones proteína-DNA a causa de las repulsiones generadas por los residuos mutantes cargados negativamente. Más aún, las sustituciones en Thr198 y Thr205 tienen un importante efecto en la fosforilación química y enzimática de DosR así como también en su defosforilación catalizada por DosS.

El sistema de dos componentes DosRST es una buena diana para el desarrollo de nuevos compuestos con actividad antimicobacteriana contra formas durmientes de *Mycobacterium tuberculosis.* Se ha iniciado un programa de investigación dirigido al desarrollo de inhibidores específicos de la proteína reguladora DosR, usando como punto de partida compuestos comerciales estructuralmente relacionados con un derivado fenilcumarínico que ha sido descrito como molécula que interfiere en la interacción DosR-DNA.

Streszczenie

Gruźlica, choroba zakaźna spowodowana przez *Mycobacterium tuberculosis*, jest globalnym problemem zdrowotnym z dwoma milionami zgonów rocznie. Jedna trzecia ludności świata jest przewlekle zakażona *Mycobacterium tuberculosis*, nie wykazując objawów klinicznych, aczkolwiek z 10% ryzykiem aktywnego rozwoju choroby, co oznacza niekontrolowany zbiornik gruźlicy. W tym bezobjawowym stanie utajonej gruźlicy, *Mycobacterium tuberculosis* jest usytuowane w ziarniniakowych zmianach w gospodarzu odpornym na działanie obecnie dostępnych leków przeciwprątkowych .

Dwuskładnikowe układy wykonawcze (two-component systems) w bakteriach są główną klasą białek transdukcji sygnału zaangażowane w adaptację bakterii do zmian środowiskowych. Typowy system zawiera kinazę histydynową, która odgrywa kluczową rolę w detekcji bodźców środowiskowych i cytozolowy regulator odpowiedzi. Ta para białek funkcjonuje jako molekularny przełącznik, który steruje różnymi zmianami adaptacyjnymi w odpowiedzi na środowisko. *Mycobacterium tuberculosis* ma jedenaście kompletnych systemów dwuskładnikowych. System DosRST, składający się z regulatora odpowiedzi, DosR oraz dwóch kinaz histydynowych, DosS i DosT, odgrywa kluczową rolę w adaptacji *Mycobacterium tuberculosis* do utajonej gruźlicy. DosS i DosT autofosforylują konserwatywne reszty histydyny i oba białka mogą przenieść grupę fosforową do reszty kwasu asparaginowego 54 w DosR. Fosforylacja Asp54 służy jako przełącznik, ktory uaktywnia DosR oraz zwiększa jego powinowactwo do odpowiedniego promotora DNA. Reszty treoninowe 198 i 205 DosR odgrywają kluczową rolę w dimeryzacji DosR i wiązaniu DNA. Dynamika molekularna z typu dzikiego i zmutowanej wersji DosR wykazuje różnice w trwałości tworzenia aktywnego dimeru DosR. Pokazuje ona także zmniejszenie lub zniesienie interakcje białko-DNA ze względu na odpychanie generowanych przez ujemnie naładowane reszty zmutowanych aminokwasów. Ponadto podstawienia w treoninach 198 i 205 w DosR mają istotny wpływ na chemiczną i enzymatyczną fosforylację DosR i na jego defosforylację katalizowaną przez DosS .

Układ dwuskładnikowy DosRST jest dobrym obiektem dla opracowania nowych leków przeciwprątkowych przeciw nieaktywnym formom *M. tuberculosis*. Strukturalny program oparty na wykrywaniu inhibitorów regulatora odpowiedzi DosR został zainicjowany z użyciem dostępnych w handlu związków wykazujących pewien stopień podobieństwa z pochodną fenylkumaryny opisaną poprzednio jako cząsteczka zakłócająca oddziaływania DosR z DNA.

Context

This thesis was initiated in the R&D Department of Ferrer Internacional S.A. (Grupo Ferrer) in the framework of a large in-house project of discovery of antibiotics against tuberculosis. It was subsequently transferred to the R&D Department of Interquim S.A. (Grupo Ferrer) and developed in the Biochemistry Laboratory of the Bioengineering Department of IQS School of Engineering, Universitat Ramon Llull. The work developed in this thesis is part of an Initial Training Network within the Marie Curie Actions of the Seventh Framework Program funded by the European Commission. The collaborative STARS (Scientific Training in Antimicrobial Research Strategies) project (www.stars-itn.eu) was directed towards the discovery and development of novel antibacterial drugs by in silico, in vitro and in vivo experiments to gain insight into the 'druggability' of different two-component systems and to screen for new designed inhibitors. This thesis was partially carried out at the Instituto de Biomedicina de Valencia (IBV-CSIC), a partner of the STARS network, where the PhD candidate was seconded twice during the development of the present work.

Moim Rodzicom

ACKNOWLEDGEMENTS

Many people have contributed in important ways to the work in this thesis and to supporting me during its development. Herewith I would like to take this opportunity to thank them all.

First of all, I would like to take the privilege to express my deep sense of gratitude to Teresa Pellicer, my supervisor and Guru throughout the course of this investigation. Her invaluable support and valued suggestions as a professional will help me in shaping my life as a better scientist and human being. Thanks for her inspiration and guidance through every stage of the research and writing process. It is indeed due to her constant encouragement that this work has materialised.

I consider myself very fortunate to have been supervised by more people during this research. I thank Toni Planas, my coadviser in the thesis, who accepted me and has been mentoring me over my undergraduate and PhD work, for his support and valuable discussions.

Special thanks go to Alberto Marina. Probably in his next life he will be a rock star, but I am glad that in this one he happened to be a crystallographer and most importantly my advisor. His expertise, insight and enthusiasm have both encouraged and restrained me periodically throughout this process, and I am very thankful to him.

Special thanks go to Andrés Fernández for giving me the opportunity to come to Spain and begin this marvelous scientific adventure. His help, support, and guidance, especially at the start of this thesis, are greatly appreciated.

I wish to express my sincere appreciation to Xevi Biarnés for his tremendous help in bioinformatics part of this thesis and many thrilling discussions. Special thanks to Ellen for all her counsels and help with ITC.

I want to thank all mates from Bioquímica Lab, Hugo, Sergi, Carles, Javi, Victoria, Marta V., Oscar, Marta P., Amanda, Estela and Patri, for their friendship and advice. Your expertise and patience were greatly appreciated.

I am especially grateful to my scientific sole mate, Cristina Val Cid, who witnessed every minute of this thesis and made it unforgettable; nothing would have been the same without her beside me every day. I could not possibly count the number of exciting (not strictly scientific) discussions that we have had till date!

I also thank all the other coleagues and professors from IQS, Xavi T., Magda, Carlos S., Xavi P. and Edo who have come with their professional and personal consultations.

To members of the IBV research group, Patricia, Laura, Jordi, Marisa, Nadya, Paqui, Elisa, thank you for adopting me as a member of your team and for having made my stay a memorable one.

In Ferrer, I was also supported by extremely kind colleagues. In particular, I thank Nuria, Wilmar, Eva, Marta, Vanessa and Gemma, for their scientific help but also for their friendship. I appreciate very much the welcoming from Miquel Armengol, former director of Interquim.

I'm proud to say that this study was part of a much bigger `dream', the STARS project led by Jerry Wells. Without his scientific leadership and coordination this study would have never been possible.

I would like to thank the European Commission for the founding given to Initial Training Network within the Marie Curie Actions of the Seventh Framework Program, which have provided me with a scholarship.

I reserve my deepest appreciation for all participants STARS team, Maria, Ana, Nadya, Simone, Agnieszka, Rogier, Edoardo, Samir and J.P. All the moments we have spent together remain as never-to-be-forgotten.

This thesis is truly dedicated to my parents Krystyna and Jan Marszałek. It's their hard work, their dream and vision that finally came true. Without them, I would never go this far. The word 'thank you' is very small for the unconditional love from them. Immense love and gratitude go to my sister Monika. I am also grateful to all my family members for providing me their whole time support and guidance during ups and downs. This PhD and anything good I will ever do in life is for my family.

I would have never finished this PhD without my friends. I appreciate all support that came from Sylwia, Justyna, Emila, Ewa R., Ewa M., Asia, Lidka, Paweł, Marek, Czarek M and Czarek N within so many years of friendship.

Thanks to Magda, for her unconditional trust in me, my mysterious life choices and my hopeless dreams. It is the blessing to have her in my life.

My special thanks to Daria, Basia, Natalia, and recently Agata for kept me sane during this period with their help and support.

My eternal gratitude to the following people: Tim, Magali, Moni, Lolo, Vero, Dani, Sven, Jan, Pedro, Mireia, for their friendship filled with moments of craziness and laughs and for creating a homely environment here in Barcelona.

Special thanks are due to Marcin Węgrecki, who has been a wonderful friend not only throughout my stays in Valencia and impacted my life and thinking tremendously. I would also like to thank Yvonne for always being there for me. It

would have been much harder to complete this thesis without her moral and practical support.

I am grateful to my committee members, Alberto Marina, Andrés Fernández, Montserrat Agut, Laura Baldoma, Luis Izquierdo, Magda Faijes and Josefa Badia, for their time and assistance.

On a personal note, I would like to thank all my friends and coleagues from Fundación Enriqueta Villavecchia and l'Hospital de Sant Pau i de la Santa Creu. Those last years with you have undoubtedly played the largest role in moulding my personality in my formative years.

I am also thankful to all those who directly or indirectly helped me during this entire work.

TABLE OF CONTENTS

LIST OF FIGURES

LIST OF TABLES

LIST OF ABBREVIATIONS

aa	amino acid
ADMET	Absorption, Distribution, Metabolism, Excretion and Toxicity
AG	arabinogalactan
AIDS	Acquired immunodeficiency syndrome
ADP	adenosine diphosphate
Amp	ampicilin
AMPPNP	adenylylimidodiphosphate
ASP	aspartic acid
ATP	adenosine-5'-triphosphate
BLAST	Basic Local Alignment Search Tool
BCG	bacille Calmette-Guérin
BSA	bovine serum albumin
CDC	Centers for Disease Control and Prevention
Chl	chloramphenicol
CHO-K1	Chinese hamster ovary cells
CO	carbon monoxide
dH_20	destilled water
DMSO	dimethyl sulfoxide
DNA	deoxyribonucleic acid
DTT	dithiothrietol
EDTA	ethylene diamine tetra-acetic acid, disodium salt
EMSA	electrophoretic mobility shift assay
FDA	Food and Drug Administration
FPLC	fast protein liquid chromatography
HABA	hydroxyl-azophenyl-benzoic acid
HEPES	4-(2-hydroxyethyl)-1-piperazineethanesulfonic acid
HepG2	human hepatocytes
HIV	human immunodeficiency virus
IGRA	Interferon-Gamma Release Assay
IMAC	Immobilised Metal Affinity Chromatography
IPTG	isopropyl-1-thio-β-D-galactopyranoside
ITC	Isothermal titration calorimetry

kb	kilobase
kDa	kiloDalton
LB	Luria-Bertani
LTBI	latent tuberculosis infection
MA	mycolic acids
MAC	*M. avium* complex
MAA	Marketing Authorisation Application
MALDI-TOF	Matrix-assisted laser desorption/ionization-time-of-flight mass
MDG	The Millennium Development Goal
MDR-TB	Multi-drug resistant tuberculosis
MHB	Müeller-Hinton agar
Mtb	*Mycobacterium tuberculosis*
MTBC	*Mycobacterium tuberculosis* complex
NDA	New Drug Application
NO	nitric oxide
NRP	nonreplicative persistence oxygen depletion model
OD	optical density
PCR	polymerase chain reaction
PhRMA	Pharmaceutical Research and Manufacturers of America
PG	peptidoglycan
PMSF	phenylmethylsulphonyl fluoride
RPF	resuscitation promoting factor
RNA	ribonucleic acid
RT	Room temperature (24-26°C)
SDS-PAGE	sodium dodecyl sulphate polyacrylamide gel electrophoresis
TB	tuberculosis
TEMED	tetramethylethylenediamine
TFA	trifluoroacetic acid
TST	tuberculin skin test
UV	ultraviolet
WHO	World Health Organisation
WT	wild-type
XDR-TB	extensively drug-resistant tuberculosis

INTRODUCTION

1 Tuberculosis

A more detailed description of epidemiological, clinical and pharmacological aspects of active tuberculosis can be found in annex 1.

Tuberculosis (TB) is an infectious disease caused by *Mycobacterium tuberculosis (M.tuberculosis, Mtb*), which most commonly affects the lungs. The World Health Organization (WHO) estimates that one third of world's total population is currently infected with *Mtb* and approximately 10% of these people are expected to develop active TB at some point in their lifetime. A new individual is infected every second whilst another one dies from the disease every 15 seconds. Furthermore, the development of multidrug-resistant tuberculosis (MDR-TB) and extensively drug-resistant tuberculosis (XDR-TB) strains, together with the spread of risk factors such as human immunodeficiency virus (HIV), acquired immunodeficiency syndrome (AIDS) and diabetes (Corbett *et al.*, 2003, Restrepo *et al.*, 2007), continue making *Mtb* a health concern in developed countries and strengthened the urge to develop new treatment infection strategies.

WHO Global Tuberculosis Report 2013 (WHO 2013) indicates that in 2012 almost 1.3 million people died of TB, new cases were estimated at 8.6 million, and the number of total TB cases worldwide is about 14 million. These figures are equivalent to 122 cases per 100,000 population (Fig. 1). Most of the estimated number of cases in 2012 occurred in Asia (58%) and Africa (27%).

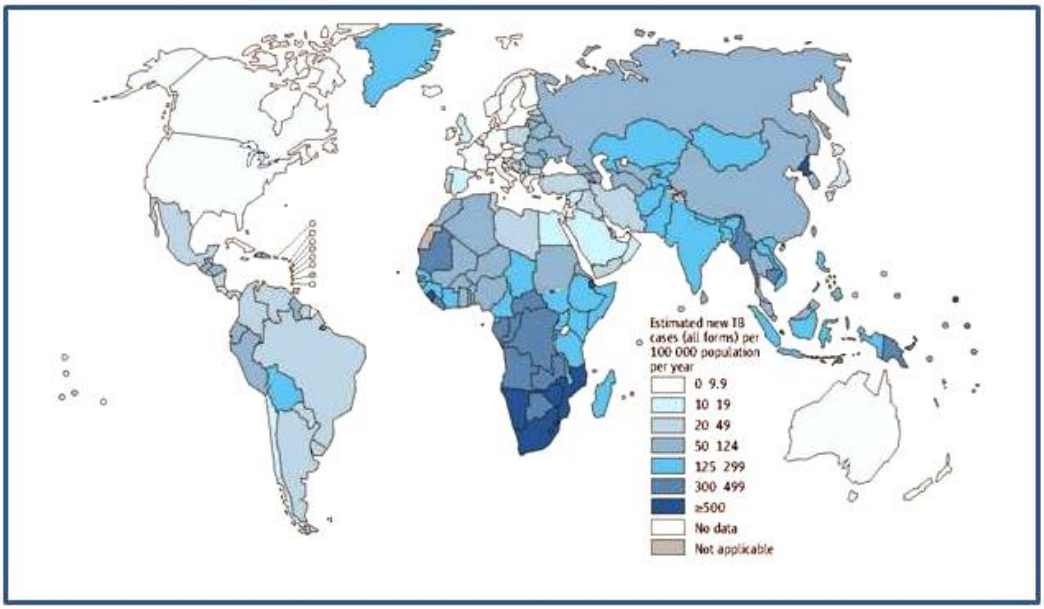

Fig. 1 Estimated TB incident rates, 2012 (WHO, 2013).

Mycobacterium tuberculosis mainly infects the lungs and causes a bad coughing. The clinical manifestations of tuberculosis can vary depending on the stage of tuberculosis, which include latency, primary disease, primary progressive (active) disease, and extrapulmonary disease.

Tuberculosis is primarily transmitted through air and spread by small airborne droplets, called droplet nuclei.

The most frequent method for diagnosing TB worldwide is sputum smear microscopy (Hopewell *et al.*, 2006). This test is relatively simple and rapid to perform, but it is not specific for tuberculosis as other mycobacteria give the same results. However, it does provide a quick method to determine if prevention should be taken while more definitive testing is performed.

Purified tuberculin protein derivative is used in tuberculin skin test (TST, Mantoux test). The degree of inflammatory reaction at the site of injection is an indication of the individual´s present or past association with the TB bacillus.

Bacille Calmette-Guerin (BCG), the oldest of the vaccines currently used throughout the world, is a commonly used prevention method in TB. New TB vaccines are an urgent part of a comprehensive plan to control and ulimately eliminate TB. Over the

past decade, researchers have made significant progress in TB vaccine development.

Antitubercular drugs can be divided into first-line drugs, those that generally have the greatest bactericidal activity when used for TB treatment, the second-line therapeutic-drugs, which are less effective, more expensive and have higher toxicities, and experimental drugs. First-line drugs include isoniazid, rifampin, pyrazinamide, ethambutol, and streptomycin. Second-line drugs contain p-aminosalicylicacid, ethionamide, cycloserine, kanamycin, capreomycin, amikacin, ciproflaxin, ofloxacin and viomycin.

Current therapy against tuberculosis is cumbersome, due to its long duration (~6months) and often leads to poor patient compliance. There is an urgent need for more effective and tolerable treatment of drug-susceptible and drug-resistant disease, latent TB infection, and dosing strategies for children. New drugs are required to shorten and simplify treatment, to improve the efficacy and tolerability of treatment for resistant strains of *Mtb* and to improve the treatment of TB among people living with HIV.

Multi-drug resistant tuberculosis (MDR-TB) is defined as resistance to the first-line drugs isoniazid and rifampin. Extensively drug resistant TB (XDR-TB) is defined as MDR-TB plus resistance to a fluoroquinolone, and at least one of three injectable second-line drugs. Treating XDR-TB is difficult and requires tailored individual care.

There are many governmental, multi-lateral and also non-governmental organizations dedicated to TB research. Their role is to accelerate progress on access to TB diagnosis and treatment, research and development for new TB diagnostics, drugs and vaccines, and tackling drug resistant- and HIV-associated.

WHO carries global leadership on matters critical to TB by monitoring TB situation in the world, including new strategies and standard implementation and measuring progress in TB care, control, and financing. WHO shapes the TB research agenda and stimulates the generation, translation and dissemination of valuable knowledge.

Main target that unites all TB organizations is The Millennium Development Goal (MDG) under which by 2015 the global burden of TB disease (deaths and prevalence) will be reduced by 50% relative to 1990 levels, and further, by 2050, the

global incidence of TB disease will be less than 1 per million population. By 2012, the prevalence rate fell 37% globally since 1990. Current forecasts suggest that the Stop TB Partnership target of halving TB prevalence by 2015 compared with a baseline of 1990 will not be met worldwide (WHO 2013).

2 The *Mycobacterium* genus

2.1 Classification and characteristics

2.1.1 Taxonomy

In the Bacteria Kingdom, Genus *Mycobacterium* belongs to the Phylum *Actinobacteria*, Order *Actinomycetales* (Suborder *Corynebacterineae*) and Family *Mycobacteriaceae*.

2.1.2 Clinical and epidemiological classification of mycobacteria

The classification of mycobacteria started in 1896 when Lehmann and Neumann proposed for the first time the genus *Mycobacterium* which included *Mycobacterium tuberculosis* and *Mycobacterium leprae* species. Phenotypic characteristics and biochemical tests have been used to classify mycobacteria into different species; more recently genotypic characteristics have been introduced as a tool for mycobacterial identification and classification. According to the latest ´´List of Bacterial Names with Standing in Nomenclature´´ there are more than 100 recognized species in the genus *Mycobacterium* (Bannister *et al.,* 2006).

Under DNA-based molecular taxonomy, mycobacteria are classified as Gram-positive bacteria due to genes high similarity with other gram-positive organisms, such as *Bacillus* (Hett & Rubin 2008).

According to their growth rate, the *Mycobacterium* genus is usually separated into two major groups: i) slow-growing species including *M. tuberculosis*, *M. bovis* and *M. leprae*; and ii) fast-growing species such as *M. smegmatis.*

Based on their epidemiological features, *Mycobacterium* includes: i) members which widely occur in natural ecosystems decomposing organic matter and due to the nitrogen binding activity they are useful and essential inhabitants of the soil and

surface waters (Hett & Rubin, 2008) (non-pathogenic or rarely pathogenic mycobacteria); ii) species strictly pathogenic to humans and/or animals (strictly pathogenic mycobacteria); iii) types usually commensal to humans, but pathogenic under certain circumstances (potentially pathogenic mycobacteria) (Brosch *et al.*, 2001;) (Table 1).

Among the pathogenic species the most relevant for human health are *M. tuberculosis* and *M. leprae*, the causative agents of two of the world's oldest diseases, tuberculosis and leprosy, respectively (Hett & Rubin, 2008).

M. canettii and *M. africanum*, which also can cause human TB, are most commonly isolated from African patients. *M. bovis* demonstrates the broadest spectrum of host infection, affecting humans, domestic or wild bovines and goats. *M. microti* can also cause disease in immunocompromised human patients (Brosch *et al.*, 2002, Niemann, 2000) and *M. pinnipedii* infects seals (Cousins *et al.*, 2003).

M. kansasii, *M. malmoense* and *M. xenopi* represent pulmonary opportunists, while *M. marinum* is the skin pathogen infecting organism by entering through damaged or ulcerated skin. *M. ulcerans* is the causative organism of buruli (tropical) ulcer (Bannister *et al.*, 2006).

Table 1 Classification of mycobacteria according to the risk of infection (Brosch *et al.,* 2001).

Rare pathogens		Potential pathogens	Strict pathogens
M. smegmatis	*M. aurum*	*M. avium*	*M. tuberculosis*
M. phlei	*M. chitae*	*M. intracellulare*	*M. bovis*
M. fallax	*M. duvalii*	*M. chelonae*	*M. africanum*
M. thermoresistibile	*M. gadium*	*M. fortuitum*	*M. ulcerans*
M. parafortuitum	*M. gilvum*	*M. kansasii*	*M. microti*
M. gastri	*M. komossense*	*M. malmoense*	*M. canetti*
M. triviale	*M. lepraemurium*	*M. marinum*	*M. caprae*
M. nonchromogenicum	*M. neoaurum*	*M. scrofulaceum*	*M. pinnipedii*
M. gordonae	*M. terrae*	*M. simiae*	*M. leprae*
M. flavescens	*M. vaccae*	*M. szulgai*	
M. farcinogenes	*M. agri*	*M. xenopi*	
M. senegalense	*M. aichiense*	*M. asiaticum*	
M. paratuberculosis	*M. austroafricanum*	*M. haemophilum*	
M. porcinum	*M. chubuense*	*M. shimoidei*	
M. diernhoferi	*M. obuense*		
M. pulveris	*M. rhodesiae*		
M. tokaiense	*M. moriokaense*		
M. poriferae			

According to the similarities in genetic and phenotypic characteristics different complexes can be differentiate within *Mycobacterium* genus.

All of the species of *Mycobacterium tuberculosis* complex (MTBC), which includes *M. tuberculosis, M. canettii, M. africanum, M. microti, M. bovis, M. caprae* and *M. pinnipedii*, are known to cause TB in humans

The *M. avium* complex (MAC) comprises *M. avium* subspecies responsible for disease in birds, but also for disseminated disease in patients with AIDS, causing systemic infections late in the progress of AIDS (Tyagi *et al.*, 2004), cervical lymphadenitis, and chronic lung disease in immunocompetent or non-HIV patients (Turenne *et al.*, 2007).

The *Mycobacterium fortuitum* complex includes *M. fortuitum, M. peregrinum, M. abcessus* and *M. chelonae,* which are frequently responsible for abscess formation in local injection or surgical wounds and can be associated with pulmonary disease (Griffith, 2007).

2.1.3 Morphology

Mycobacteria are typically rod-shaped, non–spore forming, aerobic bacteria, classified as acid-fast bacilli. The dimensions of the bacilli have been reported to be 1-10 µm in length (usually 3-5 µm), and 0.2 -0.6 µm width. Variable morphology can be observed when grown on solid media and some species exist as shorter cocci-bacilli or curved rods on artificial media (Belisle & Brennan 1989).

The reported morphological variation in *M. tuberculosis* are classified in two categories; i) those which are frequently seen at exponential phase of growth that is rod, V, Y-shape, branched or buds (Fig. 2A), and ii) those that are seen occasionally under stress or environmental conditions which are round, oval, ultra-virus, spore like, and cell wall defiant or L-forms (Fig. 2B) (Velayati *et al.,* 2009, 2011; Farnia *et al.,* 2010).

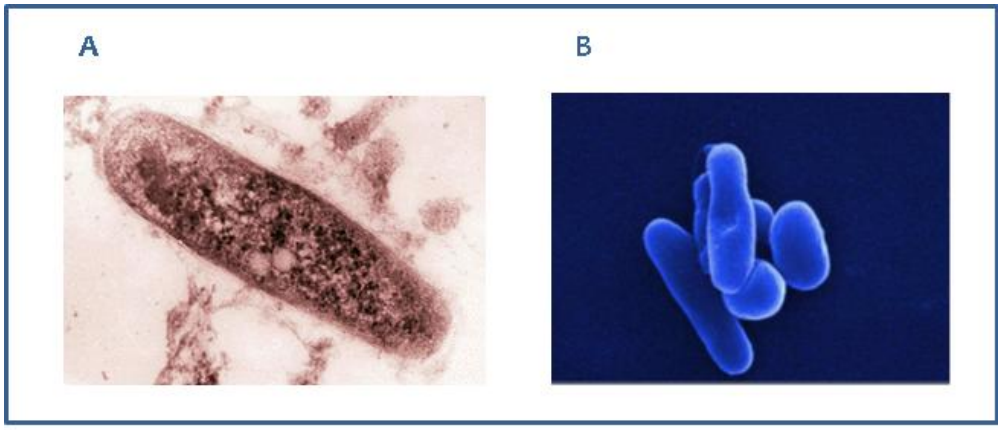

Fig. 2 Morphological variations in *M. tuberculosis*. (A). Thin section transmission electron micrograph of *Mtb* (extracted from www.wadsworth.org/databank/mycotubr.htm). (B). Scanning electron microscope shows shape variation in *Mtb* at exponential phase of growth (Ali Akbar Velayati & Parissa Farnia, 2012).

Mycobacterium tuberculosis is an obligate aerobe. For this reason *Mtb* complexes are always found in the well-aerated upper lobes of the lungs in patient with TB. The bacterium is a facultative intracellular parasite, usually of macrophages, and has generation time of 15-20 hours, which is extremely slow compared to other bacteria with division times measured in minutes (*Escherichia coli* can divide every 20 minutes).

2.2 The *Mycobacterium tuberculosis* genome

The genome of the virulent strain of *Mtb*, H37Rv was completely sequenced and published in 1998 (Cole *et al.,* 1998) and this allowed to know that the bacterium dedicates 8% of its genome to lipid metabolism alone.

It presents a sequence of 4,411,529 bp and a characteristically high guanine plus cytosine (G+C) content (65.5%). Genome analysis revealed an efficient DNA repair system with nearly 45 genes related to DNA repair mechanisms (Mizrahi & Andersen, 1998). Moreover, despite over 10,000 years of evolution, when 16 genetically diverse clinical strains were examined for conservation of 24 genes known to encode antigenic proteins, minimal variation was observed (Musser *et al.,* 2000).

H37Rv and its avirulent counterpart H37Ra strains have been widely used as reference strains for studying virulence and pathogenesis of *M. tuberculosis* worldwide since 1940s. H37Ra is used as an adjuvant to boost immunogenicity during immunization with BCG. The H37Ra genome is highly similar to that of H37Rv with respect to gene content and order (Zheng *et al.,* 2008). However, H37Ra has several characteristics that are different from its virulent sister strain H37Rv, including: i) a raised colony morphology (Steenken, 1935); ii) loss of cord formation (Middlebrook, 1947); iii) loss of neutral red dye binding (Dubos & Middlebrook, 1948); iv) decreased survival under anaerobic conditions (Heplar, 1954; Dubos, 1955) or inside the macrophages (Mackaness *et al.,* 1954); v) impaired ability to disrupt phagosomal membranes (Hart & Armstrong, 1974); and vi) loss of virulence in guinea pigs (Steenken, 1938; Alsaadi & Smith, 1973) and mice (Pierce *et al.,* 1953; Larson & Wicht, 1964). Analyses of the genomes of known avirulent strains, such as

the BCG vaccine or the H37Ra, showed mutations in PhoPR two-component system resulting in a loss of function, confirming its key role in virulence (Frigui *et al.,* 2008; Zheng *et al.,* 2008; Cimino *et al.,* 2012).

2.3 Cell wall

The cell wall structure of *Mtb*, unique among procaryotes, is associated with the pathogenicity of *Mtb* (Smith, 2003; Barry *et al.,* 1998; Dubnau *et al.,* 2000; Glickman *et al.,* 2000). The richness in high molecular weight lipids represents the complexity of the cell wall (Brennan *et al.,* 1995; Christensen *et al.*, 1999; Daffé *et al.,* 1998; Draper, 1998; Jarlier *et al.,* 1994). Unusual impermeable properties of *Mtb* cell wall are thought to be advantageous for the bacilli in stressful conditions of osmotic shock (Hett & Rubin, 2008) and the polymers, covalently linked with peptidoglycan and trehalose dimycolate, provide a thick layer involved in *Mtb* resistance to antibiotics and the host defense mechanisms (Takayama *et al.,* 2005).

The mycobacterial cell wall consists of an inner layer and an outer layer that surround the plasma membrane (Fig. 3). The outer compartment consists of both lipids and proteins. The inner compartment consists of peptidoglycan (PG), arabinogalactan (AG), and mycolic acids (MA) covalently linked together to form an insoluble complex referred to as the essential core of the mycobacterial cell wall (Brennan *et al.,* 2003).

PG, or murein, external to the bacterial cell membrane, is a major determinant of bacteria shape maintenance protecting bacilli from osmotic turgor pressure. The structure of PG is unique to bacteria and thus an excellent target for therapeutics. AG is important for cell wall integrity and for anchoring the impermeable MA layer to the PG layer (Hett & Rubin, 2008).

Another important component of the cell wall is lipoarabinomannan, a major lipoglycan involved in virulence of *Mtb* (Chan *et al.,* 1991) and in modulating the host response during infection (Cox *et al.,* 1999).

Mycolic acids, the strong hydrophobic molecules that form a lipid shell around the organism and affect permeability properties at the cell surface, has been shown to be critical for the survival of *Mtb* (Draper *et al.,* 2005).

Cord Factor, a glycolipid most abundantly produced in virulent strains of *Mtb*, is responsible for: i) inducing animal granulomas similar to those characteristic of TB infection (Hunter *et al.*, 2006b); ii) increasing cytokine production (Ryll *et al.*, 2001); iii) inhibiting the transfer of phagocytosed bacteria to acidic compartments in macrophages (Indrigo *et al.*, 2003.); and iv) influencing the morphology of mycobacterial colonies (Hunter *et al.*, 2006a).

The cell wall is a key to the survival of mycobacteria and a more complete understanding of the biosynthetic pathways and gene functions and the development of antibiotics to prevent formation of the cell wall are areas of great interest (Joe *et al.*, 2007).

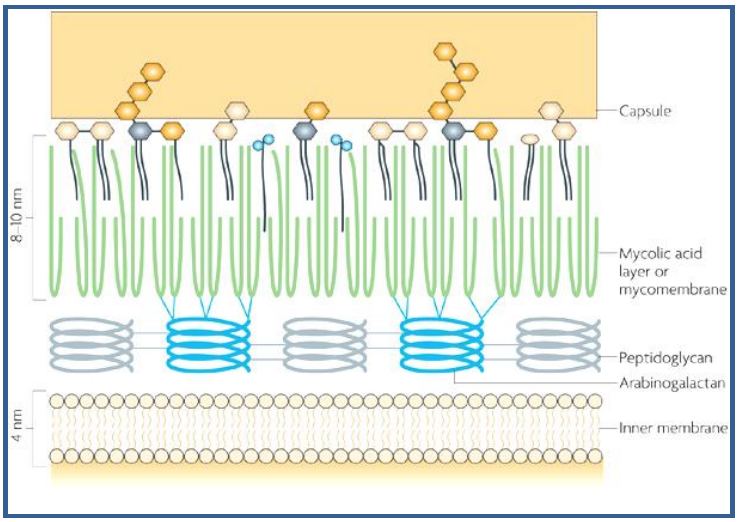

Fig. 3 Schematic of the bacterial cell wall (Abdallah *et al.*, 2007).

2.4 Virulence determinants

The virulence of *Mycobacterium tuberculosis* is extraordinarily complex. Although the organism apparently does not produce any toxins, it possesses a huge repertoire of structural and physiological properties that have been recognized for their contribution to mycobacterial virulence and to pathology of tuberculosis. Subsequently, virulent *Mtb* species have developed strategies to avoid or modulate the immune response in their favour.

Among a great number of virulence factor of *Mtb* (Table 2), exported proteins are one of the most important factors responsible for the virulence (Rajni & Meena, 2011). Culture filtrate proteins, found in the culture medium in which *Mtb* grows, are actively studied by many researchers, since a great deal of them is recognized by the sera of TB patients (Smith, 2003). The virulent components can be assembled in different clusters: i) cell envelope proteins, including cell wall proteins, lipoproteins and secretion systems; ii) proteins inhibiting antimicrobial effectors of the macrophage; iii) gene expression regulators, including two component systems, sigma factors and other transcriptional regulators; iv) enzymes involved in general cellular metabolism; and v) other proteins, including the ones of unknown function (Forrellad *et al.,* 2013; Smith, 2003).

Mtb has developed highly specialized mechanism to proliferate in the host during infection, such as: i) slow generation time, in consequence to which the immune system may not readily recognize the bacteria or may not be triggered sufficiently to eliminate them; or ii) lipid and fatty acid metabolism, including catabolism of cholesterol. It has been also shown that *Mtb* produces pili during human infection, which could be involved in initial colonization of the host (Alteri *et al.,* 2007).

Table 2 Virulence factors of *Mycobacterium tuberculosis*.

Virulence factor	Category	Role	Virulence characterization	Reference
Antigen 85 complex	Exported protein	Fibronectin-binding	Possible impact in walling off bacteria from the immune system and facilitation of tubercle formation	Belisle *et al.*, 1997
HbhA	Adhesin	Heparin-binding hemagglutin	Involvement in binding *Mtb* to epithelial cells	Delogu & Brennan, 1999
ESX-1	Secretion-associated proteins	Virulence proteins delivery during infection	Avoidance of excessive virulence by maintaining ESX-1 activity that leads to long term survival of *Mtb*	Raghavan *et al.*, 2008
WhiB3 protein	Putative transcription regulator	Implication in sensing oxygen tension and redox state	Adaptation of mycobacteria to changes in oxygen tension	Banaiee *et al.*, 2006
Acr1 (hspX)	α-crystalline protein homolog	Dormancy-associated protein	Inhibition of antimicrobial effectors of the macrophage	Yuan *et al.*, 2008
19-kDa protein	Lipoprotein antigen	Blockage of IFN-γ signaling through a TLR-2 dependent mechanism	Inhibition of MHC-II antigen processing and presentation in macrophages	Tobian *et al.*, 2003
Sigma factors	Gene expression regulators	Help in regulation of expression of specific genes during stress or morphological development	Adaptation to the changing environment within the host	Browning *et al.*, 2004
STPKs	Serine-threonine protein kinases	Regulation of cell shape; macrophages modulation	Regulation of host-pathogen interactions and developmental changes through signal transduction using reversible phosphorylation of proteins	Av-Gay & Everett, 2000; Leonard *et al.*, 1998

3 Latency, dormancy and persistence

Dormancy, latency, and persistence are related terms used to describe the ability of *M. tuberculosis* to arrest its growth in response to host-imposed stress (Rittershaus *et al.*, 2013). The difference between those terms is indistinct in various studies regarding tuberculosis.

Latency refers to an *in vivo* situation where the bacteria and the host have established a balanced state without causing clinical symptoms. Whereas the term dormant refers to the state of reduced metabolic activity adopted by many

organisms under conditions of environmental stress; organisms slow down their metabolic processes to a minimum to retain resources till the conditions are more favorable for resuscitation.

3.1 Dormancy among microbes

Dormancy, a common strategy among natural systems, is regulated by the interpretation of environmental indications. Many plant populations can adapt to changes in air temperature or photoperiod (Hairston *et al.,* 1990; Vazquez-Yanes & Orozco-Segovia, 1990). Frequently, microorganisms are capable of resisting stressors such as temperature, desiccation, oxygen tension and antibiotics by entering resting states or by forming spores (Roszak & Colwell, 1987; Whittington *et al.,* 2004; Sussman & Douthit, 1973; Lewis, 2007). Not only by constructing morphological features such as endospores, cysts, or conidia, microbes can enter convertible states of reduced metabolic activity without investment in specialized cellular structures (Sussman & Douthit, 1973; Sussman & Halvorson, 1966). Futhermore, there is some evidence that dormant and slow-growing populations can respond similarly to favorable environmental change (Choi *et al.,* 1999; Kjelleberg *et al.,* 1987).

3.2 Dormancy in *Mycobacterium tuberculosis*

Once entering the organism, *M. tuberculosis* has four potential fates: i) it can be killed by immune system, which happens in the majority of cases; ii) it can multiply causing primary TB; iii) it may become dormant and remain asymptomatic; or iv) it may proliferate after a latency period (reactivation disease).

After entering the host, typically by airborne droplets , bacteria go through a period of rapid replication until the host develops an immune response. Latent tuberculosis infection (LTBI) occurs when bacilli penetrate into the terminal alveoli where they are engulfed by phagocytic immune cells called macrophages. By slowing metabolism, spread through granuloma formation (Manabe & Bishai, 2000) and becoming dormant, *M. tuberculosis* adapts to the stressful conditions generated by host defense system and becomes as silent to the immune system

(Cardona & Ruiz-Manzano, 2004), preventing activation of the disease (Warner & Mizrahi, 2007; Rook *et al.,* 1986). The bacterial behavior during the growth phases (lag, log, stationary, and death phases) is well known, but the behavior of *M. tuberculosis* in dormant state is poorly understood.

Hypoxia, nitric oxide and nutrient starvation are some of the conditions which are believed to be associated with initiation and maintenance of *Mtb* dormancy (Wayne & Sohaskey, 2001; Betts *et al.,* 2002; Voskuil *et al.,* 2003). Carbon monoxide and ascorbic acid have also been implicated in dormancy adaptation (Kumar *et al.,* 2008; Taneja *et al.,* 2010).

Once latent infection with *M tuberculosis* has been established, viable bacilli may persist for decades in a non-replicating state, followed in some cases by reactivation (Wayne & Sohaskey, 2001).

It is commonly estimated that an individual with LTBI has ~10% lifetime risk of developing active TB. It is believed that 5% of the infected population will develop the disease after 5 years, known as "primary" TB that usually affects children and immunosuppressed hosts, and the others will suffer from "post-primary" TB at some time during their lives (Grange, 1998).

3.3 Granuloma and immunophysiology of LTBI

Although very little is known about maintenance of *M. tuberculosis* inside the host during dormant state, the growth pattern across the bacterial population appears relatively conserved in animal models.

M. tuberculosis can persist for decades without causing any clinical symptoms in multicellular structure, called granuloma. A granuloma is comprised of macrophages (resting, activated and infected), immune effector T cells on the periphery, chemokines, cytokines, adhesion molecules, and a caseous necrotic center (Lin *et al.,* 2006; Lin & Flynn, 2010). Granuloma formation is a hallmark of LTBI, and provides a microenvironment where interactions between recollected cells are facilitated and bacteria are separated from spreading into the host. Granulomas can be formed anywhere in the lung, yet 90% of the post-primary TB cases occurs in the upper lobes (Balasubramanian *et al.,* 1994).

Inside granuloma in the lungs of mice, immune cells accumulate indifferent sites that are most likely associated with their functions in different stages of infection and disease (Tsai *et al.,* 2006; Ulrichs & Kaufmann, 2006).

Granuloma formation reflects the immune response in LTBI (Fig. 4). T cells play an important role in the immune response against *M. tuberculosis*. Both CD4 and CD8 Tcells participate in control of acute tuberculosis in mice (Flynn & Ernst, 2000). Also adequate IL-12/IL-23/IFNγ signaling is required for: i) the control of *M. tuberculosis* infections; and ii) the development of mature granulomas (Ottenhoff *et al.,* 2002; Casanova & Abel, 2002). Likewise, mice deficient in IFNγ signaling fail to form granulomas following *M. tuberculosis* infection (Pearl *et al.,* 2001). Cytokines IFN-ɣ and TNF-α contribute to resistance to *M. tuberculosis* whilst in a persistent infection pursue to be produced in the lungs of mice, suggesting that continuous macrophage activation is important in preventing reactivation of the infection (Flynn *et al.,* 1998).

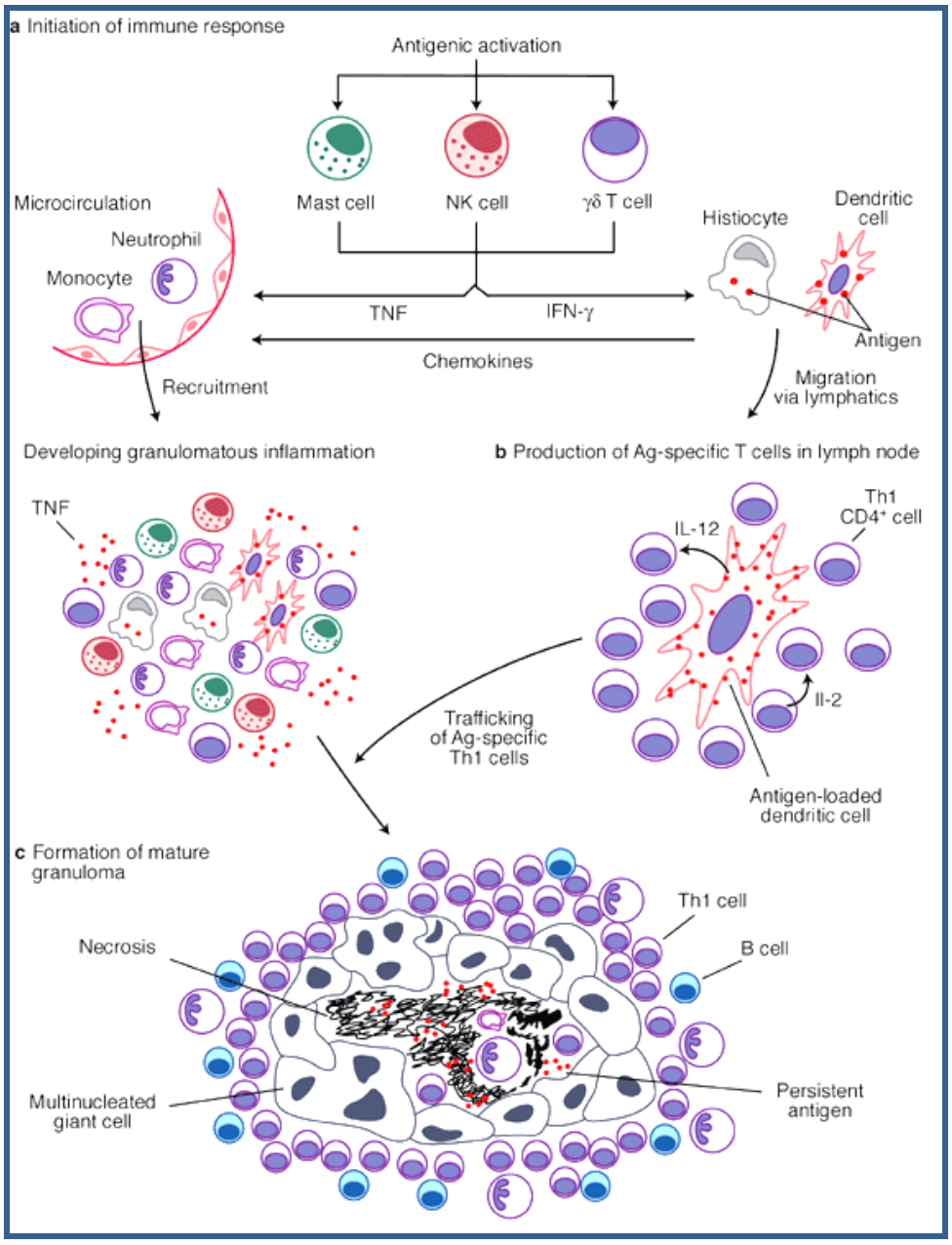

Fig. 4 Process of granuloma formation. Extracted from Expert Reviews in Molecular Medicine 2005; Published by Cambridge University Press.

3.4 Reactivation

The reactivation of TB, which is the reestablishment of *Mtb* bacilli metabolic and replicative activity, can occur in any organ in which the tubercle bacilli were seeded during the primary infection. However, in immunocompetent individuals, the

reactivation usually occurs in the upper lobes, where higher oxygen pressure supports good bacillary growth (Ahmad *et al.,* 2011).

Although detailed mechanisms of resuscitation are largely unknown, there is a plethora of information regarding the factors increasing the risk for progression into active disease. Disruption of organized structures inside granuloma, marked for deficiencies related to T-cell number or function, is a typical feature of TB reactivation and the most notable cause for that is coinfection with HIV (Dooley & Sterling, 2005; Jasmer *et al.,* 2002; McBryde & Denholm, 2012; Klossek *et al.,* 2004; Selvyn *et al.,* 1989; Hamdi *et al.,* 2006) .

Other factors, such as advanced age, uncontrolled diabetes mellitus, sepsis, renal failure, malnutrition, smoking, chemotherapy, organ transplantation, and long-term corticosteroid usage can trigger reactivation of infection (Frieden *et al.,* 2003; Wells *et al.,* 2007; Corbett *et al.,* 2003; Dooley & Chaisson , 2009).

Resuscitation has been studied at the molecular level in *Micrococcus luteus* where the resuscitation promoting factor (Rpf) has been shown to induce resuscitation. The genome of *M. tuberculosis* comprises five Rpf factors (RpfA to -E) (Mukamolova *et al.,* 2002). *In vivo* and *in vitro* studies suggest that Rpf proteins are not needed for general viability but may be required to respond to conditions specific to a later stage of disease, in particular, dormancy (Downing *et al.,* 2005; Tufariello *et al.,* 2006). Furthermore, an endopeptidase RipA of *Mtb* has recently been recognized as a vital component for revival from latency (Hett *et al.,* 2007; Kana *et al.,* 2008).

3.5 Diagnosis of LTBI

The diagnosis of LTBI is based on information gathered from the medical history, TST or IGRA result, chest radiograph, physical examination, and under certain circumstances, sputum examinations (Table 3).

Radiologic findings associated with risk of subsequent tuberculosis disease may include pulmonary scarring and granuloma, particularly in the upper lobes (Joshi *et al.,* 2007). Due to some limitations of TST, such as possible false-positive results, IGRA test has been alternatively used for LTBI diagnosis (Diel *et al.,* 2008). IGRA monitors *Mtb*-specific proteins, indicating T-cells that have previously been exposed

to TB (Lein & Reyn, 1997). Although, with its considerable specificity and predictive value, IGRA overcomes TST for LTBI diagnosis, for reasons that include increased cost and technological requirements, they are yet to be widely adopted for routine LTBI diagnosis in many parts of the world (Vinton *et al.*, 2009).

Table 3 Differentiating between LTBI and active TB disease (CDC).

LTBI	Active TB Disease
• No symptoms or physical findings suggestive of TB disease.	• Symptoms may include one or more of the following: fever, cough, chest pain, weight loss, night sweats, hemoptysis, fatigue, and decreased appetite.
• TST or IGRA result usually positive.	• TST or IGRA result usually positive.
• Chest radiograph is typically normal.	• Chest radiograph is usually abnormal. However, may be normal in persons with advanced immunosuppression or extrapulmonary disease.
• If done, respiratory specimens are smear and culture negative.	• Respiratory specimens are usually smear or culture positive. However, may be negative in persons with extrapulmonary disease or minimal or early pulmonary disease.
• Cannot spread TB bacteria to others.	• May spread TB bacteria to others.
• Should consider treatment for LTBI to prevent TB disease.	• Needs treatment for TB disease.

3.6 *In vitro* and *in vivo* models of dormancy

Studies of dormancy in TB have been hampered by the lack of *in vitro* and *in vivo* models truly representative of human LTBI. The existing models only reflect individual aspects of human TB but are good sources to learn about the metabolic state of persistent mycobacteria and host immunity.

3.6.1 *In vitro* models

Several *in vitro* models have been developed to model latency or investigate the adaptive processes of the *M. tuberculosis* to non-proliferating conditions. This can be achieved by inducing at least one of the stresses to which the tubercle bacilli are exposed in the host. These include: i) hypoxia; ii) starvation of essential nutrients, such as carbon, nitrogen, or phosphorus; iii) oxidative and nitrosative stresses; iv) iron limitation; and v) exposure to gaseous stresses such as nitric oxide and carbon monoxide (Sikri & Tyagi, 2013).

In vitro models include: i) a nonreplicative persistence oxygen depletion model (NRP) (Muttucumaru *et al.,* 2004; Voskuil *et al.,* 2004; Wayne & Hayes, 1996), where the culture is gently stirred in a sealed flask, resulting in a slow depletion of oxygen; ii) a steady-state reduced oxygen model, which makes use of a chemostat (Bacon *et al.,* 2004); iii) a static culture oxygen depletion model (Kendall *et al.,* 2004); iv) an aerated stationary-phase model (Voskuil *et al.,* 2004); v) a long-term nutritional depletion at high oxygen concentration model (Hampshire *et al.,* 2004); vi) a short-term oxygen depletion model (Park *et al.,* 2003; Sherman *et al.,* 2001; vii) addition of nitric oxide (Voskuil *et al.,* 2003); viii) a short course of complete starvation model (Betts *et al.,* 2002); ix) multiple stress model, where bacteria is exposed to the combined stresses of low oxygen, high CO2, low carbon and nitrogen nutrients and acidic pH (Deb *et al.,* 2009); and x) human macrophage model using vitamin D(3) and retinoic acid activated THP-1 macrophages (Estrella *et al.,* 2011).

3.6.2 *In vivo* models

A number of animal model systems, including mice, guinea pigs, rabbits, marmoset, cynomolgous, and macaque non-human primates, are being adapted to portray various aspects of granuloma immunopathology.

The Cornell model was the first animal model for dormant bacilli. This model involves partial clearance of *M. tuberculosis* infection by incomplete chemotherapy to induce the latent state (McCune *et al.,* 1956).

Later LTBI mouse model, known as the chronic or plateau model, involves aerosol infection or infection by intravenous routes that lead to a steady accumulation of pulmonary damage (Orme, 1988).

3.7 New targets for LTBI

Current anti-TB therapies are directed against actively replicating bacteria. There is no particular treatment for latent form of TB. Identification and validation of appropriate targets for designing drugs are critical steps in drug discovery. With different kinds of data that are now available, computational approaches can be powerful means of obtaining short-lists of possible targets for further experimental validation. Murphy & Brown bioinformatics analysis (Murphy & Brown, 2007) selected several physiological roles that can be targeted for therapeutic development against LTBI. These included: i) the significant up-regulation of genes controlled by dos*R* (also named *dev*R); ii) down-regulation of protein and ATP synthesis; and iii) the adaptation of two-carbon metabolism to the hypoxic and nutrient limited environment of the granuloma. Promising targets for inhibition were several regulatory elements (*rel*A, *mpr*AB), enzymes involved in redox balance and respiration, sulfur transport and fixation, pantothenate, isoprene, and NAD^+ biosynthesis.

Another target identification pipeline for *Mtb* through an interactome, reactome and genome-scale structural analysis (Raman *et al.,* 2008) includes high confidence targets that address mycobacterial persistence. Proteins critical for survival of *Mtb* were first identified, followed by comparative genomics with the host, finally incorporating a novel structural analysis of the binding sites to assess the feasibility of a protein as a target. This work includes a correlation study with expression data and non-similarity to gut flora proteins as well as 'anti-targets' in the host. A number of novel anti-tuberculous agents are currently in various phases of development (Annex 1 Table 11). Several of these medications such rifapentine, TMC-207 and moxifloxacin appear to have potent sterilizing activity and may potentially be of use in treatment of LTBI (Andries *et al.,* 2010).

The DosR response regulator is an essential protein that controls gene expression in latency (Voskuil *et al.,* 2003; Park *et al.,* 2003; Sherman *et al.,* 2001; Cho *et al.,* 2006). A plethora of papers (Murphy & Brown, 2007; Raman *et al.,* 2008; Hasan *et al.,* 2006; Zhang *et al.,* 2006; Saini *et al.,* 2004, 2005; Wisedchaisri *et al.,* 2005) have identified DosR as a strong candidate for therapeutic intervention against LTBI.

The mechanism of action of *dosR* targeting molecules may work not by killing *M.tuberculosis* bacilli directly, but by forcing them out of the non-replicative state (Wayne & Sohaskey, 2001) leaving them susceptible to the usual antimycobacterial agents.

4 Two-component systems

Two-component systems (TCSs) are widespread signal transduction mechanisms in prokaryotes that enable these organisms to sense, respond, and adapt to a wide range of environments, stressors, and growth conditions (Stock *et al.,* 2000). They were first described when the amino acid sequence of CheY, a response regulator involved in chemotaxis in *E. coli* and other Gram-negative bacteria, was shown to be related to regulatory proteins of other cellular processes (Stock *et al.,* 1985). TCSs are absent in mammals which makes them potential targets for antimicrobial drug design (Watanaber *et al.,* 2008).

Over three hundred TCSs have been identified in approximately one hundred different bacteria and have been catalogued in the P2CS database (http://www.p2cs.org) (Barakat *et al.,* 2011). The only bacterium studied to date where no TCS have been identified is *Mycoplasma genitalium* (Barrett *et al.,* 1998). Limited metabolic capacities and intracellular lifestyle suggest that *M. genitalium* has little need to respond to its environment by regulating gene expression.

TCS variants have also been found in yeast (Maeda *et al.,* 1994), plants (Mizuno, 2005) and in lower eukaryotes, for instance *Arabidopsis thaliana* (Imamura *et al.,* 1999), where they regulate hormone responses and circadian rhythms (Table 4A).

TCSs in bacteria are known to respond to a wide variety of conditions, such as nutrient deprivation, cold/heat shock and the presence of antimicrobial compounds (Aguilar *et al.,* 2001; Jordan *et al.,* 2008; Sun *et al.,* 1996). They can regulate a wide

variety of cellular process, including motility and chemotaxis, sporulation, biofilm formation and quorum sensing (Jiang *et al.,* 2000; López *et al.,* 2009; Lyon & Novick, 2004; Szurmant & Ordal, 2004). TCSs have been shown to play crucial role in bacterial virulence (Hoch & Silhavy, 1995; Atkinson & Ninfa, 1999) (Table 4B).

Table 4 TCSs in different bacterial species. (A). Diversity of physiological processes controlled by TCSs. (B). Examples of TCSs involved in virulence.

A. Diversity of bacterial processes controlled by TCS			
Organism	**TCS (HK/RR)**	**Function**	**Reference**
Bacillus subtilis	VanS/VanR	Vancomycin tolerance	Evers & Courvalin, 1996
Bacillus subtilis	KinA/SpoOF	Sporulation regulation	Wang *et al.,* 2001
Bacillus subtilis	ComP/ComA	Competence regulation	Weinrauch *et al.,* 1990
Bacillus subtilis	DegS/DegU	Regulation of many cellular processes e.g. exoprotease production, catabolism, competence development and motility	Ogura *et al.,* 2001
Caulobacter. crescentus	CckA/CtrA	Co-ordination of cell cycle progression and polar morphogenesis	Jacobs *et al.,* 1999; Wheeler & Shapiro, 1999
Escherichia coli	CheA/CheB	Chemotaxis	Hess *et al.,* 1988
Escherichia coli	EnvZ/OmpR	Adaptation to environmental osmotic changes by controlling expression of major outer membrane proteins	Egger *et al.,* 1997
Escherichia coli	PhoR/PhoB	Phosphate regulation	Lee *et al.,* 1989
Rhodobacter sphaeroides	PrrA/PrrB	Expression of photosynthesis and Calvin cycle CO_2 fixing operons	Emmerich *et al.,* 2000
Rhizobium spp.	FixL/FixJ	Nitrogen fixation	Weinstein *et al.,* 1992
Staphylococcus aureus	SrhS/SrhR	Regulation of energy transduction in response to changes in oxygen availability	Throup *et al.,* 2001
Staphylococcus aureus	YycG/YycF	Regulation of bacterial cell wall / membrane composition	Martin *et al.,* 1999
Streptomyces coelicolor	AbsAl/AbsA2	Antibiotic synthesis	Brian *et al.,* 1996; Anderson *et al.,* 2001
Vibrio fischeri	LuxI/LuxR	Quorum sensing and induction of bioluminescent genes	Salmond *et al.,* 1995
B. Bacterial TCS involved in the regulation of virulence determinants			
Organism	**TCS (HK/RR)**	**Function**	**Reference**
Agrobacterium tumefaciens	VirA/VirG	Crown gall tumor formation	Dziejman & Mekalanos, 1995
Bordetella pertussis	BvgS/BvgA	Activation and repression of a range of virulence factors	Akerley *et al.,* 1992
Enterococcus faecium	VanR/VanS	Vancomycin resistance	Arthur *et al.,* 1992
Klebsiella pneumoniae	NtrA/NtrC	Urease production	Collins *et al.,* 1993
Neisseria gonorrhoeae	PilA/PilB	Pilus formation	Taha *et al.,* 1991
Pseudomonas aeruginosa	PirS/PirR	Iron acquisition	Rumbaugh *et al.,* 1999
	PilS/PilR	Pilus formation	Rodrigue *et al.,* 2000
	FleS/FleR	Adhesion	Dziejman & Mekalanos, 1995

	AlgR2/ AlgR1	Alginate synthesis	Balaban *et al.*, 1998
Staphylococcus aureus	AgrC/AgrA	Expression of a range of extracellular proteins and toxins involved in various aspects of virulence (global expression)	Yarwood *et al.*, 2001
	ArlS/ArlR	Interaction with other systems to modulate virulence factor regulation	Fournier *et al.*, 2001
Streptococcus pyogenes	CsrS/CsrR	Negative regulation of hyaluronic acid production and several toxins	Bernish & Rijn, 1999; Engleberg *et al.*, 2001
Salmonella spp.	PhoQ/PhoP	Required for survival in macrophages	Groisman, 2001
Salmonella spp., Escherichia coli, Shigella spp.	EnvZ/OmpR	Outer membrane protein expression for nutrient acquisition	Bernardini *et al.*, 1989; Barrett & Hoch, 1998
Vibrio cholerae	ToxS/ToxR	Expression of virulence factors e.g. pili and toxins	DiRita, 1992

The prototypical TCS consists of a sensor histidine kinase (HK) that responds to a specific signal by modifying the phosphorylated state of its cognate response regulator (RR) (Fig. 5). First, upon the perception of environmental or intracellular signal, HK autophosphorylates (using ATP as the phosphate source) within a single, conserved histidine residue in the carboxyl-terminal region of receiver domain. Subsequently the phosphoryl group is transferred in a magnesium-dependent manner to an aspartate residue in the aminoterminal region of the partner RR protein. Phosphorylation of a RR changes the biochemical properties of its output domain, which can participate in DNA binding and transcriptional control, perform enzymatic activities, bind RNA, or engage in protein–protein interactions (Gao *et al.*, 2007; Stock *et al.*, 2000; Galperin *et al.*, 2001; Hoch, 1995,2000; Saito, 2001).

TCSs are built up from modular units: i) HK sensor domain; ii) HK kinase domain; iii) HK transmitter domain; iv) RR receiver domain; and v) RR binding DNA domain.

The signaling pathway also includes phosphatase activity that dephosphorylates the response regulator, returning it to a irresponsive state. The phosphatase activity may derive from the histidine kinase, the response regulator, or a separate protein.

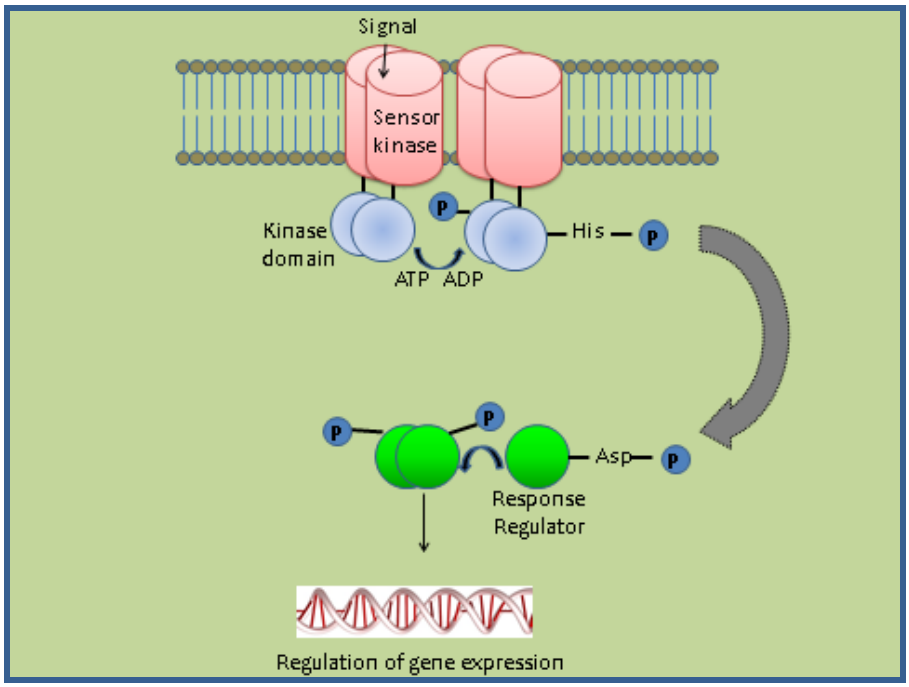

Fig. 5 A prototypical TCS signalling pathway.

4.1 Structural features

Biochemical activities and three dimensional structures are known for representatives of all conserved core domains of HKs and RRs, as well as for several variable input domains of HKs and for most of the subfamilies of output domains of RRs. Both proteins consist of (at least) two distinct domains (Mascher *et al.*, 2006).

4.1.1 Histidine kinases

Histidine kinases, that act as signal receptors, contain an N-terminal input domain and a C-terminal transmitter domain (Parkinson & Kofoid, 1992). They are typically built up of an extracellular sensing domain, two or more hydrophobic membrane-spanning segments (Stock *et at.*, 2000), and a transmitter domain localized within the cytoplasm (Fig. 6).

Some histidine kinase sensing proteins are phosphorylate in *trans*, with the kinase domain of one subunit catalysing the phosphorylation of its dimer partner (Cai *et al,.* 2003; Dutta *et at.*, 1999) while *cis*-autophosphorylation (one subunit phosphorylates itself) takes place in others (Casino *et al.*, 2010).

Due to the great number of stimuli that can be monitored by histidine kinase proteins, the regions involved in sensing show the greatest diversity within the family. Several conserved regions or boxes, used for identifying members of the histidine protein kinase superfamily, are located within the cytoplasmic domain (Grebe & Stock, 1999). Such conserved sequences extend for approximately 200 amino acid residues and are located at the C-terminal end of the protein. All histidine kinases share 20-30% sequence homology within this region (Hakenbeck & Stock, 1996).

Sensor domain of histidine kinase can be located in the cytosol, in the membrane, or in extracytosolic region. An extracytosolic sensor domain is flanked by two transmembrane (TMR1 and TMR2) helices with the N-terminus in the cytosol.

HKs also possess a dimerization domain which contains the phosphorylable histidine residue. The autophosphorylation is carried out in an ATP-dependent manner. Catalysis of the autophosphorylation reaction is facilitated by the ATP-binding domain, which contains conserved sequence motifs (N, D, F and G) (West & Stock, 2001).

The C-terminal cytoplasmic transmitter domain contains HAMP domain, also known as DHp (dimerization and histidine phosphotransfer) or HisKA domain. It is commonly found in Histidine kinases, Adenylyl cyclases, Methyl-accepting chemotaxis proteins, and Phosphatases (Aravind & Ponting ,1999), hence the name HAMP. This domain comprises a sequence with the conserved histidine residue for autophosphorylation (the H box). Activity depends on homodimer formation, with the dimerisation domains, which have two helices (referred to as Hα1 and Hα2) coming together to form a four-helix bundle.

HAMP domain is pursued by the catalytic domain (HATPase) contains the conserved N, D, F, and G boxes with the respective highly conserved amino acid residues. This domain catalyzes autophosphorylation of the HKs.

ATP-binding domain, often abbreviated as CA (for catalytic and ATP-binding properties), is located at the carboxyl terminus of the polypeptide and is required for kinase activity (Wolanin *et al.*, 2002). This domain binds ATP, which then donates its γ-phosphate group to the conserved histidine residue on the DHp domain. The

highly conserved N, D, F and G box sequence motifs of the CA domains are presumed to play crucial roles in substrate binding, catalysis and/or structure, and have also been used to classify the histidine kinases into functional subfamilies.

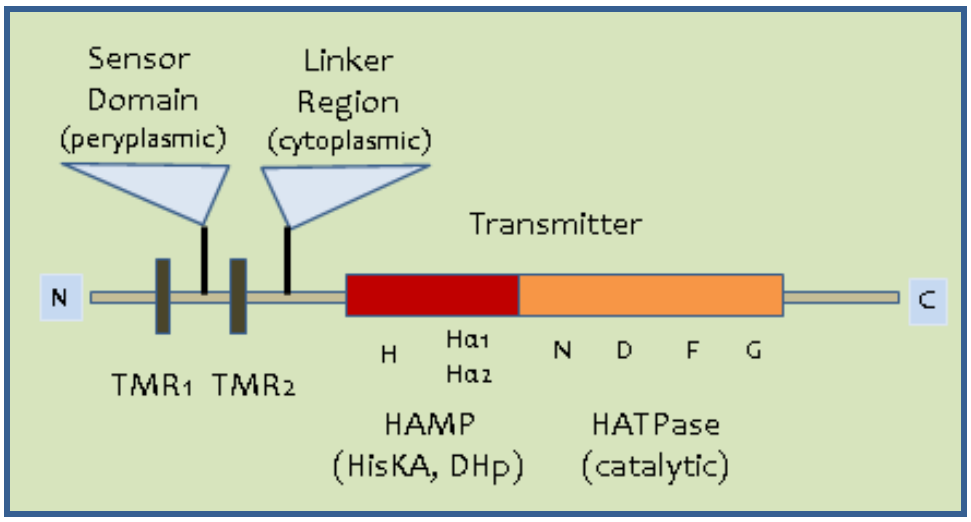

Fig. 6 Domains organization of histidine kinase (explanation in the text).

4.1.2 Response Regulators

The response regulator (RR) protein harbours the cellular output activity of the phosphorelay pathway. Response regulators contain typically two domains: an N-terminal receiver domain and a C-terminal output domain. The structures of receiver domains are well conserved with the sequence of approximately 125 amino acids (20-30% homology to other response regulators). Strongly conserved aspartic acid (Asp) residue at C-terminal domain accepts the phosphoryl group from the phosphorylated histidine kinase. In contrast, output domains show less conservation, especially at the sequence level, reflecting specificity and different affinity for promoters.

RR is a transcription factor that binds DNA. Phosphorylation of the RR receiver domain alters its affinity toward specific target proteins or DNA sequences and induces a conformational change (Lewis *et al.*, 1999), which consequently results in activation (Lange *et al.*, 1999) and/or repression of a given set of genes (Hakenbeck & Stock, 1996).

A significant fraction of RRs have effector domains as enzymes. Many others have effector domains for binding RNA, ligands, or proteins to regulate bacterial cellular process at post-transcriptional and post-translational levels. There are also single domain RRs that have only the receiver domains such as CheY and Spo0F (Galperin *et al.,* 2010).

4.2 TCSs as new drug targets

TCSs might be helpful to provide the basis for structure-based drug design. Many features make them attractive as a potential target for the development of novel antimicrobial agents.

Significant homology is shared among kinase and response regulator proteins of different bacteria (Parkinson *et al.,* 1992), which could facilitate the design of a broad-spectrum of antimicrobial drug. Similarily, regions unique to individual TCS could be targeted to produce drugs specific for a given bacterium.

Furthermore, since homologous systems have not been found in animals (Hilliard *et al.,* 1999), the drugs targeting TCSs may potentially have preferable selectivity.

Pathogenic bacteria use two-component signal transduction to regulate expression of essential virulence factors that are required to enter and survival inside the host (Dziejman & Mekalanos, 1995; Groisman & Heffron, 1995; Uhl & Miller, 1995). The inhibition of the expression of bacterial virulence factors offers an opportunity for specific intervention at the level of host invasion through biochemical processes, which are unique to the bacterial cell (Miller *et al.,* 1989).

Many TCSs play an important role in the emergence of antibiotic resistance or tolerance, and inhibition of these systems without killing the host cell may render the bacterium sensitive to antibiotics again.

Targeting the histidine kinases of two-component systems might allow the development of antibiotics with a new mode of action. Current bacterial genomics and proteomics will undoubtedly uncover further targets for related structure-based rational drug design.

Elucidated crystal structures of several RRs and HKs make it possible to carry out virtual screenings or can serve as a platform for rational design to improve the specificity of the lead compounds.

Additionally, with the increasing wealth of genome sequences available in public databases, it is now possible to identify most, if not all, TCS within an organism. Data gathered from mutagenesis research can be helpful to evaluate TCSs role in the viability and pathogenicity of the bacterium upon which framework for rational drug can be designed. This knowledge may be an adequate framework upon which rational-designed drug research and development projects could be built.

4.3 TCSs in *Mycobacterium tuberculosis*

Genomic analysis indicates that *Mtb* encodes eleven complete TCSs (Table 5), six orphan RRs, and two orphan HKs (Cole *et al.,* 1998; Tekaia *et al.,* 1999). The numbers are rather low compared with other bacteria, e.g. *E. coli*, which has more than thirty complete TCSs.

Several studies have analyzed the expression profiles during *Mtb* growth in human macrophages (Haydel & Clark-Curtiss, 2004; Zahrt & Deretic, 2001) and mice suggesting the biological role for these signal transduction systems in host-pathogens interactions.

Evidence suggests that many of the TCSs are engaged in sensing the host environment and adjusting bacterial transcription to adapt to the new environment, including PrrA (Ewann *et al.,* 2002), DosRST (Malhotra *et al.,* 2004; Roberts *et al.,* 2004), SenX3-RegX3 (Parish *et al.,* 2003), MprAB (Zahrt *et al.,* 2003), MtrAB (Fol *et al.,* 2006), and PhoPR (Perez *et al.,* 2001). The mutagenesis studies support the role of TCS in growth and survival (Sassetti *et al.,* 2001), indicating that the *senX3* , *kdpD* , and *mtrA* (Sassetti *et al.,* 2003a) gene products are required for survival in mice and that the response regulators PhoP, KdpE, PdtR, and MtrA, as well as the sensor kinases MprB, DevS, and Mtr B (Sassetti *et al.,* 2003b) are required for optimal growth *in vitro*.

Comparative genomic analyses of TCSs in *Mtb* indicate that homologues of these genes exist in other representative of *Mycobacterium* species, including *M. bovis, M*.

avium, *M. leprae*, and *M. smegmatis* (Cole *et al.,* 1998; Zahrt *et al.,* 2003). All of the paired TCSs found in *Mtb* are conserved in their genetic arrangement and location within the closely related *M. bovis* BCG vaccine strain. In contrast, only four TCSs are present and predicted to be functional in *M. leprae* (Bretl *et al.,* 2011).

Table 5 The TCSs identified in *Mtb* strain (Bretl *et al.,* 2011).

TCS (HK/RR)	ORF annotation	Regulation or effect of inactivation	Reference
SenX3/RegX3	Rv0490/Rv0491	Regulation of phosphate dependent gene expression	(Himpens *et al.,* 2000)
U/U/TcrA	Rv0600c/Rv0601c/ Rv0602c	Un-known	(Haydel & Clark-Curtiss, 2006)
PhoP/PhoR	Rv0757/Rv0758	Implication in regulating production of complex cell wall lipids	(Ludwiczak *et al.,* 2002; Zahrt & Deretic, 2001)
NarL/NarS	Rv0844c/Rv0845	Un-known	(Parish *et al.,* 2003)
PrrB/PrrA	Rv0902c/Rv0903c	Involvement in early intracellular multiplication during macrophage infection	(Ewann *et al.,* 2002, 2004)
MprA/MprB	Rv0981/Rv0982	Regulation of different genes engaged in physiology and pathogenesis	(Zahrt *et al.,* 2003)
KdpE/KdpD	Rv1027c/Rv1028c	Involvement in virulence	(Parish *et al.,* 2003)
TrcS/TrcR	Rv1032c/Rv1033c	Un-known	(Haydel *et al.,* 1999)
DevS/DevR (DosS/DosR)	Rv3132c/Rv3133c	Involvement in hypoxic adaptation	(Saini *et al.,* 2004)
MtrB/MtrA	Rv3245c/Rv3246c	Proliferation in macrophages; essential for *Mtb* viability	(Zahrt & Deretic, 2000)
TcrY/TcrX	Rv3764c/Rv3765c	Involvement in virulence	(Parish *et al.,* 2003)

5 DosR/DosS/DosT Two Component System

Dos (also known as Dev) TCS is composed of two soluble, full-length histidine kinases (HKs, DosS and DosT) and a single response regulator (RR, DosR). Dev TCS proteins were originally identified as DevR (Rv3133c) and DevS (Rv3132c) in a screen for genes **d**ifferentially **e**xpressed in the **v**irulent strain (dev) *M. tuberculosis* H37Rv compared to the avirulent H37Ra strain (Dasgupta *et al.,* 2000).

Subsequent studies demonstrated that Rv3133c was induced in the tubercle bacillus by hypoxia indicating that DevR is a key for adaptation of the bacillus to

nonreplicating survival in hypoxic environments. Therefore, the gene was named *dosR* as a regulator of **do**rmancy **s**urvival (dos) (Boon & Dick, 2012). Both gene designations remain in use today. In this study, the Dos nomenclature has been selected.

In *Mtb*, *dosR* and *dosS* are genetically linked and transcriptionally coupled with each other as well as with upstream *Rv3134c* gene forming operon *Rv3134c-devR-devS* that is transcribed from several promoters (Dasgupta *et al.,* 2000). In contrast, *dosT* does not belong to the core of DosRS operon and is located at the end of a highly induced cluster of genes regulated by DosR (Gerasimova *et al.,* 2011). While *dosR* and *dosS* are conserved and tandemly arranged in many mycobacterial species (except *M. leprae* and *M. ulcerans*), *dosT* appears to be less well conserved. DosS and DosT are capable of autophosphorylating at conserved histidine residues (DosS at His-395 and DosT at His-392), and both proteins can transfer the phosphomoiety to Asp-54 of DosR (Roupie *et al.,* 2007, Saini *et al.,* 2004a, 2004b).

DosRST upregulates a well-defined regulon of ~48 genes in *Mtb* following exposure to hypoxia, nitric oxide (NO), carbon monoxide (CO), and the cytochrome c reductant ascorbate (Boon & Dick, 2002; Honaker *et al.,* 2010; Kumar *et al.,* 2008, Taneja *et al.,* 2010; Voskuil *et al.,* 2003). The DosR regulon controls survival of the bacilli in an anaerobically-induced state of dormancy and is co-adjuvant in the transition of *Mtb* back to aerobic growth from an anaerobic or nitric oxide-induced nonrespiring state (Leistikow *et al.,* 2009; Rustad *et al.,* 2009).

It is believed that the study of the DosR–DosS signalling pathway will improve our understanding of the dormancy response in *M. tuberculosis*. DosRST two-component system has been proposed as an attractive target for the development of inhibitors against dormant organisms (Lamichhane, 2010; Murphy & Brown, 2007; Saini et al., 2004; Vohra, 2006.)

5.1 DosRST features

5.1.1 DosR response regulator

DosR response regulator controls dormancy adaptation in *Mtb*. Nearly all *Mtb* genes that are rapidly upregulated in response to low levels of oxygen and nitric oxide require DosR for their induction (Voskuil *et al.,* 2003; Park *et al.,* 2003).

DosR contains conserved amino acid residues that are implicated in its activation and that are also present in other TCSs RRs. These include: three aspartates Asp8 (D8), Asp9 (D9), Asp54 (D54), one Thr/Ser Thr82 (T82), one Tyr/Phe Tyr101 (Y101), and one Lys Lys104 (K104) (Dasgupta *et al.,* 2000; Saini et al., 2004; Wisedchaisri *et al.,* 2008). It has been demonstrated that the D8 and D9 residues together with D54, which likely form an acidic pocket (Stock *et al.,* 2000) and coordinate Mg_2^+, are functionally important for DosR phosphorylation (Saini *et al.,* 2004). The phosphorylation of D54 serves as a switch to activate DosR (Chauhan & Tyagi, 2008; Roberts *et al.,* 2004; Saini *et al.,* 2004; Wisedchaisri *et al.,* 2008).

DosR has been studied by many independent research groups and conflicting reports have been published concerning its role in *Mtb* virulence. Deletion of DosR was shown to have an increased (Parish *et al.,* 2003) or neutral effect (Rustad *et al.,* 2008) on *Mtb* virulence in mice infected with either wild type *Mtb* or a *dosR* deletion mutant. However, disruption of *dosR* was reported to increase the virulence of *Mtb* in mice (Parish *et al.,* 2003) but to lead to attenuation of *Mtb* virulence in guinea pigs (Malhotra *et al.,* 2004).

5.1.1.1 Structural insights

Crystal structure of unphosphorylated DosR has been solved (Wisedchaisri *et al.,* 2008) showing that full length DosR is composed of an N-terminal domain (receiver domain), a C-terminal domain (DNA-binding domain) and the linker region (Fig. 7). DosR belongs to the NarL subfamily of TCSs although this RR has some differential features when compared to the rest of proteins of the same family. The N-terminal domain of DosR lacks one α/β segment compared to the canonical (βα)5 arrangement. The C-terminal domain contains four α-helices named α7, α8, α9, and α10. This domain has an unusual conformation where the first α-helix in the N-

terminal domain packs against helix α10 which moves away from the core constructed by helices α7 to α9. The linker region consists of helices α5 and α6 with high flexibility of the second one.

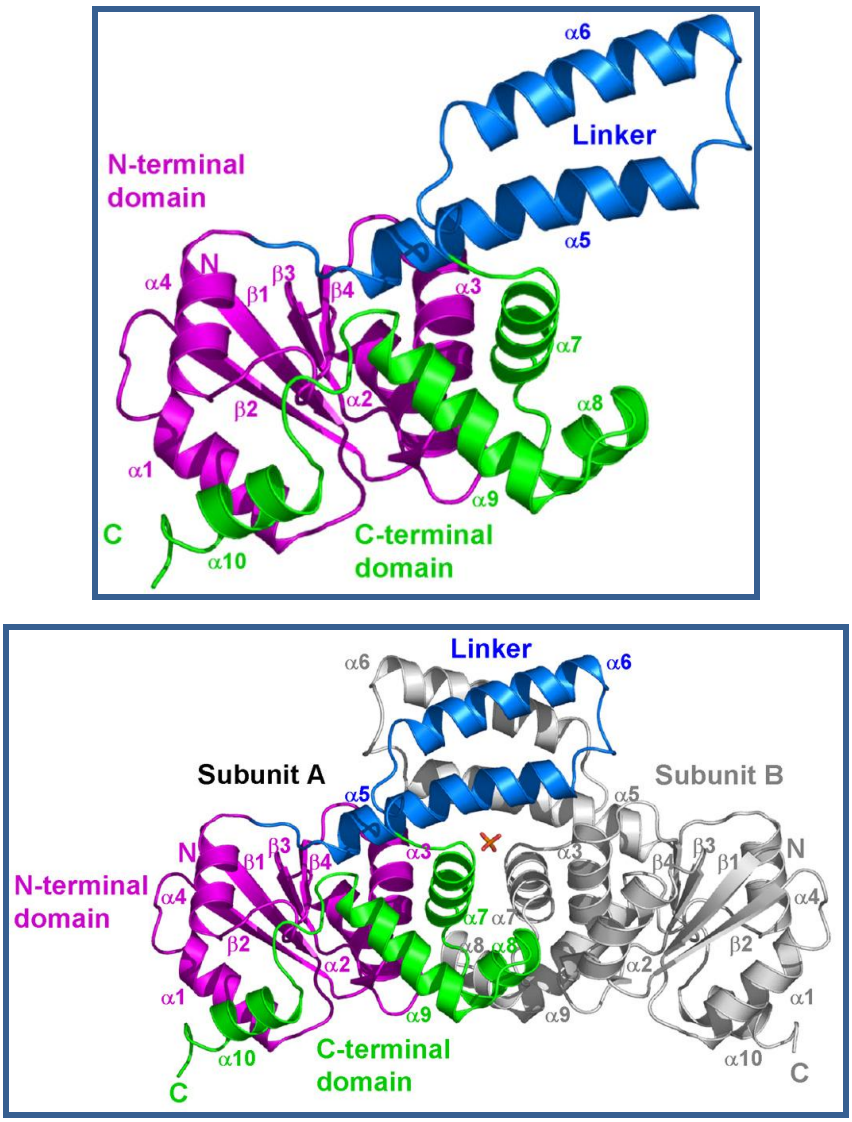

Fig. 7 Crystal structure of full-length DosR. The DosR monomer (above). The structure is shown in magenta for the N-terminal domain, blue for the linker, and green for the C-terminal DNA binding domain. The DosR dimer (below). Subunit A is shown as above. Subunit B is shown in gray.

The crystal structure of the C-terminus DosR (DosRC) in complex with DNA oligonucleotides has also been solved (Wisedchaisri *et al.*, 2005). In this structure, a DosRC dimer interacts with $G_4G_5G_6A_7C_8T_9$, a DNA motif present in each half of a palindromic consensus sequence (Fig. 8).

A helix rearrangement mechanism for DosR activation was proposed (Wisedchaisri et al., 2008). In this model, critical helix α10 is in dynamic equilibrium in the closed-inactive conformation, bound to the N-terminal regulatory domain, burying the key Asp54 residue, and in an open-inactive conformation, allowing Asp54 to be solvent-exposed part of the time and thus available for Asp phosphorylation by DosS or DosT. Upon activation by Asp54 phosphorylation, helix α10 provides the DosR dimerization interface in an open-active conformation for DNA binding.

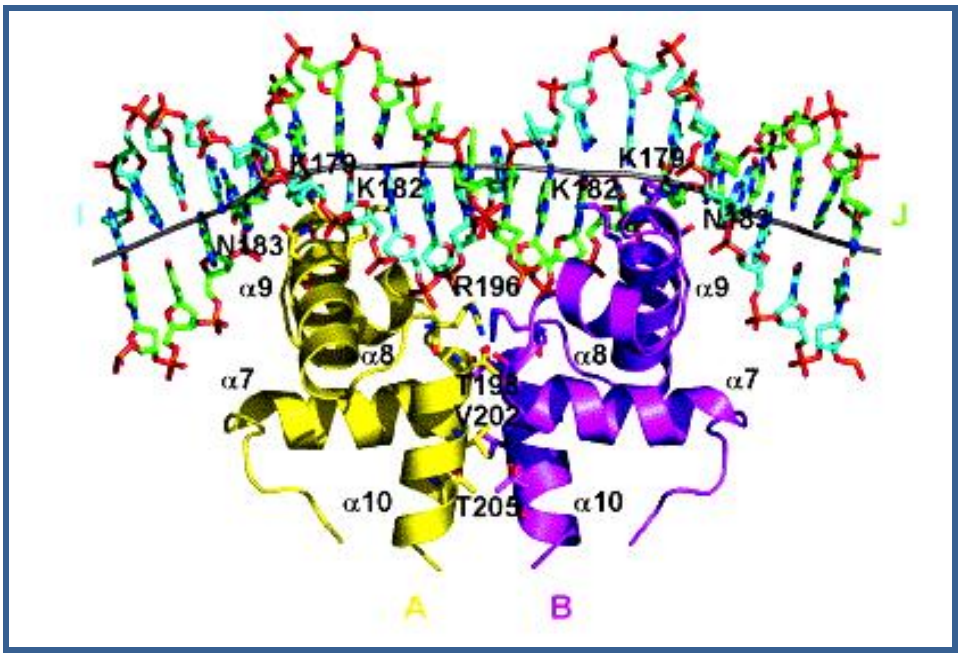

Fig. 8 Structure of the DosRC–DNA complex. DosRC uses the α10 helices to form a functional dimer for DNA binding. Arg196, Thr198, Val202, and Thr205 are residues contributing to this dimerization interface. The DNA clearly has a bent conformation, as shown by its helical axis in gray.

5.1.1.2 DosR regulon

In silico analysis of DosR regulon promoters revealed the presence of one or more copies of a consensus binding sequence located in the upstream promoter regions of target genes (Park *et al.,* 2003). It has been shown that phosphorylated DosR binds cooperatively to specific DNA sequences (Dos boxes) to activate target gene expression (Chauhan & Tyagi, 2008, 2009). The DosR regulon is composed of 48 coregulated genes that are involved in anaerobic respiration and metabolism, including genes involved in alternative electron transport pathways (*fdxA*), nitrate

metabolism (*narK2* and *narX*), and deoxynucleoside triphosphate (dNTP) synthesis under microaerophilic conditions (*nrdZ*) (Sherman *et al.,* 2001; Voskuil *et al.,* 2003). Furthermore, the *Rv3134c-dosR-dosS* operon is transcribed from multiple promoters and is autoregulated (Bagchi *et al.,* 2005). The protein alpha-crystallin (Acr) is repeatedly found to be upregulated in hypoxic conditions (Park *et al.,* 2003; Sardiwal *et al.,* 2005). *Acr* (*rv2031c*), also known as *hspX,* encodes a heat shock chaperon protein that is also a major cell wall-associated protein during stationary phase (Fig. 9). Further, *tgs1* is one of the most powerfully induced genes of the DosR regulon (Park *et al.,* 2003; Voskuil *et al.,* 2003), and it is divergently transcribed from *Rv3131. Tgs1* encodes a triacylglycerol synthase that synthesizes triacylglycerol, proposed to be an energy source during dormancy (Daniel *et al.,* 2004). Its disruption has been shown to prevent triacylglycerol accumulation under inducing conditions (Sirakova *et al.,* 2006). Rv3131 codes for a putative classical nitroreductase which may be involved in detoxification of nitrogen-containing by-products in the host (Purkayastha *et al.,* 2002).

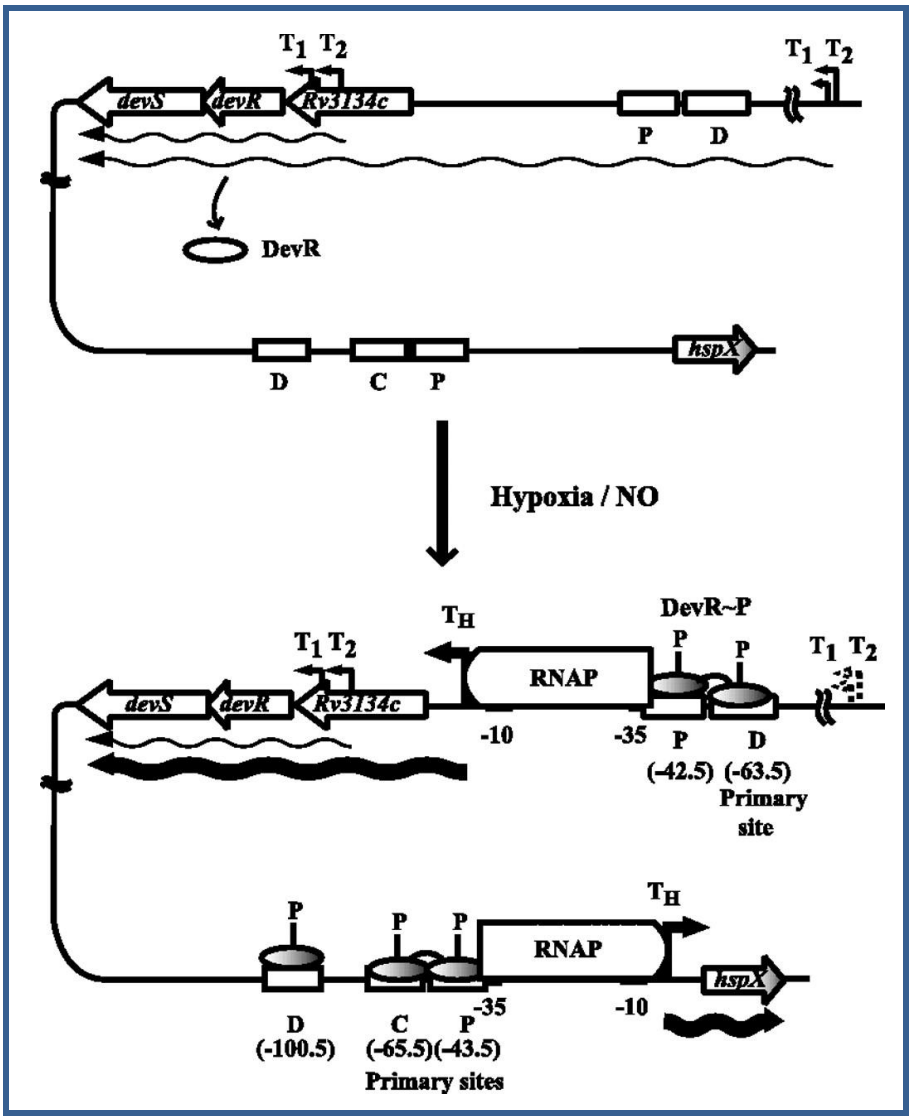

Fig. 9 Transcriptional regulation of *Rv3134c* and *hspX* promoters. (Top panel) Under normoxia, devRS operon is transcribed from aerobic promoters (thin wavy arrows) to provide basal levels of DevR and DevS. Unphosphorylated DevR does not bind or induce the operon or *hspX* gene. (Bottom panel) Upon induction, DevR~P species is generated. It binds first to the D site and cooperatively recruits another DevR~P molecule to the P site to induce the operon (thick wavy line). At the *hspX* promoter, DevR~P binds first with the P and C sites and then with the D site to induce its transcription. At both promoters, DevR~P binds to the P site overlapping the -35 promoter element and also to one or two additional upstream sites. The oligomeric status (monomer or dimer) of free and DNA-bound DevR is not known and, for simplicity, DevR is represented as an oval (white for unphosphorylated and shaded for phosphorylated) (Chauhan & Tyagi, 2008).

5.1.2 Histidine kinases DosS and DosT

DosS and DosT show high sequence similarity with each other (62.5% sequence identity in the full length protein). The N-terminal sensory domains of DosS and

DosT contain two tandem GAF domains, which are regulatory domains originally named for their association with c**G**MP-regulated cyclic nucleotide phosphodiesterases, **a**denylate cyclases, and the bacterial transcriptional regulator **F**hlA. C-terminal domains consist of histidine kinase domain (belonging to HisKA_3 family) and ATP-binding domain. The first GAF domain binds heme and acts as a gas sensor (Sardiwal *et al.,* 2005; Ioanoviciu *et al.,* 2007; Sousa *et al.,* 2007; Kumar *et al.,* 2007), while the function of the second GAF domain remains to be revealed (Sardiwal *et al.,* 2005).

Structural and biochemical analyses have provided important insights into the nature of gas ligand binding by histidine kinases DosS and DosT (Cho *et al.,* 2008, 2009; Ioanoviciu *et al.,* 2007, 2009; Kim *et al.,* 2010; Kumar *et al.,* 2007; Lee *et al.,* 2008; Podust *et al.,* 2008; Sardiwal *et al.,* 2005; Sousa *et al.,* 2007; Voskuil *et al.,* 2003; Yukl *et al.,* 2007, 2008, 2011). Two independent reports proposed a model for DosS/T signaling wherein DosS is a redox sensor and DosT is a hypoxia sensor (Cho *et al.,* 2009; Kumar *et al.,* 2007). It has been suggested that DosT is inactive when bound to oxygen under normoxic conditions (Fig. 10). However, during hypoxia, CO and NO may displace O2 in DosT, restoring its active form. Similar gas binding can also be attributed to DosS. O2 can oxidize the heme group and inhibit DosS. The oxidative form Fe^{3+}DosS does not autophosphorylate, while the reduce Fe^{2+}DosS does (Cho *et al.,* 2009). Furthermore, NO binds heme but inhibits DosS approximately 50-fold less than oxygen (Dunham *et al.,* 2003; Tuckerman *et al.,* 2002). Likewise, it was demonstrated that flavin nucleotides are capable of reducing the heme ion of DosS.

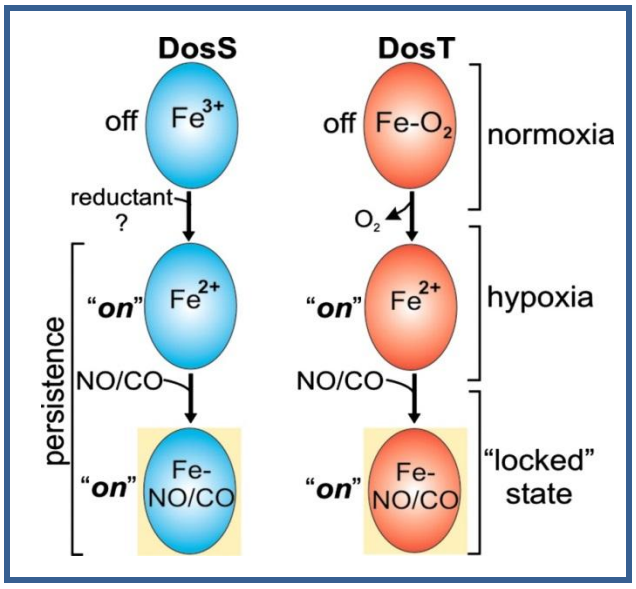

Fig. 10 Proposed mechanism for the role of *Mtb* DosS and DosT in the shift down of tubercle bacilli to the persistent state. The sense-and-lock model proposes that during disease progression hypoxia NO and CO are being sensed, independently or in conjunction, to induce the persistent state. Hypoxia, NO, and CO induce reductases to generate active ferrous DosS, whereas deoxygenation generates active ferrous DosT. Both ferrous DosS and DosT is now capable of binding NO and CO to generate NO–DosS, CO–DosS, NO–DosT, and CO–DosT, which keep the Dos regulon in a locked (active) state (Kumar *et al.,* 2007).

Few studies have focused on the biological relevance of DosT and DosS and their roles in adaptation to hypoxia and anaerobic conditions. It has been shown that after two hours under 0.2% oxygen conditions, *dosT* and *dosS* single mutants are only able to induce DosR regulon expression at 40 to 45% of normal levels, and bacteria that lack both sensors are completely unable to induce the expression of DosR-regulated genes (Roberts *et al.,* 2004). Another study reported that the *dosS* deletion mutant had no apparent effect on *acr* (a member of the DosR regulon) induction in an overnight settled culture model or after two hours in 0.2% oxygen (Sherman *et al.,* 2001). A study that used the Wayne model indicated that the *dosS* mutant had a 15-fold decrease in survival by day 40 (Boon & Dick, 2002). The *dosS* mutant, at day 5 of the model, maintains protein expression levels of DosR regulon proteins, indicating that at this time point in this particular model, DosT is able by itself to induce the expression of the DosR regulon. Another research showed that only versions of DosT and DosS lacking heme (by deletion of their N-terminal region

or treatment with denaturants) can phosphorylate themselves or DosR *in vitro* (Roberts *et al.*, 2004; Saini *et al.*, 2004a,b).

The three dimensional structures of GAF-A and GAF-B from DosT have been determined (Podust *et al.*, 2008). The heme is embedded into the GAF-A domain, which is composed of five strand anti-parallel β-sheet and four α-helices. The heme is positioned nearly perpendicular to the β-sheet (Fig. 11).

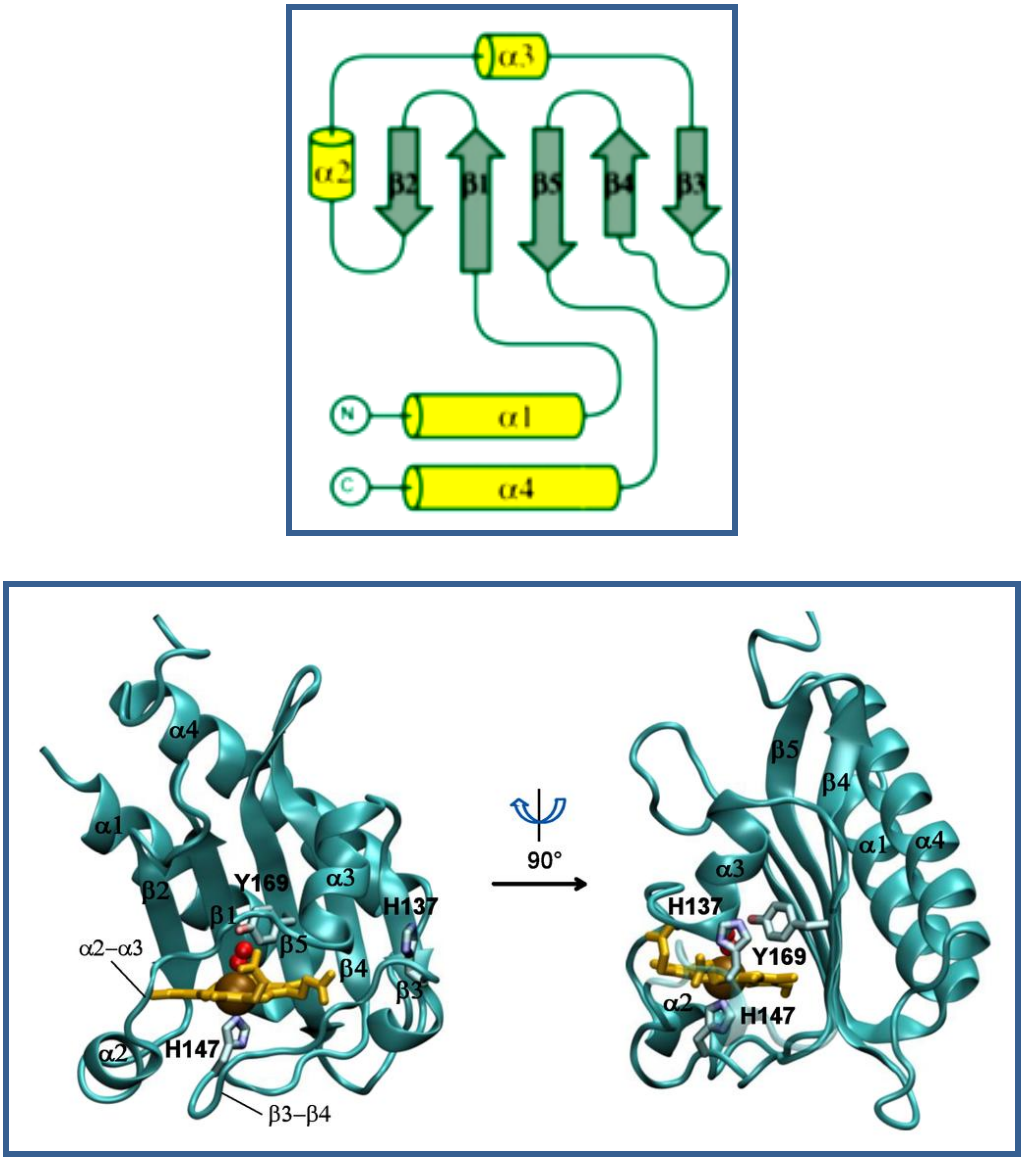

Fig. 11 Overall structure of GAF DosT. Topology diagram of GAF DosT is shown above. Below, ribbon representation of the two orthogonal views of GAF DosT. The O2 ligand is represented by red spheres, and the heme (orange), and H137, H147, and Y169 are shown as sticks.

6 Drug discovery & development pipeline

Before any potential new medicine can be discovered, the first step is to gather the knowledge about the disease to be treated. The key points are to understand how the genes are altered, how that affects the proteins they encode and how those proteins interact with each other in living cells, how those affected cells change the specific tissue they are in and finally how the disease affects the entire patient.

Target drug discovery focuses on evaluating a disease hypothesis through the process of discovery and clinical testing of a molecule designed to interact with a specific target believed to be involved in the disease pathogenesis.

With the sequencing of the human genome (Hopkins & Groom, 2002), the emergence of system biology and the development of many high throughput technologies, target-based drug discovery has emerged as the primary strategy of many pharmaceutical companies during past 20 years. This approach has advanced thanks to the development of computational and informatics tools that aid scientists in the design, selection and optimization of molecules for specific medications. Target selection is a critical task, sub-optimal target selection has become a very common cause of failure in the clinics. A multifactorial disease cannot be efficiently approached by a target located downstream or an up-stream target can fail if there is an efficient alternative pathway. System biology and its associated simulation technologies used to be on the basis of a right target selection.

Pharmaceutical research and development (R&D) of a drug consists of several stages (Fig. 12). It begins with drug discovery followed by preclinical drug development where thousands of candidate chemicals maybe screened for attractive therapeutic, pharmacological, and toxicity properties (Rowberg, 2001).

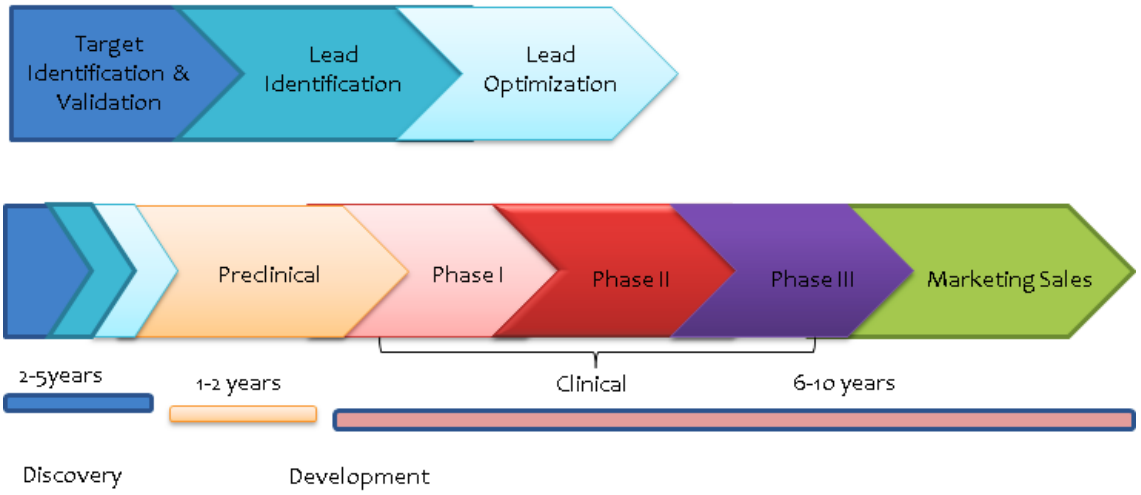

Fig. 12 Stages in the drug discovery and development (R&D) process.

6.1 Drug discovery

Typically, at this stage, chemical compounds, either naturally occurring or synthetic, are investigated for their potential to bind to and modify molecular targets (Rowberg, 2001). The sections in this chapter refer only to the drug discovery process of low-molecular weight chemical molecules, omitting different types of drugs, such as biological, cellular and gene-derived.

6.1.1 Target identification and validation

Drug discovery usually begins with the identification of potential drug targets, whose action or absence of actions result in a disease condition (Aldridge, 1998). For this purpose, it is important to understand how the disease occurs at the molecular, cellular and genetic levels. The actual process of drug discovery is characterized by a search for molecules that can bind to targets and result in an action that produces a therapeutic result. Presently, high-throughput screening is used to test a wide range of potential targets against thousands of diverse chemical compounds. This leads to the identification of promising lead compounds which interact with the target and show the potential to either neutralize or slow the disease process. The alternative method of rational drug design involves the design and synthesis of compounds based on the known structure of either a specific

target (target based drug design) or one of its natural ligands (ligand based drug design).

6.1.2 Hit identification

There are few important features to validate before the molecule could be considered for drug development: i) target selectivity, to ensure that it only or mainly acts on the disease protein; ii) target toxicity; and iii) target distribution in the body in a way that ensures it reaches the disease site.

Pharmaceutical companies, especially the "big pharma", have large small molecule compound libraries, which can include Food and Drug Administration (FDA) approved drugs, non FDA-approved drug candidates with known activity from previous screenings and compounds with unknown activity. One of the most important challenges at this point is to reduce the number of compounds to test, as chemical libraries can be very large (10,000-2,000,000 compounds) and testing is expensive but maintaining the maximal chemical diversity. Computational chemistry first helps to inform small molecule library classification and activity prediction.

6.1.3 Lead identification: hit to lead (H2L) phase

A successful hit identification phase usually yields several hit compounds (i.e. 10-200) with relatively weak affinities for the target. They can be promiscuous, but, definitively, they can add chemical diversity to the discovery process. Those hit compounds with an affordable chemistry can be selected to generate a number of independent chemical series of analogues. The aim is to obtain derived lead compounds with a higher affinity (potency) for the target and a reasonable degree of selectivity versus off-targets. In addition, *in vitro* metabolic and PK predictive tests (i.e. PAMPA, CACO, etc) are run at this stage to predict and subsequently discard those chemical structures with poor *in vivo* performance.

6.1.4 Lead optimization

This phase involves rigorous testing and optimization of the selected compounds to identify the candidate drug/s to development. This phase starts with some (i.e. 2-20) lead compounds and yield a few number of candidates to enter in the regulatory phase. Compound optimization mostly includes *in vivo* data in one or more animal species.

In vivo assays include animal models of disease as well as side effects/safety models and models of drug disposition (Absorption, Distribution, Metabolism, Excretion and Toxicity–ADMET). Candidate identification stage is required to study many processes, including metabolism, absorption into tissues and passage from the tissues back into circulation, excretion through the kidneys and liver, and, for volatile agents, exhaled from the lungs. Ideally, the dynamic kinetics of drug exposure will correlate with the appearance and decay of efficacy (pharmacodynamics) and toxicity (toxicokinetics). This information can guide drug dose schedules (Rydzewski, 2008).

6.2 Preclinical studies

Once promising drug candidates have been identified, they enter the preclinical research stage, starting the so called 'preclinical regulatory phase'. Usually this means to start the relationship with the Regulatory Agencies asking for a Scientific Advice (i.e. FDA Pre-IND meeting) to agree the development plan. The candidates undergo laboratory and animal testing focusing on the pharmacological aspects of drug development. During this phase, the pharmacological concerns of toxicity, bioavailability and efficacy are investigated (Aldridge, 1998). Safety testing takes place in animals that are administered increasing doses to look for onset of toxicity. Another feature of this stage is to determine the best method of delivery (e.g., oral, intravenous, etc.). Other tests include determining a drug candidate's shelf lifetime and shipping durability.

6.3 Clinical Drug development

Clinical trials, which constitute the most time consuming and costly portion of drug development, consist of three phases, each more complex than the preceding. Before clinical trials can begin, the sponsoring pharmaceutical company must have approval from the Regulatory Agencies involved about trial protocols.

In the clinic, there is a sequential evaluation in healthy human volunteers of tolerability, efficacy and dose range in patients, followed by widespread trials in thousands of appropriate patients to develop a broad database of efficacy and safety. New therapies typically enter the clinic through Phase I trials, which are often followed by subsequent phases. However, both the European Medicines Agency (EMA) and the US Food and Drug Administration (FDA) allow the Phase 0 trials which may enhance Phase I. Phase 0 trials will study the distribution of the drug in the human body with the usage of applications such as PET imaging, using very small non-therapeutic doses that are tagged with radiolabels.

6.3.1 Phase I

Phase I trials establish the safety of a compound; identify its behaviour and possible side effects. Further goal at this stage is to establish a dose range where the compound is safe. This is determined by testing a range of doses. Study participants initially receive a low dose of the drug; this is gradually increased as long as the drug appears to be safe. The participants in this study are healthy volunteers (rather than people who have the target disease), and they usually number between 10 and 100. Typically, a phase I trial will last about 1.5 year and cost about $10 million (Zivan, 2000).

6.3.2 Phase II

The goal of this phase is to obtain preliminary data on the effectiveness (also known as efficacy) of the test drug. The phase II trials determine the parameters for the final test (phase III trials). These parameters, among others, are the class (e.g., age, gender) and condition of the patients to include in the trial, what end points to measure, and what constitutes an effective dose (dose-range studies) and duration

of treatment. End points are those conditions that yield an unambiguous indication of the drug's success or failure. Phase II involves the use of a control group, a test group of patients to whom a placebo or another drug is given, which allows the clearest means of proving whether the drug is successful and of determining its side effects. At this point affected patients are tested in relatively small number (100 to 300 participants). They are usually randomised, double-blind studies to ensure objectivity. Typically, phase II lasts about two years, and cost about $20 million.

6.3.3 Phase III

The goal of the phase III trial is authoritative demonstration of a drug's effectiveness as defined by the end points determined in the phase II trials. Phase III seeks definitive proof of a molecule's efficacy and safety profile in a large number of patients who have the disease (from several hundred to several thousand). This extensive data provides a basis for extrapolating results to the general population and for the labelling information that will be provided with the product. In Phase III studies, the new drug is often compared to current standard therapy. Phase III trials may take several years.

During the clinical trials, companies are required to follow certain standards and procedures, like the informed consent by the particpants, to ensure good clinical practice.

6.3.4 Regulatory review and approval

At this stage, applications with all the necessary information, including quality, preclinical and clinical data collected during development of the product, are submitted to the relevant regulatory authorities in order to obtain approval to market the drug in their jurisdictions [e.g., a New Drug Application (NDA) in the US, and a Marketing Authorisation Application (MAA) in the EU].

Figure 13 (Fig. 13) gives an overview of this regulatory review and approval process. The red arrows refer to variations on the approval route that may be used when there is an identified unmet medical need or there is pressure to allow the drug for

use, even while it is being studied. These variations have specific requirements and are only applicable in limited situations.

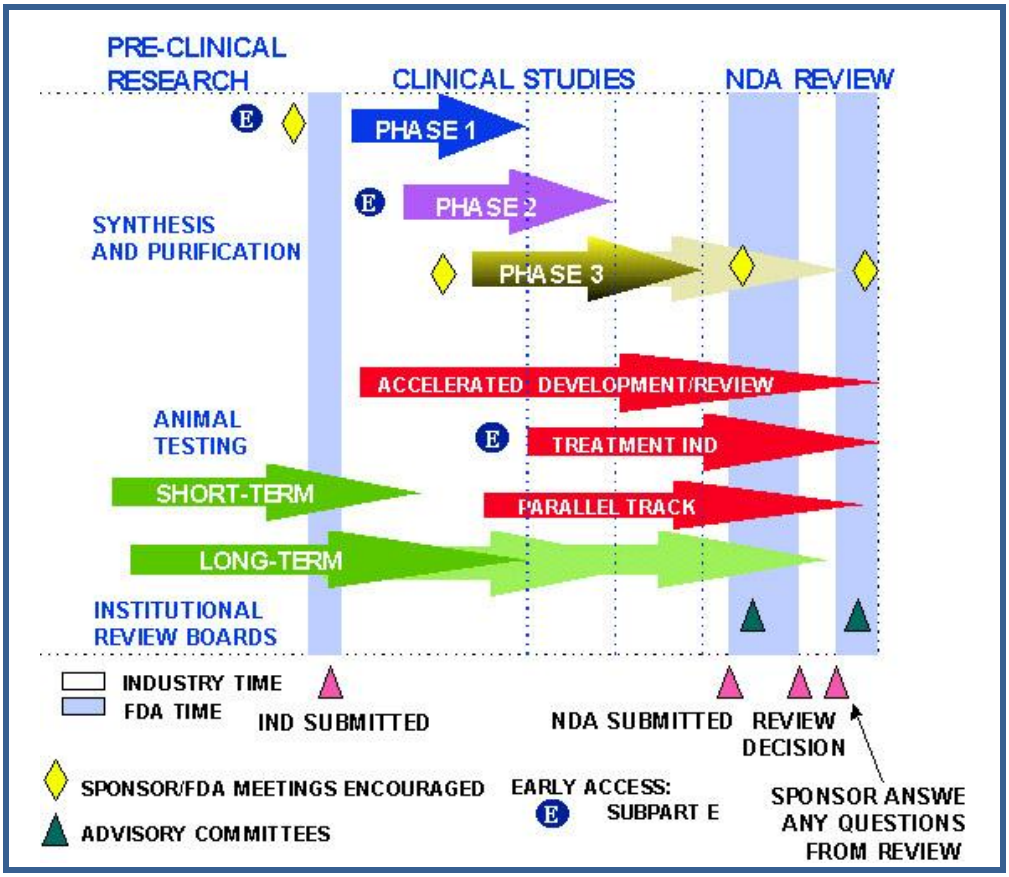

Fig. 13 Regulatory review and approval process. (Extracted from: http://www.fda.gov/cder/handbook/develop.htm)

6.3.5 Marketing

The last phase in the drug development process is the marketing or commercialization of the drug once it has been approved. The drug manufacturer must submit marketing authorization applications in every country or territory where it wants to sell the drug.

6.3.6 Life cycle management

Once the trials are completed, the treatment can be approved for general use. If approval is granted, post-marketing surveillance is carried out to monitor the drug for additional safety concerns that may not have appeared during the preapproval

clinical trials. These studies occur as post-marketing Phase IV trials. Examples are the safety and efficacy of varying doses, how the drug interacts with other drugs, or how it works in people with other diseases. Phase IV trials may include small or large numbers of subjects and may reveal uncommon side effects that are too rare to show up in Phase II or III studies.

6.4 Drug discovery and development cost

According to the Pharmaceutical Research and Manufacturers of America (PhRMA), it takes 10-17 years (Fig. 14) from disclosure to the approved medication at an average investment of $1.3- $1.7 billion (Fig. 15), where clinical trials consume the major share of the costs. Historical data, although figures are quickly evolving, point out that for every 5,000 – 10,000 potential drugs that are initially tested in an animal model of disease only 250 will progress to pre-clinical development. Of these 5 will move forward into first-in-man studies (Phase I) of which only a single compound will achieve regulatory approval (www.fda.gov).

Funding for a trial can come from various sources, with the majority sponsored by pharmaceutical companies. In addition, public funds, like the National Institutes of Health or the European Framework Programmes, venture capital, venture philanthropy, NGOs. Investigators may also receive research money from the public, from industry and from other private sources.

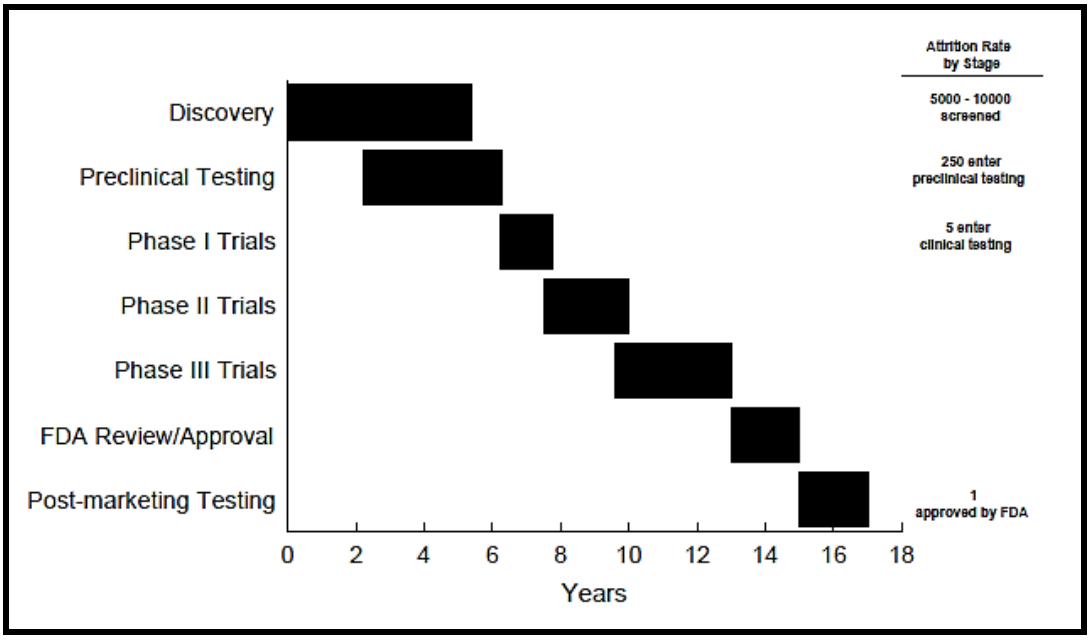

Fig. 14 Drug Development Time and Attrition Rate. Adapted from the Pharmaceutical Research and Manufacturers of America (PhRMA) 2000 Industry Profile.

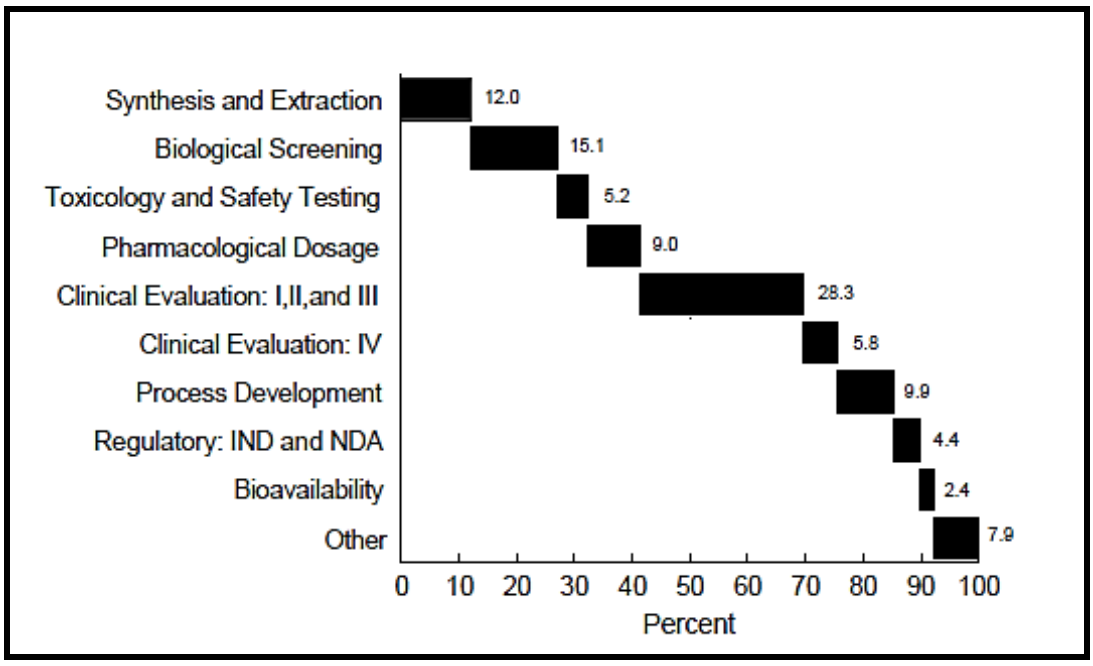

Fig. 15 R&D Cost allocations by stage, PhRMA.

OBJECTIVES

This work has two main objectives:

1. The structural and functional characterization of the DosRST two-component system with a focus on: i) the relay of phosphate groups from DosS and DosT histidine kinases to DosR response regulator; and ii) the activation of DosR as specific DNA binding protein.

Its specific objectives are:

- to clone, express and purify wild-type and mutant forms of DosR, DosS and DosT
- to solve the structure of active wild-type and mutant versions of DosR using X-ray crystallography
- to *in silico* model DosS-DosR interface, analyse the key residues implicated in HK-RR interaction and to quantify this interaction by isothermal calorimetry
- to check the autophosphorylation of DosS and DosT
- to investigate the capability of histidine kinase DosS and DosT to phosphorylate wild-type DosR and its mutant versions
- to analyse potential DosS phosphatase activity on DosR~P
- to evaluate the role of key residues of DosR in its activation and in DNA binding efficiency

2. The initiation of a structural-based discovery programme of inhibitors of DosR response regulator.

Its specific objectives are:

- to select a set of structurally diverse inhibitors of DosR based on the initial work described by Gupta *et al* (Gupta *et al.*, 2009)
- to test and implement *in vitro* assays for the analysis of the inhibitor-protein target interaction
- to analyse the activity and spectrum of the potential inhibitors of DosR through whole-cell growth inhibition assays with a set of bacterial species
- to check the selectivity of the DosR inhibitors using *in vitro* cellular assays with eukaryotic cell lines

MATERIALS & METHODS

1. Materials

1.1 Bacterial strains

Species	Strain	Purpose	Reference/source
E. coli	DH5α	Cloning	Novagen-Merck
E. coli	BL21-CodonPlus(DE3)-RIL (RIL)	Protein expression	Stratagene
E. coli	BL21 (DE3)	Protein expression	Gibco
E. coli	Rosetta (DE3)	Protein expression	Novagen-Merck
K. pneumoniae	Trevisan	Antimicrobial activity	ATCC®
E. coli	Castellani and Chalmers (Trevisan 1889)	Antimicrobial activity	ATCC®
M. smegmatis	Lehmann and Neumann 1899	Antimicrobial activity	DSMZ, Germany

1.2 Eukaryotic cell lines

Cellular line	Cell type	Purpose	Reference/source
HepG2	Human hepatocytes	Compounds selectivity	ATCC®
CHO-K1	Chinese hamster ovary cells	Compounds selectivity	ATCC®

1.3 Cloning vectors, genomic DNA and constructed plasmids

Name	Purpose	Reference/source
pET21d(+)	Cloning	Novagen-Merck
pPEU7	Cloning	IRB Barcelona
Mycobacterium tuberculosis H37Ra genomic DNA	Template for DosR, DosS and DosT cloning	ATCC®
DosR- pET21d(+)	Protein expression	This study
DosS- pET21d(+)	Protein expression	This study
DosT- pET21d(+)	Protein expression	This study
$DosS_{350-578}$ - pPEU7	Protein expression	This study
$DosS_{380-578}$ - pPEU7	Protein expression	This study
$DosT_{349-573}$ - pPEU7	Protein expression	This study
$DosT_{380-573}$ -pPEU7	Protein expression	This study

1.4 Oligonucleotides

The oligonucleotides used in this work were purchased from Sigma-Aldrich and are listed in the table below. The oligonucleotides' sequence is depicted and the restriction sites used for cloning are underlined. The codons used to generate mutant proteins are in bold in their corresponding oligonucleotides.

Fw-forward primer, Rv-reverse primer.

Table 6 Oligonucleotides used In this study.

Name	Sequence 5´-3´	Purpose	Reference
DosR Fw	CTGCCATGGTAAAGGTCTTCTTGGTCGATGAC	DosR full lenght amplification	Roberts *et al.,* 2004
DosR Rv	AATACTCGAGTGGTCCATCACCGGGTG	DosR full lenght amplification	Roberts *et al.,* 2004
DosS Fw	TGTCCATGGCTCACCACCACCACCACCACATGA CAACAGGGGGCCTCG	DosS full lenght amplification	This study
DosS Rv	TCTGGATCCCTACTGCGACAACGGTGCTGAC	DosS full lenght amplification	This study
DosT Fw	ATTAGCTAGCGTGACACACCCTGACAGGGCG	DosT full lenght amplification	This study
DosT Rv	AATACTCGAGTGCGCAGCGGTGCAGACCA	DosT full lenght amplification	This study
$DosS_{350-578}$ Fw	AAGTTCTGTTTCAGGGCCCGGACGAACAACTC GAGATGATG	DosS 350-578aa fragment amplification	This study
$DosS_{380-578}$ Rv	AAGTTCTGTTTCAGGGCCCGGAACTCGACGTA CTGACCGAC	DosS 380-578aa fragment amplification	This study
$DosT_{349-573}$ Fw	AAGTTCTGTTTCAGGGCCCGGACAAACAGCTC GATATGATGGC	DosT 349-573aa fragment amplification	This study
$DosT_{380-573}$ Fw	AAGTTCTGTTTCAGGGCCCGATCCTGACCGATC GCGACCG	DosT 380-573aa fragment amplification	This study
DosR D54A-Fw	CAGATGTCGCGGTGCTG**GCA**GTCCGGTTGC	DosR mutagenesis	This study
DosR D54A-Rv	GCAACCGGAC**TGC**CAGCACCGCATCTG	DosR mutagenesis	This study
DosR [T198A, T205A]-Fw	GAACGTCGG**GCG**CAAGCCGCGGTATTCGCG**G CG**GAGTTGAAGC	DosR mutagenesis	This study
DosR [T198A, T205A]-Rv	GCTTCAACT**CCG**CCGCGAATACCGCGGCTTG**C GC**CCGACGTTC	DosR mutagenesis	This study
DosR [T198D, T205D]-Fw	GAACGTCGG**GAT**CAAGCCGCGGTATTCGCG**GA T**GAGTTGAAGC	DosR mutagenesis	This study
DosR [T198D, T205D]-Rv	GCTTCAACTC**ATC**CGCGAATACCGCGGCTTG**AT C**CCGACGTTC	DosR mutagenesis	This study
DosR [T198E, T205E]-Fw	GAACGTCGG**GAG**CAAGCCGCGGTATTCGCG**G AG**GAGTTGAAGC	DosR mutagenesis	Chao *et al.,* 2010
DosR [T198E,	GCTTCAACTC**CTC**CGCGAATACCGCGGCTTG**CT**	DosR mutagenesis	Chao *et al.,*

T205E]-Rv	**C**CCGACGTTC		2010
EMSA-Fw	GGCCCGCGCT*TTGGGGACTAAAGTCCCTAA*CC CTGGCCACG	EMSA	Wisedchaisri *et al.,* 2005
EMSA-Rv	CGTGGCCAGGG*TTAGGGACTTTAGTCCCCAA*A GCGCGGGCC	EMSA	Wisedchaisri *et al.,* 2005

1.5 Chemicals

Acetate kinase	Sigma
Acetyl phosphate	Sigma
Acetonitrile	Merck
Acrylamide	Bio-Rad, Sigma
ADP	Sigma
Ammonium persulfate	BioRad
AMPPNP	Jena Bioscience
ATP	Roche
Bacto^{TM} Agar	Panreac
Beryllium sulfate tetrahydrate	Sigma
Bio-Safe Coomasie Stain	BioRad
Boric acid	Panreac
Bovine serum albumin (BSA)	Sigma
Bromophenol blue	BioRad
BugBuster Ni-NTA His Bind Purification Kit	Novagen-Merck
Carbamoyl phosphate disodium	Sigma
Coomassie brilliant blue G250	Pierce, Fluka
Coomassie brilliant blue R-250	Bio-Rad
Desthibiotin	Sigma
DNA ladder 100bp	Biolabs
DTT	Boehringer
EDTA	Fluka
Ethidium bromide	Boehringer
Glicerol	Merck
HEPES	Sigma
Imidazole	Sigma
Iodoacetamide (IAA)	Sigma
IPTG	Sigma
Lambda DNA/HindIII Marker	Promega
Lysozyme from hen egg white	Fluka
Matrices for MALDI analysis	Bruker Daltonics
Mercaptoethanol	Bio-Rad
MES potassium salt	Sigma
MgSO4	New England
Phenylmethanesulfonyl fluoride (PMSF)	Sigma
Polid(I)d(C)	Sigma

Precision Plus Protein® Dual Color Standards	BioRad
Protamine sulfate	Sigma
PureYield Plasmid Midiprep and Miniprep systems	Promega
Red Safe, Nucleic Acid Staining Solution	iNtRON Biotechnology
Restriction enzymes	Promega
SYBR Safe DNA gel stain	Invitrogen S. A.
T4 ligase	Novagen-Merck
T7 promotor and terminator primers	Novagen-Merck
TEMED	BioRad
Tris(2-carboxyethyl)phosphine hydrochloride	Sigma
Trypsin	Sigma
UREA	Merck
ZipTip C18	Millipore

1.6 Laboratory equipment

ÄKTA FPLC	Amersham
Fractions collector	Amersham
Laboratory balances	Mettler
	COBOS
	VULCANO
Autoclave	Selecta
Scales	Labclinic
Centrifuge	
RC5C, Tubs Corex	Du PONT
Eppendorf 5810R, 5415 d	Eppendorf
SIGMA 1-14	Sigma
SIGMA 3-16K	Sigma
Centrifuges rotor GSA, SS34	DU PONT
Column FF His·trap	VWR INTERNATIONAL EUROLAB
Column Strep·trap	GE Healthcare
Columns Superdex 75, 200	GE Healthcare
Dry bath TB15105	Fisher Scientifics
Electroporator	Eppendorf
Freezer	
-80°C	JOUAN
-20°C	ZANUSSI
Fridge	WHIRPOOL
	Zanussi
French Press Cell Disrupter	Constant Systems Ltd
Gel electrophoresis equipment	Bio-Rad
	Ecogen
Incubator	Selecta
	Barnstead international
	INNOVA
iTC200 microcalorimeter	Microcal

Laminar cabin AV100, BV100	TELSTAR
PCR PTC-200 Peltier Thermal Cycler	MJ Research
PCR System, 7500 Fast Real-Time	Applied Biosystems
Pipettes	GILSON
pH meter	CRISON
Shaker	Selecta
Spectrophotometer	Thermo Scientific
NanoDrop™ 1000	Thermo Scientific
Sonicator	BRANSON
Thermocycler PTC-150, PTC-200	MJ research
Transilluminator	UVP
UV lamp	Grogen
Vortex REAX , REAX 2000, REAX control	Heidolph
Water bath	Huber
	COLORA
	Selecta

1.7 Growth media

Antibiotics were purchased from Sigma-Aldrich. Ampicilin (Amp) stock solutions (100 mg/ml) were prepared in distilled sterile water, and filtered with 0.2 μm syringe filters. Chloramphenicol (Chl) solution (34 mg/ml) was prepared in ethanol sterilely.

LB broth (Luria-Betrani)

10 g/L bacto-tryptone

5 g/L bacto-yeast extract

10 g/L NaCl pH 7.2

LB was used to grow *E. coli* cells in the presence of the appropriate antibiotic. To prepare solid medium, 15 g/L bacto agar was added to LB and poured on Petri dishes.

Nutrient broth medium

5 g/L peptone

3 g/L meat extract

Nutrient broth medium was used to grow *Mycobacterium smegmatis* for antimicrobial activity assays.

Müeller-Hinton broth (MHB)

2 g/L beef extract

17.5 g/L acid hydrolysate of casein

1.5 g/L starch

pH 7.3

Müeller-Hinton medium was used as medium for *E.coli* and *K. pneumoniae* growth in antimicrobial activity assay.

Autoinduction medium

6 g/L Na_2HPO_4

3 g/L KH_2PO_4

20 g/L tryptone

5 g/L yeast extract

5 g/L $NaCl_2$, pH 7.2

0.2% lactose

0.6% glycerol

0.05% glucose

The autoinduction medium was used for inducible protein expression.

HepG2 cells growth medium

1.87 mM MEM with GlutaMAX™ I

1 mM sodium pyruvate

1 mM non-essential aminoacids

10% Fetal Bovine serum (FBS)

100 U/ml penicillin

100 µg/ml streptomycin

CHO-K1 cells growth medium

1176 mg/l F-12 Nutrient Mixture (Ham)

2 mM glutamine

10% Fetal Bovine serum

100 U/ml penicillin

100 µg/ml streptomycin

Cryoprotectant medium for HepG2 and CHO-K1 cells

Complete growth medium

10% DMSO

1.8 Software

- The basic local alignment search tool (**BLAST**) was used to compare sequences of interest against various gene and genome databases, such as NCBI (http://www.ncbi.nlm.nih.gov).
- The web-based **DNA calculator** (Sigma) was used to check and avoid the secondary structure and primer dimmer of designed primers (http://www.oligoevaluator.com/).
- **TMPred** was used to predict possible transmembrane regions of the proteins (http://www.expasy.org/).
- **ApE-A** plasmid Editor v2.0.37 was used for planning the plasmid constructions (http://biologylabs.utah.edu/jorgensen/wayned/ape/).
- HADDOCK software was used for molecular modelling (http://haddock.science.uu.nl/).
- Structural information about proteins was obtained from **Protein Data Bank** (http://www.rcsb.org/pdb/home/home.do).
- **PROSITE** was used for helix–turn–helix motif prediction in DosR structure (http://prosite.expasy.org/).
- **Multi Gauge** software (version 2.1) (Fujifilm) was used to analyse images from EMSA and *in vitro* phosphorylation assays (http://fujifilm.jp/lsr/).

- In MALDI-TOF, proteins and peptide fragments were examined with the **MASCOT** program (www.matrixscience.com) using following parameters: NCBI and/or Swiss-Prot sequence database.

2. Methods

2.1 Eukaryotic cell lines culture and cytotoxicity assay

2.1.1 Eukaryotic cell line culture

The cells HepG2 and CHO-K1 were frozen and thawed according to the manufacturer´s instruction. First, the cells were trypsinised with trypsin-EDTA (0.025% trypsin, 0.002% EDTA) in phosphate buffered saline (PBS). The number of cells/ml was couned with Neubeuer´s chamber and the number of vials to freeze to have 2 x 10^6 cell/vial was adjusted. Falcon tube with cells was centrifuged 3 min at 1000 rpm at 4°C. The cells were resuspended in cryoprotectant medium (1.5 ml/vial), transferred to freezing vials and froze in Mr. Frosty (Nalgene™ Cryo 1°C Freezing container) filled with absolute ethanol. Mr. Frosty was placed at -80°C for minimum 2 hours. For thawing the cells, the culture medium was warmed at 37°C. The frozen vials were thawed rapidly and centrifuged 3 min at 1000 rpm at 4°C. Next, the cells were resuspended with 1 ml of culture medium per vial and seeded in a culture dish (1 dish/vial). The cells were cultured at 37°C incubator with 5 %CO_2.

2.1.2 Cytotoxicity assay

Cytotoxicity of selected compounds was analysed in HepG2 human hepatocytes and CHOK1 Chinese hamster ovary cells, using CellTiter-Glo® Luminescent Cell Viability Assay. The cells were incubated for 24 h at 37°C with 5% carbon dioxide. Control wells containing medium without cells to obtain a value for background luminescence were prepared. The test compounds (final concentration: 10 µM, 30 µM, 100 µM) were added to the cell-containing wells and incubated for 24 h at 37°C with 5% carbon dioxide. 15 µl Celltiter- Glo 3/7 was added to each well and incubated at RT for 1 h, before reading the luminescence.

2.2 Microbiological methods

2.2.1 Glycerol stock preparation

Glycerol stocks of all bacterial strains were prepared by growing a bacterial culture from a single, colony to mid-exponential phase (OD_{600} 0.5-0.6). Glycerol was added to a final concentration of 12% (v/v). 1 ml aliquots were prepared and frozen at –80°C in cryotubes

2.2.2 Bacterial growth in LB medium

The cells were grown overnight at 37° C, 250 rpm in LB medium and diluted 200 fold to obtain starting main culture.

2.2.3 Preparation of electrocompetent cells

A single colony of *E. coli* was inoculated into 2 ml LB medium and incubated at 37°C o/n, 250 rpm. The o/n culture was then used to inoculate 200 ml LB. Cells were grown to OD_{600} of ~0.4, placed on ice for 20 min and then harvested by centrifugation at 5000 g for 10 min at 4°C. The pellet was washed two times with 250 ml of ice-cold distilled water, harvested by centrifugation as described above and gently resuspended in 50 ml dH_20, containing 10% glycerol. After the final centrifugation the cells were resuspended in 0.5 ml dH_20, containing 10% glycerol. The aliquots were stored at -80°C prior snap freezing in liquid nitrogen.

2.2.4 Preparation of heat shock competent cells

A single colony of *E. coli* was inoculated into 10 ml LB medium and incubated at 37°C o/n, 250 rpm. The o/n culture was then used to inoculate 500 ml LB. Cells were grown to OD_{600} of ~0.4, placed on ice for 20 min and then harvested by centrifugation at 3000 g for 10 min at 4°C. Cell pellets were gently resuspended in 30 ml of ice-cold 100mM $CaCl_2$ and incubated on ice for 30 min. Cells were harvested by centrifugation as described above and gently resuspended in 8 ml 100 mM $CaCl_2$,

containing 15% glycerol. The aliquots were stored at -80°C prior snap freezing in liquid nitrogen.

2.2.5 Antimicrobial activity

Compounds were screened for their antibacterial activity against *M. smegmatis, E.coli* and *K. pneumoniae* using a high-throughput, turbidometric bacterial growth assay. In this assay, Müeller-Hinton agar (MHB) was used as medium for *E.coli* and *K. pneumoniae* growth and nutrient agar medium was used to *Mycobacterium smegmatis* growth.

Compounds were added at a final concentration of 10 μM. In all plates, the OD_{612} was measured before and after 18 h (*E. coli* and *K. pneumoniae*) or 40 h (*M. smegmatis*) incubations at 35°C. Negative controls (1% DMSO vehicle) and positive controls (Ciprofloxacin, 3.0 μg/mL) were run in each plate. The experiment was repeated three times and the results given were the mean of three independent reads.

2.3 DNA analysis

2.3.1 Primers design

Primers for PCR experiments were designed according to the following standard. The length of most primers was ranged from 18-25 nucleotides with a >50% of guanine/cytosine (GC) content greater than 50% in order to result in a melting temperature (Tm) from 50-65°C.

2.3.2 Plasmid construction

2.3.2.1 Insert and vector preparation

The primers used in this work are described in (Table 6). Plasmid construction was planned using ApE-A plasmid Editor. Amplification reactions for all *M. tuberculosis* gene targets were designed and optimized to be used under standardized set of thermocycling parameters.

Cloning the full-length of DosR, DosS and DosT

The *dos*R and *dos*S genes were amplified from *Mycobacterium tuberculosis* H37Ra genomic DNA using KOD XL DNA polymerase. Amplification was carried out in a 50 µl final volume reaction mixture containing nuclease-free water, PCR buffer, 2 mM PCR nucleotide mix deoxynucleoside triphosphates (dNTPs) (0.2 mM final concentration for each dNTP), 2.5 U/µl KOD XL DNA polymerase (0.05 U/µl final concentration), and genomic DNA from *Mycobacterium tuberculosis* H37Ra. A 3 min initial denaturation at 95°C was followed by 30 cycles: 95°C 15 sec, 65°C 20 sec (DosR) or 25 sec (DosS, DosT), 72°C 50 sec (DosR) or 2.5 min (DosS, DosT) and a 10 min final extension at 72°C. Cloning primers incorporated restriction sites for directed cloning. Both amplified fragment and vector were digested with appropriate endonucleases following the manufacturer's instructions. To inhibit restriction enzymes, the digested mixtures were heated at 65°C for 10 min in the case of heat labile enzymes. For heat resistant enzymes, the DNA fragments resulting from the digestion were purified from an agarose gel after electrophoresis. PCR products were mixed with 6x DNA loading buffer (360 mM Tris-HCl, pH 8.8, 9% SDS, 0.9% bromophenol blue, 15% β-mercaptoethanol, 30% glycerol) and electrophoresed on a 1% agarose gel. Electrophoretic separation of products was carried out for 60 min at 0.8 mV/cm2 in 1x TAE buffer (40 mM Tris base, 20 mM glacial acetic acid, 1 mM EDTA pH 8.0). Amplicons were visualized under UV transillumination, and size estimation was made using Lambda DNA/HindIII Ladder. Both, fragment and vector were purified using a commercially available purification kits; fragment DNA (GenElute TM PCR Clean-Up Kit, Sigma) and vector (QIAquick® Gel Extraction Kit, Qiagen), according to manufacturer´s instructions.

Ammonium acetate purification

For purification of low concentrated DNA fragments, 0.5 volumes of 2.5 M ammonium acetate solution was added, and the samples were mixed and chilled on ice. The samples were then centrifuged for 30 min (10,000xg, 4°C) and the supernatant was transferred to a clean tube. In order to precipitate the DNA, two

volumes of absolute ethanol was added to the samples and the contents were mixed by inversion and stored for 20 min at –20°C. The DNA pellet was subsequently collected by centrifuging for 10 minutes at 5000 g, 4°C, washed in 70% ethanol and allowed to dry. The final pellet was dissolved in required volume of dH_2O or TE buffer (10 mM Tris-HCl, 1 mM EDTA, pH 8.0) and stored at –20°C till further use.

Cloning the truncated forms of DosS and DosT

Truncated forms of histidine kinases DosS and DosT were PCR-amplified from *Mycobacterium tuberculosis* H37Ra genomic DNA using the appropriate primers (see Table 6) and were cloned into the pPEU7 vector. The clones were obtained by using the CloneEZ® PCR Cloning Kit (GenScript) according to manufacturer´s instructions.

2.3.2.2 Ligation and transformation

Ligation was carried out in a 20 µl final volume reaction mixture containing nuclease-free water, 2 µl of 10x ligation buffer (500 mM Tris HCl pH 8.0, 100 mM MgCl2, 0.5 mg/ml acetylated BSA), 2.5 U/µl T4 DNA polymerase , 2 µl of 25 mM dATP, 1 µl 100 mM DTT (DNA-ligation kit, Novagen-Merck). The ligation reaction was allowed to proceed 18 hours at 16°C. A control ligation was set up without insert. DNA ligase inactivation was performed by heating the reaction mixture 10 min at 70°C.

Heat shock transformation

Competent cells were incubated on ice for 30 min in 20 µl ligation reaction. Then they were heat shocked at 42°C for 2 min. Tubes were placed back on ice for a further 5 min. 500 µl of LB media was added and cells were incubated for 1 h at 37°C, with shaking (250 rpm). Transformation mixtures were spread onto LB agar plates containing adequate antibiotic for transformants selection. Plates were incubated o/n at 37°C.

Electroporation

Electrocompetent bacteria were thawn on ice for 5–10 min. For a single transformation 50 µl of bacterial suspension were mixed in a cold transformation cuvette with 1-8 µl of the ligation reaction, equalling approximately 1–10 ng of circular plasmid DNA. Immediately after the electroporation (U = 1.7 kV; time pulse = 5 ms) 500 µl of LB-medium were added and this suspension was transferred to an Eppendorf tube. After incubating the cells at 37°C for 1 h, 100 µl were plated on an agar plate containing the appropriate selection antibiotic and incubated at 37°C o/n.

Selection of recombinant clones

To screen for recombinant plasmids, colony PCR was performed. Insert-specific primers or vector-specific primers were used for amplifying a portion of the plasmid. Plasmid DNA from positive clones was isolated and sequence integrity was checked by automatic sequencing. Following sequencing confirmation, purified plasmids were used to transform *E.coli* Rosetta (DosR and DosS full lenght) or BL21 (truncated forms of DosS and DosT) for the proteins expression.

DNA sequencing

DNA sequencing was performed for each new clone using PCR to amplify the DNA region of interest prior to Sanger sequencing.T7 forward and reverse primers were used. PCR reactions were sent to Technical and Scientific Services of University of Barcelona to be automated sequenced by the fluorescent Sanger method.

2.4 Construction of mutant clones

Mutagenesis of specific residues of DosR was carried out using the QuikChange XL site-directed mutagenesis kit following the manufacturer's instructions. In this method, mutations were generated by PCR using a pair of oligonucleotide primers designed with mismatching nucleotides at the centre of the primers (Table 6). Mutations were confirmed by DNA sequencing and the final constructs were used to transform Rosetta or Bl21 *E. coli* cells.

2.5 Purification and analysis of proteins

2.5.1 Protein expression

E.coli Rosetta (for DosR, DosS and mutant proteins of DosR) or Bl21 (for truncated forms of DosS and DosT) cells were transformed with the recombinant clones and grown in plates with LB medium with the appropriate antibiotics. The pre-inoculum was inoculated with one colony, grown o/n at 37°C (250 rpm) and then used to inoculate flasks containing 1L of LB medium with the appropriate antibiotics.

Protein expression was induced by the addition of isopropyl-1-thio-β-D-galactopyranoside (IPTG) or with autoinduction system. In the first case, cells were grown in LB medium with adequate antibiotics at 37°C until OD_{600} ~0.6. Protein expression was induced with 1 mM IPTG at 37°C for 3-18 h. Cells were centrifuged at 4,000 rpm for 20 min at 4°C and stored at -80°C before use. In autoinduction system, cells were grown in auto induction medium with adequate antibiotics at 37°C until OD_{600} ~1.5 and shifted at 20°C for 18 h. The cells were harvested by centrifugation at 4,000 rpm for 20 min at 4°C and stored at -80°C before use.

2.5.2 Denaturating poly-acrylamide gel electrophoresis (SDS-PAGE)

For the separation and analysis of proteins, SDS-polyacrylamide gel electrophoresis technique was used (Laemmli, 1970). Resolving gels (125 mM Tris-HCl, pH 6.8, 0.1% SDS, 10-20% ammonium persulfate, 0.5-1% TEMED) of either 12% or 15% acrylamide (acrylamide:bis-acrylamide 29:1) and a stacking gel (375 mM Tris-HCl, pH 8.8, 0.1% SDS, 10-20% ammonium persulfate, 0.5-1% TEMED) of 6% were prepared and casted in the electrophoresis apparatus according to the manufacturer's instructions. Protein samples were mixed with an appropriate amount of loading buffer (63 mM Tris-HCl, 10% glycerol, 2% SDS, 5% ß-mercaptoethanol, 0.0025% bromophenol blue, pH 6.8) and boiled for 5 min before loading onto the gel. The gels were run in running buffer (25 mM Tris-HCl pH 8.3, 190 mM glycine, 0.1% SDS). Coomasie buffer was used for visualising the proteins in the gel. Gels were immersed in Coomassie Blue stain for 30-60 min on a shaking platform. Gels were subsequently rinsed several times in metanol:AcOH:H2O (5:1:4) to destain for 1-2 hours, rinsed in dH_2O and analysed.

2.5.3 Cell disruption and crude extract production

After protein expression, induced cultures were thawed on ice and resuspended in buffer (150 mM NaCl, 100 mM Tris-HCl, pH 8.0 and 1 mM EDTA for Strep-tagged proteins) supplemented with 1% protamine sulfate and lysed. Cells were disrupted by repeated sonication cycles (12 μm amplitude, 15 sec on, 45 sec off for 25 cycles), or using a French press Cell Disrupter (21,000 psi pressure). Protein integrity was accomplished by keeping the cell suspension and the subsequent crude extract cooling on ice.

The insoluble fraction was isolated by centrifugation at 16,000 g for 40 min. Presence of induced recombinant protein in soluble and insoluble cell fractions was determined by SDS-PAGE with Coomassie staining.

2.5.4 Protein purification and quantification

Immobilized Metal Ion Affinity Chromatography (IMAC) is based on the interaction of certain protein residues (histidines, cysteines, and to some extent tryptophans) with cations of transition metals. The Nickel Chelating Resin is specifically designed for the purification of recombinant proteins fused to the 6 x histidine (6XHis) tag. Ni-Affinity Chromatography uses the ability of His to bind nickel.

The strep-tag purification system is based on the highly selective binding of engineered streptavidin, called strep-tactin, to strep-tag fusion proteins.

The proteins were purified under denaturating conditions using liquid chromatography system ÄKTA. Proteins were fractionated by automatic collector and detected in the eluent by determination by UV absorbance at 280 nm.

The cell lysate was applied to a 5 ml pre-equilibrated affinity column (His•trap or Strep•tractin) with washing buffer (150 mM NaCl, 100 mM Tris-HCl, pH 8.0 and 1mM EDTA for Strep-tagged proteins composition) at a rate of 1 ml/min. The nonspecifically bound proteins were eluted with washing buffer. Recombinant proteins were eluted from the column with elution buffer (washing buffer with addition of 500 mM imidazole or washing buffer with addition of 2.5 mM desthiobiotin for His•tag or Strep•tag proteins, respectively). Protein fractions

were analyzed by SDS-PAGE, pooled and further purified by size exclusion chromatography.

For size exclusion chromatography, pooled fractions from the affinity chromatography were injected onto a Superdex 75 or 200 gel filtration column equilibrated in washing buffer used with affinity columns. Fractions were collected and analyzed by SDS-PAGE. Gels were stained with Coomassie staining.

For crystallization trials or ITC, fractions containing protein were dialysed against washing buffer. Proteins were concentrated using Amicon Centriplus spin concentrators. The protein content for all proteins was determined by Bradford method or with Thermo Scientific NanoDrop™ 1000 Spectrophotometer.

2.5.5 Matrix-assisted laser desorption/ionization-time-of-flight mass spectrometry (MALDI-TOF)

Matrix-assisted laser desorption/ionization (MALDI) is a "soft" ionization technique used in mass spectrometry, allowing the analysis of biomolecules (e.g. proteins, peptides or sugars) and large organic molecules (e.g. polymers, dendrimers or other macromolecules), which tend to be fragile and fragment when ionized by more conventional ionization methods. The utility of MALDI-TOF for protein analyses lies in its ability to provide highly accurate molecular weight information on molecules. The ability to generate such accurate information can be extremely useful for protein identification and characterization (e.g. post-translational modifications). Typical MALDI protocols for protein modification characterization begin with the enzymatic digestion of the protein sample, resulting in a complex mixture of peptides. When a protein's primary structure is known, the molecular weight of a peptide can be used to corroborate the presence of any modification by its specific molecular-weight difference between the observed mass of peptide and that calculated on the basis of the sequence.

The identity of all the proteins produced in this thesis was verified by MALDI-TOF. MALDI-TOF/TOF analysis was performed with the Microflex system spectrophotometer (Bruker Daltonics).

The dried extract of protein band excised from SDS-PAGE was dissolved in 10 µl of 0.1% trifluoroacetic acid (TFA) and purified by ZipTip C4 tips prior to MS analysis. The eluate was mixed with 50% acetonitrile and 0.1% TFA in water for spotting onto sample plate, and dried for MALDI-TOF/TOF MS analysis. For phosphoprotein characterization, proteins, previously pretreated with either 20 mM AcP, 100 mM CmP or 5 mM BeF_3^-, were incubated with 100 ng/L trypsin (50 mM , pH 8.3) on ice. Phosphopeptides were dissolved, purified and eluted as above using ZipTip C18. The solution was spotted on a polish stainless steel MALDI target plate. Linear Detector was used for samples 5-100 kDa (proteins), while reflector detector was used for samples 0-5 kDa (peptides). Proteins and peptide fragments were examined with the MASCOT program using following parameters: NCBI and/or Swiss-Prot sequence database.

2.5.6 Regeneration of columns

Columns regeneration was performed when different proteins were isolated or when there was a significant loss in the yield of protein. Columns used in polyhistidine-tagging were regenerated with nickel sulfate (NiSO4). His•Trap column was striped by washing with 5–10 column volumes of stripping buffer (20 mM sodium phosphate, 0.5 M NaCl, 50 mM EDTA, pH 7.4). Next, it was washed with 5–10 column volumes of washing buffer and 5–10 column volumes of distilled water before re-charging the column with nickel sulfate. The water-washed column was re-charged by loading 0.5 ml or 2.5 ml of 0.1 M NiSO4 in distilled water on column. Again, the column was washed with 5 column volumes of distilled water, and 5 column volumes of washing buffer for pH adjustment before storage in 20% ethanol.

To regenerate Strep•Tactin column, an excess of a yellow azo dye 1 mM hydroxyl-azophenyl-benzoic acid (HABA) was added to the column. HABA displaces the desthiobiotin from the binding pocket on the Strep•Tactin and being removed by adding 1 x Strep•Tactin washing buffer before using the column.

2.5.7 Proteins crystallization and diffraction trials

Protein structural characterization was attained by crystallization and diffraction trials. Pure protein preparations were used to obtain protein crystals by the sitting drop vapor diffusion method. This technique employs special 96-well plates with reservoir solution (Fig. 16). Crystallization of the purified protein was initially performed at 21°C with commercially available screens: JBScreen Classic HTS I, II (Jena Bioscience, Germany) and JCSG+ (Qiagen, Netherlands) using a robotic system. Subsequent modifications of conditions were performed for crystals optimization. DosR and DosR mutant proteins (10 mg/ml) were treated with BeF_3^- (7mM $MgCl_2$, 30 mM NaF, 5 mM $BeSO_4$) before setting up the crystallization plates. Crystals appeared between 2 hours and 2 weeks and reached their maximum size after 1 week to 1 month. Crystals were subsequently transferred to a cryo-protectant solutions and flash frozen under liquid nitrogen. Diffraction trials were performed at the European Synchrotron Radiation Facility (ESRF), Grenoble, France.

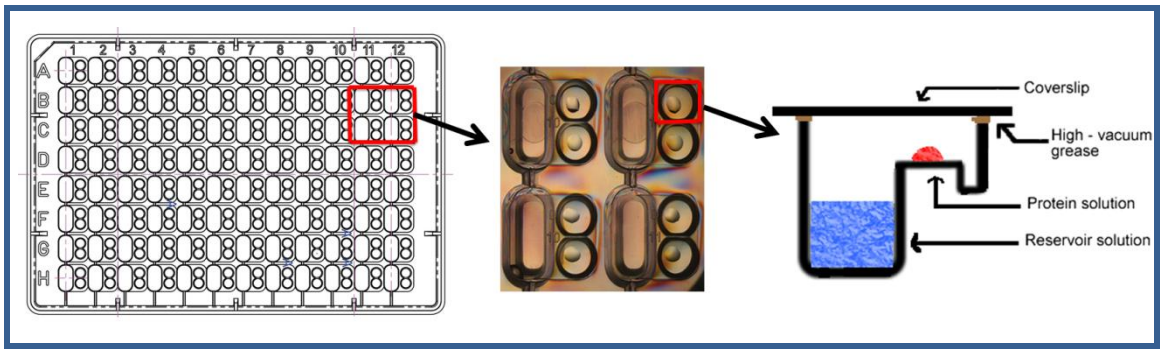

Fig. 16 An illustration of 96-well crystallization plate with diagram of sitting drop vapor diffusion method. In this method, the protein drop sits on a pedestal above the reservoir solution.

2.6 Analysis of protein interactions

2.6.1 Electrophoretic mobility shift assay (EMSA)

The gel electrophoretic mobility shift assay (EMSA) was used to detect the formation of protein-DNA complexes. A double-stranded oligonucleotide containing the palindromic consensus promoter sequence of hypoxic response genes was used as a DNA probe. EMSA-Fw and EMSA-Rv 5'-fluorescein labelled oligonucleotides (Table 6) were annealed (incubation at 85°C for 5 minutes and gradually reduction

of the heat until room temperature) and used as DNA probe. Binding of protein to DNA fragments was carried out by incubation on ice for 30 min in a 20 µl reaction mixture. The mixture was composed of labelled probe (5-10 ng), 1–10 µg of protein DosR, 50 mM Tris-HCl, pH 8.0, 1 mM EDTA, 40 mM KCl, 12 mM MgCl2, 1 µg/µl poly-(dI–dC) and 10% of glycerol. After incubation, the reaction was resolved in a 15% non-denaturing polyacrylamide gel in 1 x Tris-borate-EDTA (TBE) buffer (Tris base 89 mM, boric acid 89 mM, EDTA 2 mM). The positions of the fluorescein labelled DNA in the gels were detected using a flatbed scanner that detects fluorescence (Fujifilm FLA-5000 machine) or with transiluminator. Cell extracts contain many DNA-binding proteins that are capable of interacting with DNA in a sequence-independent manner and thus they may compete with the protein of interest for binding to a specific DNA. Nonspecific competitor DNA, poly-(dI–dC), was included in the binding reaction to minimize nonspecific interactions by facilitating detection of the complexes of interest. The assay was accomplished in the presence or absence of phosphoryl donors, such as carbamoyl phosphate (100 mM) and acetyl phosphate (20 mM), or Asp-phosphate mimetics like BeF_3^- (5 mM). The analysis of these experiments was carried out using Multi Gauge Fujifilm software (version 2.1).

Apart from protein-DNA binding, EMSA can also measure the ability of the small molecules to inhibit the DNA-binding or change the conformation of examined protein. The inhibitors screening was performed with EMSA to validate the inhibitory properties of the compounds and provide additional criteria for eliminating the least effective compounds.

2.6.2 *In vitro* phosphorylation assay

2.6.2.1 Autophosphorylation of DosS and truncated forms of DosS and DosT

For autophosphorylation assay, DosS full length, DosS and DosT truncated forms were incubated with 0.5 µCi [γ-^{32}P]ATP in 10 ml reaction buffer (500 mM Tris/HCl, pH 6.8, 1M KCl, 100 mM MgCl2, 1 mM ATP) at 24°C and aliquots were withdrawn at different time points and the reaction was stopped by SDS buffer (120 mM Tris-HCl, pH 6.8, 20% glycerol, 4% SDS, 10% -mercaptoethanol, and 0.2% bromphenol blue). Unincorporated [γ-^{32}P]ATP was removed by applying the reaction mixture to a

Centricon Centrifugal Filter Devices (Amicon Millipore). All aliquots were analyzed by SDS-PAGE and blotted to polyvinylidene difluoride membrane. The membranes were exposed to film o/n at 25°C and visualised with Fujifilm FLA-5000 machine.

2.6.2.2 Phosphotranfer from DosS and truncated forms of DosS and DosT to DosR

Phosphotransfer was accomplished by adding DosR to autophosphorylated DosS sample to in the same buffer, maintaining a molecular ratio of 1:1. The reaction was carried out at 24°C and stopped at different time-points with SDS-sample buffer. Proteins were separated by 15% polyacrylamide gel, which was dried and visualized through autoradiography.

2.6.2.3 Phosphorylation of DosR and mutant proteins by acetyl phosphate

[^{32}P]-acetyl phosphate was prepared using 1.5 unit of acetate kinase in buffer (2.5 mM Tris-HCl, pH 8.0, 6 mM CH3CO2K, 1 mM $MgCl_2$).

Freshly prepared [^{32}P]-AcP was used to phosphorylate DosR and mutant proteins. For each reaction 0.25 mg/ml of protein was incubated with [^{32}P]-AcP in phosphorylation buffer (2,5 mM Tris-HCl pH 8,0, 6 mM CH3CO2K, 1 mM MgCl2) at 24°C at different times. The reaction was stopped with SDS-sample buffer and products were separated on 15% SDS-PAGE. After drying, detection was performed by autoradiography.

2.6.2.4 Phosphatase Activity of DosS

DosR was phosphorylated by [^{32}P]-AcP as described above and DosS was added to a final reaction. The reaction mixture was incubated for various time points at 24°C. A control reaction was prepared in parallel, where DosS was replaced with buffer. The reaction was stopped with SDS- buffer and products were separated on 15% SDS-PAGE. After drying the gels, detection was performed by autoradiography.

2.6.3 Isothermal titration calorimetry (ITC)

Isothermal titration calorimetry (ITC) is a physical technique that measures the heat changes associated with the interactions occurring between components in

solution, and thus it is useful to measure thermodynamic parameters between interacting biomolecules. ITC measures all binding parameters in a single label-free, in-solution experiment. ITC is used for characterization of mechanism of the molecular interaction, confirmation of intended binding targets in small molecule drug discovery and determination of binding specificity and stoichiometry.

ITC was used to examine protein-protein interactions and to measure the affinity of a set of potential inhibitors for DosR. The assays were performed at 21°C with purified proteins by using iTC200 microcalorimeter. All solutions were dialysed into washing buffer (with the addition of DMSO for protein-ligand interaction) to minimize the noise and thoroughly treated by vacuum stirring before loading into the syringe and the cell of the calorimeter. For protein-protein interaction measurement, a solution containing various protein concentrations was used as titrant, whereas solutions containing various concentration of other protein were used in the calorimetry cell. For protein-ligand interaction measurement, a solution containing various compound concentrations was used as titrant, whereas solutions containing various concentration of protein were used in the calorimetry cell. The machine was settled to inject 27 successive aliquots of 1.5 µl samples from the syringe with a 150 seconds interval into the cell under continuous stirring at 100 rpm. The binding data were collected according to the heat effects (heat of reaction per injection) measured in microcalories per second and analysed by non-linear regression using a simple one-site binding model. The fitted data yielded the association constant (KA), number of binding sites on the protein (N), the enthalpy of binding (ΔH) and the entropy of binding (ΔS) by Origin software (version 7.0).

2.7 Molecular modelling DosR-DosS complex

The three dimensional structure of the HisKA_3 domain of *M. tuberculosis* DosS (aminoacids 382 to 446) was modelled with MODELLER software (Sali & Blundell, 1993) using the *B. subtillis* DesK crystal structure (PDB accession code: 3EHF) as a reference template. A 'slow' refinement of the structure was performed during the modelling. Five different models were generated, and the one with better DOPE-score was selected for analysis and further calculations. The structure of the

DosR:DosS complex was predicted with HADDOCK software (Dominguez *et al.*, 2003). The *M. tuberculosis* DosR structure was obtained from the PDB (accession code: 3C3W). Only the response regulator domain was considered (aminoacids 1 to 99) as the receptor in the docking algorithm. The *M. tuberculosis* DosS structure was directly taken from the previous modelling. Two structural units of DosS were considered as two independent ligands. Structural information from the homolog *T. maritima* HK:RR complex (PDB accession code: 3DGE) was used to set-up a list of distance restrains between receptor and ligands aminoacids to reduce the protein-protein docking search space. One thousand structures were generated by rigid body docking. The two-hundred best structures were then refined by a semi-flexible simulated-annealing protocol in explicit water as implemented in HADDOCK. Structures were visualized and analyzed with Visual Molecular Dynamics (Humphrey *et al.*, 1996).

2.8 Molecular dynamics simulations

The starting coordinates for the simulation of the DosR-DNA complex were taken from the Protein Data Bank (PDB accession code: 1ZLK). The system was prepared for simulation using the GROMACS 4.5.3 simulation package. Molecular dynamics in explicit solvent at an atomic resolution were performed using a TIP3P water model (Jorgensen *et al.*, 1983) and the CHARMM force-field (MacKerell *et al.*, 1998) to describe the bonding and non-bonding interactions of the whole system. The system is embedded in a 111.5 x 68 x 57 A^3 volume box and it was equilibrated following standard procedures (structure optimization followed by temperature and volume equilibration). All bonds were constrained with the LINCS algorithm (Hess *et al.*, 1997) after optimization and the simulation time-step set to 2 fs. The production simulation used for analysis was performed in the micro-canonical ensemble at 300K using the PME treatment of long range electrostatic interactions (Essmann *et al.*, 1993) with a distance cut-off of 8 Å for updating the neighbouring list. Separate NOSE-HOOVER thermostats (Evans & Holian, 1985) were used for protein, DNA and water atoms. The simulation was extended for 3.5 ns, and non-solvent structures were sampled every 1 ps.

2.9 Compounds selection

All compounds used as inhibitor candidates were purchased from Specs Compound Handling BV (http://www.specs.net/snpage.php?snpageid=home), except for compound 10 that was purchased from ChemBridge (www.chembridge.com). These two companies are suppliers of screening compounds and building blocks to the Life Science industry. Compounds dilutions were freshly prepared before each experiment.

RESULTS

For the study of DosRST two-component system, recombinant protein production methods were applied. Those methods offer the possibility of attaching purification tags to the proteins which facilitates the purification procedures. Hexahistidine tag (His-tag) was chosen for easy affinity chromatography (Hoffmann & Roeder, 1991) when designing the constructs for expressing the full length DosR, DosS and DosT proteins. Compared to other affinity tags like glutathione-S-transferase which is a protein on its own, the small size of a hexahistidine tag does not interfere with function and crystallisation ability of many recombinant proteins, and therefore shortens the protein preparation procedures of having to cleave the tag.

Another advantage of using recombinant proteins is that their production can be boosted by the use of an efficient expression system, which is normally a better alternative to protein extraction from the native source, if the goal is to produce proteins in a large quantity to meet the need of crystallisation. Additionally, proteins belonging to a pathogenic bacteria (*Mycobacterium tuberculosis*), which demands P3 containment safety level, could be produced in different strains of non-pathogenic *Escherichia coli*, the expression system of choice in this study.

1. Cloning

1.1 Cloning of DosR

1.1.1 Cloning of wild type DosR

The *dos*R gene of *M. tuberculosis* H37Rv was amplified using *Mtb* H37Ra genomic DNA as template. The DosR amino acid sequence of *Mtb* virulent strain H37Rv is identical to that of avirulent strain H37Ra (see Annex 2).

The cloning oligonucleotides (Table 6) incorporated restriction sites at their 5' end for directed cloning: the forward primer included *Nco*I cleavage site and the reverse primer contained *Xho*I site. The selected cloning vector was pET21d(+), which allows

the cloning and expression of recombinant proteins with a C-terminal six histidine tag (His_6-tag). The amplified DNA fragment and circular vector were digested with *Nco*I and *Xho*I endonucleases. The digested fragments were ligated and the ligation reaction was transformed into *E. coli* DH5α competent cells. Transformants were selected on LB-Amp agar plates and analysed by colony-PCR. Plasmid DNA from positive clones was isolated and sequence integrity was checked by automatic sequencing.

1.1.2 Cloning of mutant forms of DosR

The mutagenesis research was performed in order to gather the data which could be helpful to evaluate the molecular switches leading to DosRST TCS activation, upon which a framework for rational drug project can be initiated.

It has been shown that phosphorylation of Asp54 serves as a switch to activate DosR and it occurs through phosphorylation in a reaction catalysed by DosS and DosT(Chauhan & Tyagi, 2008; Roberts *et al.,* 2004; Saini *et al.,* 2004a; Wisedchaisri *et al.,* 2008).

It has been also demonstrated that DosR is a substrate of Ser/Thr kinase PknH (Chao *et al.,* 2010). PknH phosphorylates DosR in residues threonine 198 (Thr198) and threonine 205 (Thr205), located in the key regulatory helix 10, involved in the activation and dimerization of DosR. PknH and DosS phosphorylation of DosR cooperatively enhance DosR binding to cognate DNA sequences (Chao *et al.,* 2010). To assess the role of phosphorylation in DosR activity a series of mutants in residues Asp54, Thr198 and Thr205 was constructed in this study and their roles in the Dos TCS signal transduction pathway (i.e. phosphorylation, dephosphorylation and DNA binding) compared to the wild-type response regulator protein were evaluated.

Asp-54 residue of DosR was mutated to alanine. Three different double mutants were constructed at Thr198 and Thr205 residues of DosR: i) mutation to alanine, DosR [T198A, T205A]; ii) mutation to aspartic acid, DosR [T198D, T205D]; and iii) mutation to glutamic acid, DosR [T198E, T205E]. Triple mutant DosR [D54A, T198D, T205D] was also constructed. A schematic representation of DosR with mutant derivatives residues is shown in Fig. 17.

Mutagenesis of specific residues of DosR was carried out with the QuickChange XL site-directed mutagenesis kit using DosR-pET21d(+) construct as template. Mutations were confirmed by DNA sequencing and the final constructs were used to transform Rosetta *E. coli* cells for the expression and purification of mutant recombinant proteins.

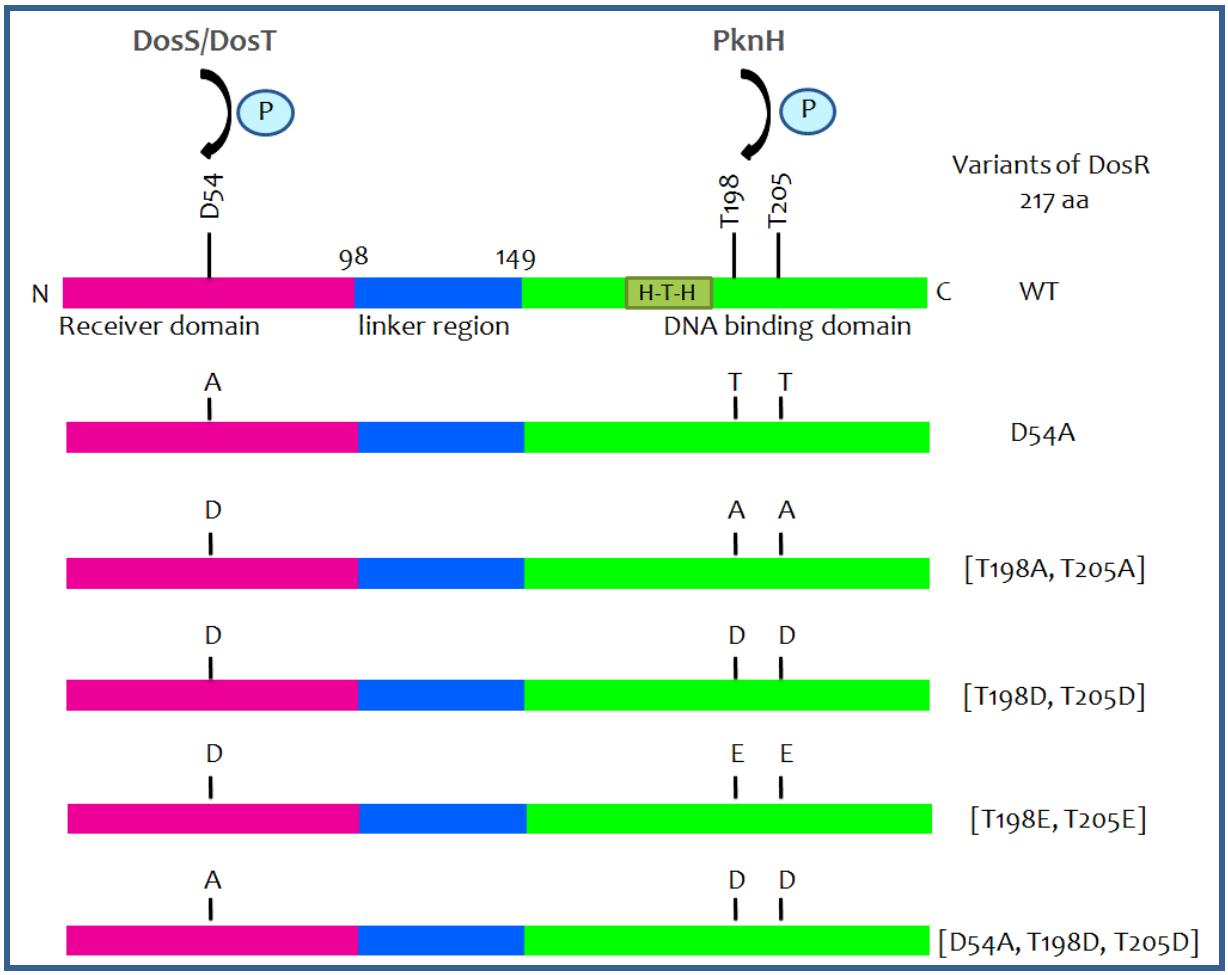

Fig. 17 Schematic outline of DosR of *M. tuberculosis* wild type and mutant proteins domains structure. Mutated amino acid residues are indicated in one-letter code. Helix–turn–helix motif (H-T-H) was predicted by PROSITE.

1.2 Cloning of DosS

1.2.1 Cloning of full length DosS

The *dos*S gene of *M. tuberculosis* H37Rv was amplified using *Mtb* H37Ra genomic DNA as template. The DosS amino acid sequence of *Mtb* virulent strain H37Rv is identical to that of avirulent strain H37Ra (see Annex 2).

Cloning oligonucleotides (Table 6) incorporated restriction sites at their 5' end for directed cloning: the forward primer included *Nco*I cleavage site with an additional N-terminal six histidine tag (His6-tag) and the reverse primer contained *BamH*I cleavage site. The selected cloning vector was pET21d(+). The amplified DNA fragment and circular vector were digested with *Nco*I and *BamH*I endonucleases. The digested fragments were ligated and the ligation reaction was transformed into *E. coli* DH5α competent cells. Transformants were selected on LB-Amp agar plates and analysed by colony-PCR. Plasmid DNA from positive clones was isolated and sequence integrity was checked by automatic sequencing.

1.2.2 Cloning of truncated forms of DosS

By sequence similarity comparison with known proteins belonging to two-component systems, the conserved His residue at position 395 in DosS was predicted to be the site of phosphorylation (Dasgupta *et al.,* 2000). Its involvement in the phosphorylation reactions was confirmed by the analysis of mutant proteins (Roberts *et al.,* 2004; Saini *et al.,* 2004a, b). In Saini *et al,* for instance, the mutation to glutamine (unable to receive phosphodonor) at His395 resulted in abolishment of DosS autophosphorylation, confirming that phosphorylation occurs at the conserved His395 residue.

Furthermore, the histidine kinases are membrane-bound sensor kinases, which denote the probable complexity in protein purification. TMPred prediction of the DosS revealed possible transmembrane (TM) regions that flank predominantly at the N-terminus of the protein (Fig. 18). The C-terminus of DosS protein contains all the domains required for phosphorelay and signal output. Taking into account the above mentioned structural and functional considerations, diverse truncated forms of histidine kinase DosS were constructed (Fig. 19). To avoid the difficulties in protein solubility and subsequent purification problems that could be encountered with full length of DosS, the predicted transmembrane regions were detached. In order to be used in *in vtro* phosphorylation assays, in each truncated form of protein the conserved histidine residue was preserved. One of the truncated forms carries the histidine kinase domain exclusively ($DosS_{380-578}$). In the other truncated

form ($DosS_{350-578}$) few additional amino acids at N-terminal of HisK domain were included to elude possible disruption in secondary structure of protein.

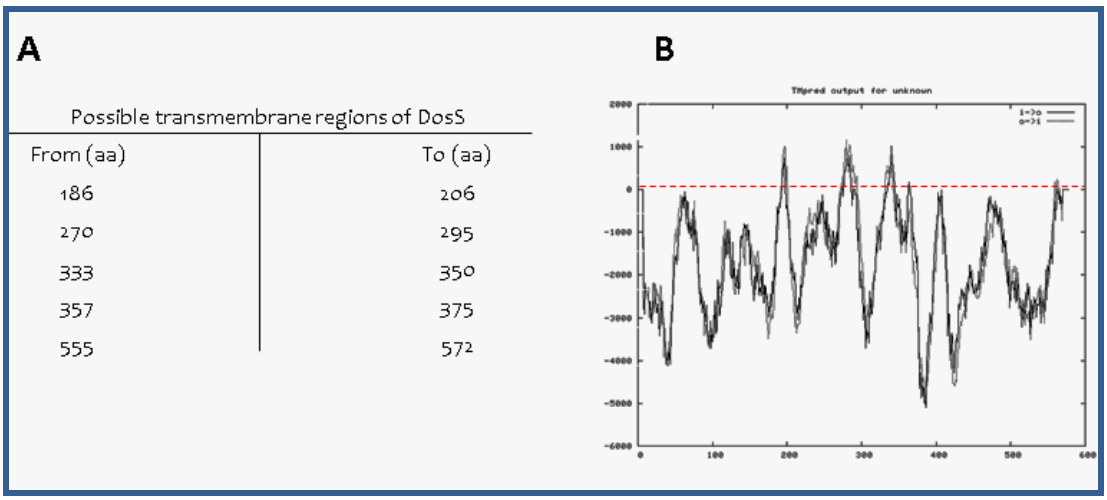

Fig. 18 TMPred prediction of the DosS revealed possible transmembrane (A). The prediction of transmembrane regions. (B). The orientation of transmembrane regions of DosS. Anything above zero on the scale is considered to be a possible TM.

The truncated forms of *dos*S gene were amplified using *M. tuberculosis* H37Ra genomic DNA as template and the corresponding cloning oligonucleotides (Table 6). The pPEU suite of vectors have been developed in the IRB Barcelona Protein Expression Core Facility for HTP cloning and expression of proteins in a number of affinity tag/fusion protein/expression host combinations. The selected cloning vector was pPEU7, which has t7/lacO promoter/operon combination for inducible expression in *E. coli* strains and N-terminal StrepII-Cherry tag. The clones were obtained using the CloneEZ Kit according to manufacturer´s instruction.

The digested fragments were ligated and the ligation reaction was transformed into *E. coli* DH5α competent cells. Transformants were selected on LB-Amp agar plates and analysed by colony-PCR. Plasmid DNA from positive clones was isolated and sequence integrity was checked by automatic sequencing.

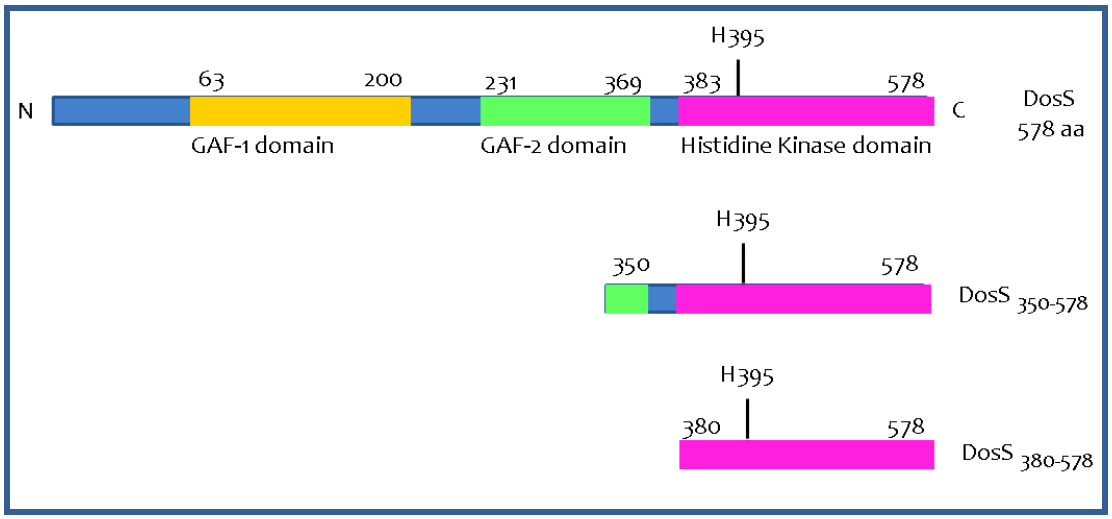

Fig. 19 Schematic outline of DosS of *M. tuberculosis* wild type and truncated proteins domains structure prepared in this work. Indicated amino acid residue represents conserved histidine residue (H395) in single-letter code.

1.3 Cloning of DosT

1.3.1 Cloning of full length DosT

The *dos*T gene of *M. tuberculosis* H37Rv was amplified using *Mtb* H37Ra genomic DNA as template. The DosT amino acid sequence of *Mtb* virulent strain H37Rv is identical to that of avirulent strain H37Ra (see Annex 2).

Cloning oligonucleotides (Table 6) incorporated restriction sites at their 5' end for directed cloning: the forward primer included *Nhe*I cleavage site and the reverse primer contained *Xho*I site. The selected cloning vector was pET21d(+), which allows the cloning and expression of recombinant with a C-terminal His_6-tag. The amplified DNA fragment and circular vector were digested with *Nhe*I and *Xho*I endonucleases. The digested fragments were ligated and the ligation reaction was transformed into *E. coli* DH5α competent cells. Transformants were selected on LB-Amp agar plates and analysed by colony-PCR. Plasmid DNA from positive clones was isolated and sequence integrity was checked by automatic sequencing.

1.3.2 Cloning of truncated forms of DosT

The conserved His residue at position 392 in DosT was predicted to be the site of phosphorylation of DosT (Dasgupta *et al.*, 2000). Its involvement in the phosphorylation reactions was confirmed by the analysis of mutant proteins (Roberts *et al.*, 2004), like in the case of DosS. TMPred prediction of DosT revealed possible transmembrane (TM) regions that flank predominantly at the N-terminus of the protein with strong transmembrane helice at position 238-256aa (Fig. 20). The C-terminus of DosT protein contains all the domains required for phosphorelay and signal output indicating that this region is cytoplasmic. For *in vitro* phosphorylation and EMSA assays, the diverse truncated forms of histidine kinase DosT were constructed (Fig. 21). Alike for truncated forms of DosS, in each truncated form of DosT the conserved histidine residue was preserved and predicted possible transmembrane regions detached. The truncated forms of *dos*T gene were amplified using *M. tuberculosis* H37Ra genomic DNA as template and the cloning oligonucleotides (Table 6). Cloning was performed as it is described in chapter 1.2.2.

A

Possible transmembrane regions of DosT

From (aa)	To (aa)
238*	256*
280	298
354	372

B

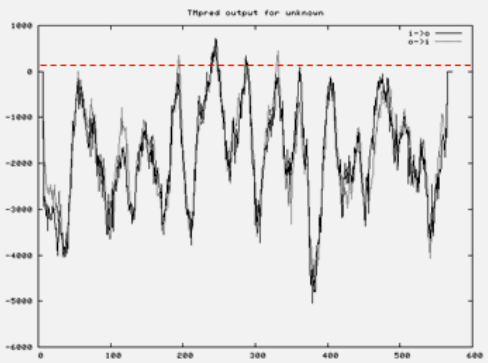

Fig. 20 TMPred prediction of the DosT revealed possible transmembrane (A). The prediction of transmembrane regions. (B). The orientation of transmembrane regions of DosT. Anything above zero on the scale is considered to be a possible TM. *The probable strong transmembrane helice of DosT is indicated by the large peak at aa 238-256.

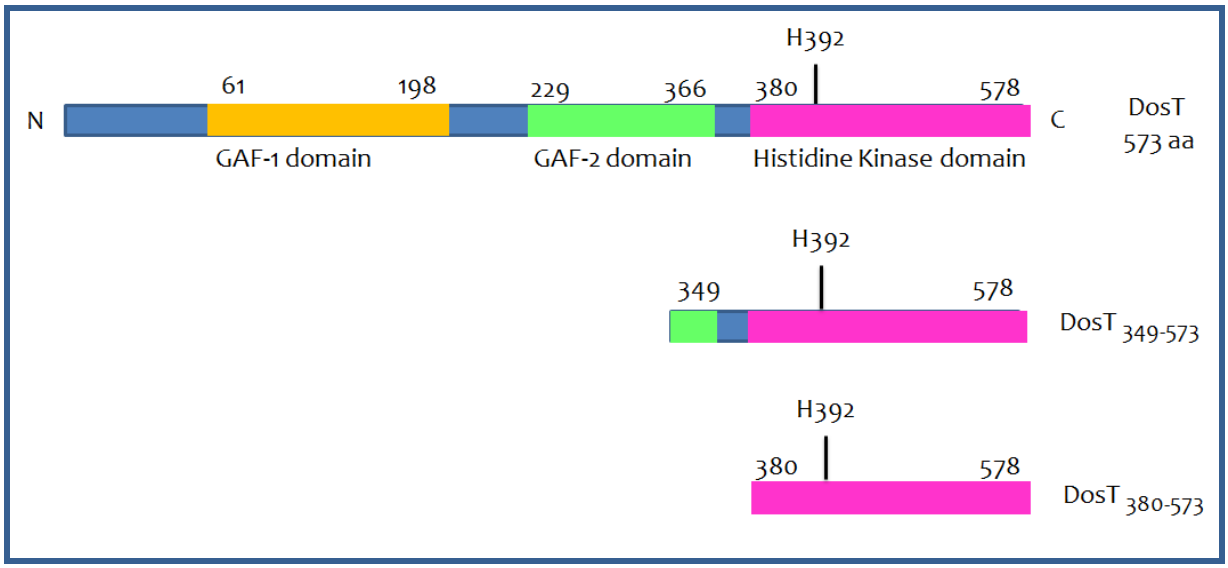

Fig. 21 Features of DosT of *M. tuberculosis*. Full length and truncated forms prepared in this work. Indicated amino acid residue represents conserved histidine residue (H392) in single-letter code.

1.4 Expression and purification of proteins

Induction of recombinant protein expression was performed either by the addition of IPTG to cells growing on LB or by autoinduction in cells growing in autoinducing medium.

IPTG induction

The T7 expression system is widely used for the production of inducible target proteins from cloned genes in *E. coli*. T7 polymerase is so selective, active and processive that most resources of the cell can become directed to producing a great variety of target proteins (Studier & Moffatt, 1986). The expression of recombinant proteins was achieved by IPTG induction of a chromosomally integrated cassette in which the T7 RNA polymerase is expressed from the lacUV5 promoter.

Autoinduction

The autoinduction bacterial expression method (Studier, 2005) is based on the presence of medium components that are metabolized differentially to promote culture growth to high cell densities and subsequently induce protein expression

from *lac*-based promoters. The method allows high cell densities and spontaneous gene induction without monitoring cell growth.

Autoinduction systems often increase cell mass and target-proteins yield substantially compared to conventional IPTG induction in *E. coli* cell cultures (Grabski *et al.*, 2003). In some studies autoinduction produced 5-20 fold increase in target protein per volume of culture compared to IPTG induction (Studier, 2005).

Expression trials

The expression trials were performed for each protein with both autoinduction system and with the use of IPTG as inducing agent. For IPTG induction, proteins expression levels were optimized by adjusting the amount of inducing agent used, time allowed for expression and temperature.

As an example of these trials, DosS overexpression was analysed by SDS-PAGE (Fig. 22). Here, the experiment with different IPTG concentrations (from 0.5 to 2.0 mM), temperatures (20°C, 30°C, 37°C) and induction times (2 h, 4 h, o/n) was performed.

The lower IPTG concentration (0.5 mM) resulted in lower levels of recombinant protein (data not shown). Comparable amounts of recombinant protein were produced in 2 h and o/n cultures, induced at 20°C or 30°C. The best conditions for expression of this protein were selected: 4 h, 37°C, where the protein is overexpressed in high yield.

The trials carried out with autoinduction system showed proteins expression higher in the soluble yield of most proteins, comparing to IPTG induction (data not shown).

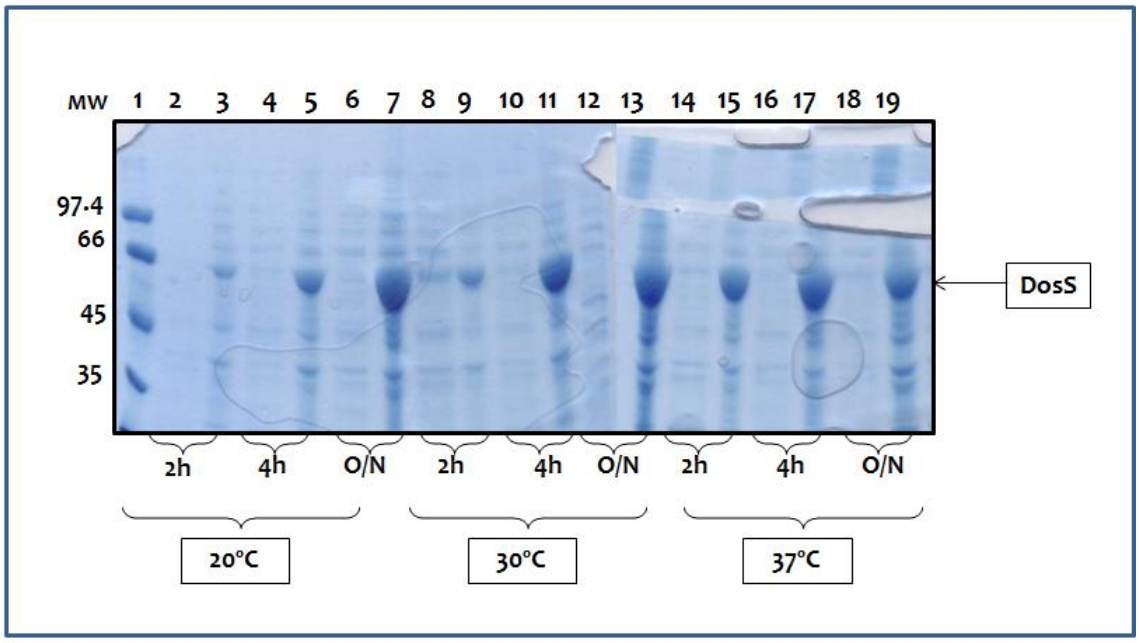

Fig. 22 DosS protein expression trials with 1 mM IPTG. Cell lysates of DosS were analysed. Different conditions (time and temperature) were analysed in this experiment. MW lanes show protein molecular weight marker (kDa); Non-induced cultures: lanes 1, 3, 5, 7, 9, 11, 13, 15, 17; induced cultures: lanes 2, 4, 6, 8, 10, 12, 14, 16, 18.

1.4.1 DosR

1.4.1.1 Expression and purification of wild type DosR and mutant forms of DosR

Overexpressed (IPTG or autoinduction) DosR WT or DosR mutant proteins were purified by IMAC chromatography with 500 mM imidazole in buffer (150 mM NaCl, 100 mM Tris-HCl, pH 8.0). SDS-PAGE analysis revealed that proteins migrated as diffuse bands with the predicted molecular mass of approximately 26 kDa (Fig. 23). All the constructions were expressed as soluble proteins.

The average yields of DosR WT, D54A, [T198A, T205A], [T198D, T205D], [T198E, T205E] proteins were 10 mg/ml, 8 mg/ml, 8 mg/ml, 10 mg/ml and 18 mg/ml, respectively. All the proteins were considered to be >90% pure by Coomassie staining after SDS-PAGE.

The identity of wild-type DosR and mutant proteins DosR were verified by MALDI-TOF.

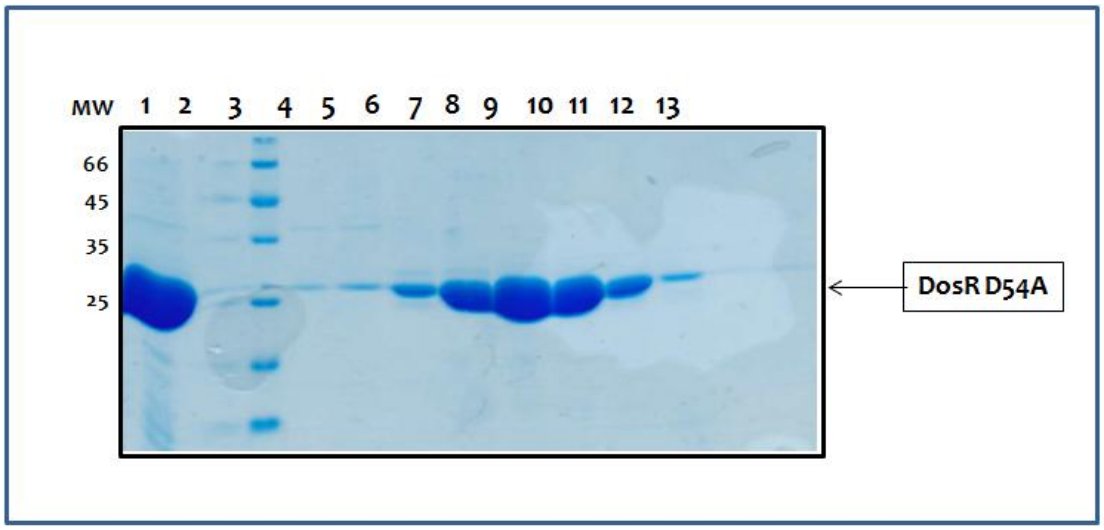

Fig. 23 SDS-PAGE analysis purified DosR D54A mutant protein. Purification fractions: lane 1, concentrated DosR fractions after HisTrap column purification; lanes 2, 4-6, contaminant proteins eluted from column; 7-9, purified DosR; lane 3, protein molecular mass marker.

1.4.2 DosS

1.4.2.1 Expression and purification of full length DosS

Overexpressed (IPTG induction or autinduction) recombinant protein was purified by IMAC chromatography with 500 mM imidazole in buffer (150 mM NaCl, 100 mM Tris-HCl, pH 8.0). SDS-PAGE analysis revealed that proteins migrated as diffuse bands with the predicted molecular mass of approximately 65 kDa. Despite presenting many difficulties in purification (e.g. high aggregation in solution), DosS was expressed as soluble protein with average yield of 15 mg/ml (Fig. 24).

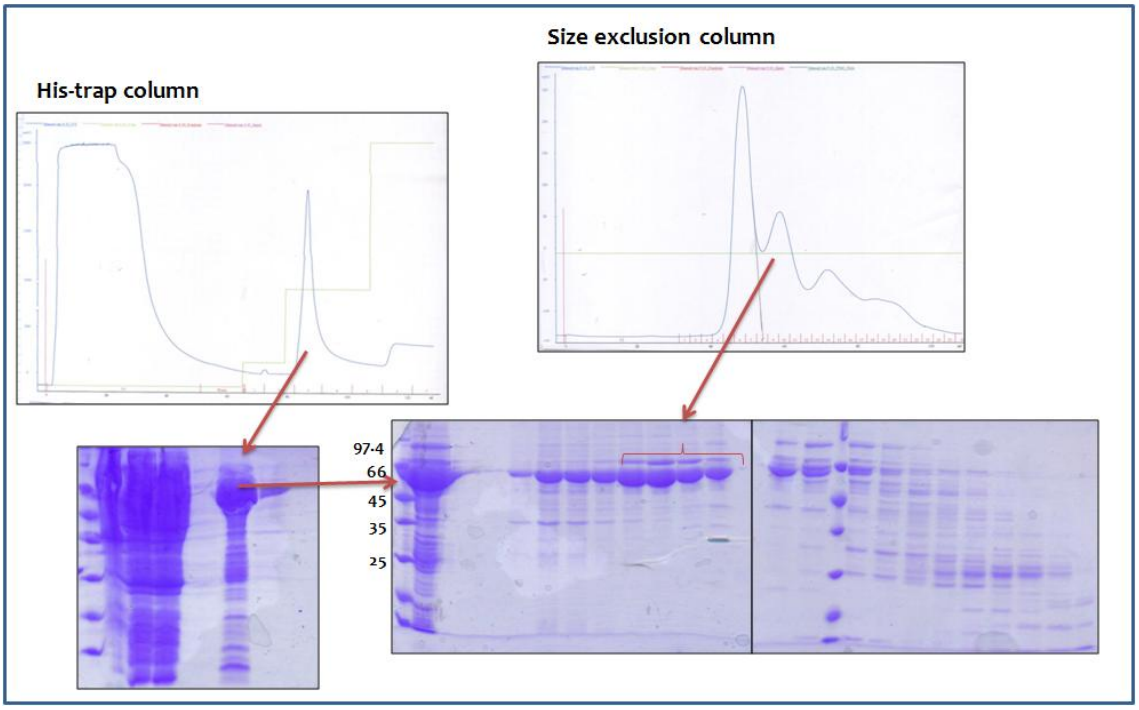

Fig. 24 DosS purification trial. Chromatograms and SDS-PAGE analysis of *E. coli* lysates and purified protein DosS. DosS purified with Ni-affinity column (on the left) was loaded onto size exclusion column. The aggregate and contaminants were separated and purified fractions of DosS were collected.

1.4.2.2 Expression and purification of truncated forms of DosS

Truncated forms of DosS were overexpressed in *E. coli* Bl21 cells by induction with IPTG or by autoinduction. The soluble fractions were purified by IMAC chromatography with 2.5 mM desthiobiotin in buffer (150 mM NaCl, 100 mM Tris-HCl, pH 8.0, 1 mM EDTA). SDS-PAGE analysis revealed that proteins migrated as diffuse bands with the predicted molecular mass of approximately 37 kDa. The average yields of $DosS_{350-578}$ and $DoS_{380-578}$ were 1.6 mg/ml and 3.4 mg/ml, respectively. All the proteins were contaminated by the overexpressed protein ~23 kDa and the contamination was impossible to remove neither by Strep-tactin column nor by size exclusion chromatography. In spite of the contaminants, the proteins were checked for their autophosphorylation capacity.

The identity of full length DosS and truncated forms DosS were verified by MALDI-TOF.

1.4.3 DosT

1.4.1 Expression and purification of full length DosT

Overexpressed (IPTG induction or autoinduction) recombinant protein were purified by IMAC chromatography with 500 mM imidazole in buffer (150 mM NaCl, 100 mM Tris-HCl, pH 8.0). SDS-PAGE analysis revealed that proteins migrated as diffuse bands with the predicted molecular mass of approximately 65 kDa. DosT was expressed as insoluble protein, and refolding trials were unsuccessful (Fig. 25).

Fig. 25 DosT purification trial. Expression trial of DosT with IPTG (left) shows band ~65kDa indicating that IPTG has induced DosT.

1.4.2 Expression and purification of truncated forms of DosT

Truncated forms of DosT were overexpressed in *E. coli* Bl21 cells by induction with IPTG or by autoinduction. The soluble fractions were purified by IMAC chromatography with 2.5 mM desthiobiotin in buffer (150 mM NaCl, 100 mM Tris-HCl, pH 8.0, 1 mM EDTA). SDS-PAGE analysis revealed that proteins migrated as diffuse bands with the predicted molecular mass of approximately 37 kDa. The average yields of $DosT_{349-573}$ and $DosT_{380-573}$ were 2.9 mg/ml and 4.6 mg/ml, respectively. Alike with truncated forms of DosS , the proteins from this experiment were contaminated by the overexpressed protein ~23kDa. Even though the contamination was impossible to be removed neither by Strep-tag column nor by

size exclusion chromatography, the proteins were checked for their ability to autophosphorylate.

The identity of full length DosT and truncated forms DosT was verified by MALDI-TOF.

1.4.4 DosR phosphorylation

Response regulators phosphorylate at their active aspartic acid residue, i.e. Aps54 in the case of DosR, in the presence of phosphoryl donors, such as acetyl phosphate or carbamoyl phosphate. BeF_3^- is reported to mimic phosphorylation on active aspartate residues in response regulators (Cho *et al.,* 2001). To determinate DosR WT phosphorylation the protein was treated with different phosphoryl donors and prepared for MALDI screening as described in M&M chapter (2.5.5.). The MALDI-TOF spectrum of non-treated protein showed a broad peak centred at m/z 24.3664, indicating a molecular mass of DosR of approximately 24 kDa in accordance with the predicted molecular mass (Fig. 26). Analysis of DosR pre-treated with BeF_3^- (Fig. 27A), AcP (Fig. 27B) or CmP (Fig. 27C), revealed other peaks with different molecular masses (Table 7), suggesting the modification of DosR at certain residues.

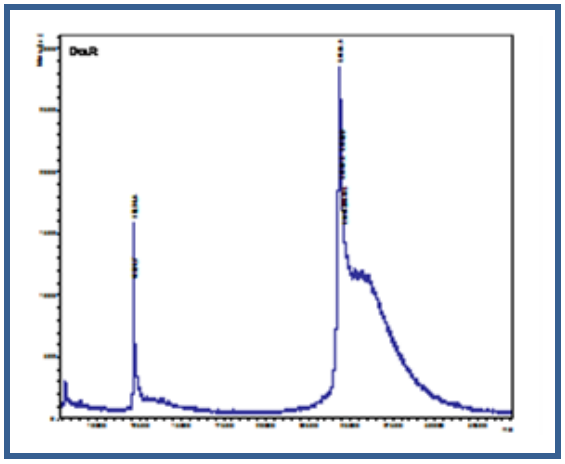

Fig. 26 MALDI spectrum obtained for untreated DosR WT protein.

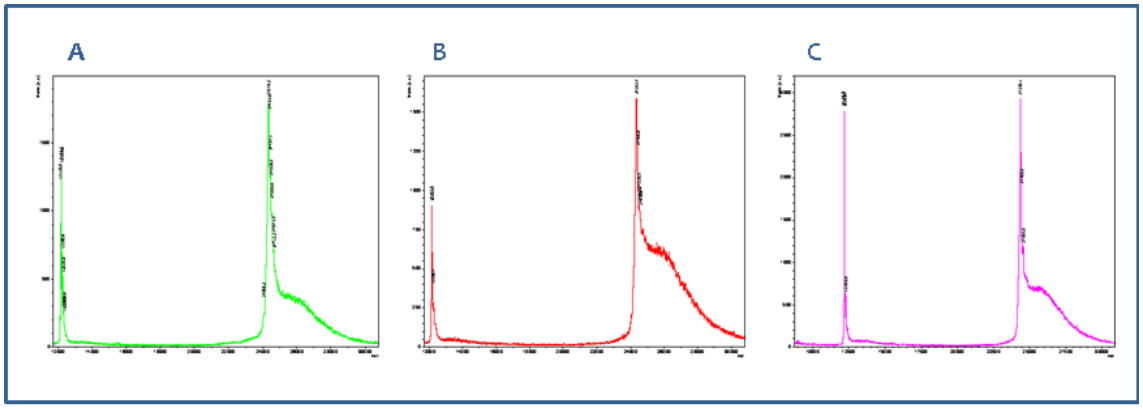

Fig. 27 MALDI spectrum obtained for DosR WT protein pre-treated with BeF_3^- (A), AcP (B) and CmP (C).

Table 7 Proteins recognized by MALDI-TOF. Molecular size (Da): DosR WT: 23261.9; DosR WT in pET21d+, containing His•tagx 6: 24360; BeF_3^-: 103.95; $PO4^{3-}$: 94.97. The weights of the main peaks are highlighted in yellow.

	DosR	DosR + BeF_3^-	DosR+AcP	DosR+CmP
Molecular weights of detected proteins (kDa)	24366.4	24460.6	24454.1	24460.2
	24520.9	24362.4	24348.3	24356.1
	24540.2	24520.5	24432.6	24565.5
	24640.3	24560.8	24536.1	
	24684.4			

To reveal if the residues of interest had been phosphorylated, the pre-treated proteins were digested with trypsin in order to obtain peptides profile by MALDI-TOF screening. DosR pre-treated with BeF_3^- could not be estimated due to the lack of recognition of peptide carrying residue Asp54 by MALDI MS (Fig. 28A). In case of DosR pretreated with AcP (Fig. 28B) or CmP (data not shown), the peptide with the residue of interest Asp54 was recognized, but the molecular weight of the peptide was the exact as of the sample non-treated sample.

The signals from the trypsinised peptides did not result in target phosphopeptides identification. It is often difficult to observe phosphopeptides in protein enzyme digests and map them by MALDI-TOF. Signal intensity from the phosphopeptide is often lower than that of most other peptides due to its low abundance and high instability, so disappearance of such a weak peak after phosphatase treatment is

more difficult to detect. After additional trials of phosphopeptide detection by MALDI TOF and subsequent failures, no further experiments were performed.

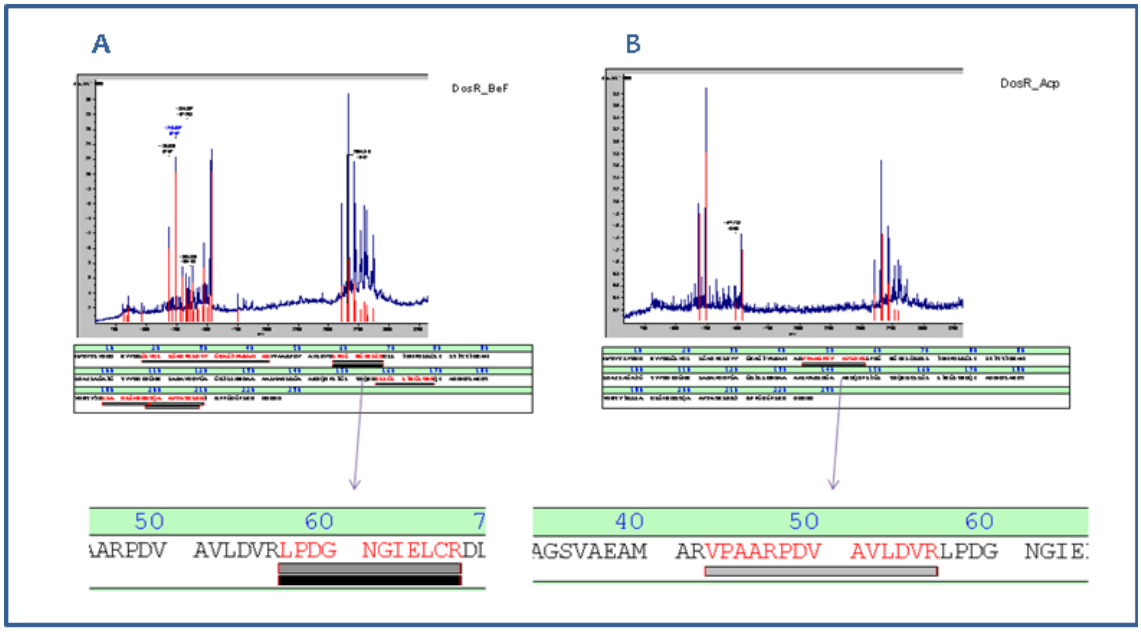

Fig. 28 MALDI-TOF peptides analysis of DosR pre-treated with BeF_3^- (A) or AcP (B).

1.5 Structural determination of active form of DosR

1.5.1 Protein crystallization and diffraction trials

The crystal structure of full-length unphosphorylated (inactive) DosR has already been reported (Wisedchaisri *et al.*, 2008). In this study the production and structural characterization of the phosphorylated (activated) DosR crystal protein has been attempted. The crystal structures of other TCS response regulators in active conformations have been reported before in the presence of BeF_3^- (Yan, 1999; Lee 2001), For this reason, DosR wild type and mutant variants were pre-treated with BeF_3^- prior to being submitted to crystallization trials.

Crystals were obtained using the sitting drop vapour diffusion method. Each experiment consisted of mixing protein solution with reservoir solution and then equilibrating it against reservoir solution.

Only crystals of variants of DosR proteins were obtain when proteins were pre-treated with BeF_3^-. Many crystals of different symmetry were obtained, but few

crystals were reproducible. The best crystals chosen for diffraction trials (Fig. 30, Fig. 33), diffracted very poorly (7-10 Å). Diffraction trials were performed at the European Synchrotron Radiation Facility (ESRF), Grenoble, France.

1.5.1.1 Wild type DosR

In an intensive crystallization screen for wild type DosR many crystal of different forms were obtained: hexagonal, rhombic and needle-like crystals. The best crystals were obtained in the pH range varies from 4 to 8.5.

Small crystals were obtained after ~48 h incubation and accomplished maximum size after ~2 weeks.

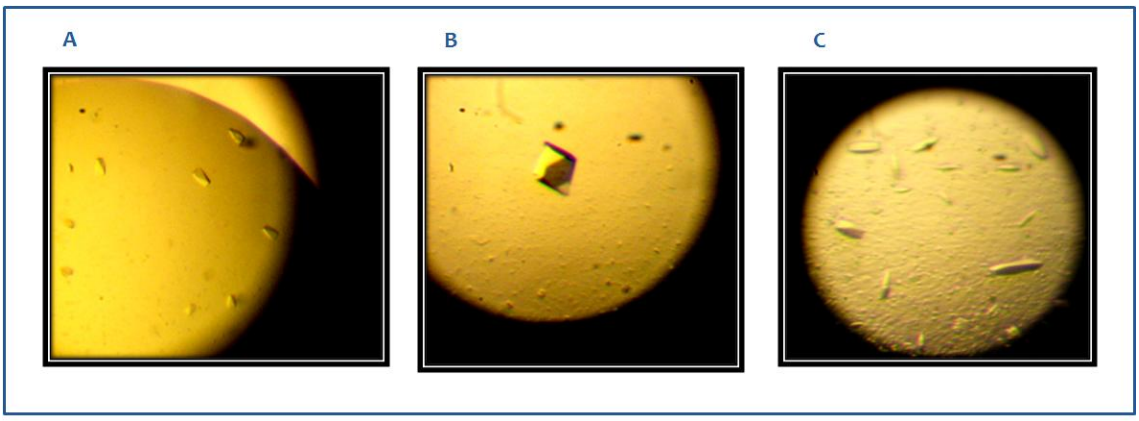

Fig. 29 DosR WT crystals obtained in the crystallization plates. (A). 5 mM BeF_3^-, 2.6 M sodium chloride, 0.15 M ammonium phosphate, 0.1 M Bis-Tris, pH 7.8. (B). 5 mM BeF_3^-, 4% isopropanol, 2.5 M sodium chloride, 0.1 M Bis-Tris, pH 7.8. (C). 5 mM BeF_3^-, 4% isopropanol, 2,5 M sodium chloride, 0.1 M MMT, pH 4.0.

The best crystal was transferred to a cryoprotectant solution and flash frozen in liquid nitrogen. The crystal diffracted to 10 Å ressolution.

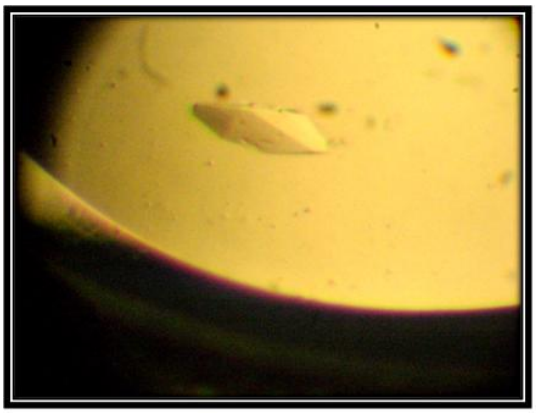

Fig. 30 DosR crystal chosen for diffraction trial. 5 mM BeF_3^-, 4% isopropanol, 2.75 M NaCl, 0.1 M MMT, pH7.4.

1.5.1.2 DosR [T198A, T205A]

Very few crystals were obtained for DosR [T198A, T205A] and most of them were not reproducible.

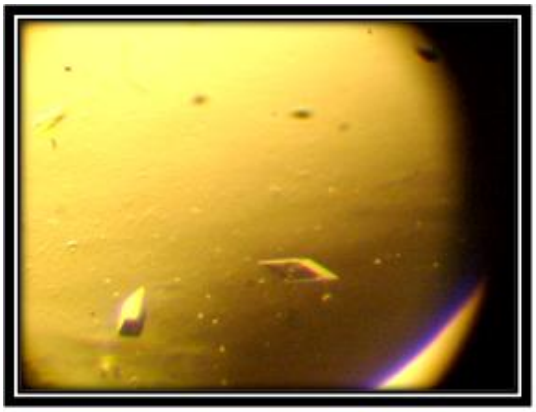

Fig. 31 Example of DosR [T198A, T205A] crystal. 5 mM BeF_3^-, 1.6 M magnesium sulfate, 0.1 M MES sodium salt, pH 6.5.

1.5.1.3 DosR [T198D, T205D]

DosR [T198D, T205D] crystallized rapidly and in wide range of different conditions. Different crystal forms were observed. The best crystals were obtained in the pH range varies from 6.5 to 8.0. Needle-shaped crystals appeared after ~2 h incubation. Hexagonal crystals were obtained after ~24 hours and accomplished maximum size after ~1 week.

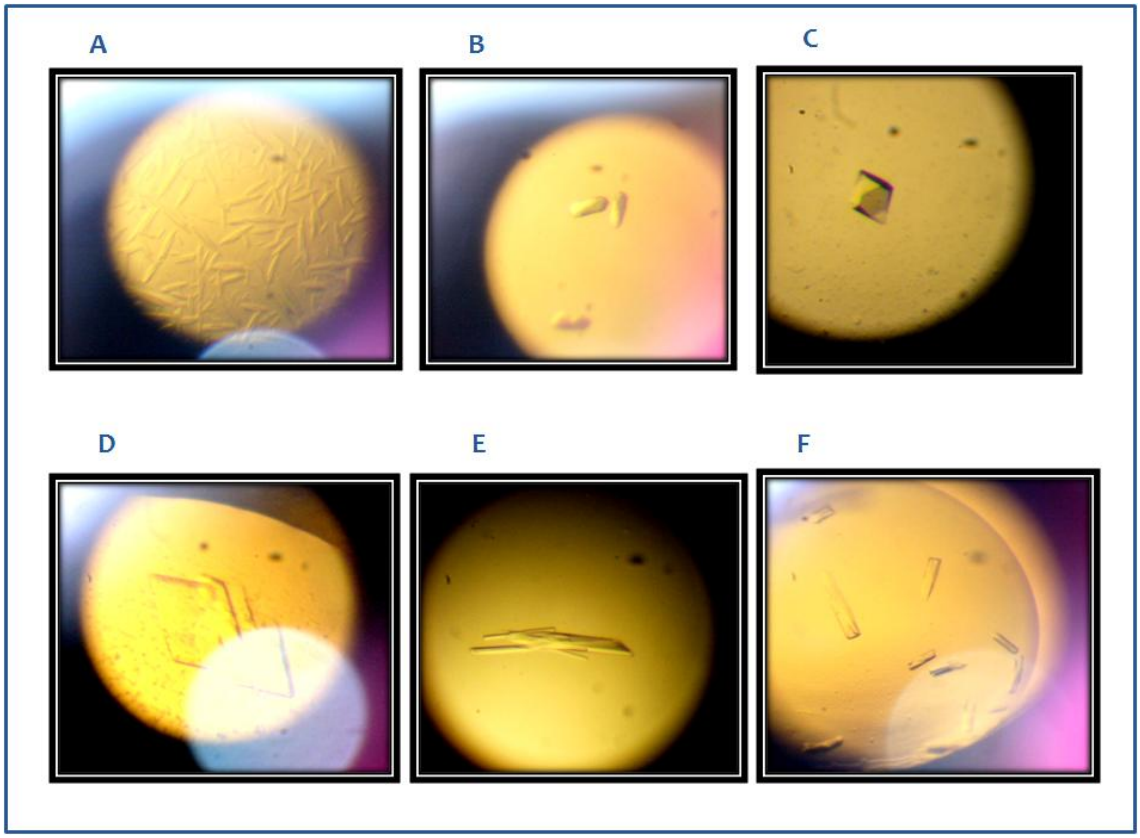

Fig. 32 DosR [T198D, T205D] crystals obtained in the crystallization plates (A). 5 mM BeF_3^-, 8% PEG 8000 MME, 0.2 M lithium chloride, 0.05 M magnesium sulphate. (B). 5 mM BeF_3^-, 0.1 M potassium chloride, 4% PEG 6000, 0.1 M Bis-Tris pH 6.5. (C). 5 mM BeF_3^-, 0.15 M magnesium chloride, 10% PEG 2000 MME, 0.1 M MES pH6.8. (D). 5 mM BeF_3^-, 0.1 M magnesium chloride, 8% PEG 6000, 0.1 M Tris pH 8.0. €. 5 mM BeF_3^-, 0.1 M potasium chloride, 3% PEG 6000, 0.1 M Tris-HCl pH 8.0. (F). 5 mM BeF_3^-, 0.2 M Sodium acetate, 15% PEG 8000, 0.1 M MES sodium salt, pH6.5

The best crystal was transferred to a cryoprotectant solution and flash frozen in liquid nitrogen. The crystal diffracted to 7 Å ressolution.

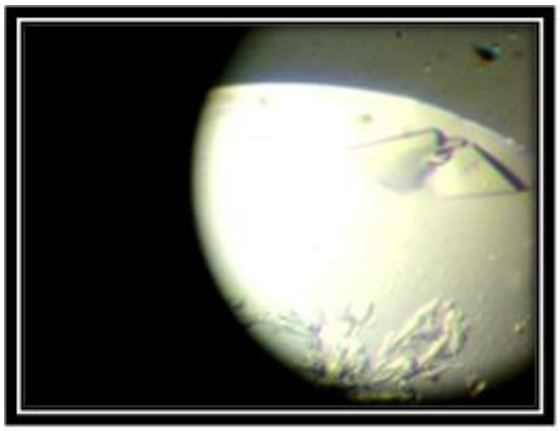

Fig. 33 DosR [T198D, 205D] chosen for diffraction trial. 5 mM BeF_3^-, 15% PEG 8000, 0.2 M sodium acetate, 0.1 M MES sodium salt, pH 6.5.

1.6 DosR-DosS interaction

Protein–protein interaction between DosR and DosS were analysed through ITC and *in vitro* phosphorylation assays.

1.6.1 ITC

ITC was used to analyse protein-protein interactions between DosR and DosS. The assays were performed at 21°C with purified proteins dialyzed against the same buffer.

ITC technique is very sentitive to little changes in the protein environment and even though various conditions and proteins concentrations were examined, the interaction between response regulator DosR and correspond histidine kinase DosS was not potent enough to be clearly observed with ITC. In experiment shown in Fig. 34, a solution containing 5 mM of DosR was used as titrant, whereas solution containing 25 µM of DosS was used in the calorimetry cell.

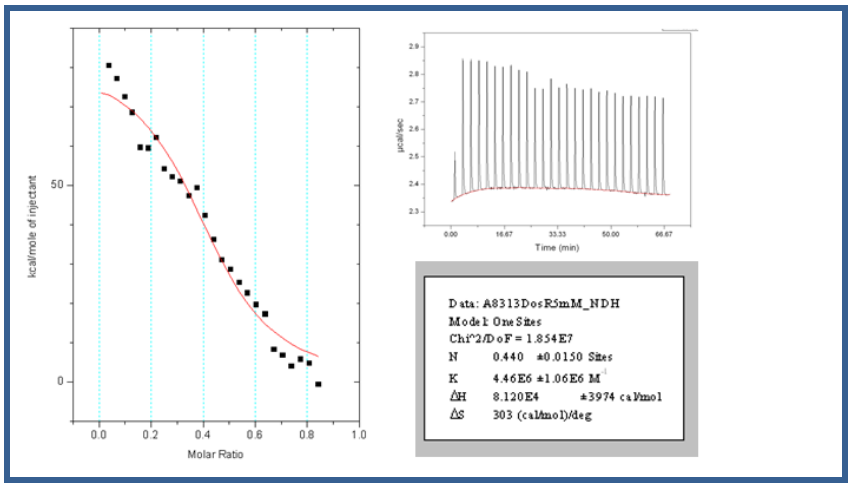

Fig. 34 DosR-DosS interaction measured by ITC. 5 mM of DosR and 25 µM DosS was used. Figure represents raw binding heats (on the right) and the integrated heat data (on the left).

1.6.2 Autophosphorylation of DosS and truncated forms of DosS and DosT

The first steps in two-component signal transduction are the signal recognition by the sensor histidine kinase followed by dimerization and autophosphorylation at a specific His residue (Hoch & Silhavy, 1995). Purified DosS was incubated at room temperature with 0.5 µCi [γ-^{32}P]ATP, and aliquots of the reaction were removed for analysis at 5, 30 and 120 min. The aliquots were electrophoresed in 12% SDS-PAGE gels, which were subsequently dried and visualized by autoradiography (Fig. 35).

The autophosphorylation assay showed that full-length DosS was able to autophosphorylate and that it incorporated the maximum amount of radiolabelled ATP at 2 hour time point (data not shown). In a time course phosphorylation assay (1 to 120 min) DosS was rapidly labelled with [γ-^{32}P]ATP: about 85% and 97% of the maximum radioactivity incorporated in the protein was detected at 60 min and 90 min, respectively (Fig. 35).

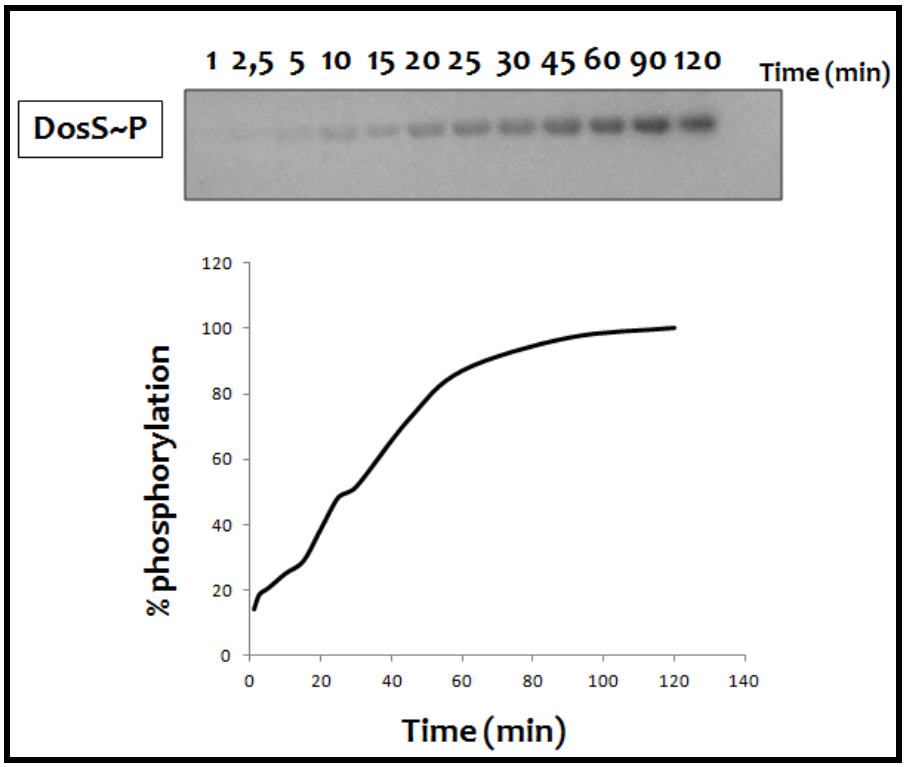

Fig. 35 Time-dependent autophosphorylation of DosS. Protein was incubated in reaction buffer as described and samples were removed at indicated time points and analysed by 12% SDS-PAGE.

To investigate whether full length of histidine kinases is required for autophosphorylation, truncated versions of histidine kinases were tested for their *in vitro* autokinase activity in the same manner as full length DosS. $DosS_{350-578}$, $DosT_{349-573}$ and $DosT_{380-573}$ autophosphorylated in the presence of [γ-^{32}P]ATP, which proved their autophosphorylation activity (Fig. 36). The truncated form $DosS_{380-578}$ did not autophosphorylate, which might be due to possible disruption in the secondary structure caused by too short amino acid sequence when designing the truncation.

Taking into account these activity results and the degree of protein purity obtained with full-length and truncated protein samples, only full length DosS was used for further enzymatic phosphorylation assays.

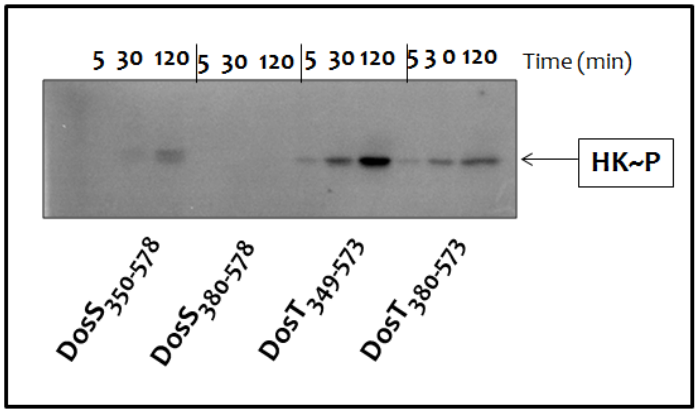

Fig. 36 *In vitro* autophosphorylation of truncated forms of DosS and DosT. Truncated forms of proteins DosS and DosT: $DosS_{350-578}$, $DosT_{349-573}$, $DosT_{380-573}$ and $DosS_{380-578}$ were incubated in reaction buffer as described and samples were removed at indicated time points and analysed by 15% SDS-PAGE.

1.6.3 Phosphotransfer from histidine kinase to response regulator

In TCS signalling cascades, once HK is autophosphorylated, HKs transfer the phosphate moiety from His-P to the active aspartic acid residue of their cognate RR. This phosphotransfer was analysed for wild type and mutant versions of DosR using full length of DosS protein.

1.6.3.1 Phosphotransfer from DosS to wild-type DosR

To assess phosphotransfer from DosS to DosR, wild type DosR was added to the autophosphorylated DosS. A fast phosphotransfer from DosS to DosR (0.5 min) was observed with a maximum of DosR phosphorylation at 1 min and quick decrease to nearly complete dephosphorylation of both proteins within 20 min (Fig. 37).

To rule out the possibility that DosR phosphorylation was due to autophosphorylation, a control phosphotransfer reaction was performed, where DosR was incubated with [γ-^{32}P]ATP in the absence of DosS. No phosphorylation of DosR was observed under those conditions as no labelling was observed (data not shown).

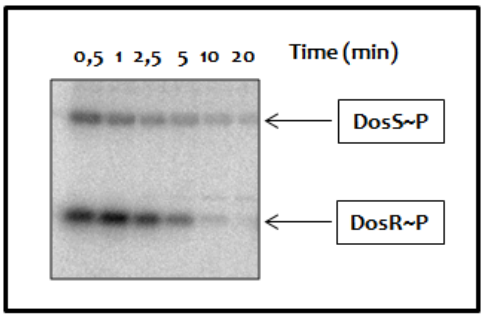

Fig. 37 Phosphotransfer from DosS~P to wild-type DosR. DosS was incubated with 0.5 µCi [γ-^{32}P]ATP for 60 minutes and added to DosR. Samples were removed at indicated time points and analysed by 15% SDS-PAGE. It is observed that DosS~P transfers the phosphate donor to cognate response regulator DosR.

1.6.3.2 Phosphotransfer from DosS to DosR D54A

Aspartic acid residue Asp54 in *Mtb* DosR has been described to be the receiver residue of DosS histidine kinase phosphatase activity. Mutagenesis of the Asp54 residue to Val (Saini *et al.*, 2004a) or Glu (Roberts *et al.*, 2004), the residues incapable of receiving the donor phosphate, rendered DosR protein unable to accept the phosphoryl moiety from DosS~P. That result determined that the phosphorelay proceeded in a manner consistent with two-component response regulators.

To confirm the specificity of the phosphorelay from DosS to DosR proteins of this study, phosphotransfer assays using DosR D54 mutant was performed. Autophosphorylated DosS could not transfer the phosphate moiety to DosR D54A (Fig. 38), in agreement with Asp54 being the acceptor residue of DosR for phosphotransfer.

1.6.3.3 Phosphotransfer from DosS to DosR double mutants

As it was mentioned before, DosR can be phosphorylated by PknH in residues Thr198 and Thr205. To evaluate the implication of Thr198 and Thr205 residues in the phosphotransfer from DosS to DosR, three double mutant proteins at these residues were constructed. The change of threonines to aspartic acid and glutamic acid residues was chosen because these negatively charged amino acids are

considered to function as phosphomimetic substitutions. The mutation to alanines was selected as control of silencing substitutions (Wang & Klemke, 2008).

To evaluate the synergism of DosS phosphorylation with PknH we carried out phosphotransfer assays form DosS to the different DosR Thr mutant proteins. In the presence of DosR double mutants, (DosR [T198A, T205A], DosR [T198D, T205D] and DosR [T198E, T205E]) phosphorylated DosS transfered the phosphor moiety to each response regulator (Fig. 38). DosR [T198A, T205A] behaved similarly to the wild type responseIn contrast, the threonine phosphomimicking versions, DosR [T198D, T205D] and DosR [T198E, T205E] were more efficiently phosphorylated by DosS, since both the level of phosphorylation (2-fold higher level of phosphorylation at time point 10 minutes) and the speed (almost 100% of the DosS-associated phosphosignal is being transferred within 1 min of reaction) increased This significant finding is discussed in details in the discussion section.

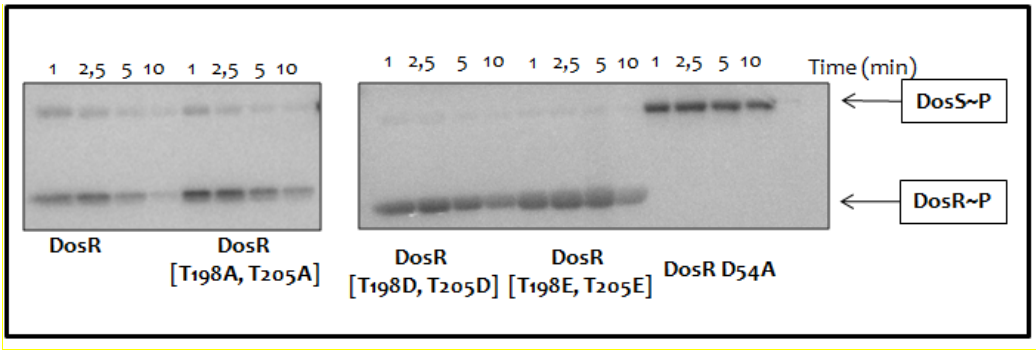

Fig. 38 Phosphotransfer from DosS~P to DosR and DosR mutant proteins. DosS was incubated with 0.5 µCi [γ-^{32}P]ATP for 60 minutes and added to DosR. Samples were removed at indicated time points and analysed by 15% SDS-PAGE.

1.6.3.4 Phosphotransfer from DosS to triple mutant DosR

To analyse if the increased and more stable phosphorylation in DosR [T198D, T205D] and DosR [T198E, T205E] was due to a more efficient phosphotransfer from DosS to DosR's Asp54 or to phosphotransfer to other potential HKs phosphoaccepting groups (i.e. aspartate or glutamate residues along the response regulator protein), a triple mutant, DosR [D54A, T198D, T205D] was constructed. There was no observable phosphotransfer throughout the 10-min time course, with the triple mutant behaving as the DosR D54A mutant (Fig. 39). These results indicated that

Asp54 was still the DosS specific phosphoacceptor in DosR [T198D, T205D] and DosR [T198E, T205E] mutants.

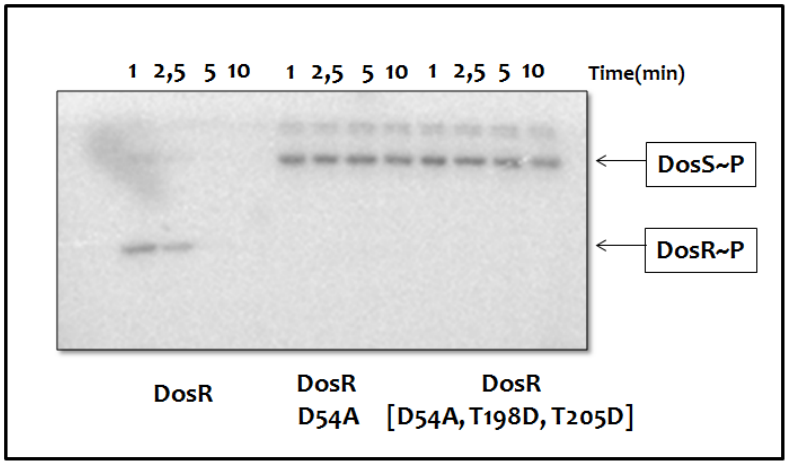

Fig. 39 Phosphotransfer from DosS~P to DosR [D54A, T198D, T205D]. DosS was incubated with 0.5 µCi [γ-^{32}P]ATP for 60 minutes and added to DosR. Samples were removed at indicated time points and analysed by 15% SDS-PAGE.

1.6.3.5 Acetyl-phosphate phosphorylation

To study if the observed higher efficiency in phosphorylation was DosS-dependent, we compared phosphorylation of wild-type DosR, DosRT198A/T205A, DosRT198D/T205D and DosRT198E/T205E using [^{32}P]-acetyl phosphate as the phosphodonor. Low-molecular-weight compounds such as acetyl phosphate (AcP) have been described to serve as phosphodonors for response regulators phosphorylation both *in vitro* and *in vivo* (Lukat *et al.*, 1992; Kenney *et al.*, 1995; Klein *et al.*, 2007). The phosphorylation pattern of wild-type DosR, DosR [T198A, T205A], DosR [T198D, T205D] and DosR [T198E, T205E] using [^{32}P]-acetyl phosphate as phosphodonor was analysed. Radioactive [^{32}P]-AcP and DosR WT or mutant proteins were incubated for up to 120 min. The experiment showed that DosR [T198A,T205A], phosphorylated in the presence of acetyl phosphate slightly more efficiently than wild-type. However, the AcP-dependent phosphorylation of DosR [T198D, T205D] and DosR [T198E, T205E] were clearly enhanced compared to wild type DosR protein (Fig. 40). Quantification of phosphorylation level showed that DosR [T198A,T205A], DosR [T198D, T205D] and DosR [T198E, T205E]

phosphorylated 2-fold, 4-fold and 5-fold faster than WT, respectively. Mutant DosR D54A was not phosphorylated when treated with ^{32}P-acetyl phosphate (data not shown).

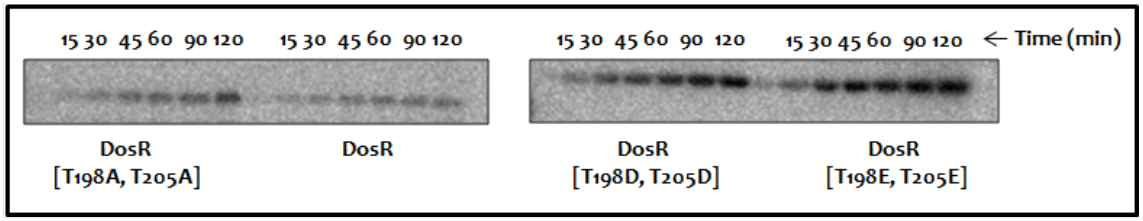

Fig. 40 DosR and DosR mutant proteins phosphorylation by [^{32}P]-acetyl phosphate. Radioactive [^{32}P]-AcP and DosR WT or mutant proteins were incubated for up to 120 min. DosR. Samples were removed at indicated time points and analysed by 15% SDS-PAGE.

1.6.4 Phosphatase activity of DosS

Histidine kinases can exhibit phosphatase activity towards their cognate response regulators.

The phosphatase activity of DosS has not been described before, so in this study it was investigated if DosS has the capacity to dephosphorylate DosR~P. To rule out the potential phosphatase activity coming from DosR itself, negative control reaction were set up in the absence of DosS. First, we checked the stability of DosR~P phosphorylated by AcP in Asp54. DosR~P was highly stable with an apparent half-life of 30 min. When DosS was added, the radiolabelled signal on DosR started to disappear after 5 min and it was almost completely eliminated after 30 min (Fig. 41). Therefore, DosS has a significant phosphatase activity that accelerates 6 fold the dephosphorylation of DosR. However, DosS did not show phosphatase activity on phosphorylated DosR [T198E, T205E].

Phosphatase activity of DosS against DosR~P is extensively debated in the discussion section.

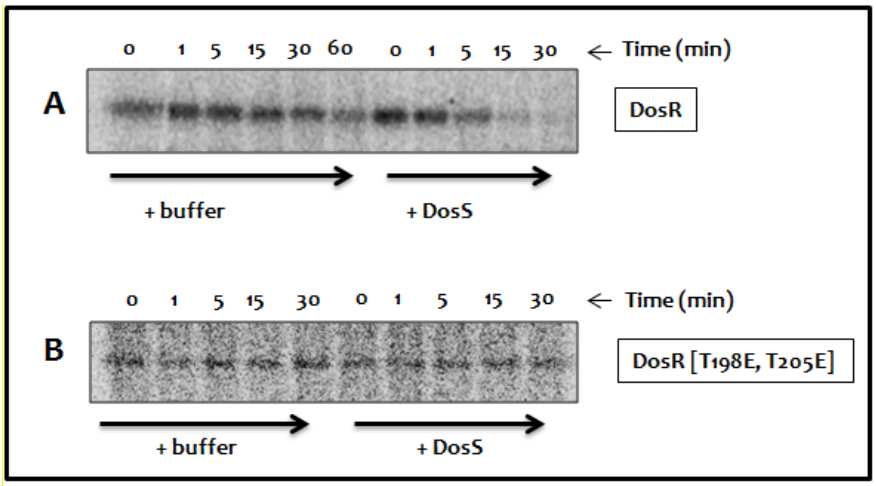

Fig. 41 Phosphatase activity of DosS on phosphorylated wild type DosR (A) and mutant DosR [T198E, T205E] (B). Wild-type DosR and DosR [T198E, T205E] previously phosphorylated with [^{32}P]-AcP were treated for 30 min time course with unphosphorylated DosS. Samples were removed at indicated time points and analysed by 15% SDS-PAGE.

1.6.5 Modelling HK-RR interaction

Disclosure of protein-protein interaction is crucial for the investigation of intracellular signaling pathways. Using *in silico* molecular modeling, the mechanism of intermolecular phosphotransfer between response regulator DosR and histidine kinase DosS was proposed in this study. The key residues involved in this interaction were studied.

Structures of some response regulators have been revealed and can be used as templates to predict the 3D structure of other regulators by homology modelling. The known structures of response regulators have receiver domains composed of alternating α-helices and β-sheets. The 3D shape resembles a barrel composed of five α/β sequential segments [(αβ)5], with parallel β-sheets surrounded by the α-helices. The aspartate residue that is phosphorylated occurs at the tip of one of the internal β-sheets, almost in the loop that connects it to the next α-helix. These structural feature appear to be conserved in the receiver domains of the majority of response regulators whose structure has been determined or modelled so far (Alves *et al.*, 2003).

Crystal structure of non-phosphorylated inactive DosR has been solved (Wisedchaisri *et al.*, 2008) showing that full length DosR is composed of an N-

terminal domain (receiver domain), a C-terminal domain (DNA-binding domain) and the linker region. DosR belongs to the NarL subfamily of TCSs although this RR has some differential features when compared to the rest of proteins of the same family. The N-terminal domain of DosR lacks one α/β segment compared to the canonical (αβ)5 arrangement. The C-terminal domain contains four α-helices named α7, α8, α9, and α10. This domain has an unusual conformation where the first α-helix in the N-terminal domain packs against helix α10 which moves away from the core constructed by helices α7 to α9. The linker region consists of helices α5 and α6 with high flexibility of the second one. Sequence alignments of DosR with other RRs, for example RR468 from *Thermotoga maritima*, confirmed that *M. tuberculosis* DosR lacks one αβ segment (Fig. 42).

The crystal structure of the C-terminus DosR (DosRC) in complex with DNA oligonucleotides has also been solved (Wisedchaisri *et al.*, 2005). In this structure, DosRC uses the α10 helix to form a functional dimer for DNA binding. These available structures were considered in this study, when modelling DosR-DosS complex with HADDOCK software.

DosS structure has not been reported hitherto. Previously solved structure of histidine kinase HK853 in complex with its cognate response regulator RR468 of *Thermotoga maritima* (Casino *et al.*, 2009) was also used to construct DosR-DosS model. Interfacing residues in *T. maritima* HK853-RR468 complex were proposed and identified by site-directed mutagenesis (Casino *et al.*, 2009). In HK853 they were: Thr267, Tyr272, and in response regulator they were: Ile17, Phe20.

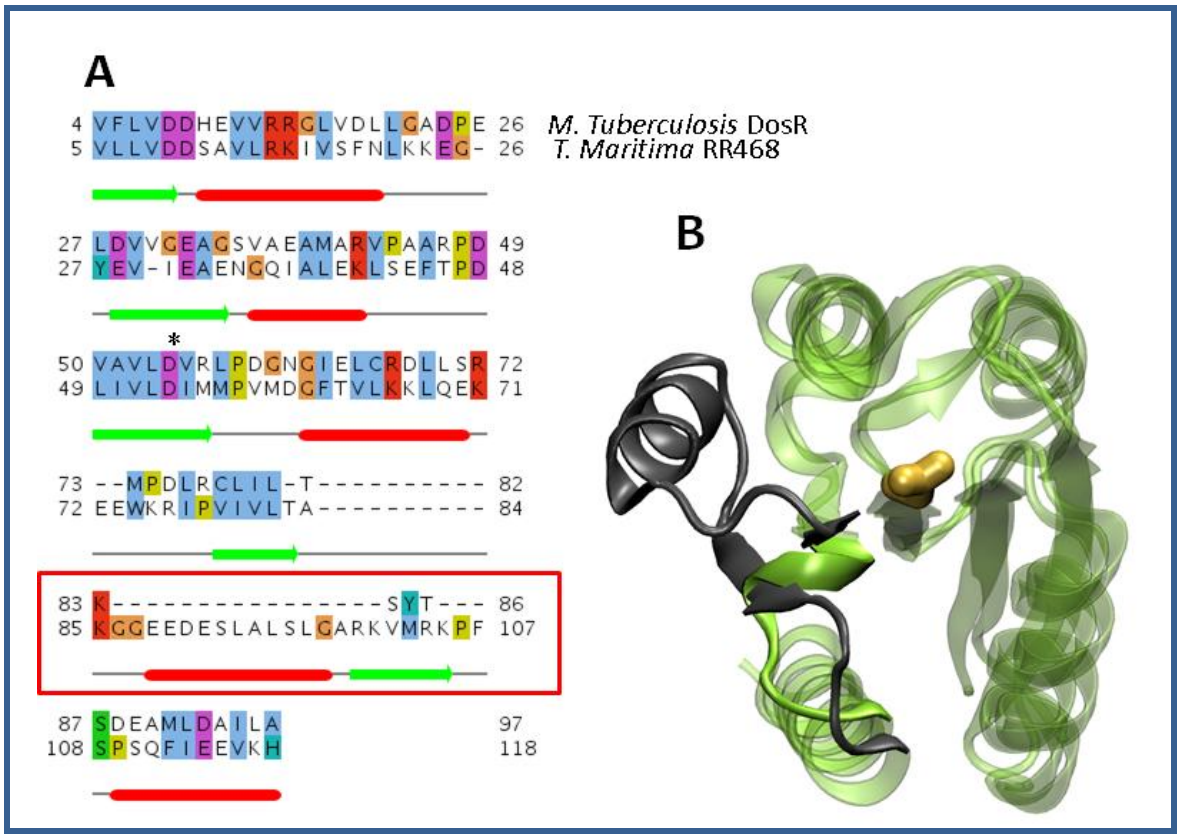

Fig. 42 Sequence and structural alignments of *M. tuberculosis* DosR and *T. maritima* RR468. (A). Sequence alignment of *M. tuberculosis* DosR and *T. maritima* RR468. The red box denotes the missing αβ segment in DosR. Similarities in aminoacids are marked with colours. The star indicates the conserved aspartic residue in receiver domain of response regulators: Asp54 in DosR and Asp53 in RR468. (B). Structural alignment of DosR (green) and RR468 (grey). Conserved Asp residue is highlighted in gold.

Mtb DosS and *T. maritima* HK853 histidine kinases consist of two GAF domains and histidine kinase domain. There are seven families in clan His_Kinase_A of histidine kinase domains. Histidine kinase domain from *T. maritima* HK853 belongs to HisKA family while histidine kinase domain from *M. tuberculosis* DosS belongs to HisKA_3. Moreover, sequence comparison show that phosphate donor site (conserved histidine) is shifted one amino acid position in the sequence alignment with respect to other subfamilies (Fig. 43).

These proteins are mainly built up from alpha-helices, this shift in sequence was translated into a rotation about 60 degrees in the 3D structure. In the model of DosS structure, the conserved histidine residue is rotated 60 degrees when compared to the structure of the histidine kinase from *T. maritima* HK853. The

location of phosphoacceptor in DosS and subsequent rotation of DosR caused *T. maritima* model unhelpful for DosR-DosS structural prediction.

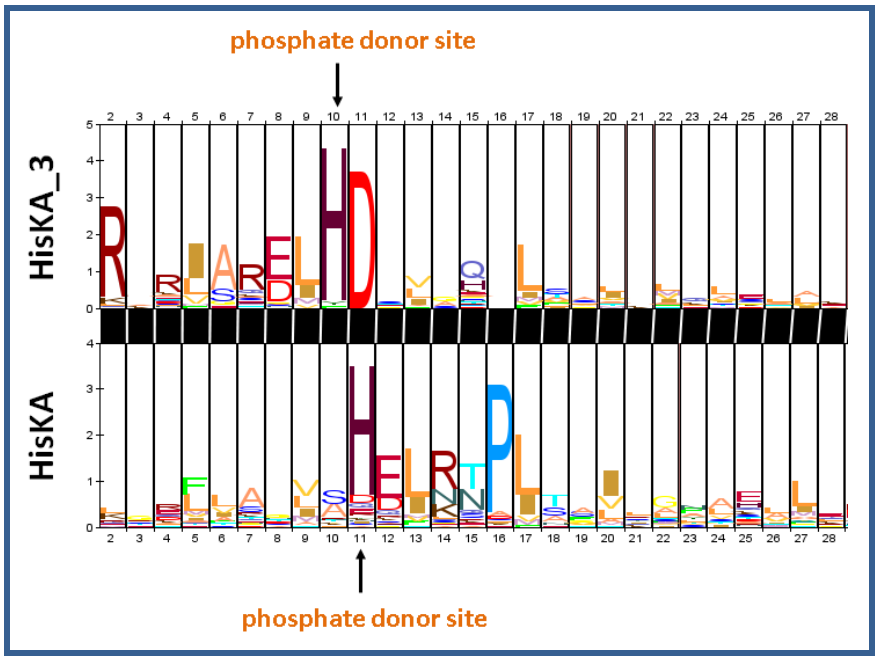

Fig. 43 Sequence comparison of HisKA and HisKA_3 families. The phosphate donor site (conserved histidine) are highlighted in purple and annotated with arrows.

Upon BLAST search of DosS homologous genes (HisKA_3) with known protein structure, DesK from *B. subtilis* was identified. The sequence comparison of DosS and DesK showed that both proteins are homologous with a 90% of sequence identity (5e-12 E-value) in the histidine kinase domain (Fig. 44). Thus, the solved structure of histidine kinase of DesK served in this study, apart from *T. maritima* complex, as a template for modelling DosS in DosS-DosR complex.

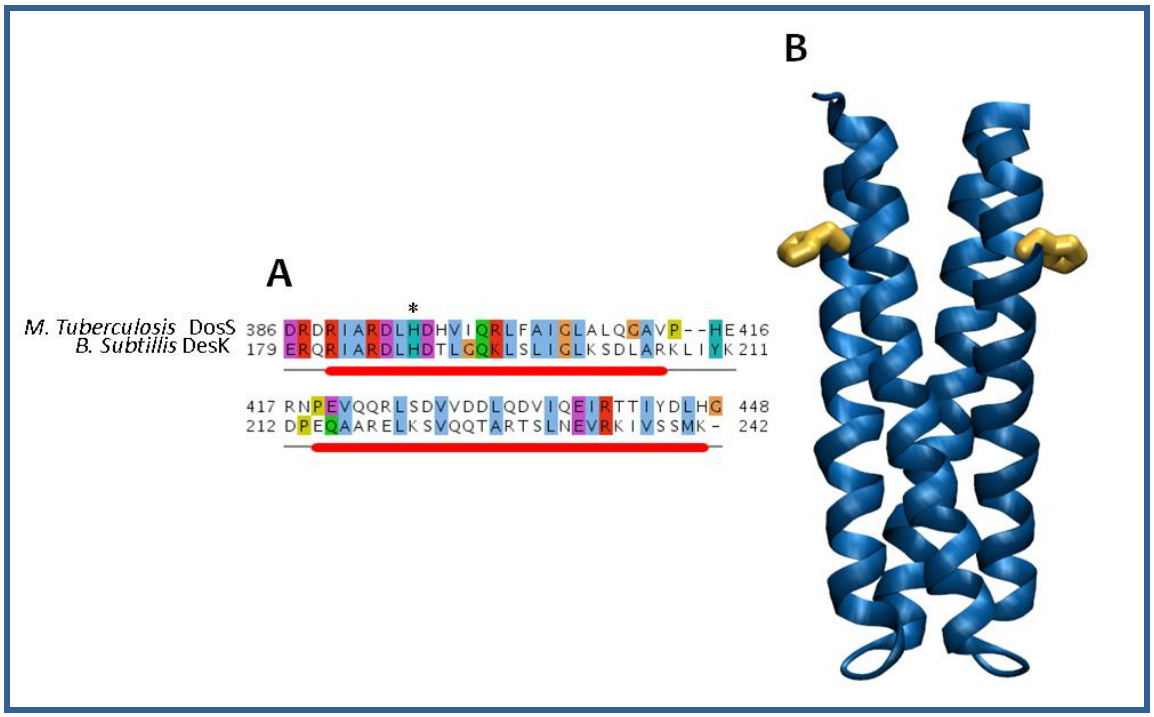

Fig. 44 Sequence alignment and structure of histidine kinase domains. (A). Sequence alignment of histidine kinases domains of *M. tuberculosis* DosS and *B. subtillis* DesK. The star indicates the conserved His residue in histidine kinase domains (His395 in DosS and His188 in DesK). Similarities in aminoacids are marked with colours. (B). Structure of histidine kinase domain of DesK. His188 is highlighted in gold.

For modelling the structure of the complex, protein-protein virtual docking was performed with HADDOCK software. Only those models in which histidine H395 (from DosS) and aspartate D54 (DosR) were facing each other at an interacting distance lower than 3 Å were considered.

Prediction model of DosR-DosS complex upon the structures of non-phosphorylated response regulator DosR from *Mtb* and histidine kinase DesK from *B. subtillis* showed the rotation about 60 degrees of response regulator DosR against histidine kinase DosS (Fig. 45). A genuine overlap between hydrophobic and polar aminoacids (Val12 of DosR with Gln400 of DosS and Ala404 of DosS; Leu20 of DosR with Leu407 of DosS, Glu88 of DosR with Gln410 of DosS, Phe403 of DosS with Val13 of DosR and Leu17 of DosR) was maintained at the DosR-DosS interface, generating His395 directly pointing at Asp54 ready for proper phosphoryl transfer.

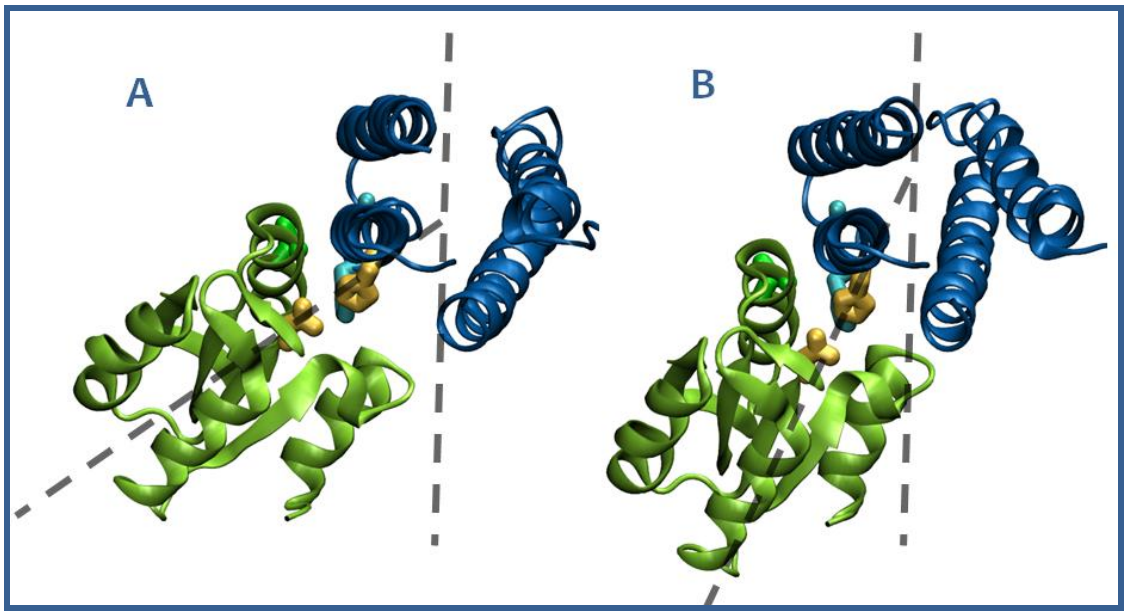

Fig. 45 The complexes of HK-RR. (A). Reported structure of HK853-RR468 complex of *T. maritima*. (B). Predicted model for DosR–DosS complex. Conserved aspartic residues (RR) and histidine residues (HK) are highlighted in gold. Histidine kinases are shown in green and response regulators are shown in blue.

The analysis of the interfaces of DosR and DosS showed good overlap of amino acid types and allowed detection of key residues for the proteins interactions. Exposed hydrophobic amino acids were: Val12 and Leu20 in DosR; Phe403 and Leu407 in DosS.

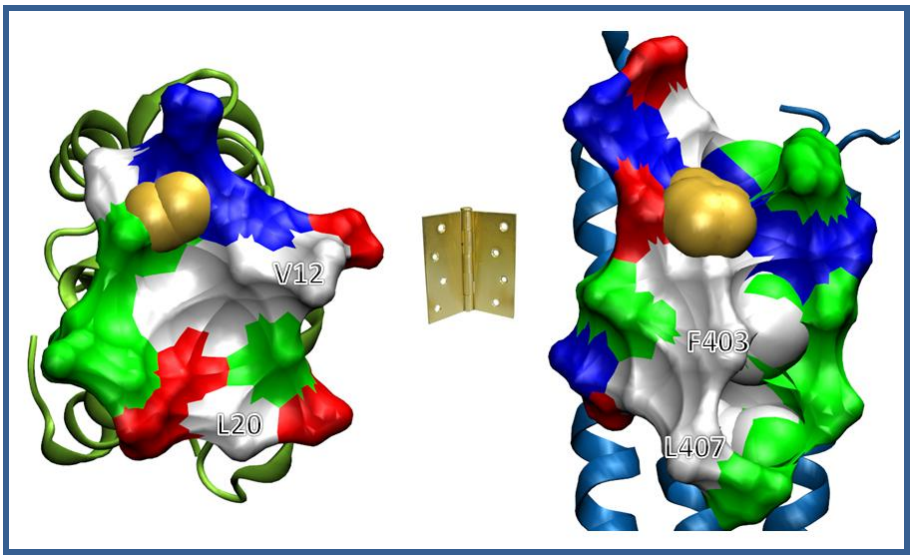

Fig. 46 The interfaces of DosR (left) and DosS (right) with exposed hydrophobic amino acids: Val12 and Leu20 in DosR; Phe403 and Leu407 in DosS. Polar amino acids are highlighted in green, non-polar in white, positive in blue and negative in red.

1.7 DosR-DNA binding

The electrophoretic mobility shift assay (EMSA) was developed based on the observation that a DNA fragment mobility is retarded in a gel when it complexes with a DNA-binding protein (Garner and Revzin, 1981). DNA binding efficiency of the DosR and its mutant counterparts were examined using this technique. It had been previously determined that DosR recognizes variations of a 20-bp palindromic sequence that precedes nearly all of the *Mtb* genes initially upregulated by hypoxia (Park *et al.,* 2003; Florczyk *et al.,* 2003). Furthermore, the crystal structures of the DosR C-terminal domain in complex with DNA sequence including the proper consensus was reported (Wisedchaisri *et al.,* 2005). This precise DNA sequence containing a 20 bp consensus motif was used as probe for EMSAs.

It has been reported that phosphorylation of DosR in Asp54 promotes its DNA-binding capacity (Roberts *et al.,* 2004) and that phosphorylation in Thr198 and Thr205 by PnkH enhances this ability (Chao *et al.,* 2010). In this study, exploiting DosR mutant forms, EMSAs were performed to evaluate the role of key residues of DosR in its activation and in DNA binding efficiency.

1.7.1 Wild-type DosR binding to DNA

To analyse the interaction of DosR with its cognate DNA, EMSAs were carried out using purified wild-type DosR protein with or without pre-treatment with different phosphoryl donors, such as acetyl phosphate (AcP) or carbamoyl phosphate (CmP) to induce protein phosphorylation. BeF_3^-, which has been reported to serve as a phosphate analogue in proteins phosphorylated on aspartate residues (Cho *et al.,* 2001) was also used (Fig. 50). DosR-DNA binding was observed in the presence of 0.5 μM of DosR (Fig. 47).

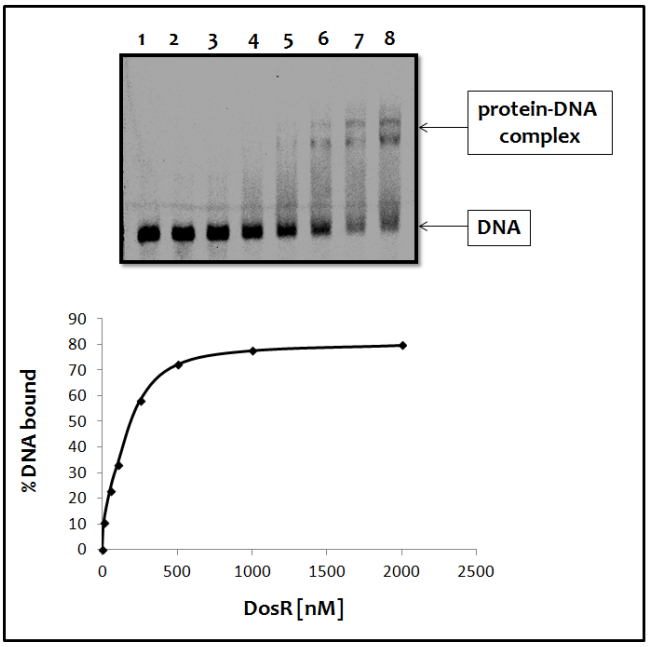

Fig. 47 Wild-type DosR binding to their cognate DNA fragment. EMSA was performed in the absence of DosR (lane 1) or in the presence of 10 nM, 50 nM, 100 nM, 250 nM, 0.5 µM, 1 µM, 2 µM DosR (lanes 2-8).

The specificity of DosR-DNA binding was demonstrated by competition assays with increasing amounts of non-labelled DNA probe (Fig. 48).

Addition of excess cold DNA (self-specific competitor) effectively reduced binding by DosR to labelled DNA. Furthermore, incubation with non-specific competitor showed no interruption in the binding, which demonstrates specificity of this binding interaction.

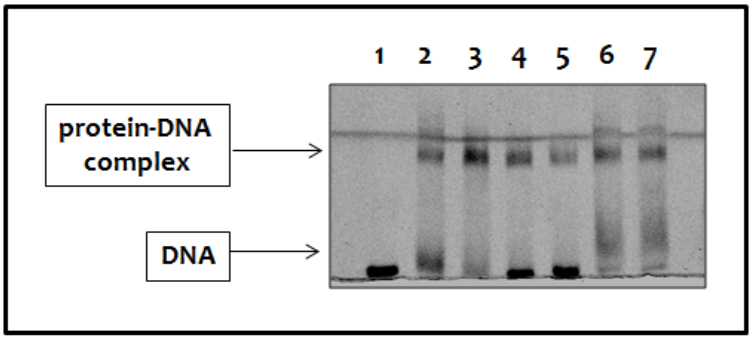

Fig. 48 Specificity of DosR-DNA binding. Competition was performed with 5 ng of DNA without (lane1) or with DosR (2 µM) with no competitor (lane 2) or with 50x, 250x, 500x of self-competitor (lanes 3-5) and 100x, 500x of non-specific competitor (lanes 6,7).

DosR bound to the DNA probe in the absence of phosphorylation. However, when DosR was pre-treated with AcP enhanced DosR binding was observed (Fig. 49). 0.2

μM of DosR was sufficient to observe DosR-DNA complex, whilst 0.5 μM of non-phosphorylated DosR was required for DosR-DNA binding. The enhancement in the affinity of DosR~P (pre-treated with AcP) to bind to cognate DNA has been shown also in other studies (Roberts *et al.*, 2004; Chauhan *et al.*, 2008). Increased DosR-DNA binding was also seen for DosR pre-treated with CmP (data not shown). There was no enhancement of DosR binding to DNA when the protein was previously pre-treated with BeF_3^- (Fig. 50).

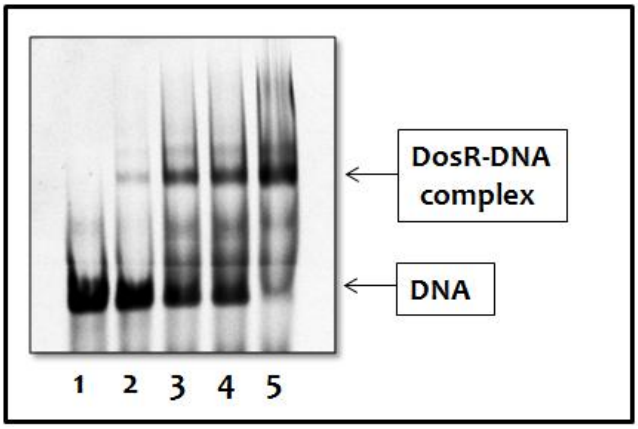

Fig. 49 Phosphorylated DosR binding to their cognate DNA fragment. EMSA was performed in the absence of DosR (lane 1) or in the presence of: 0.2 μM, 0.7 μM, 1.38 μM, 2.75 μM DosR pre-treated with AcP (lanes 2-5).

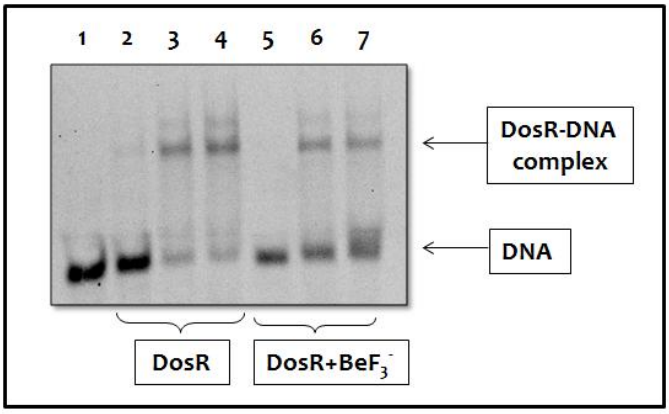

Fig. 50 DosR and DosR pre-treated with BeF_3^- binding to their cognate DNA fragment. EMSA was performed in the absence of DosR (lane 1) or in the presence of: 0.2 μM, 0.5 μM, 0.7 μM DosR (lanes 2-4) or DosR pre-treated with BeF_3^- (lanes 5-7).

1.7.2 DosR D54A binding to DNA

The lack of phosphotransfer from DosS to DosR D54A (Fig. 38) pointed at Asp54 as the only amino acid that can be specifically phosphorylated by DosS. EMSA was performed in order to examine if the phosphorylation impairment had an effect on DNA binding. Wild-type DosR and DosR D54 were incubated with labelled DNA and the reaction was resolved in a non-denaturing polyacrylamide gel. DosR D54A bound poorly to DNA compared to DosR WT protein (Fig. 51).

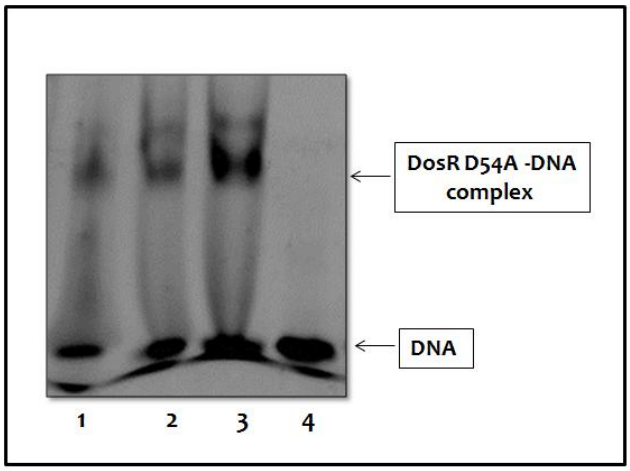

Fig. 51 DosR and DosR D54A DNA binding. EMSA was performed in the absence of protein (lane 1) or in the presence of 2 μM DosR or DosR D54A (lanes 2 and 3 respectively).

1.7.3 DosR double mutants binding to DNA

To evaluate the effect of mutations in residues Thr198 and Thr205 on DosR-DNA binding, the ability of wild-type, DosR [T198A, T205A], DosR [T198D, T205D] and DosR [T198E, T205E] to bind to their cognate DNA was analysed. At 1 μM of wild-type DosR, almost all DNA was bound to the protein. The binding was also observed between DNA and DosR [T198A, T205A] even though the mutant protein bound more weakly than the wild type. Most notably, the DosR [T198D, T205D] and DosR [T198E, T205E] mutants were unable to bind to cognate DNA at any of the assayed protein concentrations (Fig. 52).

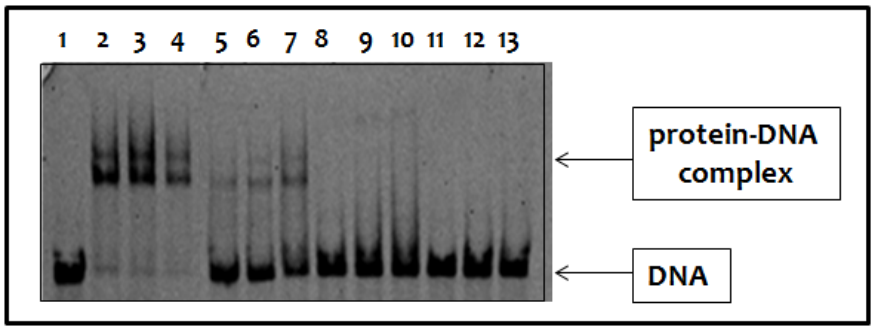

Fig. 52 Wild-type DosR and mutant proteins binding to cognate DNA. EMSA was performed in the absence of protein (lane 1) or in the presence of 0.5 µM, 0.75 µM, 1 µM wild-type DosR (lanes 2-4), 0.5 µM, 0.75 µM, 1 µM DosR [T198A, T205A] (lanes 5-7), 0.5 µM, 0.75 µM, 1 µM DosR [T198D, T205D] (lanes 8-10), 0.5 µM, 0.75 µM, 1 µM DosR [T198E, T205E] (lanes 11-13) .

To analyse if the enhancement of protein-DNA binding induced by DosR phosphorylation occurred with DosR mutants, EMSA was performed with proteins pre-treated with BeF_3^-, acetyl phosphate (Fig. 53) or carbamoyl phosphate. The assay showed that the pattern of DNA binding did not change by the pre-treatment with phosphoryl donors or phosphomimetic.

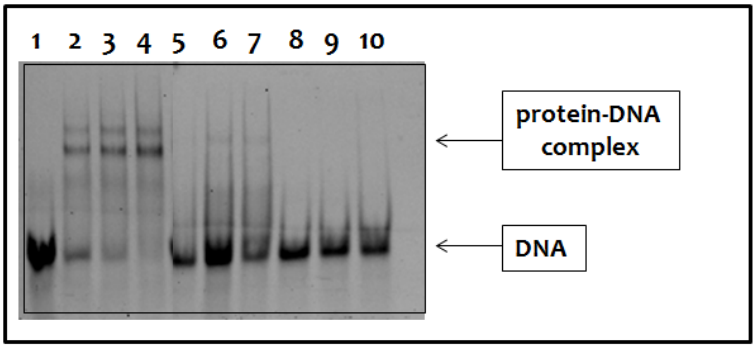

Fig. 53 Wild-type DosR and mutant proteins binding to cognate DNA in the presence of 20 mM AcP. EMSA was performed in the absence of protein (lane 1) or in the presence of 0.2 µM, 0.4 µM, 0.8 µM wild-type DosR (lanes 2-4), 0.2 µM, 0.4 µM, 0.8 µM DosR [T198A, T205A] (lanes 5-7), 0.2 µM, 0.4 µM, 0.8 µM DosR [T198D, T205D] (lanes 8-10).

1.7.4 Molecullar modelling of DosR-DNA interaction

The effect of the double mutations at positions Thr198 and Thr205 on the structural stability of the DosR dimer and the complex it forms with DNA was analysed by means of molecular dynamics simulations. The structure of the wild-type DosR-DNA complex remained stable fluctuating around the initial X-ray coordinates for the

total simulation period. On the other hand, when the double mutant DosR [T198E, T205E] was introduced into the structure, two important effects occurred. Firstly, the DosR dimer started bending and breaking apart (Fig. 54A), showing an average RMSD of 2.7 Å with respect to the initial structure (the RMSD is kept low at 1.5 Å for the wild type DosR) after 4 ns of simulation. This is mainly due to the fact that position 198 and 205 are actually located at the dimerization interface formed by alpha-helix 10. A small threonine to a voluminous and negatively charged glutamate substitution in these positions notably disfavoured the protein-protein interactions. Secondly, and as a consequence of the DosR dimer rearrangement, the interaction with DNA was progressively lost with an initial separation of 4 Å between the center of masses of DosR and DNA (Fig. 54B). Moreover, the DosR [T198E, T205E]-DNA complex was further destabilized by the T198E substitution because a strong negative electrostatic potential was formed at the deeper site of the DNA binding pocket (data not shown).

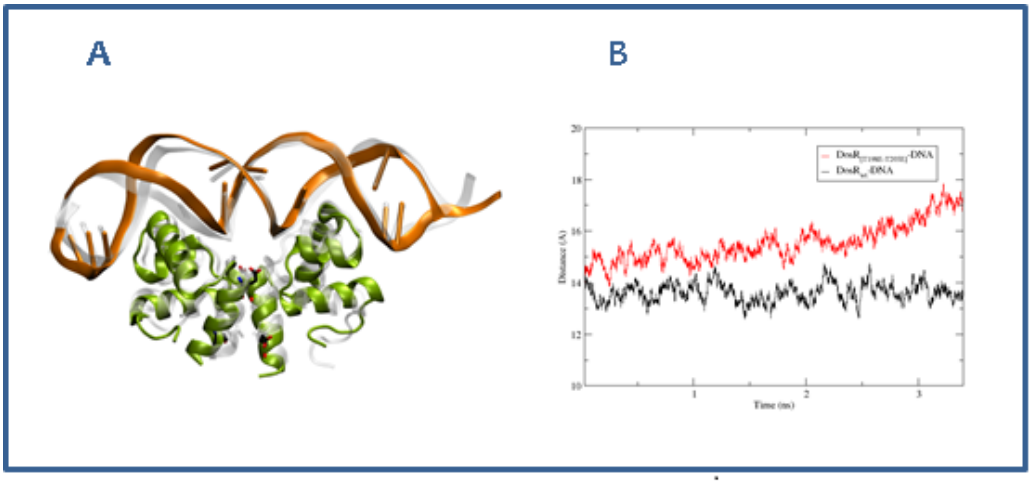

Fig. 54 Molecular dynamics simulations for DosR and DosR [T198E, T205E]. (A). Superposition of the wild-type DosR (white) and DosR [T198E, T205E] mutant (green) in complex with DNA (orange) at the end of the molecular dynamics simulation. (B). Evolution of the distance between DosR dimer and DNA strand along the simulation of the complex for different DosR variants.

1.8 Screening for potential inhibitors of DosR-DNA binding

This thesis was initiated because of the attractiveness of *Mtb* Dos TCS of as a novel antitubercular drug target. The mechanism of action of DosRST targeting molecules

may work not by killing *M. tuberculosis* bacilli directly, but by forcing them out of the non-replicative state leaving them susceptible to currently available antimycobacterial agents. Response regulators had been suggested to be good targets for this and a significant number of molecules targeting response regulators as a strategy for the development of novel broad-spectrum anti-infectives had been reported. In this work a group of small-molecules were designed as potential inhibitors of DosR TCS.

1.8.1 Compounds selection

During bacterial adaptation to hypoxia and other stress signals, DosR response regulator mediates the induction of 48 genes that constitute the DosR regulon.

In view of the role of DosR in dormancy regulation and in hypoxic survival, the identification of compounds that inhibit the ability of DosR to bind to its target genes is likely to provide novel antitubercular chemotherapeutic agents against persistent bacilli. DosRST two-component system has been proposed as an attractive target for the development of inhibitors against dormant mycobacteria (Lamichhane, 2010; Murphy & Brown, 2007; Saini *et al.,* 2004; Vohra, 2006).

In Gupta *et al*, a homology-based model of DosR was generated to be used as a tool for the rational design of potential inhibitor compounds. The model was based on the structure of NarL response regulator of *E. coli* as the primary template for the N-terminal region, whereas the known crystal structure of C-terminal DosR was used as the template for the C-terminal region. In that study, a phenylcoumarin derivative molecules named as compound 10 (Fig. 55) showed its ability to abrogated DNA-protein interaction with an IC50 < 26.2 µg/ml (45 µM). Compound 10 showed its ability to prevent DosR binding to target DNA without inhibiting its phosphorylation. Exposure of *Mtb* to this compound prevented the upregulation of genes from the DosR regulon. Furthermore, exposure to this compound reduced the ability of *Mtb* to establish nonreplicating dormancy *in vitro* following gradual oxygen depletion. Thus, compound 10 appeared like a good starting point for the development of small molecules inhibiting DosR-DNA binding.

Consistent with results from Gupta and colleagues, for this study ten commercially available small molecules (compounds 1-9, 11, Table 8), structurally similar to compound 10, were selected for biological and chemical screenings in order to search for potential DosR-DNA binding inhibitors. Fig. 55 shows the chemical structure of compound 10 and the three different regions on which the design of the chosen compounds was based are highlighted. All the compounds were freshly prepared in DMSO for every experiment.

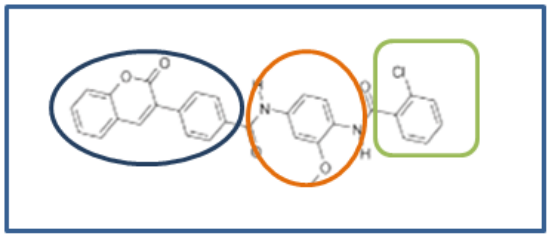

Fig. 55 Chemical structure of compound 10 **(phenylcoumarin derivative) (ChemBridge, 7862123) (Gupta *et al.*, 2009). The shapes of different colours represent the chemical structures on which the selection of other screening compounds for this study was based.**

Table 8 The compounds 1-9 and 11 used in this study.

Compound number	Name & Formula	ID number (SPECS)	Chemical structure
1	N-{4-[(2-chlorobenzoyl) amino]-3-methoxyphenyl }-3,5-dimethylbenzamide $C_{23}H_{21}ClN_2O_3$	AP-970/42250064	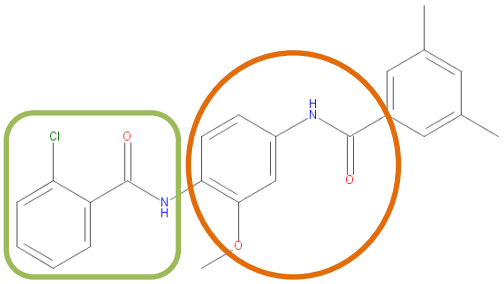
2	2-chloro-N-(3,4-dimethoxyphenyl)benzamide $C_{15}H_{14}ClNO_3$	AO-548/10416031	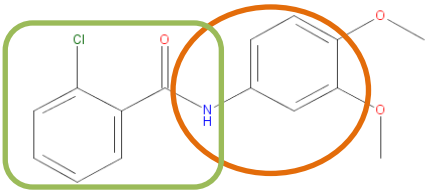

3	2-chloro-N-[4-(2-oxo-2H-chromen-3-yl)phenyl]benzamide C22H14ClNO3	AG-690/36105015	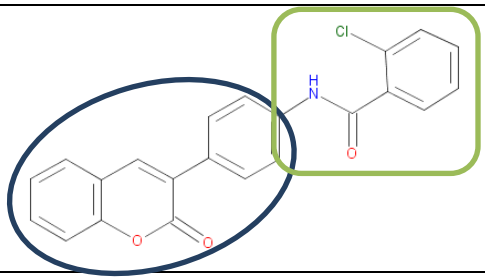
4	N-{4-[(2-chlorobenzoyl)amino]-3-methoxyphenyl}-1,3-benzodioxole-5-carboxamide C22H17ClN2O5	AP-970/42736696	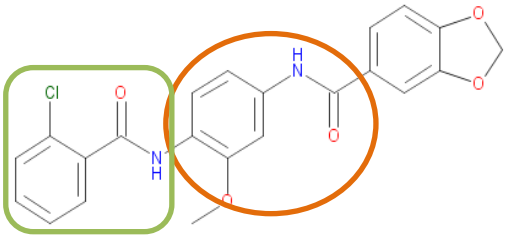
5	2,3-dichloro-N-[3-methyl-4-(2-oxo-2H-chromen-3-yl)phenyl]benzamide C23H15Cl2NO3	AG-670/11901084	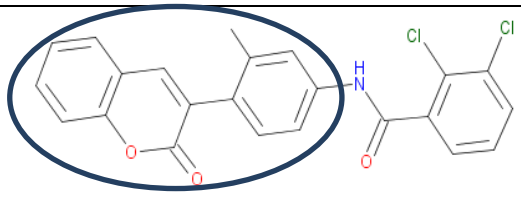
6	3-methoxy-N-[4-(2-oxo-2H-chromen-3-yl)phenyl]benzamideC23H17NO4	AK-778/37026083	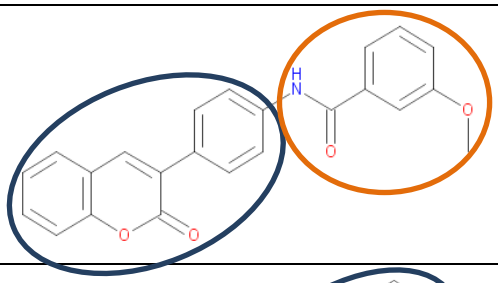
7	2-chloro-5-iodo-N-[4-(2-oxo-2H-chromen-3-yl)phenyl]benzamide C22H13ClINO3	AK-778/36975010	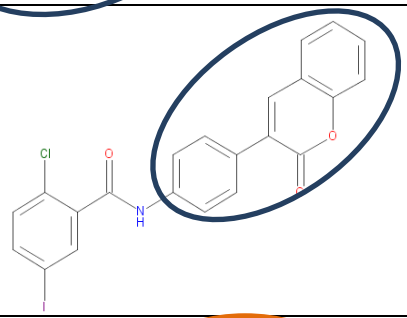
8	N-(3,4-dimethoxyphenyl)-4-methylbenzamide C16H17NO3	AO-548/10416025	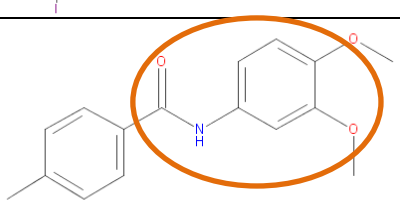
9	4-(2-oxo-2H-chromen-3-yl)benzoic acid C16H10O4	AN-465/25105015	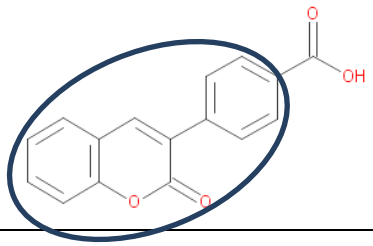

11	N-(3,4-dimethoxyphenyl)[1,1'-biphenyl]-4-carboxamide C21H19NO3	AO-548/11903037	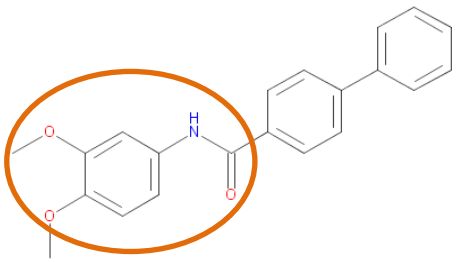

1.8.2 Activity assays

1.8.2.1 ITC

ITC analysis was carried out to determine the binding ability of each compound to wild-type DosR. The assays were performed at 21°C with solutions dialyzed into buffer (150 mM NaCl, 100 mM Tris-HCl, pH 8.0 and 10% DMSO). A solution containing different compound concentrations was used as titrant, whereas solutions containing 100 µM of DosR were used in the calorimetry cell. Compound 10 and compound 2 showed affinity to DosR (Fig. 56). Compounds 1, 5 and 9 displayed very weak binding. Compounds 3, 4, 6, 7, 8 and 11 showed no affinity to DosR (Table 9).

Table 9 Displayed affinity of compounds 1-11 to DosR measured by ITC. Strong binding (+++), weak binding (+) and no binding (-) were observed.

compound #	1	2	3	4	5	6	7	8	9	10	11
Affinity to DosR	+	+++	-	-	+	-	-	-	+	+++	-

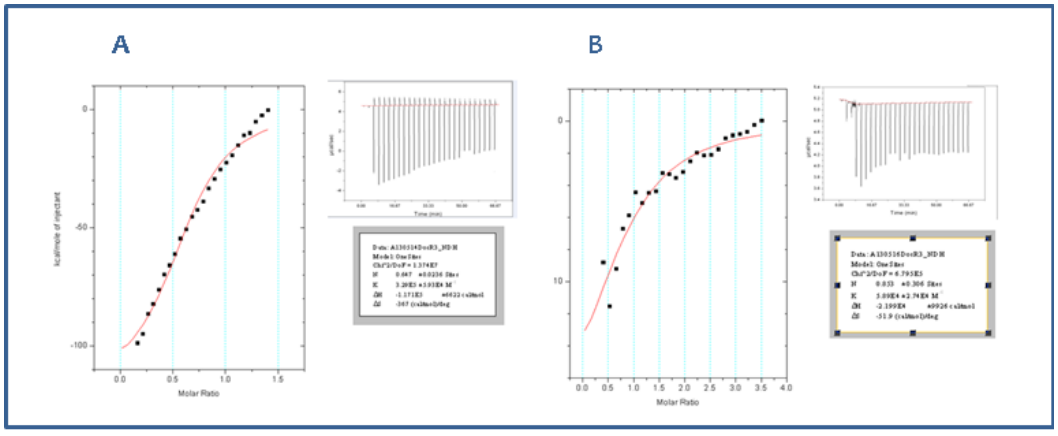

Fig. 56 Compounds binding to DosR. (A). Compound 10. (B). Compound 2. The right upper part of each figure shows the raw binding heats and the left part represents the integrated heat data. The aliquots of a compound (500 µM) were injected into the cell containing DosR (100 µM) solution.

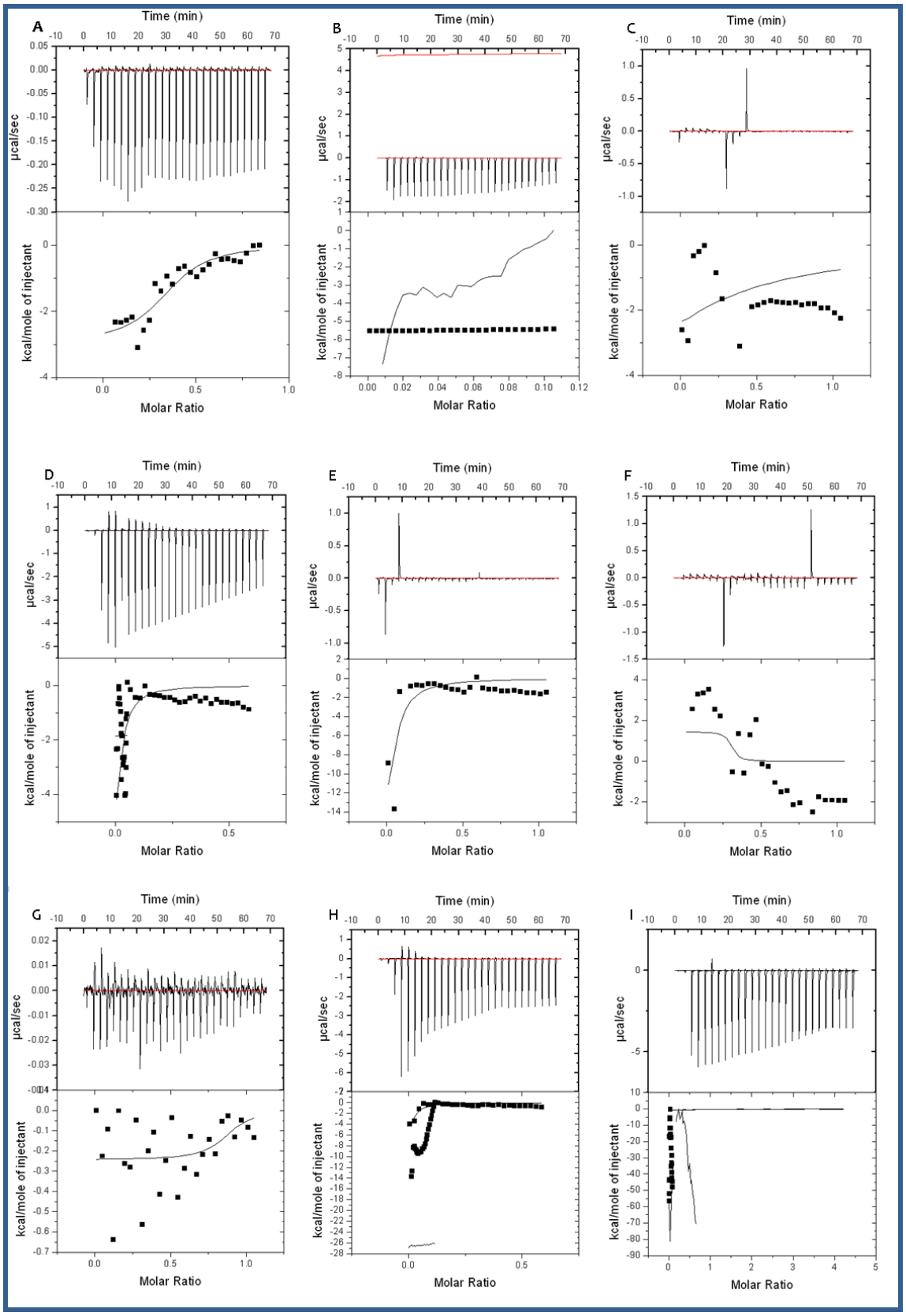

Fig. 57 Compounds binding to DosR [(A): compound 1, (B): compound 3, (C): compound 4, (D): compound 5, (E): compound 6, (F): compound 7, (G): compound 8, (H): compound 9, (I): compound 11). The top part of each figure shows the raw binding heats and the bottom the integrated heat data. The aliquots of a compound (500 µM) were injected into the cell containing DosR (100 µM) solution.

1.8.2.2 EMSA

EMSA trials have been shown to be a good experimental approach to test potential inhibitors (Gupta *et al.*, 2009). The compounds showed good solubility in DMSO and for each experiment they were freshly prepared in this solvent. To set up the experimental conditions, different concentrations of DMSO were added to each sample to analyse its potential influence on the binding of DosR to DNA and on the migration of the free DNA probe (Fig. 58). Although some effect on DNA binding was observed at concentrations higher than 5% DMSO, the compromise between product solubility and a DMSO concentration where DNA shift was observable made us select 10% DMSO as the final concentration in each reaction.

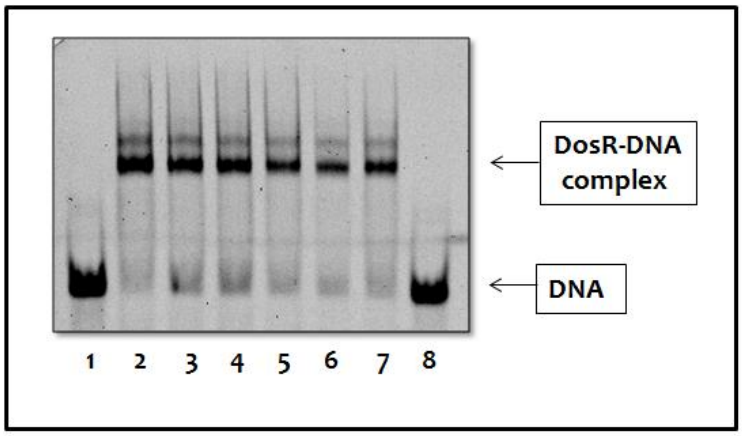

Fig. 58 DMSO influence on DosR-DNA binding estimated by EMSA. DosR (2 µM) was incubated with different concentration of DMSO: 0, 2.5%, 5%, 7.5%, 10%, 15% (lanes 2-7, respectively). DNA (5 nM) incubated with 15 µM DMSO, lane 8, only DNA, lane 1.

ITC analysis showed affinity of compounds 2 and 10 for DosR protein. To evaluate if those compounds had influence on DosR-DNA binding, EMSA was performed initially for those two compounds. Decreased binding of DosR to DNA was showed in the presence of compound 2 in all the assayed concentrations. Decreased binding of DosR to DNA was showed in the presence of compound 10 already at 500 µM and an increase in compound concentration caused higher decrease in binding.

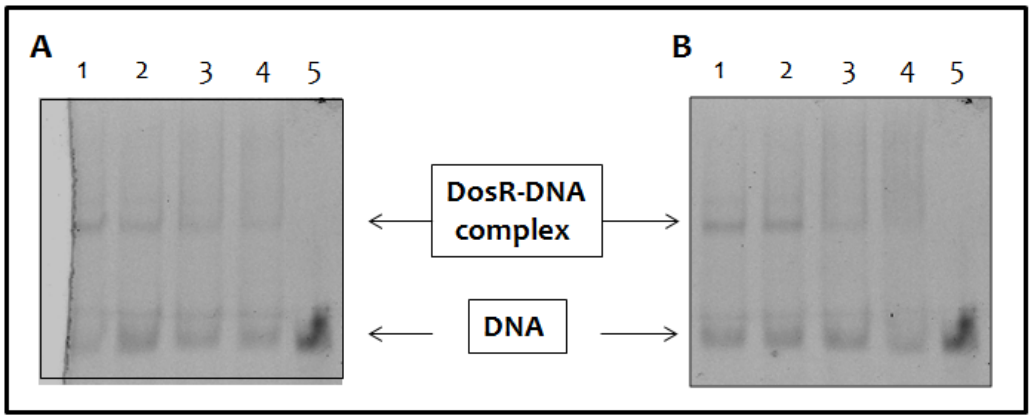

Fig. 59 The effect of the compounds 2 and 10 on DosR binding to DNA. (A). Compound 2. (B). Compound 10. EMSA was carried out without (lane 5) or with 2 μM DosR (lanes 1-4). The compounds were added at 0.125 mM 0.25 mM, 0.5 mM, 1 mM (lanes 1-4). 5 nM of DNA was used.

The compounds 1, 3, 9-11 were tested with EMSA at concentrations 250 μM (lanes b in Fig. 60) or 500 μM (lanes a in Fig. 60) with the protein DosR alone (Fig. 60A) or pre-treated with 20 mM AcP (Fig. 60B). Any of the tested chemicals showed significant inhibitory effect on the DNA-binding properties of the response regulator DosR. In the presence of DosR pre-treated with AcP, compound 5 inhibited DosR-DNA binding at 250 μM. Hypothesis about these findings are presented in discussion section.

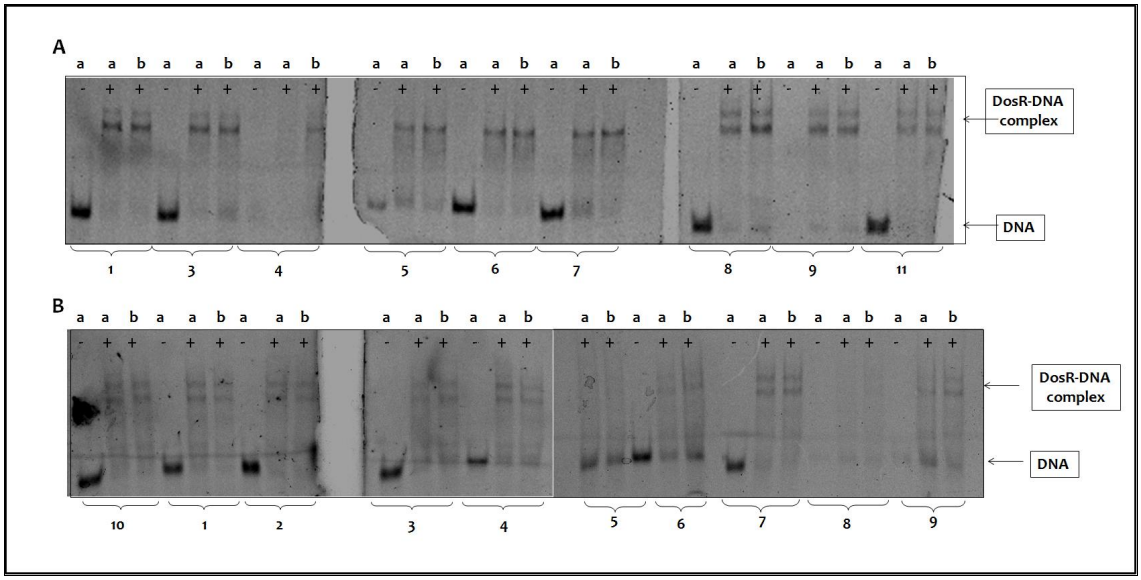

Fig. 60 Effect of test compounds on DosR (2 μM) binding to DNA (5 nM). EMSAs were carried out with compounds 1-11 at 500 μM (a) and 250 μM (b) in the absence (-) or presence (+) of wild-type DosR protein. (A). Non phosphorylated DosR. (B). DosR pretreated with 20 mM AcP.

1.8.2.3 Whole cell antimicrobial activity

Compounds were screened for antibacterial activity against *E.coli*, *K. pneumoniae* and *M. smegmatis* using a high-throughput, turbidometric assay of bacterial growth in a 384-well plate format. In this assay, Müeller-Hinton broth (MHB) was used as medium for *E.coli* and *K. pneumoniae* growth and nutrient medium was used to *M. smegmatis* growth. Compounds were added at a final concentration of 10μM. In all plates, the OD_{612} was measured before and after 18 h (*E. coli* and *K. pneumoniae*) or 40 h (*M. smegmatis*) incubations at 35°C. Negative controls (1% DMSO vehicle) and positive controls (Ciprofloxacin, 3.0 μg/ml) were run in each plate. The experiment was repeated three times and the reported results are means of three individual readings. Fig. 61 shows the effect of the eleven compounds on the growth of *E. coli*, *K. pneumoniae* and *M. smegmatis* in liquid medium, as determined by monitoring optical density at 612 nm. The assayed compounds only inhibited *E. coli* and *K. pneumoniae* growth by 10%. For *M. smegmatis*, compounds showed growth inhibition between 30%-83 %, except for compound 8, which showed no effect on growth of *M. smegmatis.*

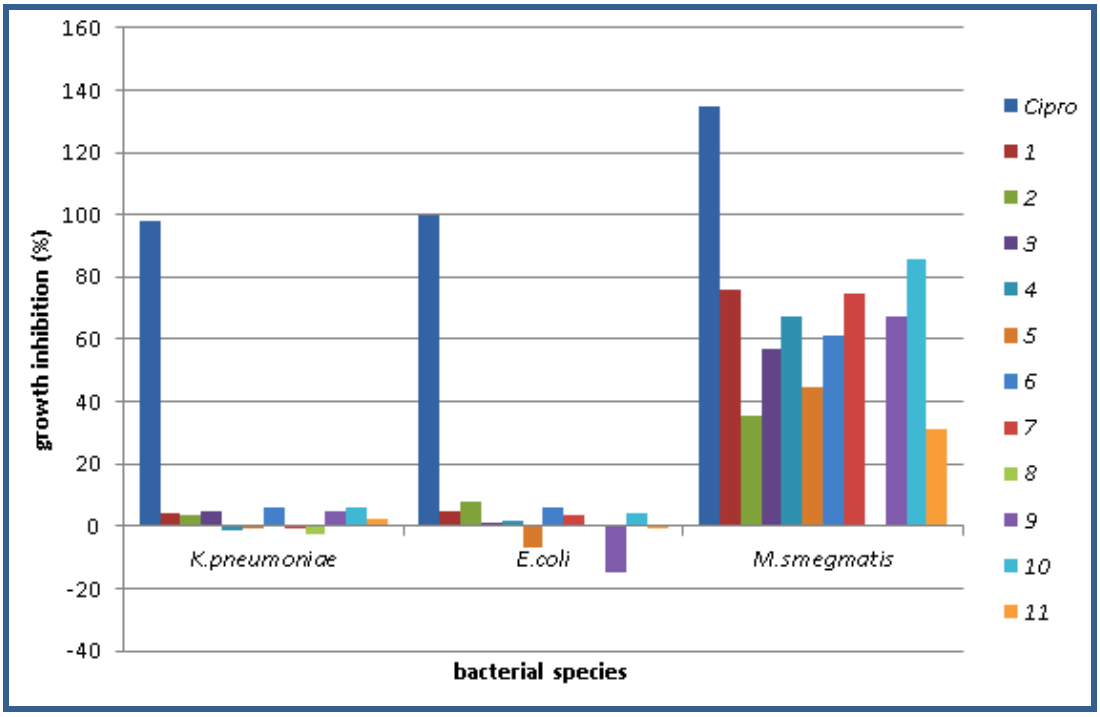

Fig. 61 Growth inhibition of *K. pneumoniae, E. coli* and *M. smegmatis* by compounds 1-11 (10 μM). The percentage of inhibition was determined with relation to the control 3.0 μg/mL ciprofloxacin (Cipro).

1.8.3 Compounds selectivity- cytotoxicity assays

Selectivity of compounds is a major determinant in selecting agents for further inhibitors development. The analysis of the *in vitro* cytotoxicity of each compound on human hepatocytes HepG2 cells and Chinese hamster ovary CHO-K1 cells was performed using the CellTiter-Glo® Luminescent Cell Viability Assay. This is a homogeneous method to determine the number of metabolically active viable cells in culture which correlates the ATP present in the sample. The amount of ATP is directly proportional to the number of cells present in culture in agreement with previous reports (Crouch *et al.,* 1993). The assay was used to analyse each compound. HepG2 cells (2500 cells/well) and CHO-K1 cells (2000 cells/well) were seeded in MTP-384 assay plates and incubated for 24 h at 37°C with 5% carbon dioxide. Control wells containing medium without cells to obtain a value for background luminescence were prepared. As a control, tamoxifen was used. The test compounds (final concentration: 10 µM, 30 µM, 100 µM) were added to experimental wells and incubated for 24 h at 37°C with 5% carbon dioxide. 15 µl Celltiter- Glo 3/7 was added to each well and incubated at RT for 1h, before reading the luminescence.

The HepG2 cells viability was >80% for all the assayed compounds. death was not induced by any compound at any concentration, causing only a slightly decrease in cell viability. Very small reduction of CHO-K1 cells viability was observed when the cells were incubated with compounds at 10 µM (≥ 80% cell viability). CHO-K1 viability was lower than 80% at 100 µM of compounds 1, 2, 5, 8, 9, 11.

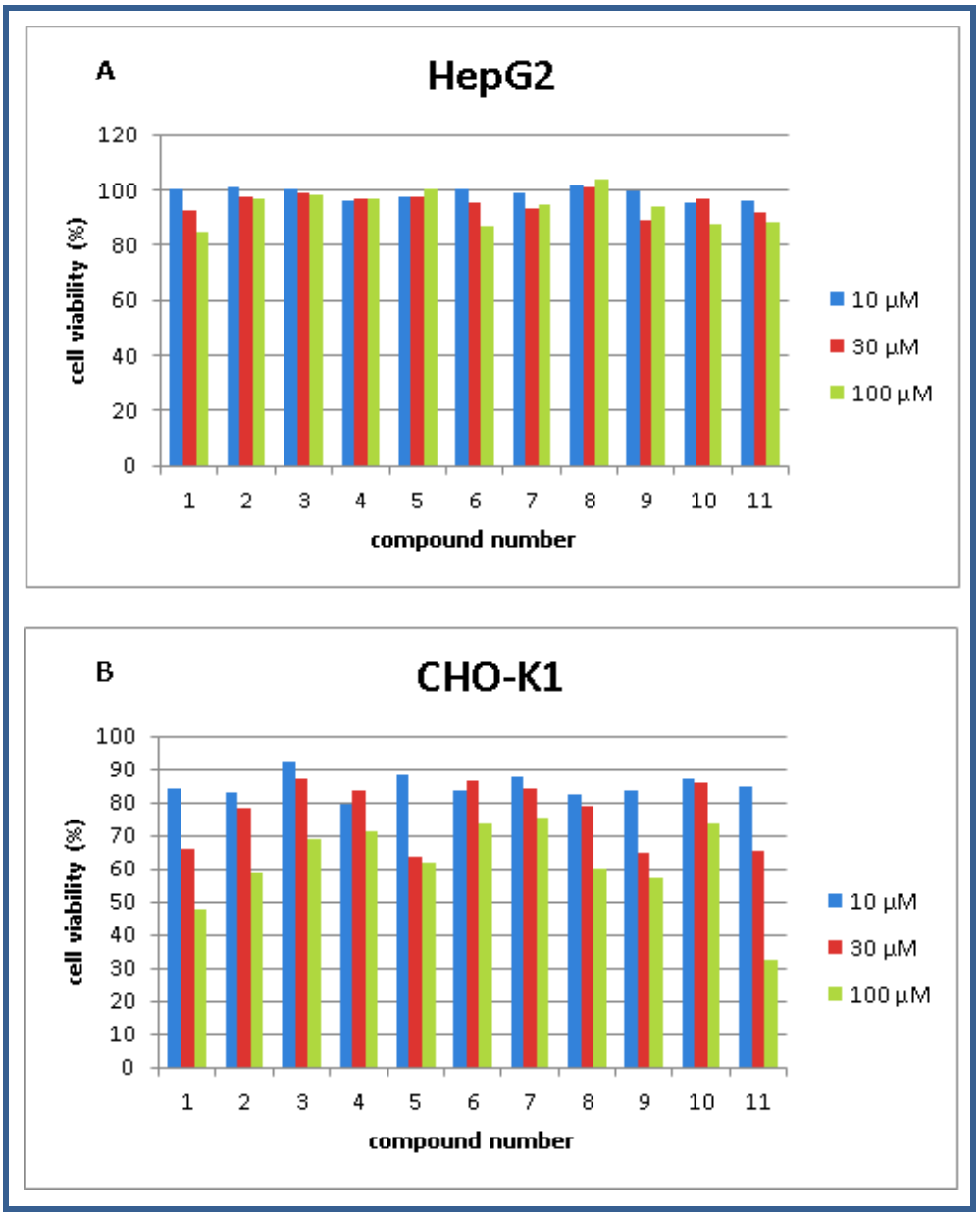

Fig. 62 Cell viability of HepG2 (A) and CHO-K1 (B) cells. The test compounds (final concentration: 10µM, 30 µM, 100 µM).

DISCUSSION

The core of bacterial two-component system pathways is a phosphotransfer reaction between two components, a histidine kinase (HK) and a response regulator (RR). Firstly, upon the perception of environmental of cytosolic specific signal(s), HK autophosporylates at conserved His residue using ATP as phosphodonour. Cis-autophosphorylation (one subunit phosphorylates itself) occurs in some HKs while trans-autophosphorylation takes place in others (Casino *et al.,* 2010). The HK communicates with a response regulator protein that possesses a receiver domain containing a conserved site of aspartate phosphorylation. Aspartate phosphorylation of the response regulator acts as a molecular switch to control output activity, thus transducing the original signal.

The DosR regulon is composed of ~48 co-regulated genes essential for *Mtb* survival during latency. The DosR regulon, activated in response to hypoxia, NO, CO or ascorbic acid exposure, is regulated by a two-component regulatory system consisting of two sensor kinases, DosS and DosT, and a response regulator DosR.

One of the main objectives of this study was the structural and functional characterization of the activation mechanism of DosR response regulator of the DosRST two-component system.

1 Activation mechanisms of DosR

1.1 Activation of DosR through *in vitro* phosphorylation

The ability to phosphorylate is essential for response regulators to activate gene expression and allow adaptation of bacteria to their natural habitats. Phosphorylation of the active site aspartate residue in a receiver domain of RR is coupled to conformational changes that regulate the function of its output domains (Ninfa & Magasanik, 1986), many of which activate or repress transcription (Parkinson& Kofoid, 1992; Stock *et al.,* 1995).

The crystal structure of unphosphorylated inactive DosR has been reported (Wisedchaisri *et al.,* 2008) showing that full length DosR is composed of an N-terminal receiver domain, a C-terminal DNA-binding domain and the linker region and revealing several features never seen before in other response regulators. The N-terminal domain of DosR lacks one α/β segment compared to the canonical (αβ)5 arrangement. The C-terminal domain contains four α-helices named α7, α8, α9, and α10. This domain has an unusual conformation where the first α-helix in the N-terminal domain packs against helix α10 which moves away from the core constructed by helices α7 to α9. The linker region consists of helices α5 and α6 with high flexibility of the second one. Sequence similarity analysis of DosR with other RRs, for example RR468 from Thermotoga maritima, confirmed that *M. tuberculos*is DosR lacks one αβ segment. The structural characterization of phosphorylated active form of DosR was one of the objectives during this research. This information would allow to gain detailed structural information of the active site and would consequently help in the design of target based inhibitors of DosR. Therefore, crystallization trials of wild-type and variants of DosR protein were performed.

Phosphorylation-mediated conformational changes in the response regulator pre-treated with BeF_3^- have been reported. Comparison of the structures of receiver domains that are phosphorylated or bound to BeF_3^- with their nonphosphorylated counterparts revealed key differences between the active and inactive conformations (Lee *et al.,* 2001, Wassmann *et al.,* 2007). In CheY, the response regulator of bacterial chemotaxis, BeF_3^- bound to Asp57, the normal site of phosphorylation, forming a hydrogen bond and salt bridge with Thr87 and Lys109, respectively (Lee *et al.,* 2001).The BeF3– modification of receiver domain of response regulator PleD from *Caulobacter crescentus* causes rearrangement with respect to an adaptor domain, which, in turn, promotes dimer formation, allowing for the efficient encounter of two symmetric catalytic domains (Wassmann *et al.,* 2007). Consequently, in this study, the proteins were pre-treated with BeF_3^- prior to being submitted to crystallization trials. Although many crystals with different geometries were obtained, they diffracted poorly. This might be due to the small size and low-quality crystals, or problems with aberrations coming from cryoprotectant treatment. The potential formation of multimers of wild-type DosR

might be one of the reasons for unsuccesfull diffraction. The mutant proteins may have a high degree of structural flexibility and therefore structural heterogeneity, which results difficult to obtain rigid conformation of proteins.

Although RRs are typically phosphorylated by HK-catalysed phosphotransfer *in vivo*, RRs can be phosphorylated *in vitro* using suitable small molecule phosphodonors, such as acetyl phosphate (AcP) or carbamoyl phosphate (CmP). The phosphorylation of DosR protein by [γ-^{32}P]AcP was shown before and also in this study.

To analyse how the DosR phosphorylation correlate with the interaction of DosR with its cognate DNA, EMSAs were carried out using purified wild-type DosR protein with or without pre-treatment with different phosphoryl donors, AcP or CmP to induce protein phosphorylation or phosphate analogue, BeF_3^-, to mimic phosphorylation.

DosR bound to the DNA probe in the absence of phosphorylation. In fact, the unphosphorylated response regulators are still able to recognize promoters (Cariss, *et al.,* 2008); however, it is unlikely for microbes to over-produce the response regulators to activate or repress transcription. In causing the disease, the activation of response regulator is important largery, for instance by coordination of virulence factors (Leday, *et al.,* 2008). Therefore, when DosR was pre-treated with AcP or CmP, DosR binding enhancement was observed confirming the positive effect of DosR phosphorylation in DNA binding. There was no enhancement of DosR binding to DNA when the protein was previously pre-treated with BeF_3^-, although it was previously demonstrated by gel shift assays that BeF_3^- stimulates the DNA binding properties of RRs. The problems with DosR protein precipitation after BeF_3^- might have interfered in the DNA- binding capacities of protein.

1.2 DosS-dependent phosphorylation of DosR Asp54 is affected by DosR Thr198 and Thr205 mutations

Two functional histidine kinases, DosS and DosT, phosphorylate DosR response regulator specifically at aspartic acid residue Asp54 and form a *bona fide* two-component system (Saini *et al.,* 2004a). DosR, DosS and DosT proteins of M.

tuberculosis exhibited properties typical of TCS´s proteins, namely autophosphorylation of a conserved histidine residues in the cytoplasmic domain of the histidine kinase DosS and DosT and phosphotransfer of phosphoryl moiety from HK to a conserved aspartic acid residue (Asp54) in the response regulator DosR.

In this study, full length of DosS was expressed and purified as C-terminal His_6-tag protein and used for *in vitro* assays. To exclude possible transmembrane (TM) regions that flank predominantly at the N-terminus of the protein and used to result in problems with proteins purification, diverse truncated forms of histidine kinases DosS and DosT were constructed. In each truncated form of the protein, a HisKA domain, which contains the phosphoryl group-accepting histidine residue, and a HATPase domain, which is the ATP binding site, were preserved.

Full-length N-terminal His-tagged DosS was able to autophosphorylate in the presence or [γ-^{32}P]ATP, which proved its catalytic autophosphorylation activity and subsequently was used for the enzymatic phosphorylation of DosR variants. DosS autophosphorylated in the presence of [γ-^{32}P]ATP and transferred the phosphomoiety to full-length C-terminally His-tagged DosR. The stability of DosS~P was modulated by DosR; the phosphorylated DosS protein had a very short half-life (<1 min) in the presence of DosR but was very stable in its absence (the entire radioactivity retained in DosS~P at 2 h). *In vivo*, the rapid phosphotransfer from DosS to DosR would enable the rapid adaptation to hypoxic conditions and thus would increase the bacilli survival by entering into dormancy. The lack of phosphotransfer from DosS~P to DosR D54A mutant confirmed the specificity of DosS phosphorylation in Asp54. It also points out the essentiality of Asp54 residue for the phosphorylation of RR and for protein–protein interactions between RR and HK, as it was demonstrated for DosR-DosS TCS of *M.smegmatis, Mtb* homolog, (Lee *et al.,* 2013). In their study, the replacement of Asp54 with Ala in DosR completely abolished protein interactions of DosR with DosS in yeast two-hybrid assay, which was further confirmed in the pull-down assay.

Bacterial homologues of eukaryotic type serine/threonine kinases have been found to be necessary for cellular functions such as growth, differentiation, pathogenicity, and secondary metabolism (Kennelly, 2002; Deutscher & Saier, 2005; Jayakumar *et al.,* 2008). They have been described to be kinases of response regulators in specific

threonines. For instance, VirS, a transcriptional regulator of *Mtb* that controls the transcription of the *mymA* operon, can be phosphorylated by the serine/threonine kinase PknK, and this phosphorylation increases the affinity for the *mymA* promoter (Kumar *et al.,* 2009). PknH, a Ser/Thr kinase of *Mtb*, phosphorylates InhA, a key enzyme of the fatty-acid synthase II system involved in mycolic acid biosynthesis (Khan *et al.,* 2010), and EmbR, a putative transcriptional regulator of the *embCAB* operon (Sharma *et al.,* 2006). It has been also demonstrated that DosR is a substrate of Ser/Thr kinase PknH (Chao *et al.,* 2010). PknH phosphorylates DosR in threonine residues 198 (Thr198) and 205 (Thr205). These phosphorylable residues are located in helix α10 at the C-terminal domain of DosR, which has been implicated in the activation and binding of the response regulator to DNA. The combination of Asp54, Thr198 and Thr205 phosphorylation has been described to cooperatively enhance the ability of DosR to bind its cognate promoter sequences in one of the two *dos*R boxes of *hsp*X. For the exposed reasons, mutants mimicking Thr198 and Thr205 phosphorylated state were designed. Expected results (i.e. increase in DNA binding affinity), were not achieved, which partially contradicted Chao and collaborators work. This unexpected results are discussed in detail here. Response regulators are in equilibrium between inactive and active conformations, with phosphorylation acting as a molecular switch towards the active form (Cho *et al.,* 2001; Ames *et al.,* 1999; Simonovic *et al.,* 2001; Volkman *et al.,* 2001) and vice versa. For *E. coli* CheY, four states of activation and inactivation of clockwise signaling have been identified. The four states correspond to the combinations of phosphorylated and unphosphorylated, active and inactive conformations (Silversmith & Bourret, 1999).

In this study, the particular interest was to understand the role of DosR amino acid residues Thr198 and Thr205 in its activation mechanism. Previous studies established that PknH phosphorylation of DosR in Thr198 and Thr205 together with DosS-catalysed phosphorylation in DosR Asp54 enhanced DosR binding to its cognate DNA promoter sequences (Chao *et al.,* 2010).

A set of mutants in Thr198 and Thr205 were constructed (DosR [T198A, T205A], DosR [T198D, T205D], DosR [T198E, T205E], DosR [D54A, T198D, T205D]) and their behavior regarding phosphorylation, DNA binding, and dephosphorylation analysed.

Phosphotransfer from DosS to DosR [T198A, T205A] had a similar pattern to that of wild-type DosR, indicating that the introduction of silencing neutral mutations did not affect largely the conformation of the regions surrounding Asp54 of the response regulator. However, phosphotransfer from DosS to DosR [T198D, T205D] and DosR [T198E, T205E] was clearly enhanced compared to wild-type and DosR [T198A, T205A], increasing the quantity and speed of the HK→RR phosphorelay and the stability of the phosphor signal in the RR. This result seems to indicate that the change from threonines to the negatively charged residues induced a conformational change in DosR which made Asp54 more accessible to phosphorylation by DosS. This result is in accordance with the DosR helix rearrangement activation mechanism proposed by Wisedchaisri *et al.*, where, at neutral pH, helix α10 is likely to be in equilibrium between different conformations including one with no contact with the N-terminal domain (Wisedchaisri *et al.*, 2008). The electrostatic repulsion between electronegative charges of Asp54, Asp198 and Asp205 or Asp54, Glu198 and Glu205 could displace the equilibrium of the conformations towards the one where there are no contacts between helix α10 and Asp54, thus exposing Asp54 to the solvent and making it more accessible to DosS active His395 thus enhancing phosphotransfer. The lack of phosphotransfer from DosS~P to triple mutant DosR [D54A, T198D, T205D] confirmed Asp54 necessity for phosphotransfer from DosS to DosR.

Prolonged phosphorylation of DosR by mutagenesis of one of its residue was published recently (Cho *et al.,* 2014). In this study, DosR S83A mutant showed slower autodephosphorylation than the wild type. Ser83 was proposed to play a role in DosR transition from an activated, phosphorylated state to an inactive, unphosphorylated state.

In vitro phosphorylation experiments were performed with wild-type DosR and its mutant variants using acetyl phosphate to see if the observed increase in phosphorylation of the mutant variants was DosS dependent. The results were comparable to those of DosS catalysed phosphotransfer, suggesting that an increase in accessibility of phosphor donors to active phosphorylable Asp54 residue may be the reason why mutants DosR [T198D, T205D] and DosR [T198E, T205E] were more rapidly and stably phosphorylated. This result indicates that the effect of

the introduction of mutations in Thr198 and Thr205 is independent of the type of phosphorylation, whether it is a chemical process or a DosS-catalysed reaction.

1.3 DosS is a phosphatase of DosR~P

In addition to acting as phosphoryl donors of aspartic acid residues located in the receiver domain of response regulators, some sensor histidine kinases have been described to display phosphatase activity toward their cognate phosphorylated regulators. Willett and Kirby (2012) dissected the autokinase and the phosphatase activity of histidine kinases of diverse origin. This mechanism of control is a means of auto-regulation of the TCS activation and has been described for a number of HK-RR pairs such as in WalRK of *Bacillus anthracis* (Dhiman, 2014). Saini *et al* suggested the presence of phosphatase activity in the cytoplasmic portion of DosS. In our phosphotransfer experiments with wild-type and mutants of DosR, DosS~P seemed to have a certain phosphatase activity as DosR dephosphorylated when the Dos~P was present. To probe DosS phosphatase activity and rule out a possible autophosphatase activity by DosR, whether full-length DosS was capable of dephosphorylating [^{32}P]-acetyl phosphate phosphorylated DosR was tested. Dephosphorylation of wild-type DosR was observed in the presence of DosS. Contrary, the radiolabel signal on DosR [T198D, T205D] and DosR [T198E, T205E] remained stable in the presence of the histidine kinase, indicating that DosS could not exert its phosphatase activity against these proteins. It is tempting to speculate that the structural modifications induced in helix α10 in the mutant proteins have a pleiotropic effect on the protein structure which renders it unable to be substrate of DosS phosphatase activity. Once phosphorylated, the protein structure would rearrange in such a way that Asp54~P is no longer available for DosS and is protected from dephosphorylation. It would be highly interesting to repeat the experiment incorporating PknH protein and investigating the effect of specific phosphorylation of Thr198 and Thr205. This has been attempted in this work but the production of PknH, either full-length of truncated forms of the protein, has proved unsuccessful.

1.4 The role of DosR Thr198 and Thr205 in DosR dimerization and DNA binding

Non-phosphorylated response regulators can bind their cognate DNA sequences, although phosphorylation increases their binding affinity. In views of this statement, the ability of wild-type and mutant versions of DosR to bind a DNA fragment comprising a consensus promoter sequence in the *hspX* gene was analysed. Precise 3D crystallographic information from co-crystals of DosR C-terminal and this DNA sequence is available; for this reason the very same DNA sequence was used as probe in the EMSAs. The results showed that wild-type DosR bound specifically to DNA, and this binding was stronger than in the case of DosR D54A as it had been shown before (Park *et al.,* 2003; Saini *et al.,* 2004a). Surprisingly, the results of the EMSAs with mutant versions of DosR were contradictory with our hypothesis: mutant DosR [T198A, T205A], phosphorylated at Asp54, was able to bind DNA although with much less affinity than wild-type DosR. Even more striking was the observation that no band shift appeared with DosR [T198D, T205D] and DosR [T198E, T205E]. The change of threonines to aspartic acid and glutamic acid residues was chosen because these negatively charged amino acids are considered to function as phosphomimetic substitutions. The mutation to alanines was selected as control of silencing substitutions (Wang & Klemke, 2008). The mutant's inability to bind DNA could not be attributable to a less efficient phosphorylation at Asp54 as we had previously showed that phosphorylation was enhanced in the mutants. Thus the effect may be due to inappropriate interactions between the DNA and the C-terminal binding domain of DosR mutants.

The effect of the double mutation at positions Thr198 and Thr205 on the structural stability of the DosR dimerization and DosR-DNA complex was analysed by molecular dynamics simulations and shed light on the unexpected results of the DNA-binding experiments. The solved structure of C-terminal DosR in complex with DNA (Wisedchaisri *et al.,* 2005) and a model of mutant DosR [T198E, T205E] were used in this simulation. Conventional protein-DNA interfaces showed a positive electrostatic potential all along the interaction surface of the protein, as was presented for WT DosR. The structure of the wild-type DosR-DNA complex remained stable fluctuating around the initial X-ray coordinates for the total

simulation period. By mutation from threonines to glutamic acids, this positive electrostatic potential was disrupted in the center of the binding pocket and two important effects occurred. Firstly, the DosR dimer started bending and breaking apart, which is mainly due to the fact that position 198 and 205 are actually located at the dimerization interface formed by alpha-helix 10. A small threonine to a voluminous and negatively charged glutamate substitution in these positions notably disfavours the protein-protein interactions. Second important observation was a progressive loss of the DosR-DNA interaction, which is a consequence of the DosR dimer rearrangement. This shows the necessity of stable dimerization of DosR for full activation and DNA-binding. Furthermore, the DosR [T198E,T205E]-DNA complex was further destabilized by the T198E substitution because a strong negative electrostatic potential was formed at the deeper site of the DNA binding pocket.

Mutations in threonines 198 and 205 have two clear and confronted effects on DosR activity: on one hand they enhance Asp54 phosphorylation but on the other impair the protein ability to bind DNA.

The observations made in this study are somehow contradictory with the work of Chao *et al.,* where it was postulated that phosphorylation of DosR threonines Thr 198 and 205 enhanced the binding of DosR to cognate DNA sequences. Chao observed this phenomenon in one of the two DNA probes used in their EMSA experiments. Little differences in the DNA sequence used as probes and DosS constructs (full-length in this study and truncated DosS in Chao *et al*) may be the cause of the different observations. Additional studies with DNA promoters belonging to other DosR regulated genes would be worth to analyse if the observed cooperative effect of Asp54, Thr198 and Thr205 phosphorylation is general for all the genes of the Dos regulon or just applicable to *hsp*X regulation.

The results altogether help increase our understanding of the molecular events leading to the activation of DosR and its interactions with DNA. They also support the thesis that stable dimerization of DosR is essential for correct DNA binding and that any disruption of this process may result in *dos*R regulon inhibition.

Further experiments in *M. tuberculosis* under inducing conditions (hypoxia or nitric oxide exposure, for example) will help delineate the role of Thr198 and Thr205 residues in regulating the activity of DosRST two-component system.

The knowledge of the certain residues significance among DosR response regulator protein will provide enormous insight into modularity and robustness of a given system. It will also find great value in applications such as identification and validation of drug targets, prediction of critical points, which when perturbed lead to system failure.

2. DosRST as potent therapeutic target

This thesis was initiated because of the attractiveness of DosRST as a novel antitubercular drug target against latent tuberculosis infections. In particular, DosR response regulator was analysed as potential target for the development of novel antimicrobials. A number of inhibitors of DosR were designed and biochemical and cellular assays for the evaluation of novel inhibitors were implemented.

Dormant *Mtb* may persist for decades in a non-replicating state in the infected host, with an estimated 10% lifetime risk of developing active TB. Existing anti-TB therapies are directed against actively replicating bacteria, while there is no particular treatment for LTBI (latent TB infection). Moreover, the development of new antibiotics is not keeping pace with the rapid evolution of resistance to almost all clinically available drugs, and novel strategies are required to fight bacterial infections. One such strategy is the control of pathogenicity as opposed to inducing bacteria death directly. In this case, by forcing *Mtb* to leave the non-replicative state, bacilli would be made susceptible to currently available antimycobacterial treatments.

In recent decades important advances have been made in deciphering the role of TCSs in a variety of physiological processes in bacteria, such as virulence, biofilm formation and antibiotic resistance. Several properties of TCSs have made them attractive targets for the discovery of new antibacterial agents (Introduction, chapter 4.2) and the efforts to develop small molecules that inhibit TCSs are on-going. Some approaches have targeted specific TCSs, such as AgrCA (Lyon *et al.*,

2000), whereas other approaches have been aimed at identifying inhibitors that target a broad collection of TCSs (Matsushita & Janda, 2002; Stephenson & Hoch, 2002). During this study one of the main aims focused on the optimization of biochemical assays used for target-based drug development. Identification and validation of appropriate targets for designing drugs are critical steps in drug discovery.

Several sites have been identified in TCSs that are amenable to disruption by the action of inhibitors and that may interfere with the intracellular signalling activities of these systems (Fig. 63). Interference by chemical compounds could occur at key junctions in the cascade including perception of the triggering signal, binding of ATP and consequent HK autophosphorylation (HK~P), HK-RR interaction, phosphotransfer from HK~P to RR, and binding of phosphorylated RR (RR~P) to the promoter of its target genes.

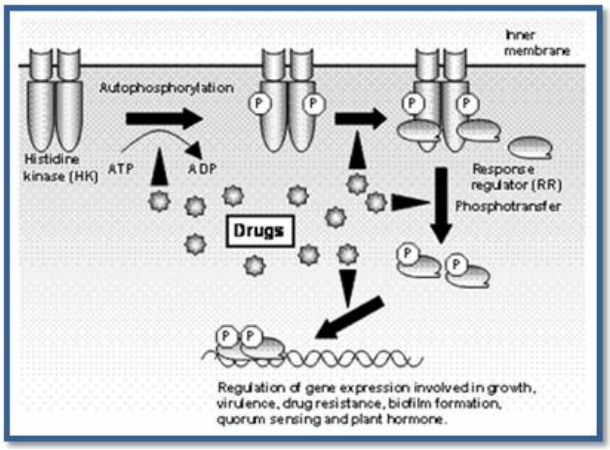

Fig. 63 Two-component system signalling pathway. Black triangles indicate potential targets sites amenable to inhibition by molecules generated in drug discovery projects (Watanabe *et al.,* 2008).

Certain screening campaigns for small-molecule inhibitors targeting TCSs have been directed towards autophosphorylation of histidine kinases or phosphotransfer from histidine kinases to response regulators (Matsushita & Janda, 2002; Stephenson & Hoch, 2002). One of the reasons for having chosen these targets is the possibility of running the screening assays in a high-throughput mode. Initial hits that target the histidine kinases have been discovered, although most of them have shown poor selectivity (Hilliard *et al.*, 1999; Stephenson & Hoch, 2004).

Response regulators have been suggested to be preferable targets because the HK's activity may be overcome by small molecule phosphate donors and because they are the effector molecules in the signaling transduction pathway (Stephenson & Hoch, 2002; Gotoh *et al.,* 2010a).

A significant number of molecules targeting response regulators as a strategy for the development of novel broad-spectrum anti-infectives have been reported. One example of this is the identification of compounds that inhibit alginate gene expression by inhibiting response regulator AlgR1-DNA binding in *Pseudomonas aeruginosa* (Roychoudhury *et al.,* 1993). Another example presents Rap proteins from *B. subtilis*, named after the founding members of the family, which were shown to be response regulator aspartate phosphatases (Perego *et al.,* 1994). The essential WalK/WalR (YycG/YycF) two-component system is highly conserved and specific to low-GC percentage of Gram-positive bacteria. The development of a high-throughput screening assay for WalR inhibitors and the identification of two novel inhibitors targeting the WalR response regulator have been reported (Gotoh *et al.,* 2010b).

Structure-based design of DosR inhibitors against non-replicating *M. tuberculosis* has been reported (Gupta *et al.,* 2009). A phenylcoumarin derivative (named compound 10 by Gupta and also this study) inhibited DosR binding to target DNA, downregulated dormancy genes transcription and drastically reduced survival of hypoxic organisms. Consistent with those results, ten structurally similar and commercially available compounds were purchased. These small molecules were selected for biological and chemical screenings in order to search for potential DosR-DNA binding inhibitors.

The thermodynamic information of the interactions of protein-small molecule obtained from ITC facilitates the understanding of the binding modes and is helpful to the development of novel drugs for some diseases (Yang *et al.,* 2007; Engel *et al.,* 2006; Lorca *et al.,* 2007; Thompsett *et al.,* 2005). ITC has been used for evaluation of many proteins studied as targets for pharmaceutical drug development. In most cases, ITC has been used to study the contribution of enthalpy and entropy to binding, which is important when designing the ligands. Furthermore, a significant

correlation of the thermodynamic (ITC) and structural (X-ray crystallography, models) data was observed suggesting that ITC measurements provide valuable information for optimizing inhibitor binding in drug discovery (Perspicace *et al.*, 2013).

One of the interests of the present work was to investigate whether ITC could be used as screening assay to quantify the interactions between DosR and thus to screen for potential inhibitors.

ITC was carried out to determine the binding ability of each compound to wild-type DosR. The ITC results of compound 10, which showed affinity to DosR, are in accordance with previous findings about this compound, where it was suggested that compound 10 interacts with DosR by locking it in a conformation that cannot bind to cognate DNA (Gupta *et al.*, 2009). Another examined compound, 2-chloro-N-(3,4-dimethoxyphenyl) benzamide (named compound 2 in this study) also showed affinity to DosR, pointing at the regions in compound 10 that may be essential for interaction with DosR. The binding to DosR was abolished for compounds 3, 4, 6, 7, 8 and 11, while compounds 1, 5 and 9 displayed very weak binding. Despite the wide application of the ITC method, it has some inherent limitations, which makes it difficult to explore data generated with this technique for the DosR protein. The routine problems were encountered during ITC attempts, such as alterations in protein and ligand pH final solutions, a common issue when working with high concentrations of ligand, e.g. 500 µM. It is unclear why no heat was observed in some trials. This may be linked to the weak binding or low affinity, but also could be possible due to the problems with dilution, or protein aggregation. Another trouble encountered in this study was high sensitivity of the method on any environmental changes coming from poor dialysis, for instance. From the experience gained with the DosR system, ITC does not seem to be ideal as primary screening technique due to the difficulties in its standardisation. Nevertheless, it could be used as secondary screening in the hit to lead phase (Introduction, chapter 4.1.3). ITC could be used as secondary screening technique with a reduced number of molecules for gathering thermodynamic information about the interaction of DosR and the evaluated compounds.

In addition to ITC, all the compounds were screened with the electrophoretic mobility shift assay (EMSA). EMSA can be used to validate the inhibitory properties of screening compounds and could provide additional criteria for selecting the most promising ones. In fact, EMSA trials have been shown to be a good experimental approach to test potential inhibitors of response regulators such as DosR (Gupta *et al.*, 2009) or PhoP response regulator from *Salmonella enterica* (Tang *et al.,* 2012).

EMSA was used to evaluate if the screened compounds could bind to DosR and prevent this protein from binding to cognate DNA promoter. Most of the tested chemicals had no significant effect on the DNA-binding properties of the response regulator DosR. Compound 2 displayed poor inhibitory effects in DosR-DNA binding. The results confirmed the inhibitory activity against DosR-DNA binding of compound 10 at 500 µM and an increase in compound concentration (1 mM), measured for compound 10 caused an increase in binding inhibition.

These results confirmed the inhibitory activity against DosR-DNA binding of compound 10 at 500 µM and an increase in compound concentration (1 mM), measured for compound 10 caused an increase in binding inhibition.

Surprisingly, the affinity of compound 10 was not potent enough to inhibit the binding when DosR was pre-treated with AcP. These results are not in correlation with previous study (Gupta *et al.,* 2009), where compound 10 inhibited pre-treated with AcP DosR-DNA binding. This disagreement might derive from the differences in DNA fragments used as DNA probles in both studies. Gupta *et al.,* used the whole fragment of *fdxA* promoter, while in this experiment the short fragment of *hspX* promoter was employed. Furthermore, fluorescein labelled DNA probe might result in lower signal comparing to radioactive labelled DNA fragments, that is why 500 µM (compound 10) and 1 mM (compound 2) was required for noticeable inhibition.

It is interesting to note the significant inhibitory effect of 2,3-dichloro-N-[3-methyl-4-(2-oxo-2H-chromen-3-yl)phenyl]benzamide (compound 5) already at lower 250 µM in the binding when DosR was pre-treated with AcP. Compound 5 was, in this experiment, the unique molecule able to inhibit binding of DosR-DNA with the protein previously phosphorylated. Compound 5 did not inhibit the binding when the protein DosR was not phosphorylated. It is tempting to speculate that

compound 5 interferes with DosR conformational changes by inhibiting the phosphorylation of DosR.

This result is in accordance with other study, where Lactoferricin B (Lfcin B), a natural antimicrobial peptide, did not affect the DNA binding ability of the unphosphorylated response regulators, BasR and CreB. Instead, Lfcin B was observed to attach to the receiver domains of BasR and CreB to inhibit their phosphorylation activity. As it was mentioned before, the unphosphorylated response regulators are still able to recognize promoters; however, it is unlikely for microbes to over-produce the response regulators to activate or repress transcription.

The screening for antimicrobial activity of the chemical compounds as potential drug candidates represents an additional strategy in the development of novel drugs. The acquired information may assist in the optimisation of a lead compound's activity, provide a focus for toxicological attention and aid in the anticipation of resistance. Characterization of the interaction between antimicrobial compounds and their target sites could potentially allow the design of second generation inhibitors. Antibacterial activity has been reported in the literature with diverse sets of methodologies, degrees of sensitivity, amount of test–compounds and microbial strains.

In this study, the growth inhibition assay was used to estimate the activity of the inhibitors to arrest bacterial growth. Compounds were screened for antibacterial activity against *Escherichia coli, Klebsiella pneumoniae* and *Mycobacterium smegmatis*. Susceptibility testing was performed using Müeller-Hinton agar (*E. coli* and *K. pneumoniae*) or nutrient agar medium (*M. smegmatis*).

It was observed that the broadest activity of the screened compounds was against *M. smegmatis* while lower activity was noticed against *E. coli* and *K. pneumoniae*. This different behaviour may be a consequence of the specificity of the assayed compounds towards DosR. An identified response regulator of *M. smegmatis*, which plays an important role in adaptation to oxygen-starved stationary phase, has exhibited a strong sequence similarity to DosR of *M. tuberculosis* and is also named DosR (O'Toole *et al.,* 2003). It has been determined that the response regulator

DosR plays an important role in stationary-phase gene expression, adaptation to oxygen stavation-induced growth arrest, and resistance to environmental stress in *M. smegmatis.* It can be hypothesised that the compounds activity against *M. smegmatis* in this study could be due to affinity of those molecules to DosR.

Differences in compounds activities in the different bacterial species assayed could also be explained by the different classification of evaluated bacteria according to Gram stain (Gram-positive *M. smegmatis* against Gram-negative *E. coli* and *K. pneumoniae*). For most antimicrobial molecules that are not active against Gram-negative bacteria, the outer membrane is believed to be a major barrier (Matsuzaki *et al.,* 1999; Nikaido, 1994). However, the details of the interactions of the molecules with these membranes are still not fully known. The outer membrane of Gram-negative bacteria mostly (>90%) contains the glycolipid lipopolysaccharides (LPS) on its surface, which is generally thought to be a protective wall, rendering bacteria resistant to a variety of host defense molecules. This may be one of the reasons for the negative results with the compounds screened with Gram-negative bacteria.

In vitro profiling of compounds encouraged the study of *in vitro* toxicological profiles that may be valuable for prioritizing compounds for more intensive toxicological investigation, and ultimately, predicting *in vivo* toxicity.

In order to measure the selectivity of the compounds, the examination of the *in vitro* cytotoxicity on human hepatocytes HepG2 cells and Chinese hamster ovary CHO-K1 cell lines was studied. The percentage of cell viability was quantified in the presence of each compound.

The HepG2 cell death was not induced by any compound at any concentration, causing only a slightly decrease in cell viability (>80% cell viability). The compounds tested with CHO-K1 showed different mortality rate at different concentrations. Previous studies (Xia *et al.,* 2008) demonstrated that *in vitro* cytotoxicity is often cell-type specific and that cytotoxicity in one cell type does not necessarily predict cytotoxicity in another. In this study, commonly used in cell viability assays HepG2 and CHO-K1 cell lines were used due to their genuine toxicity predictions in animal models.

The good antimicrobial activity of compounds 2, 5 and 10 against *M. smegmatis* and low toxicity against HepG2 and CHO-K1 cells, together with their target based inhibition profile, suggest that they may be regarded as potential hits for drug development of novel antimycobacterial drugs against dormant forms of *M. tuberculosis*.

CONCLUSIONS

1. The DosR response regulator and the DosS histidine kinase of *Mycobacterium tuberculosis* cloned, expressed and purified in this work, conform a *bona fide* two-component system.

2. The predicted molecular model of DosS-DosR interactions reveals a genuine overlap between hydrophobic and polar amino acids. The analysis of the complex interface shows that exposed hydrophobic amino acids Phe403 and Leu407 in DosS and Val12 and Leu20 in DosR are key in maintaining the complex stability.

3. DosR D54A mutant is not phosphorylated by DosS, showing the specificity of the DosS-catalysed phosphorylation of DosR in its active aspartic acid residue.

4. The truncated form of DosS histidine kinase, $DosS_{350-578}$, has the ability to autophosphorylate with ATP similarly to wild type full-length DosS *in vitro*.

5. The truncated forms of DosT histidine kinase, $DosT_{349-573}$ and $DosT_{380-573}$, have the ability to autophosphorylate with ATP *in vitro*.

6. Phosphorylation on Asp54 of DosR enhances its ability to bind specifically to its cognate promoter sequences.

7. Mutant DosR [T198A, T205A] shows a slight increase in chemical and DosS-mediated phosphorylation compared to wild type DosR. However, this mutant binds to DNA less efficiently than wild type DosR.

8. Mutants DosR [T198D, T205D] and DosR [T198E, T205E] show a notorious increase in chemical and DosS-mediated phosphorylation compared to wild type DosR. However, these mutants are completely unable to bind their cognate promoters.

9. Molecular dynamics calculations of the interactions between C-terminal domain of DosR and DNA show stability of the protein-DNA complex along time.

10. Molecular dynamics calculations of C-terminal DosR [T198E, T205E]-DNA interactions, based on the available 3D structure of this complex with wild type DosR, reveal an increase in the distance between protein and DNA along time. This result explains the observed lack of protein-DNA complex formation because of the

inability to form a dimer with the appropriate conformation compatible with DNA interactions.

11. Molecular modelling of DosR [T198E, T205E]-DNA shows repulsion between negatively charged DNA and glutamate 198, contributing to the lack of DNA binding observed in this mutant.

12. DosS is a phosphatase of wild type DosR~P. However, DosS has limited phosphatase activity on mutant DosR [T198A, T205A] and is unable to dephosphorylate mutants DosR [T198D, T205D] and DosR [T198E, T205E].

13. Compound 10 (a phenylcoumarin derivative), together with compound 2 show affinity to DosR. Compound 5 inhibits binding of phosphorylated DosR to DNA. Compound 5 does not interfere with DNA-binding when DosR is not phosphorylated as is the case of compound 10. These molecules have good activity profile in the bacterial growth inhibition assay and low toxicity against HepG2 and CHO-K1 cells. These findings suggest that they may be interesting hits for the development of novel antimycobacterial drugs.

BIBLIOGRAPHY

Aguilar, P.S., Hernandez-Arriaga, A.M., Cybulski, L.E., Erazo, A.C., and de Mendoza, D. (2001) Molecular basis of thermosensing: a two-component signal transduction thermometer in *Bacillus subtilis*. Embo J 20: 1681-1691.

Ahmad S. (2011) Pathogenesis, immunology, and diagnosis of latent *Mycobacterium tuberculosis* infection," Clinical and Developmental Immunology, Article ID 814943, 17 pages.

Akerley B.J., Monack D., Falkow S. and Miller J.F. (1992) The bvgAS locus negatively controls motility and synthesis of flagella in *Bordatella bronchisceptica*. Journal of Bacteriology 174 980-90

Akira S. (2003) Toll-like receptor signaling," Journal of Biological Chemistry, vol. 278, no. 40, pp. 38105–38108.

Algood H.M., Chan J., Flynn J.L. (2003) Chemokines and tuberculosis. Cytokine Growth Factor Rev.;14(6):467-77

Alsaadi A.I., Smith D.W. (1973) The fate of virulent and attenuated *Mycobacteria* in guinea pigs infected by the respiratory route. Am Rev Respir Dis 107: 1041–1046.

Alteri *et al.*, (2007) Proc Natl Acad Sci U S A; 104(12): 5145–5150

Alves R. and Savageau M.A. (2003) Comparative analysis of prototype two-component systems with either bifunctional or monofunctional sensors: differences in molecular structure and physiological function. Mol Microbiol.;48:25–51

Ames S.K., Frankema N., Kenney L.J. (1999) C-terminal DNA binding stimulates N-terminal phosphorylation of the outer membrane protein regulator OmpR from *Escherichia coli*. Proc. Natl. Acad. Sci. USA;96:11792–11797.

Anderson T.B., Brian P. and Champness W.E. (2001) Genetic and transcriptional analysis of absA, an antibiotic gene cluster-linked two-component system that regulates multiple antibiotics in Streptomyces coelicolor. Molecular Microbiology 39: 553-66

Andries K., Gevers T., Lounis N. (2010) Bactericidal potencies of new regimens are not predictive of their sterilizing potencies in a murine model of tuberculosis. Antimicrob Agents Chemother.; 54(11):4540–4544.

Aravind L. and Ponting C.P. (1999) The cytoplasmic helical linker domain of receptor histidine kinase and methyl-accepting proteins is common to many prokaryotic signalling proteins. FEMS Microbiol Lett.17611116

Arthur M., Molinas C. and Courvalin P. (1992) The VanS-VanR two-component regulatory system controls synthesis of depsipeptidide peptidoglycan precursors in Enterococcus faecium BM4147. Journal of Bacteriology 174: 2582-91

Atkinson M. R. and Ninfa A. J. (1999) Two-component systems. In S. Baumberg, editor, Prokaryotic Gene Expression, pages 194–228. Oxford University Press, Oxford, UK.

Av-Gay Y. and Everett M. (2000) The eukaryotic-like Ser/Thr protein kinases of *Mycobacterium tuberculosis.* Trends Microbiol. 8:238–244.

Bacon J., James B. W., Wernisch L., Williams A., Morley K. A., *et al.*. (2004). The influence of reduced oxygen availability on pathogenicity and gene expression in *Mycobacterium tuberculosis.* Tuberculosis (Edinburgh) 84:205–217.

Badri M., Wilson D., Wood R. (2002) Effect of highly active antiretroviral therapy on incidence of tuberculosis in South Africa: a cohort study. Lancet.;359(9323):2059–2064.

Bagchi G., Chauhan S., Sharma D., Tyagi J.S. (2005) Transcription and autoregulation of the Rv3134c-devR-devS operon of *Mycobacterium tuberculosis.* Microbiology 151: 4045–4053.

Bakir M., Millington K.A., Soysal A., *et al.* (2008) Prognostic value of a T-cell-based, interferon-gamma biomarker in children with tuberculosis contact. Ann Intern Med.;149(11):777–787.

Balaban N., Goldkorn T., Nhan R.T., Dang L.B., Scott S., *et al.* (1998) Autoinducer of virulence as a target for vaccine and therapy against *Staphylococcus aureus.* Science 280: 438-40

Balasubramanian V., Wiegeshaus E. H., Taylor B. T., and Smith D. W. (1994) Pathogenesis of tuberculosis: pathway to apical localization. Tuber. Lung Dis. 75: 168-178.

Banaiee N., Jacobs W.Jr., and Ernst J. (2006)Regulationof *Mycobacterium tuberculosis* whiB3 in the mouse lung and macrophages. Infect. Immun. 74, 6449–6457.doi: 10.1128/IAI.00190-06

Bannister B., Gillespie S., Jones J. (2006) Infection. Microbiology and Management. Third edition, Blackwell Publishing, pages365-386

Barakat M.; Ortet P., Whitworth D.E. (2011) P2CS: a database of prokaryotic two-component systems. Nucleic Acids Res. (in eng) (England) 39 (Database issue): D771–6. doi:10.1093/nar/gkq1023. PMC 3013651. PMID 21051349.

Barrett J.F. and Hoch Ja. (1998) Two-component signal transduction as a target for microbial antiinfective therapy. Antimicrobial Agents and Chemotherapy 42: 1529-36

Barry III C.E., Lee R.E., Mdluli K., Simpson A.E., Schroeder B.G., *et al.* (1998) Mycolic acids: Structure, biosynthesis and physiological functions. Prog Lipid Res 37:143–179. DOI:10.1016/S0163-7827(98)00008-3

Belisle J.T. and Brennan P.J. (1989) Chemical basis of rough and smooth variation in mycobacteria. J. Bacteriol. 171: 3465-3470.

Belisle J.T., Vissa V.D., Sievert T., Takayama K. and Brennan P.J. (1997) Role of the major antigen of *Mycobacterium tuberculosis* in cell wall biogenesis. Science, 276: 1420-1422. PMID: 9162010

Bernardini M.L., Fontaine A. and Sansonetti P.I. (1990) The two-component regulatory system ompR-envZ controls the virulence of *Shigella flexneri.* Journal of Bacteriology 172: 6274-81

Bemish B. and van de Rijn I. (1999) Characterisation of a two-component system in Streptococcus pyogenes which is involved in regulation of hyaluronic acid production. Journal of Biological Chemistry 274: 4786-93

Betts J. C., Lukey P. T., Robb L. C., McAdam R. A., Duncan K. (2002) Evaluation of a nutrient starvation model of Mycobacterium tuberculosis persistence by gene and protein expression profiling. Mol. Microbiol. 43: 717–731.

Beutler B. (2004) Innate immunity: an overview. Mol Immunol.;40(12):845-59.

Hart D.N. (1997) Dendritic cells: unique leukocyte populations which control the primary immune response. Blood.;90(9):3245-87.

Blower S. M., Small P. M., and Hopwell P. C. (1996) Control strategies for tuberculosis epidemics: New models for old problems, Science, 273:497–500.

Boon, C. and Dick, T. (2002) *Mycobacterium bovis* BCG response regulator essential for hypoxic dormancy. J. Bacteriol. 184, 6760–6767.

Boon C. and Dick T. (2012) How *Mycobacterium tuberculosis* goes to sleep: the dormancy survival regulator DosR a decade later. Future Microbiol, 7:513–518

Boyd R.F. (1995) Basic Medical Microbiology 5th edition, Little, Brown and Company

Brennan P.J. and Nikaido H. (1995) The envelope of mycobacteria. Annu Rev Biochem. 64: 29–63.

Brennan P. J. (2003) Structure, function, and biogenesis of the cell wall of *Mycobacterium tuberculosis.* Tuberculosis (Edinburgh) 83:91–97.

Bretl D.J., Demetriadou C., Zahrt T.C. (2011) Adaptation to environmental stimuli within the host: two-component signal transduction systems of *Mycobacterium tuberculosis*. Microbiol Mol Biol Rev; 75:566-82; PMID:22126994; 05004-11

Brian P., Riggle P.J., Santos R.A. and Champness W.C. (1996) Global negative regulation of Streptomyces coelicolor antibiotic synthesis mediated by an absA-encoded putative signal transduction system. Journal of Bacteriology 178: 3221-31

Brosch R., Pym A.S., Gordon S.V. and Cole S.T. (2001) The evolution of mycobacterial pathogenicity: clues from comparative genomics. Trends Microbiol. 9: 452–458.

Brosch R., Gordon S.V., Marmiesse M., Brodin P., Buchrieser C., *et al.* (2002) A new evolutionary scenario for the *Mycobacterium tuberculosis* complex. Proc Natl Acad Sci USA; 99:3684-9; PMID: 11891304;

Browning D. F. and Busby S. J. (2004) The regulation of bacterial transcription initiation. Nat. Rev. Microbiol. 2:57–65.

Cai S., Khorchid A., Ikura M. and Inouye M. (2003) Probing catalytically essential domain orientation in histidine kinase EnvZ by targeted disulfide crosslinking. J. Mol. Biol., 328, 409–418.

Calmette A. (1927) Sur la vaccination pre´ ventive des enfants nouveau-ne´ s contre la tuberculose par le BCG. Annales de l'Institut Pasteur 41, 201–232.

Cardona P.J. and Ruiz-Manzano J. (2004) On the nature of *Mycobacterium tuberculosis*-latent bacilli. Eur. Respir, J., 24: 1044-1051. DOI: 10.1183/09031936.04.00072604

Casanova J. L. and Abel L. (2002) Genetic dissection of immunity to mycobacteria: the human model. Annu.Rev.Immunol. 20: 581-620.

Casino P., Rubio V., Marina A. (2009) Structural insight into partner specificity and phosphoryl transfer in two-component signal transduction. Cell, 139:325-336.

Casino P., Rubio V., Marina A. (2010) The mechanism of signal transduction by two-component systems Curr. Opin. Struct. Biol., 20, pp. 763–771

Castillo-Chavez C. and Feng Z. (1997) To treat or not to treat: The case of tuberculosis, J. Math. Biol., 35:629–656.

Castillo-Chavez C. and Feng Z. (1998) Mathematical models for the disease dynamics of tuberculosis, in Advances in Mathematical Population Dynamics: Molecules, Cells and Man, O. Arino, D. Axelrod, and M. Kimmel (Eds.), World Scientific, 629–656.

Castillo-Chavez C. and Song B. (2004) Dynamical models of tuberculosis and applications, Mathematical Biosciences and Engineering, 1, 361–404.

Chakraborti P.K., Matange N., Nandicoori V.K., Singh Y., Tyagi J.S., Visweswariah S.S. (2011) Signalling mechanisms in *Mycobacteria. Tuberculosis* (Edinb). Sep;91(5):432-40

Chan J., *et al.,* (1991) Lipoarabinomannan, a possible virulence factor involved in persistence of *Mycobacterium tuberculosis* within macrophages. Infect Immun, 59(5): p. 1755-61.

Chao J.D., Papavinasasundaram K.G., Zheng X., Chávez-Steenbock A., Wang X., *et al.* (2010) Convergence of Ser/Thr and Two-component Signaling to Coordinate Expression of the Dormancy Regulon in *Mycobacterium tuberculosis.* J. Biol. Chem., 285, 29239-29246.

Chauhan S. and Tyagi J. S. (2008) Cooperative binding of phosphorylated DevR to upstream sites is necessary and sufficient for activation of the Rv3134c-devRS operon in *Mycobacterium tuberculosis:* implication in the induction of DevR target genes. J. Bacteriol. 190:4301–4312.

Chauhan S. and Tyagi J.S. (2009) Powerful induction of divergent tgs1-Rv3131 genes in *Mycobacterium tuberculosis* is mediated by DevR interaction with a high-affinity site and an adjacent cryptic low-affinity site. J Bacteriol 191: 6075–6081.

Cho H., *et al.* (2001) BeF(3)(-) acts as a phosphate analog in proteins phosphorylated on aspartate: Structure of a BeF(3)(-) complex with phosphoserine phosphatase. Proc Natl Acad Sci USA;98:8525–8530.

Cho H.S., Pelton J.G., Yan D., Kustu S., Wemmer D.E. (2001) Phosphoaspartates in bacterial signal transduction. Curr. Opin. Struct. Biol;11:679–684.

Cho H. Y., Cho H. J., Kim Y. M., Oh J. I., Kang B. S. (2008) Crystallization and preliminary crystallographic analysis of the second GAF domain of DevS from *Mycobacterium smegmatis.* Acta Crystallogr. Sect. F Struct. Biol. Cryst. Commun. 64:274–276

Cho H.Y., Cho H.J., Kim Y.M., Oh J.I., Kang B.S. (2009) Structural insight into the heme-based redox sensing by DosS from *Mycobacterium tuberculosis*. J Biol Chem.; 284:13057–13067.

Cho H.Y. and Kang B.S. (2014) Serine 83 in DosR, a response regulator from *Mycobacterium tuberculosis*, promotes its transition from an activated, phosphorylated state to an inactive, unphosphorylated state. Biochemical and Biophysical Research Communications, 444: 651- 655

Cho S.H., Goodlett D., Franzblau S. (2006) ICAT-based comparative proteomic analysis of non-replicating persistent *Mycobacterium tuberculosis.* Tuberculosis (Edinb), 86:445-460. 38.

Choi J.W., Sherr B.F., Sherr E.B. (1999) Dead or alive? A large fraction of ETS-inactive marine bacterioplankton cells, as assessed by reduction of CTC, can become ETS-active with incubation and substrate addition. Aquat Microb Ecol 18:105–115.

Christensen H., Garton N.J., Horobin R.W., Minnikin D.E., Barer M.R. (1999) Lipid domains of mycobacteria studied with fluorescent molecular probes. Mol. Microbiol. 31: 1561–1572.

Cimino M., Thomas C., Namouchi A., Dubrac S., Gicquel B., Gopaul D.N.(2012) Identification of DNA Binding Motifs of the *Mycobacterium tuberculosis* PhoP/PhoR Two-Component Signal Transduction System.PLoS ONE,7,e42876.

Colditz G, Brewer T, Berkey C, *et al.* (1994) Efficacy of BCG vaccine in the prevention of tuberculosis. Meta-analysis of the published literature. JAMA.;271(9):698–702. doi: 10.1001/ jama.271.9.698.

Colditz G.A., Berkey C.S., Mosteller F., *et al.* (1995) The efficacy of bacillus Calmette-Guerin vaccination of newborns and infants in the prevention of tuberculosis: meta-analysis of the published literature. Pediatrics.;96:29–35.

Cole S. T., Brosch R., Parkhill J., *et al.,* (1998) Deciphering the biology of *Mycobacterium tuberculosis* from the complete genome sequence," Nature, vol. 393, no. 6685, pp. 537–544.

Collins C.M., Gutman D.M. and Laman H. (1993) Identification of a nitrogen-regulated promoter controlling expression of *Klebsiella pneumoniae* urease genes. Molecular Microbiology 8: 187- 98

Cooper A.M. (2009) Cell-mediated immune responses in tuberculosis. Annu Rev Immunol 27: 393–422.

Corbett E. L., Watt C.J., Walker N., Maher D., Williams B.G., *et al.* (2003) The growing burden of tuberculosis: global trends and interactions with the HIV epidemic. Arch. Intern. Med. 163, 1009–1021.

Cousins D.V., Bastida R., Cataldi A., Quse V., Redrobe S., *et al*. (2003) Tuberculosis in seals caused by a novel member of the *Mycobacterium tuberculosis* complex: *Mycobacterium pinnipedii* sp. nov. Int J Syst Evol Microbiol; 53:1305-14; PMID:13130011;

Cox J.S., *et al.,* (1999) Complex lipid determines tissue-specific replication of *Mycobacterium tuberculosis* in mice [In Process Citation]. Nature. 402(6757): p. 79-83.

Crouch S.P. *et al.* (1993) The use of ATP bioluminescence as a measure of cell proliferation and cytotoxicity. J. Immunol. Methods 160, 81–8.

Daffé M., Draper P. (1998) The envelope layers of mycobacteria with reference to their pathogenicity. Adv. Microb. Physiol. 39: 131–203.

Daniel T.M. (2006) The history of tuberculosis. Resp Med 100: 1862–1870.

Dasgupta N., Kapur V., Singh K.K., Das T.K., Sachdeva S., *et al.* (2000) Characterization of a two-component system, devR-devS, of *Mycobacterium tuberculosis.* Tuber. Lung. Dis; 80:141–159

Ddungu H, Johnson JL, Smieja M, Mayanja- Kizza H. (2006) Digital clubbing in tuberculosis-relationship to HIV infection, extent of disease and hypoalbuminemia. BMC Infect Dis.;6:45.

Deb C. *et al.*(2009) A novel in vitro multiple-stress dormancy model for *Mycobacterium tuberculosis* generates a lipid-loaded, drug-tolerant, dormant pathogen. PLoS One.

Delogu G., Brennan M.J. (1999) Functional domains present in the mycobacterial hemagglutinin, HBHA. J Bacteriol; 181:7464-9; PMID:10601202

Deutscher J., Saier M.H. Jr. (2005) Ser/Thr/Tyr protein phosphorylation in bacteria – for long time neglected, now well established. J Mol Microbiol Biotechnol.; 9:125–131. [PubMed: 16415586]

Dhiman A., Bhatnagar S., Kulshreshtha P., Bhatnagar R. (2014) Functional characterization of WalRK: A two-component signal transduction system from Bacillus anthracis. FEBS Open Bio. 2014 Jan 2;4:65-76. doi: 10.1016/j.fob.2013.12.005. eCollection.

Diel R., Loddenkemper R., Meywald-Walter K., Niemann S., Nienhaus A. (2008) Predictive value of a whole blood IFN-gamma assay for the development of active tuberculosis disease after recent infection with *Mycobacterium tuberculosis*. Am J Respir Crit Care Med.;177:1164-70.

DiRita V.J. (1992) Co-ordinate expreSSIOn of virulence genes by ToxR III *Vibrio cholerae*. Molecular Microbiology 6: 451-8

Dominguez C., BoelensR. and Bonvin A. M.J.J. (2003). HADDOCK: a protein-protein docking approach based on biochemical and/or biophysical information. J. Am. Chem. Soc. 125, 1731-1737

Dooley K.E. and Sterling T.R. (2005)Treatment of latent tuberculosis infection: challenges and prospects. Clinics Chest Med.;26:313-26.

Dooley K. E. and Chaisson R. E., (2009) Tuberculosis and diabetes mellitus: convergence of two epidemics, The Lancet Infectious Diseases, vol. 9, no. 12, pp. 737–746.

Dorman S.E. and Holland S.M. (1998) Mutation in the signal-transducing chain of the interferon-γ receptor and susceptibility to mycobacterial infection. J Clin Invest 101:2364–2369.

Dormandy T. (1999). The White Death – A History of Tuberculosis. London: Hambledon Press.

Downing K. J., Mischenko V. V., Shleeva M. O., Young D. I., Young M., *et al.* (2005) Mutants of *Mycobacterium tuberculosis* lacking three of the five rpf-like genes are defective for growth in vivo and for resuscitation in vitro. Infect. Immun. 73:3038–3043.

Draper P. (1998) The outer parts of the mycobacterial envelope as permeability barriers. Front. Biosci. 3: 1253–1261.

Draper P. and Daffé M. (2005) Thee cell envelope of *Mycobacterium tuberculosis* with special reference to the capsule and outer permeability barrier. In ST Cole, KD Eisenach, DN McMurray, and WR Jacobs Jr, eds., Tuberculosis and the tubercle bacillus, pp. 261–273. American Society of Microbiology Press. ISBN 978-1555812959

Dubnau E., Chan J., Raynaud C., Mohan V.P., Lanéelle M.A., *et al*. (2000) Oxygenated mycolic acids are necessary for virulence of *Mycobacterium tuberculosis* in mice. Mol Microbiol 36(3):630–637. DOI:10.1046/j.1365-2958.2000.01882.x

Dubos R.J., Middlebrook G. (1948) Cytochemical reaction of virulent tubercle bacilli. Am Rev Tuberc 58: 698–699.

Dubos R.J. (1955) A Symposium of the Society for General Microbiology. 5: 103–125.

Dutta R., Qin L. and Inouye M. (1999) Histidine kinases: diversity of domain organization. Molecular Microbiology 34: 633-40

Dziejman M. and Mekalanos N. (1995) Two-component signal transduction and its role in the expression of bacterial virulence factors. In Two-component signal transduction, ed. JA Hoch, TJ Silhavy: ASM 305-17

Egger L.A., Park H. and Inouye M. (1997) Signal transduction VIa the histidyl-aspartyl phosphorelay. Genes to cells 2: 167-84

Emmerich R., Hennecke H. and Fischer H. (2000) Evidence for a functional similarity between the two-component regulatory systems RegSR, ActSR and RegBA (PrrBA) in alpha-proteobacteria. Archives Microbiology 2000: 307-13

Engel M., Hindie V., Lopez-Garcia L.A., Stroba A., Schaeffer F., *et al.* (2006) Allosteric activation of the protein kinase PDK1 with low molecular weight compounds. EMBO J, 25: 5469– 5480

Engleberg N.C., Heath A., Miller A., Rivera C. and DiRita V.I. (2001) Spontaneous mutations in the CsrRS two-component regulatory system of *Streptococcus pyogenes* result in enhancd virulence in a murine model of skin and soft tissue infection. Journal of Infectious Diseases 183: 1043-54

Essmann U., Perera L., Berkowitz M. L., Darden T., Lee H. and Pedersen L. G. (1995) A smooth particle mesh Ewald method J. Chem. Phys. 103, pp. 8577-8593

Estrella J.L., Kan-Sutton C., Gong X., Rajagopalan M., Lewis D.E., *et al.* (2011) A Novel in vitro Human Macrophage Model to Study the Persistence of *Mycobacterium tuberculosis* Using Vitamin D(3) and Retinoic Acid Activated THP-1 Macrophages. Front Microbiol 2: 67. doi: 10.3389/fmicb.2011.00067

Ewann F., Jackson M., Pethe K., Cooper A., Mielcarek N., *et al.* (2002) Transient requirement of the PrrA-PrrB two-component system for early intracellular multiplication of *Mycobacterium tuberculosis.* Infect Immun, 70:2256-2263.

Ewann F., Loch C. and Supply P. (2004) Intracellular autoregulation of the *Mycobacterium tuberculosis* PrrA response regulator. Microbiology 150, 241–246.

Evans D. J. and Holian B. L. (1985) The Nose–Hoover thermostat J. Chem. Phys. 83, 4069

Evers Sand Courvalin P. (1996) Regulation ofVanB-type vancomycin resistance gene expression by the VanSB-VanRB two-component regulatory system in *Enterococcus faecalis* V583. Journal of Bacteriology 178: 1302-9

Farnia P., Masjedi M.R., Farnia P., Merza M.A., Tabarsi P., *et al.* (2010) Growth and cell –division in extensive (XDR) and extremely drug resistany (XXDR) tuberculosis strains: transmission and atomic force observation. Int. J. Clin. Exp. Med . 3:320-326

Feng Z., Iannelli M., and Milner F. (2002) A two-strain TB model with age-structure, SIAM J. Appl. Math., 62(5):1634–1656.

Ferwerda G., Kullberg B. J., De Jong D. J. *et al.* (2007) *Mycobacterium paratuberculosis* is recognized by Toll-like receptors and NOD2," Journal of Leukocyte Biology, vol. 82, no. 4, pp. 1011–1018.

Ferwerda G., Girardin S. E., Kullberg B. J. *et al.* (2005) NOD2 and toll-like receptors are nonredundant recognition systems of *Mycobacterium tuberculosis,"* PLoS Pathogens, vol. 1, no. 3, pp. 279–285.

Florczyk M. A., *et al*. (2003) A family of acr-coregulated *Mycobacterium tuberculosis* genes shares a common DNA motif and requires Rv3133c (dosR or devR) for expression. Infect. Immun. 71:5332–5343.

Flynn, J. L., Scanga C. A., Tanaka K. E., and Chan J. (1998) Effects of aminoguanidine on latent murine tuberculosis. J. Immunol. 160:1796–1803.

Flynn J. L., and Ernst J. D. (2000) Immune responses in tuberculosis. Curr. Opin. Immunol. 12:432–436.

Fol M., Chauhan A., Nair N. K., Maloney E., Moomey M., *et al.* (2006) Modulation of *Mycobacterium tuberculosis* proliferation by MtrA, an essential two-component response regulator. Mol. Microbiol. 60:643–657.

Forrellad M. A., Klepp L.I., Gioffré A., Sabio García J.,, Morbidoni H. R., *et al.* (2013) Virulence factors of the *Mycobacterium tuberculosis* complex. Virulence 4:1, 3–66; January 1,

Fournier B., Klier A. and Rapoport. (2001) The two-component system ArlS-ArlR is a regulator of virulence gene expression in *Staphylococcus aureus*. Molecular Microbiology 41: 247-61

Frieden T.R., Sterling T.R., Munsiff S.S., Watt C.J., Dye C. (2003) Tuberculosis. Lancet.;362: 887-899.

Frigui W. *et al.* (2008) Control of *M. tuberculosis* ESAT-6 secretion and specific T cell recognition by PhoP. PLoS pathogens, 4(2), p.e33.

Frucht D.M., Holland S.M. (1996) Defective monocyte costimulation for IFN-γ production in familial disseminated *Mycobacterium avium* complex infection: abnormal IL-12 regulation. J Immunol 157:411–416.

Galperin M.Y., Nikolskaya A.N., and Koonin E.V. (2001) Novel domains of the prokaryotic two-component signal transduction systems. FEMS Microbiol. Lett. 203: 11–21.

Gao R., Mack T.R., and Stock A.M. (2007) Bacterial response regulators: Versatile regulatory strategies from common domains. Trends Biochem. Sci. 32: 225–234.

Garner, M. and Revzin, A. (1981). A gel electrophoresis method for quantifying the binding of proteins to specific DNA regions: application to components of the *Escherichia coli* lactose operon regulatory system. Nucleic Acids Research, Vol.9, No.13, pp. 3047-3060

Geijtenbeek T. B. H., Van Vliet S. J., Koppel E. A. *et al.,* (2003)Mycobacteria target DC-SIGN to suppress dendritic cell function," Journal of Experimental Medicine, vol. 197, no. 1, pp. 7–17.

Gerasimova A., Kazakov A.E., Arkin A.P., Dubchak I., Gelfand M.S. (2011) Comparative genomics of the dormancy regulons in mycobacteria. J Bacteriol, 193(14):3446-3452.

Getahun H., Gunneberg C., Granich R., Nunn P. (2010) HIV infection-associated tuberculosis: the epidemiology and the response. Clin Infect Dis 50: S201–207.

Girardin S. E., Boneca I. G., Viala J. *et al*., (2003)Nod2 is a general sensor of peptidoglycan through muramyl dipeptide (MDP) detection," Journal of Biological Chemistry, vol. 278, no. 11, pp. 8869–8872.

Glickman M.S., Cox J.S., and Jacobs Jr W.R. (2000) A novel mycolic acid cyclopropane synthetase is required for cording, persistence, and virulence of *Mycobacterium tuberculosis*. Mol Cell 5(4):717–727. DOI:10.1016/S1097-2765(00)80250-6

Glynn J.R., Murray J., Bester A. (2008)Effects of duration of HIV infection and secondary tuberculosis transmission on tuberculosis incidence in the South African gold mines. AIDS.;22(14):1859–1867

Gonzalo-Asensio J., Mostowy S., Harders-Westerveen J., Huygen K., Hernandez-Pando R., *et al.* (2008) PhoP: a missing piece in the intricate puzzle of *Mycobacterium tuberculosis* virulence. PLoS ONE 3: e3496.

Gordon S. (2003) Alternative activation of macrophages," Nature Reviews Immunology, vol. 3, no. 1, pp. 23–35,.

Gotoh Y., Eguchi Y., Watanabe T., Okamoto S., Doi A., and Utsumi R. (2010a) Two-component signal transduction as potential drug targets in pathogenic bacteria. Curr. Opin. Microbiol. 13, 232–239

Gotoh Y., Doi A., Furuta E., Dubrac S., Ishizaki Y., *et al.* (2010b) Novel antibacterial compounds specifically targeting the essential WalR response regulator. J Antibiot (Tokyo) 63: 127–134.

Grabski A., Mehler M. and Drott D. (2003) Unattended high-density cell growth and induction of protein expression with the Overnight Express Autoinduction System. inNovations 17, 3–6.

Graham J.E. and Clark-Curtiss J.E. (1999) Identification of *Mycobacterium tuberculosis* RNAs synthesized in response to phagocytosis by human macrophages by selective capture of transcribed sequences (SCOTS). Proc. Natl. Acad. Sci. U. S. A. 96:11554 –11559.

Grange J.M. (1998)Immunophysiology and immunopathology of tuberculosis. In: Davies PDO, ed. Clinical tuberculosis. London, Chapman & Hall, 1998; pp. 129–152.

Grebe T.W. and Stock J.B. (1999) The histidine protein kinase superfamily. Advances in Microbial Physiology 41: 139-214

Griffith D.E. (2007) Therapy of nontuberculous mycobacterial disease. Curr. Opin. Infect. Dis. 20: 198–203.

Groisman E. A. and Heffron F. (1995) in Two-Component Signal Transduction, eds. (Am. Soc. Microbiol., Washington, DC), pp. 319–332.

Groisman E.A. (2001) The pleitropic two-component regulatory system PhoP-PhoQ. Journal of Bacteriology 183: 1835-42

Gupta R.K., Thakur T.S., Desiraju G.R., Tyagi J.S. (2009) Structure-based design of DevR inhibitor active against nonreplicating *Mycobacterium tuberculosis*. J Med Chem; 52: 6324-34.

Gutierrez C., Brisse S., Brosch R., Fabre M., Omais B., *et al.* (2005) Ancient origin and gene mosaicism of the progenitor of *Mycobacterium tuberculosis*. PLoS Pathogens 1: 1–7. doi:10.1371/journal.ppat.0010005.

Hairston N.G. Jr., Dillon T.A., De Stasio B.T. Jr. (1990) A field test for the cues of diapauses in a freshwater copepod. Ecology 71:2218–2223.

Hakenbeck R. and Stock J.B. (1996) Analysis of two-component signal transduction systems involved in transcriptional regulation. Methods in Enzymology 273: 281-300

Hamdi H., Mariette X., Godot V., Weldingh K., Hamid A., *et al*. (2006) Inhibition of anti-tuberculosis T-lymphocyte function with tumour necrosis factor antagonists. Arthritis Res Ther.;8(4):R144.

Hampshire T., Soneji S., Bacon J., James B. W., Hinds J., *et al.* (2004) Stationary phase gene expression of *Mycobacterium tuberculosis* following a progressive nutrient depletion: a model for persistent organisms? Tuberculosis (Edinburgh) 84:228–238.

Harding C.V., Boom W.H. (2010) Regulation of antigen presentation by *Mycobacterium tuberculosis:* a role for Toll-like receptors. Nat Rev Microbiol.;8(4):296–307. doi: 10.1038/nrmicro2321

Hart P,D., Armstrong J.A. (1974) Strain virulence and the lysosomal response in macrophages infected with *Mycobacterium tuberculosis*. Infect Immun 10: 742–746.

Hasan S., Daugelat S., Rao P.S., Schreiber M. (2006) Prioritizing genomic drug targets in pathogens: application to *Mycobacterium tuberculosis*. PLoS Comput Biol, 2:e61.

Haydel S. E., Dunlap N. E., Benjamin W. H., Jr. (1999) In vitro evidence of the twocomponent system phosphorylation between the *Mycobacterium tuberculosis* TrcR/TrcS proteins. Microb. Pathog. 26, 195–206. 123–1

Haydel S.E. and Clark-Curtiss J.E. (2004) Global expression analysis of two-component system regulator genes during *Mycobacterium tuberculosis* growth in human macrophages. FEMS Microbiol. Lett. 236:341–347.

Haydel S. E., Malhotra V., Cornelison G. L., Clark-Curtiss J. E., (2012) The prrAB two-component system is essential for *Mycobacterium tuberculosis* viability and is induced under nitrogen-limiting conditions," J. Bacteriol., vol. 194, pp. 354{ 361

Heplar J.Q., Clifton C.E., Raffel S., Futrelle C.M. (1954) Virulence of the tubercle bacillus. I. Effect of oxygen tension upon respiration of virulent and avirulent bacilli. J Infect Dis 94: 90–98.

Herrera C., Lima S., Munoz R., Ramos G., Rodriguez A., and Salzberg C. (1996) A model describing the response of immune system to *Mycobacterium tuberculosis,* Department of Biometrics Technical Report Series # BU-1364-M, Biometrics Department, Cornell University.

Hess B., Bekker H., Berendsen H.J.C., Fraaije J. (1997) A linear constraint solver for molecular simulations Comput. Chem., Vol. 18, No. 12., pp. 1463-1472, doi:10.1002

Hess K.R., Zhang W., Baggerly K.A., Stivers D.N. and Coombes K.R. (2001) Microarrays: handling the deluge of data and extracting reliable information. Trends in Biotechnology 19: 463-7

Hett E. C., Chao M. C., Steyn A. J., Fortune S. M., Deng L. L., and Rubin E. J. (2007) A partner for the resuscitationpromoting factors of *Mycobacterium tuberculosis.* Molecular Microbiology, vol. 66, no. 3, pp. 658–668, 2007.

Hett E.C. and Rubin E.J. (2008) Bacterial growth and cell division: a mycobacterial perspective. Rs Microbiol. Mol. Biol.; 72, 126-56.

Hilliard J. J., Goldschmidt R. M., Licata L., Baum E. Z., and Bush K. (1999) Multiple mechanisms of action for inhibitors of histidine protein kinases from bacterial two-component systems. Antimicrob. Agents Chemother. 43, 1693–1699

Himpens S., Locht C., Supply P. (2000) Molecular characterization of the mycobacterial SenX3-RegX3 two-component systems: Evidence for autoregulation. Microbiology 146, 3091–3098.

Hoch J.A. (2000) Two-component and phosphorelay signal transduction. Curr. Opin. Microbiol. 3, 165–170.

Hoch J. A. and Silhavy T. J. (1995) Two-Component Signal Transduction. American Society for Microbiology, Washington, DC, USA.

Hoffmann A. and Roeder R. G. (1991) Purification of his-tagged proteins in non-denaturing conditions suggests a convenient method for protein interaction studies. Nucleic Acids Res, 19(22):6337-8., Nov 25.

Holmes C.B., Wood R., Badri M. (2006) CD4 decline and incidence of opportunistic infections in Cape Town, South Africa: implications for prophylaxis and treatment. J Acquir Immune Defic Syndr.;42(4):464–469

Honaker R.W., Leistikow R.L., Bartek I.L., Voskuil M.I. (2009) Unique roles of DosT and DosS in DosR regulon induction and *Mycobacterium tuberculosis* dormancy. Infect Immun.; 77:3258–3263. [PubMed: 19487478]

Honaker R. W, Dhiman R. K, Narayanasamy P, Crick D. C, Voskuil M. (2010)DosS responds to a reduced electron transport system to induce the *Mycobacterium tuberculosis* DosR regulon. J Bacteriol 192: 6447–6455.

Hopewell P.C., Pai M., Maher D., Uplekar M., Raviglione M.C. (2006) International standards for tuberculosis care. Lancet Infect Dis 6: 710–725.

Hopkins A.L., Groom C.R. (2002) The druggable genome. Nat Rev Drug Discov 1(9): 727–730

Humphrey W., Dalke A. and Schulten K., (1996) VMD - Visual Molecular Dynamics, J. Molec. Graphics, vol. 14, pp. 33-38.

Hunter R.L., Venkataprasad N., Olsen M.R. (2006a) The role of trehalose dimycolate (cord factor) on morphology of virulent *M. tuberculosis* in vitro. Tuberculosis (Edinb) 86: 349–356.

Hunter R.L., Olsen M., Jagannath C., Actor J.K. (2006b) Trehalose 6,6'-dimycolate and lipid in the pathogenesis of caseating granulomas of tuberculosis in mice. Am. J. Pathol. 168: 1249–1261.

Imamura A, Hanaki N, Nakamura A, Suzuki T, Taniguchi M, *et al.* (1999) Compilation and characterization of Arabiopsis thaliana response regulators implicated in His-Asp phosphorelay signal transduction. Plant Cell Physiol, 40:733-742.

Indrigo J., Hunter R.L. Jr, Actor J.K. (2003) Cord factor trehalose 6,6'-dimycolate (TDM) mediates trafficking events during mycobacterial infection of murine macrophages. Microbiology 149: 2049–2059.

Inglis J.J., Simelyte E., McCann F.E., Criado G., Williams R.O. (2008) Protocol for the induction of arthritis in C57BL/6 mice. Nat Protoc 3: 612–618. doi: 10.1038/nprot.2008.19

Ioanoviciu A., Meharenna Y.T., Poulos T.L., Ortiz de Montellano P.R. (2009) DevS oxy complex stability identifies this heme protein as a gas sensor in *Mycobacterium tuberculosis* dormancy. Biochemistry 48: 5839–48.

Jacobs C., Domian I.J., Maddock J.R. and Shapiro L. (1999) Cell cycle-dependent polar localization of an essential bacterial histidine kinase that controls DNA replication and cell division. Cell 97: 111-20

Jarlier V., Nikaido H. (1994) Mycobacterial cell wall: structure and role in natural resistance to antibiotics. FEMS Microbiol. Lett. 123: 11–18.

Jasmer R.M., Nahid P., Hopewell P.C. (2002) Latent tuberculosis infection. N Eng J Med.;347(23):1860-6.

Jayakumar D., Jacobs W.R., Jr., Narayanan S. (2008) Protein kinase E of *Mycobacterium tuberculosis* has a role in the nitric oxide stress response and apoptosis in a human macrophage model of infection. Cell Microbiol; 10:365-74; PMID:17892498

Jiang, M., Shao, W., Perego, M., and Hoch, J.A. (2000) Multiple histidine kinases regulate entry into stationary phase and sporulation in *Bacillus subtilis.* Mol Microbiol 38: 535-542.

Jo E.K., Yang C.S., Choi C.H., Harding C.V. (2007) Intracellular signalling cascades regulating innate immune responses to Mycobacteria: branching out from Toll-like receptors. Cell Microbiol.;9(5):1087–1098. doi: 10.1111/j.1462-5822.2007.00914.x.

Joe M., Bai Y., Nacario R.C., Lowary T.L. (2007) Synthesis of the docosanasaccharide arabinan domain of mycobacterial arabinogalactan and a proposed octadecasaccharide biosynthetic precursor. J Am Chem Soc.;129 (32):9885-9901.

Jordan S., Hutchings M.I. and Mascher T. (2008) Cell envelope stress response in Gram-positive bacteria. FEMS Microbiol Rev 32: 107-146.

Jorgensen W. L., Chandrasekhar J., Madura J. D., Impey R. W. Klein, M. L. (1983) Comparison of simple potential functions for simulating liquid water. J. Chem. Phys, 79, 926-935. doi:10.1063/1.445869

Joshi R., Pati S., Kalantri S., Schwartzman K., Menzies D., Pai M. (2007)Prevalence of abnormal radiological findings in health care workers with latent tuberculosis infection and correlations with T cell immune response. PLoS One.;2(8):e805.

Kana B.D., Gordhan B.G., Downing K.J., Sung N., Vostroktunova G., et al. (2008) The resuscitation-promoting factors of Mycobacterium tuberculosis are required for virulence and resuscitation from dormancy but are collectively dispensable for growth in vitro. Mol Microbiol 67: 672–684.

Cariss S. J., Tayler A. E., and Avison M. B. (2008) Defining the growth conditions and promoter-proximal DNA sequences required for activation of gene expression by CreBC in Escherichia coli. J. Bacteriol. 190, 3930–3939

Kendall S. L., Movahedzadeh F., Rison S. C., Wernisch L., Parish T., *et al.* (2004) The *Mycobacterium tuberculosis* dosRS two-component system is induced by multiple stresses. Tuberculosis (Edinburgh) 84:247–255.

Kennelly P. J. (2002) Protein kinases and protein phosphatases in prokaryotes: a genomic perspective. FEMS Microbiol. Lett. 206:1-8

Kenney L.J., Bauer M.D., Silhavy T.J. (1995) Phosphorylation-dependent conformational changes in OmpR, an osmoregulatory DNA-binding protein of *Escherichia coli*. Proc.Natl.Acad.Sci.USA 92:8866-0

Khan S., Nagarajan S.N., Parikh A., Samantaray S., Singh A., *et al.* (2010) Phosphorylation of enoyl-acyl carrier protein reductase InhA impacts mycobacterial growth and survival. J Biol Chem; 285:37860-71.

Kim M., Park K., Ko I., Kim Y.M., Oh J. (2010) Different roles of DosS and DosT in the hypoxic adaptation of mycobacteria J. Bacteriol., 192 pp. 4868–4875

Kirschner D. (1999) Dynamics of co-infection with *M. tuberculosis* and HIV-1, Theoretical Population Biology, 55:94–109.

Kjelleberg S., Hermansson M., Marden P., Jones G.W. (1987) The transient phase between growth and nongrowth of heterotrophic bacteria, with emphasis on the marine environment. (Translated from eng). Annu Rev Microbiol 41:25–49.

Klein A.H., Shulla A., Reimann S.A., Keating D.H. and Wolfe A.J. (2007) The intracellular concentration of acetyl phosphate in Escherichia coli is sufficient for direct phosphorylation of two-component response regulators. J Bacteriol 189, 5574–5581.

Klossek A., Dannenberg C., Feuerhahn M., Korholz D. (2004) Pulmonary tuberculosis in a child receiving intensive chemotherapy for acute myeloblastic leukemia. J Ped Haem Onc.;26(1):64-7.

Kumar A., Toledo J.C., Patel R.P., Lancaster J.R. Jr, Steyn A.J.C. (2007) *Mycobacterium tuberculosis* DosS is a redox sensor and DosT is a hypoxia sensor. Proc Natl Acad Sci USA.; 104:11568–11573.

Kumar A., Deshane J.S., Crossman D.K., Bolisetty S., Yan B.S., *et al.* (2008) Heme oxygenase-1-derived carbon monoxide induces the *Mycobacterium tuberculosis* dormancy regulon. J. Biol. Chem., 283, 18032–18039.

Kumar P., Kumar D., Parikh A., Rananaware D., Gupta M., *et al*. (2009) The *Mycobacterium tuberculosis* protein kinase K modulates activation of transcription from the promoter of mycobacterial monooxygenase operon through phosphorylation of the transcriptional regulator VirS. J Biol Chem; 284:11090-9;

Kundu M. and Thompson C. B. (2008) Autophagy: basic principles and relevance to disease," Annual Review of Pathology, vol. 3, pp. 427–455.

Lamichhane G. (2010) Novel targets in M. tuberculosis: search for new drugs. Trends Mol. Med. 17:25–33.

Lange R., Wagner C., Saizieu A., Flint N., Molnos J., Stieger *et al.* (1999) Domain organization and molecular characterization of 13 two-component systems identified by genome sequencing of Streptococcus pneumoniae. Gene 237: 223-34

Larson C.L. and Wicht W.C. (1964) Infection of mice with *Mycobacterium tuberculosis*, strain H37Ra. Am Rev Respir Dis 90: 742–748.

Lawn S.D., Wood R., De Cock K.M., Kranzer K., Lewis J.J., *et al.* (2010) Antiretrovirals and isoniazid preventive therapy in the prevention of HIV-associated tuberculosis in settings with limited health-care resources. Lancet Infect Dis 10: 489–498. doi: 10.1016/s1473-3099(10)70078-5

Lee H.N., Lee N.O., Ko I.J., Kim S.W., Kang B.S. and Oh J.I. (2013) Involvement of the catalytically important Asp54 residue of *Mycobacterium smegmatis* DevR in protein–protein interactions between DevR and DevS. FEMS Microbiology Letters, 343: 26–33

Lee J.M., Cho H.Y., Cho H.J., Ko I.J., Park S.W., *et al.* (2008) O2- and NO-sensing mechanism through the DevSR two-component system in *Mycobacterium smegmatis.* J Bacteriol 190: 6795–6804.

Lee S.Y., Cho H.S., Pelton J.G., Yan D., Berry E.A., Wemmer D.E. (2001) Crystal structure of activated CheY. Comparison with other activated receiver domains. J Biol Chem;276:16425–16431.

Lee T.Y., Makino K., Shinagawa H., Amemura M. and Nakata A. (1989) Phosphate regulon in members of the family Enterobacteriaceae: comparison of the phoB-phoR operons of Escherichia coli, Shigella dysenteriae, and Klebsiella pneumoniae. Journal of Bacteriology 171: 6593-9

Lein A., Von Reyn C. (1997) In vitro cellular and cytokine responses to mycobacterial antigens: application to diagnosis of tuberculosis infection and assessment of response to mycobacterial vaccines. Am J Med Sci.;313:364-71.

Leistikow R.L., Morton R.A., Bartek I.L., Frimpong I., Wagner K., Voskuil M.I. (2009) The *Mycobacterium tuberculosis* DosR regulon assists in metabolic homeostasis and enables rapid recovery from nonrespiring dormancy J. Bacteriol., 192, pp. 1662–1670

Leonard C. J., Aravind L., and Koonin E. V. (1998) Novel families of putative protein kinases in bacteria and archaea: evolution of the "eukaryotic" protein kinase superfamily. Genome Res. 8:1038–1047.

Leung C.C., Yam W.C., Yew W.W., *et al.* (2010) T-Spot.TB outperforms tuberculin skin test in predicting tuberculosis disease. Am J Respir Crit. Care Med.;182(6):834–840.

Levin S. A. and Pimentel D. (1981) Selection of intermediate rates of increase in parasite host systems, Am. Nat., 117:308–315.

Lewis R. J., Brannigan J. A., Muchova K., Barak I., Wilkinson A. J. (1999) Phosphorylated aspartate in the structure of a response regulator protein. J. Mol. Biol. 294:9–15

Lewis K. (2007) Persister cells, dormancy and infectious disease. Nat Rev Microbiol 5: 48–56.

Lietman T. and Blowe S. M. (2000) Potential impact of tuberculosis vaccines as epidemic control agents, Clinical Infectious Diseases, 30(Suppl. 3): S316–322

Lin P.L., Pawar S., Myers A., Pegu A., Fuhrman C., Reinhart T.A., *et al.* (2006) Early events in *Mycobacterium tuberculosis* infection in cynomolgus macaques. Infect.Immun. 74, 3790–3803.doi: 10.1128/IAI.74.4.2052-2062.2006

Lin P.L. and Flynn J.L.(2010) Understanding latent tuberculosis: amoving target. J. Immunol. 185, 15–22. doi:10.4049/jimmunol.0903856

Lin X., Hethcote H. W. and van den Driessche P. (1993) An epidemiological models for HIV/AIDS with proportional recruitment, Math. Biosci., 118:181–195.

López D., Vlamakis H., and Kolter R. (2009) Generation of multiple cell types in *Bacillus subtilis.* FEMS Microbiol Rev 33: 152-163.

Lorca G.L., Ezersky A., Lunin V.V., Walker J.R, Altamentova S., *et al.* (2007) Glyoxylate and pyruvate are antagonistic effectors of the Escherichia coli IclR transcriptional regulator. J Biol Chem 2007, 282: 16476–16491

Lowell A. M., Edwards L. B. and Palme C. E. (1969) Tuberculosis, Harvard University Press, Cambridge, MA.

Ludwiczak P., Gilleron M., Bordat Y., Martin C., Gicquel B., Puzo G. (2002) *Mycobacterium tuberculosis* phoP mutant: lipoarabinomannan molecular structure. Microbiology 148:3029-3037

Lukat G.S., McCleary W.R., Stock A.M., Stock J.B. (1992)Phosphorylation of bacterial response regulator proteins by low molecular weight phosphodonors. Proc Natl Acad Sci U S A;89:718–722.

Lugosi L. (1992) Theoretical and methodological aspects of BCG vaccine from the discovery of Calmette and Guerin to molecular biology. A review. Tuber. Lung Dis. 73:252–261

Lyon G. J., Mayville P., Muir T. W. and Novick R. P. (2000) Rational design of a global inhibitor of the virulence response in *Staphylococcus aureus*, based in part on localization of the site of inhibition to the receptor-histidine kinase, AgrC. Proc Natl Acad Sci U S A 97, 13330–13335.

Lyon G.J. and Novick R.P. (2004) Peptide signaling in *Staphylococcus aureus* and other Gram-positive bacteria. Peptides 25: 1389-1403.

Mackaness G.B., Smith N., Wells A.Q. (1954) The growth of intracellular tubercle bacilli in relation to their virulence. Am Rev Tuberc 69: 479–494.

MacKerell Jr. A.D., *et al.* (1998) All-atom empirical potential for molecular modeling and dynamics studies of proteins. J Phys Chem B 102 (18): 3586–3616. doi:10.1021/jp973084f

Malhotra V., Sharma D., Ramanathan V. D., Shakila H., Saini D. K., *et al.* (2004). Disruption of response regulator gene, devR, leads to attenuation in virulence of *Mycobacterium tuberculosis.* FEMS Microbiol. Lett. 231:237–245.

Maeda T., Wurgler-Murphy S. M. and Saito H. (1994) A two-component system that regulates an osmosensing map kinase cascade in yeast. Nature, 369, 242–245.

Manabe Y.C., Bishai W.R. (2000) Latent *Mycobacterium tuberculosis* - persistence, patience and winning by waiting. Nat Med.;6:1327-9.

Martin C., Williams A., Hernandez-Pando R., Cardona P.J., Gormley E., et al. (2006) The live *Mycobacterium tuberculosis* phoP mutant strain is more attenuated than BCG and confers protective immunity against tuberculosis in mice and guinea pigs. Vaccine 24: 3408–3419.

Martin P.K., Li T., Sun D., Biek D.P. and Schmid M.B. (1999) Role in cell permeability of an essential two-component system in *Staphylococcus aureus.* Journal of Bacteriology 181: 3666- 73

Mascher T., Helmann J.D., Unden G. (2006) Stimulus perception in bacterial signal-transducing histidine kinases. Microbiol. Mol. Biol. Rev. 70: 910–938.

Matsushita M. & Janda K. D. (2002) Histidine kinases as targets for new antimicrobial agents. Bioorg Med Chem 10, 855–867.

Matsuzaki K., Sugishita K. and Miyajima K. (1999) Interactions of an antimicrobial peptide, magainin 2, with lipopolysaccharide-containing liposomes as a model for outer membranes of gram-negative bacteria. FEBS Lett.;449(2-3):221–224.

McBryde E. and Denholm J.T. (2012) Risk of active tuberculosis in immigrants: effects of age, region of origin and time since arrival in a low-exposure setting. Med J Aust.;197(8):458-61.

McCune Jr. R.M., McDermott W., Tompsett R. (1956) The fate of *Mycobacterium tuberculosis* in mouse tissues as determined by the microbial enumeration technique. II. The conversion of tuberculous infection to the latent state by the administration of pyrazinamide and a companion drug. J. Exp. Med. 104: 763-802.

Middlebrook G., Dubos R.J., Pierce C. (1947) Virulence and morphological characteristics of mammalian tubercle bacilli. J Exp Med 86: 175–184.

Miller J. F., Mekalanos J. J. and Falkow S. (1989) Coordinate regulation and sensory transduction in the control of bacterial virulence. Science 243, 916–922.

Mishra B.B., Moura-Alves P., Sonawane A., Hacohen N., Griffiths G., *et al.* (2010) *Mycobacterium tuberculosis* protein ESAT-6 is a potent activator of the NLRP3/ASC inflammasome. Cell. Microbiol. 12: 1046–1063.

Mizrahi V. and Andersen S.J. (1998) DNA repair in *Mycobacterium tuberculosis.*What have we learnt from the genome sequence? Mol. Microbiol. 29: 1331–1339.

Mizuno T. (2005) Two-component phosphorelay signal transduction systems in plants: from hormone responses to circadian rhythms. Bioscience, Biotechnology, and Biochemistry , 69(12), 2263–2276.

Mukamolova G. V., Turapov O. A., Young D. I., Kaprelyants A. S., Kell D. B., and Young M. (2002) A family of autocrine growth factors in *Mycobacterium tuberculosis*. Mol. Microbiol. 46:623–635.

Murphy D. J. and Brown J. R. (2007) Identification of gene targets against dormant phase *Mycobacterium tuberculosis* infections. BMC Infect. Dis. 7:84.

Musser J.M., Amin A., Ramaswamy S. (2000) Negligible genetic diversity of *Mycobacterium tuberculosis* host immune system protein targets: evidence of limited selective pressure. Genetics. 155(1): p. 7-16.

Muttucumaru D. G., Roberts G., Hinds J., Stabler R. A., and Parish T. (2004) Gene expression profile of *Mycobacterium tuberculosis in* a nonreplicating state. Tuberculosis (Edinburgh) 84:239–246.

Niemann S., Richter E., Rüsch-Gerdes S. (2000) Differentiation among members of the *Mycobacterium tuberculosis* complex by molecular and biochemical features: evidence for two pyrazinamide-susceptible subtypes of M. bovis. J Clin Microbiol; 38:152-7; PMID: 10618079

Nigou J., Zelle-Rieser C., Gilleron M., Thurnher M., and Puzo G. (2001) Mannosylated lipoarabinomannans inhibit IL-12 production by human dendritic cells: evidence for a negative signal delivered through the mannose receptor," Journal of Immunology, vol. 166, no. 12, pp. 7477–7485.

Nikaido H. (1994) Prevention of drug access to bacterial targets: permeability barriers and active efflux. Science 264: 382–388.

Ninfa A.J., Magasanik B. (1986) Covalent modification of the glnG product, NRI, by the glnL product, NRII, regulates the transcription of the glnALG operon in Escherichia coli. Proc Natl Acad Sci U S A.;83(16):5909–5913

Norton B.L. and Holland D.P. (2012) Current management options for latent tuberculosis: a review. Infection and drug resistance 5: 163–173

O'Toole R., Smeulders M.J., Blokpoel M.C., Kay E.J., Lougheed K., Williams H.D. (2003) A two-component regulator of universal stress protein expression and adaptation to oxygen starvation in *Mycobacterium smegmatis*. J. Bacteriol. 185(5), 1543–1554.

Oddo M., Renno T., Attinger A., Bakker T., MacDonald H.R., *et al.* (1998) Fas ligand-induced apoptosis of infected human macrophages reduces the viability of intracellular *Mycobacterium tuberculosis.* J Immunol 160: 5448–5454.

Ogura M., Yamaguchi H., Yoshida K., Fujita Y. and Tanaka T. (2001) DNA micro array analysis of Bacillus subtilis DegU, ComA and PhoP regulons: an approach to comprehensive analysis of *B. subtilis* two-component regulatory systems. Nucleic Acids Research 29: 3804-13

Orme I.M. (1988) Mouse model of the recrudescence of latent tuberculosis in the elderly. Am. Rev. Respir. Dis. 137: 716-718.

Ottenhoff T.H., Verreck F.A., Lichtenauer-Kaligis E.G., Hoeve M.A., Sanal O. and van Dissel J.T. (2002) Genetics, cytokines and human infectious disease: lessons from weakly pathogenic mycobacteria and salmonellae. Nat.Genet. 32: 97-105.

Pai M., Zwerling A., Menzies D. (2008) Systematic review: T-cell-based assays for the diagnosis of latent tuberculosis infection: an update. Ann Intern Med.;149(3):177–184.

Pang X., Samten B., Cao G., Wang X., Tvinnereim A.R., *et al.* (2013) MprAB Regulates the espA operon in *Mycobacterium tuberculosis* and modulates ESX-1 function and host cytokine response. J Bacteriol 195:66–75

Park H. D., Guinn K. M., Harrell M. I., Liao R., Voskuil M. I., *et al.* (2003) Rv3133c/dosR is a transcription factor that mediates the hypoxic response of *Mycobacterium tuberculosis*. Mol. Microbiol. 48:833–843.

Parish T., Smith D. A., Kendall S., Casali N., Bancroft G. J., Stoker N. G. (2003) Deletion of two-component regulatory systems increases the virulence of *Mycobacterium tuberculosis*. Infect. Immun. 71, 1134–1140.

Parkinson J. S. and Kofoid E. C. (1992) Communication modules in bacterial signaling proteins. Ann. Rev. Genet., 26, 71–112.

Paton N.I., Chua Y.K., Earnest A., Chee C.B. (2004) Randomized controlled trial of nutritional supplementation in patients with newly diagnosed tuberculosis and wasting. Am J Clin Nutr.;80:450-465.

Pearl J. E., Saunders B., Ehlers S., Orme I. M. and Cooper A. M. (2001) Inflammation and lymphocyte activation during mycobacterial infection in the interferon-gamma-deficient mouse. Cell Immunol. 211: 43-50.

Peloquin C.A. (2002)Tuberculosis, in Pharmacotherapy: A Pathophysiologic Approach, Dipiro, JT; et al., Editors., McGraw-Hill: New York, NY. p. 1917-38.

Perego M, Hanstein C, Welsh KM, Djavakhishvili T, Glaser P, *et al.* (1994) Multiple protein-aspartate phosphatases provide a mechanism for the integration of diverse signals in the control of development in *B. subtilis.* Cell 79: 1047–1055.

Perez E., Samper S., Bordas Y., Guilhot C., Gicquel B., Martin C. (2001) An essential role for phoP in *Mycobacterium tuberculosis* virulence. Mol. Microbiol. 41:179–187.

Perspicace S., Rufer A. C., Thoma R., Mueller F., Hennig M., *et al.* (2013) Isothermal titration calorimetry with micelles: Thermodynamics of inhibitor binding to carnitine palmitoyltransferase 2 membrane protein.

Pierce C.H., Dubos R.J. and Schaefer W.B. (1953) Multiplication and survival of tubercle bacilli in the organs of mice. J Exp Med 97: 189–206.

Plotkin S. and Vidor E. (2004) Poliovirus Vaccine-Inactivated. In Vaccines, ed. S. A. Plotkin, and W. A. Orenstein. Philadelphia: Saunders

Podust L.M., Ioanoviciu A., Ortiz de Montellano P.R. (2008) 2.3 Å X-ray structure of the heme-bound GAF domain of sensory histidine kinase DosT of *Mycobacterium tuberculosis.* Biochemistry.

Pouchot J., Grasland A., Collet C., Coste J., Esdaile J.M., Vinceneux P. (1997) Reliability of tuberculin skin test measurement. Ann Intern Med.; 126(3):210–214.

Raghavan S., Manzanillo P., Chan K., Dovey C. and Cox J.S. (2008) Secreted transcription factor controls *Mycobacterium tuberculosis* virulence. Nature, 454: 717-721. DOI: 10.1038/nature07219

Rajni and Laxman S. Meena. (2011) Unique Characteristic Features of *Mycobacterium Tuberculosis* in Relation to Immune System. American Journal of Immunology 7 (1): 1-8. ISSN 1553-619X

Raman K., Yeturu K. and Chandra N. (2008) targetTB: a target identification pipeline for *Mycobacterium tuberculosis* through an interactome, reactome and genome-scale structural analysis. BMC Syst Biol. 2:109

Restrepo B. I. (2007) Convergence of the tuberculosis and diabetes epidemics: renewal of old acquaintances. Clin. Infect. Dis. 45, 436–438.

Rickman L., Saldanha J. W., Hunt D. M., Hoar D. N., Colston M. J., *et al.* (2004) A two-component signal transduction system with a PAS domain-containing sensor is required for virulence of *Mycobacterium tuberculosis* in mice. Biochem Biophys Res Commun 314, 259–267.

Rifat D., Bishai W. R., Karakousis P. C. (2009) Phosphate depletion: a novel trigger for *Mycobacterium tuberculosis* persistence. J Infect Dis 200, 1126–1135.

Rittershaus E.S.C., Baek S-H., Sassetti C.M. (2013) The normalcy of dormancy: common themes in microbial quiescence. Cell Host Microbe 13: 643–651. doi: 10.1016/j.chom.2013.05.012

Roberts D. M., Liao R. P., Wisedchaisri G., Hol W. G., Sherman D. R. (2004) Two sensor kinases contribute to the hypoxic response of *Mycobacterium tuberculosis*. J. Biol. Chem. 279:23082–23087.

Rook G., Steele J., Ainsworth M., Champion B. (1986) Activation of macrophages to inhibit proliferation of *Mycobacterium tuberculosis*: comparison of the effects of recombinant gamma-interferon on human monocytes and murine peritoneal macrophages. Immunol.;59:333-8.

Roszak D.B., Colwell R.R. (1987) Survival strategies of bacteria in the natural environment. Microbiol Rev 51:365–379.

Roupie V., Romano M., Zhang L., Korf H., Lin M.Y., *et al*. (2007) Immunogenicity of eight dormancy regulon-encoded proteins of *Mycobacterium tuberculosis* in DNA-vaccinated and tuberculosis-infected mice. Infect Immun 75: 941–949

Roychoudhury S., Zielinski N.A., Ninfa A.J., Allen N.E., Jungheim L.N., *et al.* (1993) Inhibitors of two-component signal transduction systems: inhibition of alginate gene activation in *Pseudomonas aeruginosa.* Proc Natl Acad Sci U S A 90: 965–969.

Rowberg R.E. (2001) Pharmaceutical Research and Development: A Description and Analysis of the Process, CRS Report for Congress RL30913 (Congressional Research Service), p. 23.

Rumbaugh K.P., Griswold J.A., Iglewski B.H. and Hamood A.N. (1999) Contribution of quorum sensing to the virulence of *Pseudomonas aeruginosa* in bum wound infections. Infection and Immunity 67: 5854-62

Rustad T.R., Sherrid A.M., Minch K.J., Sherman D.R. (2009) Hypoxia: a window into *Mycobacterium tuberculosis* latency. Cell Microbiol.

Ryll R., Kumazawa Y., Yano I. (2001) Immunological properties of trehalose dimycolate (cord factor) and other mycolic acid-containing glycolipids – a review. Microbiol. Immunol. 45: 801–811.

Saini D.K., Malhotra V., Dey D., Pant N., Das T.K., Tyagi J.S. (2004a) DevR-DevS is a bona fide twocomponent system of *Mycobacterium tuberculosis* that is hypoxia-responsive in the absence of the DNA-binding domain of DevR. Microbiology. 150:865–875. [PubMed: 15073296]

Saini D. K., Malhotra V., and Tyagi J. S. (2004b) Cross talk between DevS sensor kinase homologue, Rv2027c, and DevR response regulator of *Mycobacterium tuberculosis.* FEBS Lett. 565:75–80.

Saini D.K. and Tyagi J.S. (2005) High-throughput microplate phosphorylation assays based on DevR-DevS/Rv2027c 2-component signal transduction pathway to screen for novel antitubercular compounds. J Biomol Screen, 10(3):215-224

Saito H. (2001) Histidine phosphorylation and two-component signaling in eukaryotic cells. Chem Rev;101:2497–2509.

Sali A. and Blundell T.L. (1993) Comparative protein modelling by satisfaction of spatial restraints. J. Mol. Biol. 234, 779-815.

Salmond G.P.C., Bycroft B.W., Stewart G.S.A.B. and Williams P. (1995) The bacterial 'enigma': Cracking the code of cell-cell communication. Molecular Microbiology 16: 615-24

Samten B., Wang X., Barnes P.F. (2011) Immune regulatory activities of early secreted antigenic target of 6-kD protein of *Mycobacterium tuberculosis* and implications for tuberculosis vaccine design. Tuberculosis (Edinb.) 91(Suppl 1):S114 –S118.

Sardiwal S., Kendall S. L., Movahedzadeh F., Rison S. C., Stoker N. G., and Djordjevic S. (2005). A GAF domain in the hypoxia/NO-inducible *Mycobacterium tuberculosis* DosS protein binds haem. J. Mol. Biol. 353:929–936.

Sassetti C. M., Boyd D. H. and Rubin E. J. (2001) Comprehensive identification of conditionally essential genes in mycobacteria. Proc. Natl. Acad. Sci. USA 98, 12712–12717.

Sassetti C. M., Boyd D. H. and Rubin E. J. (2003a) Genetic requirements for mycobacterial survival during infection. Proc. Natl. Acad. Sci. USA 100, 12989–12994.

Sassetti C. M., Boyd D. H. and Rubin E. J. (2003b) Genes required for mycobacterial growth defined by high density mutagenesis. Mol. Microbiol. 41, 179–187.

Schmitz S-F. Shu (2000) Treatment and vaccination against HIV/AIDS in homosexuals with genetic heterogenity, Math. Biosci.,167:1–18.

Schwartz, Mindy A. (2009) Tuberculosis: a journey across time.

Selwyn P., Hartel D., Lewis V., Schoenbaum E., Vermund S., *et al.* (1989) A prospective study of the risk of tuberculosis among intravenous drug users with human immunodeficiency virus infection. N Eng J Med.;320(9):545-50.

Sharma K., Gupta M., Krupa A., Srinivasan N. and Singh Y. (2006) EmbR, a regulatory protein with ATPase activity, is a substrate of multiple serine/threonine kinases and phosphatase in *Mycobacterium tuberculosis*. FEBS J; 273:2711-21;

Sherman D. R., Voskuil M., Schnappinger D., Liao R., Harrell M. I., and Schoolnik G. K. (2001) Regulation of the *Mycobacterium tuberculosis* hypoxic response gene encoding alpha-crystallin. Proc. Natl. Acad. Sci. USA 98:7534–7539.

Silversmith R. E. and Bourret R. B. (1999) Throwing the switch in bacterial chemotaxis. Trends Microbiol. 7:16 –22.

Simonovic M. and Volz K. (2001) A distinct meta-active conformation in the 1.1-A resolution structure of wildtype ApoCheY. J. Biol. Chem;276:28637–28640.

Smith I. (2003) *Mycobacterium tuberculosis* pathogenesis and molecular determinants of virulence. Clin Microbiol Rev 16(3):463–496. DOI:10.1128/CMR.16.3.463-496.2003

Sonnenberg P., Glynn J.R. and Fielding K. (2005) How soon after infection with HIV does the risk of tuberculosis start to increase? A retrospective cohort study in South African gold miners. J Infect Dis.;191(2):150–158.

Sousa E.H., Tuckerman J.R., Gonzalez G., Gilles-Gonzalez M.A. (2007) DosT and DevS are oxygen-switched kinases in *Mycobacterium tuberculosis.* Protein Sci 16: 1708–1719.

Starke J.R., Jacobs R. and Jereb J. (1992) Resurgence of tuberculosis in children. J Pediatr 1992;120:839-55.

Steenken W. JR. (1935) Lysis of tubercle bacilli in vitro. Proc Soc Exptl Biol Med 33: 253–255.

Steenken W. JR. (1938) Spontaneous lysis of tubercle bacilli on artificial culture media. Am Rev Tuberc 38: 777–790.

Stephenson K. and Hoch J. A. (2002) Two-component and phosphorelay signal-transduction systems as therapeutic targets. Curr. Opin. Pharmacol. 2, 507–512

Stephenson K. and Hoch, J. A. (2004) Developing inhibitors to selectively target two-component and phosphorelay signal transduction systems of pathogenic microorganisms. Curr. Med. Chem. 11, 765–773

Stock A.M., Koshland D.E. and Stock J.B. (1985) Homologies between the *Salmonella typhimurium* Che Y protein and proteins involved in the regulation of chemotaxis, membrane protein synthesis and sporulation. Proceedings of the National Academy of Sciences, USA 82: 7989-93

Stock A. M., Robinson V. L. and Goudreau P. N. (2000) Two-component signal transduction. Annu. Rev. Biochem. 69:183–215.

Studier F.W. and Moffatt B.A. (1986) Use of bacteriophage T7 RNA polymerase to direct selective high-level expression of cloned genes. J. Mol. Biol. 189, 113-130.

Studier F.W. (2005) Protein production by auto-induction in high-density shaking cultures. Protein Expr. Purif. 41, 207-234.

Sun G., Birkey, S.M. and Hulett, F.M. (1996) Three two-component signal-transduction systems interact for Pho regulation in *Bacillus subtilis.* Mol Microbiol 19: 941-948.

Sussman A.S., Halvorson H.O. (1966) Spores Their Dormancy and Germination (Harper & Row, New York, NY).

Sussman A.S., Douthit H.A. (1973) Dormancy in microbial spores. Annu Rev Plant Physiol 24:311–352.

Szurmant H. and Ordal G.W. (2004) Diversity in chemotaxis mechanisms among the bacteria and archaea. Microbiol Mol Biol Rev 68: 301-319.

Takayama K., Wang L., David H.L. (1972) Effect of isoniazid on the in vivo mycolic acid synthesis, cell growth, and viability of *Mycobacterium tuberculosis*. Antimicrob Agents and Chemother.;2(1):29–35.

Takayama K., Wang C., and Besra G.S. (2005) Pathway to synthesis and processing of mycolic acids in *Mycobacterium tuberculosis.* Clin Microbiol Rev 18:81–101. DOI:10.1128/CMR.18.1.81-101.2005

Takeda K. and Akira S. (2004) TLR signaling pathways," Seminars in Immunology,vol. 16, no. 1, pp.3–9

Taneja N.K., Dhingra S., Mittal A., Naresh M., Tyagi J.S. (2010) *Mycobacterium tuberculosis* transcriptional adaptation, growth arrest and dormancy phenotype development is triggered by vitamin C. PLoS One, 5, e10860. North RJ, Jung YJ. Immunity to tuberculosis. Annu Rev Immunol. 2004; 22:599–623. [PubMed: 15032590]

Tang Y.T., Gao R., Havranek J.J., Groisman E.A., Stock A.M., *et al.* (2012) Inhibition of Bacterial Virulence: Drug-Like Molecules Targeting the *Salmonella enterica* PhoP Response Regulator. Chem Biol Drug Des 79 (6) 1007–1017. doi: 10.1111/j.1747-0285.2012.01362.x

Tekaia F., Gordon S.V., Garnier T., Brosch R., Barrell B.G., Cole S.T. (1999) Analysis of the proteome of *Mycobacterium tuberculosis* in silico. Tuber. Lung Dis. 79:329–342.

Thompsett A.R., Abdelraheim S.R., Daniels M. and Brown D.R. (2005)High affinity binding between copper and full-length prion protein identified by two different techniques. J Biol Chem, 280: 42750–42758

Throup J.P., Zappacosta F., Lunsford R.D., Annan R.S., Carr S.A., *et al.* (2001) The srhSR gene pair from *Staphylococcus aureus*: genomic and proteomic approaches to the identification and characterisation of gene function. Biochemistry 40: 10392-401

Thurlbeck W., Churg A. (1995) Pathology of the Lung 2nd edition. Thieme Medical Publishers. Chapter 13, p234

Tobian A.A., Potter N.S., Ramachandra L., Pai R.K., Convery M., *et al.* (2003) Alternate class I MHC antigen processing is inhibited by Toll-like receptor signaling pathogen-associated molecular patterns: *Mycobacterium tuberculosis* 19-kDa lipoprotein, CpG DNA, and lipopolysaccharide. J Immunol; 171:1413-22; PMID:12874233

Tsai M. C., Chakravarty S., Zhu G., Xu J., Tanaka K., *et al.* (2006) Characterization of the tuberculous granuloma in murine and human lungs: cellular composition and relative tissue oxygen tension. Cell Microbiol. 8: 218-232.

Tufariello J. M., Mi K., Xu J., Manabe Y. C., Kesavan A. K., *et al.* (2006) Deletion of the *Mycobacterium tuberculosis* resuscitation-promoting factor Rv1009 gene results in delayed reactivation from chronic tuberculosis. Infect. Immun. 74:2985– 2995.

Turenne C.Y., Wallace R. Jr and Behr M.A. (2007) *Mycobacterium avium* in the postgenomic era. Clin. Microbiol. Rev. 20: 205–229.

Tyagi J.S. and Sharma D. (2004) Signal transduction systems of mycobacteria with special reference to M. tuberculosis. Current Science 86: 93–102.

Uhl M. A. and Miller J. F. (1995) in Two-Component Signal Transduction, eds. Hoch, J. A. & Silhavy, T. J. (Am. Soc. Microbiol., Washington, DC), pp. 333–349.

Ulrichs T. and Kaufmann S. H. (2006) New insights into the function of granulomas in human tuberculosis. J.Pathol. 208: 261-269.

Underhill D. M., Ozinsky A., Smith K. D. and Aderem A. (1999) Toll-like receptor-2 mediates mycobacteria-induced proinflammatory signaling in macrophages," Proceedings of the National Academy of Sciences of the United States of America, vol. 96, no. 25, pp. 14459–14463.

Waaler H. T., Gese A. and Anderson S. (1962) The use of mathematical models in the study of the epidemiology of tuberculosis, Am. J. Publ. Health, 52:1002–

Wade M.M. and Zhang Y. (2004) Anaerobic incubation conditions enhance pyrazinamide activity against *Mycobacterium tuberculosis.* J Med Microbiol. 53(Pt 8): p. 769-73.

Wang J.Y., Hsueh P.R., Wang S.K., *et al.* (2007) Disseminated tuberculosis: a 10-year experience in a medical center. Medicine (Baltimore).; 86(1):39-46.

Wang L., Fabret C., Kanamaru K., Stephenson K., Dartois V., *et al.* (2001) Dissection of the functional and structural domains of phosphorelay histidine kinase A of Bacillis subtilis. Journal of Bacteriology 183: 2795-802

Wang Y. and Klemke R.L. (2008) PhosphoBlast, a Computational Tool for Comparing Phosphoprotein Signatures among Large Datasets. Mol Cell Proteomics 7: 145-62

Watanabe T., Okada A., Gotoh Y., Utsumi, R. (2008) Inhibitors targeting two-component signal transduction. Adv Exp Med Biol 631: 229–236. doi: 10.1007/978-0-387-78885-2-16

Weinrauch Y., Penchev R., Dubnau E., Smith I. and Dubnau D. (1990) A *Bacillus subtilis* regulatory gene product for genetic competence and sporulation resembles sensor protein members of the bacterial two component systems. Genes and Development 4: 860-72

Wayne L. G. and Hayes L. G. (1996) An in vitro model for sequential study of shiftdown of *Mycobacterium tuberculosis* through two stages of nonreplicating persistence. Infect. Immun. 64:2062–2069.

Wayne L. G. and Sohaskey C. D.(2001) Nonreplicating persistence of *Mycobacterium tuberculosis.* Annu. Rev. Microbiol. 55:139–163.

Warner D.F. and Mizrahi V. (2007) The survival kit of *Mycobacterium tuberculosis*.NatMed.;13(3):282-4.

Watanabe T., Okada A., Gotoh Y., Utsumi R. (2008) Inhibitors targeting two-component signal transduction. Adv Exp Med Biol 631: 229–236.

Weinstein M., Lois A.F., Monson E.K., Ditta G.S. and Helinski D.R. (1992) Isolation of phosphorylation-deficient mutants of the Rhizobium meliloti two-component regulatory protein, FixJ. Molecular Microbiology 6: 2041-9

Wells C.D., Cegielski J.P., Nelson L.J., *et al*. (2007) HIV infection and multidrug-resistant tuberculosis—the perfect storm," Journal of Infectious Diseases, vol. 196, no. 1, pp. S86–S107.

Wheeler R.T. and Shapiro L. (1999) Differential localisation of two histidine kinases controlling bacterial cell differentiation. Molecular Cell 4: 683-94

WHO (2013). World Health Organisation Global Tuberculosis Report.(2013)

Whittington R.J., Marshall D.J., Nicholls P.J., Marsh I.B. and Reddacliff L.A. (2004) Survival and dormancy of *Mycobacterium avium* subsp. paratuberculosis in the environment. Appl Environ Microbiol 70:2989–3004.

Willett J.W., Kirby J.R. (2012) Genetic and biochemical dissection of a HisKA domain identifies residues required exclusively for kinase and phosphatase activities. PLoS Genet.;8:e1003084. PGENETICS-D-12–00740

Winder F.G. and Collins P.B. (1970) Inhibition by isoniazid of synthesis of mycolic acids in *Mycobacterium tuberculosis.* J Gen Microbiol.;63(1):

Wisedchaisri G., Wu M., Rice A.E., Roberts D.M., Sherman D.R. and Hol W.G. (2005) Structures of *Mycobacterium tuberculosis* DosR and DosRDNA complex involved in gene activation during adaptation to hypoxic latency. J Mol Biol, 354:630-641.

Wisedchaisri G., Wu M., Sherman D.R. and Hol W.G. (2008) Crystal structures of the response regulator DosR from *Mycobacterium tuberculosis* suggest a helix rearrangement mechanism for phosphorylation activation. J. Mol. Biol. 378:227–242.

Wolanin P.M., Thomason P.A. and Stock, J.B. (2002) Histidine protein kinases: Key signal transducers outside the animal kingdom. Genome Biol. 3: REVIEWS3013. doi:10.1186/gb-2002-3-10-reviews3013.

VanCrevel R., Ottenhoff T. H. M. and Van derMeer J.W. M.(2002) Innate immunity to *Mycobacterium tuberculosis,"* Clinical Microbiology Reviews, vol. 15, no. 2, pp. 294–309.

van Hest R., Baars H., Kik S., van Gerven P., Trompenaars M. C., *et al.* (2004) Hepatotoxicity of Rifampin-Pyrazinamide and Isoniazid Preventive Therapy and Tuberculosis Treatment. Clinical Infectious Diseases; 39:488–96

Vazquez-Yanes C. and Orozco-Segovia A. (1990) Ecological significance of light controlled seed germination in two contrasting tropical habitats. Oecologia 83:171–175.

Velayati A.A., Farnia P., Masjedi M.R., Ibrahim T.A., Tabarsi P., *et al.* (2009) Totally drug-resistant tuberculosis strains: evidence of adaptation at the cellular level. Eur Respir J. 34:1202-1203.

Velayati A.A., Farnia P., Masjedi M.R., Zhavnerko G.K., Merza M.A., *et al*. (2011) Sequential adaptation in latent tuberculosis bacilli: observation by atomic force microscopy (AFM). Int J Clin Exp Med 2011;4

Velayati A.A. and Farnia P. (2012) Morphological Characterization of *Mycobacterium tuberculosis*, Understanding Tuberculosis - Deciphering the Secret Life of the Bacilli, Dr. Pere-Joan Cardona (Ed.), ISBN: 978-953-307-946-2

Via L.E., Curcic R., Mudd M.H., Dhandayuthapani S., Ulmer R.J. and Deretic V. (1996) Elements of signal transduction in *Mycobacterium tuberculosis:* in vitro phosphorylation and in vivo expression of the response regulator MtrA. J Bacteriol 178: 3314–3321.

Vinton P., Mihrshahi S., Johnson P., Jenkin G.A., Jolley D., Biggs B-A. (2009) Comparison of QuantiFERON-TB Gold In-Tube test and tuberculin skin test for identification of latent *Mycobacterium*

tuberculosis infection in healthcare staff and association between positive test results and known risk factors for infection. Infect Cont Hosp Epi.;30(3):215-21.

Vohra R., Gupta M., Chaturvedi R. and Singh Y. (2006) Attack on the scourge of tuberculosis: patented drug targets. Recent Pat. Antiinfect. Drug Discov. 1:95–106.

Volkman B.F., Lipson D., Wemmer D.E., Kern D. (2001) Two-state allosteric behavior in a single-domain signaling protein. Science 2001;291:2429–2433.

Voskuil M.I., Schnappinger D., Visconti K.C., Harrell M.I., Dolganov G.M., Sherman D.R., Schoolnik G.K. (2003) Inhibition of respiration by nitric oxide induces a *Mycobacterium tuberculosis* dormancy program. J Exp Med. 198:705–713.

Voskuil M. I., Visconti K. C. and Schoolnik G. K. (2004) *Mycobacterium tuberculosis* gene expression during adaptation to stationary phase and low-oxygen dormancy. Tuberculosis (Edinburgh) 84:218–227.

Xia M., Huang R., Witt K.L., Southall N., Fostel J., Cho M.H., et al. (2008) Compound cytotoxicity profiling using quantitative high-throughput screening. Environ Health Perspect.;116:284–91. doi: 10.1289/ehp.10727.

Yan D., Cho H., Hastings C., Igo M., Lee S., *et al*. (1999) Beryllofluoride mimics phosphorylation of NtrC and other bacterial response regulators. Proc Natl Acad Sci USA 96, 14789–14794.

Yarwood J.M., McConnick J.K. and Schlievert P.M. (2001) Identification of a novel two-component regulatory system that acts in global regulation of virulence factors of *Staphylococcus aureus.* Journal of Bacteriology 183: 1113-23

Yuan Y., Crane D.D., Simpson R.M., Zhu Y.Q., Hickey M.J., *et al.* (1998) The 16-kDa alpha-crystallin (Acr) protein of *Mycobacterium tuberculosis is* required for growth in macrophages. Proc Natl Acad Sci U S A; 95:9578-83.

Yukl E.T., Ioanoviciu A., de Montellano P.R. and Moënne-Loccoz P. (2007) Interdomain interactions within the two-component heme-based sensor DevS from *Mycobacterium tuberculosis.* Biochemistry; 46:9728–9736.

Yukl E.T., Ioanoviciu A., Nakano M.M., de Montellano P.R.and Moënne-Loccoz P. (2008) A distal tyrosine residue is required for ligand discrimination in DevS from *Mycobacterium tuberculosis.* Biochemistry; 47:12532–12539.

Yukl E. T., *et al*. (2011) Nitric oxide dioxygenation reaction in DevS and the initial response to nitric oxide in *Mycobacterium tuberculosis.* Biochemistry 15:1023–1028.

Zahrt T.C. and Deretic V. (2001) *Mycobacterium tuberculosis* signal transduction system required for persistent infections. Proc Natl Acad Sci USA 98: 12706–12711.

Zahrt T. C., Wozniak C., Jones D. and Trevett A. (2003) Functional analysis of the *Mycobacterium tuberculosis* MprAB two-component signal transduction system. Infect. Immun. 71:6962–6970.

Zhang Y., *et al.,* (1992) The catalase-peroxidase gene and isoniazid resistance of *Mycobacterium tuberculosis.* Nature. 358(6387): p. 591-93.

Zhang Y., Permar S. and Sun Z., (2002) Conditions that may affect the results of susceptibility testing of *Mycobacterium tuberculosis* to pyrazinamide. J Med Microbiol. 51(1): p. 42-49.

Zhang Y., Post-Martens K., Denkin S. (2006) New drug candidates and therapeutic targets for tuberculosis therapy. Drug Discov Today 2006, 11:21-27.

Zheng H., Lu L., Wang B., Pu S., Zhang X., *et al.*(2008) Genetic basis of virulence attenuation revealed by comparative genomic analysis of *Mycobacterium tuberculosis* strain H37Ra versus H37Rv.PLoS One, 3:e2375

Zink A.R., Sola C., Reischl U., Grabner W., Rastogi N., *et al.* (2003) Characterization of *Mycobacterium tuberculosis* complex DNAs from Egyptian mummies by spoligotyping. J Clin Microbiol 41: 359–367. doi: 10.1128/jcm.41.1.359-367.2003

Annex 1

1 Tuberculosis

Tuberculosis (TB) is an infectious disease caused by *Mycobacterium tuberculosis (M.tuberculosis, Mtb*), which most commonly affects the lungs. The World Health Organization (WHO) estimates that one third of world's total population is currently infected with *Mtb* and approximately 10% of these people are expected to develop active TB at some point in their lifetime. A new individual is infected every second whilst another one dies from the disease every 15 seconds. Furthermore, the development of multidrug-resistant tuberculosis (MDR-TB) and extensively drug-resistant tuberculosis (XDR-TB) strains, together with the spread of risk factors such as human immunodeficiency virus (HIV), acquired immunodeficiency syndrome (AIDS) and diabetes (Corbett *et al*., 2003, Restrepo *et al*., 2007), continue making *Mtb* a health concern in developed countries and strengthened the urge to develop new treatment infection strategies.

TB has been historically known by different names, such as consumption, phthisis, wasting disease, Pott's disease or scrofula and has infected humans for millennia.

Evidence of TB has been found in Egyptian mummies of several thousand years BC and also in antique Babylonian and Chinese writings. Recent molecular genetic studies have shown that *M. tuberculosis* is ~3 million years old (Zink *et al*., 2003, Gutierrez *et al*., 2005).

The tuberculosis epidemic in Europe, which probably started in the 17th century and lasted two hundred years, was known as the Great White Plague and caused more than 1 billion deaths (Dormandy *et al*., 1999).

Until mid-1800s, many people believed that TB was hereditary. In 1865 Jean Anoine-Villemin demonstrated that TB was contagious. In 1882 Robert Koch discovered *Mtb*, the bacterium that causes TB. These two findings changed the medical community's understanding of how to prevent and treat the disease.

Another important development in the 19th century were sanatoriums, a special type of hospitals, where infectious persons were isolated from society, treated and provided with supervised recuperation and convalescence. The sanatoriums, usually

located in the countryside, demonstrated the value of rest, fresh air, good nutrition and isolation to prevent the spread of infection. Initially started in Silelsia in 1859 by Hermann Brehmer, sanatoriums became widespread by the late 19th and early 20th centuries being used also as centers of discovery (Schwartz *et al.,* 2009).

One of the great advances in TB treatment, commenced in the nineteenth century, was the development of the vaccination. In the 1880s, Louis Pasteur began his studies on immunization against anthrax, chicken cholera, and, later, rabies. Koch hoped to develop an effective vaccine from an extract of the protein coat of the tuberculin organism. In 1908, the French scientists Albert Calmette and Camille Guerin grew Koch's bacillus in a variety of media in an attempt to decrease their virulence and increase the capacity to produce immunity. This led to the development of one of the worldwide most popular vaccine called Bacille Calmette-Guérin (BCG) introduced in 1921 for the first time (Schwartz *et al.,* 2009).

In 1944 Albert Schatz, Elizabeth Bugie, and Selman Waksman isolated streptomycin from *Streptomyces griseus*, the first antibiotic and first bacterial agent effective against *Mycobacterium tuberculosis*. This finding is generally considered the beginning of the modern era of tuberculosis, although the true revolution began some years later, in 1952, with the development of isoniazid, the first oral mycobactericidal drug (Daniel *et al*., 2006). The discovery of rifampin in the 1970s significantly reduced the number of tuberculosis cases until the 1980s.

The expansion of drug-resistant strains in the 1980s tempered the complete elimination of TB .

1.1 Mortality, incidence, prevalence and HIV co-infection

The burden of disease caused by TB can be measured in terms of mortality, incidence or prevalence.

WHO Global Tuberculosis Report 2013 (WHO 2013) indicates that in 2012 almost 1,3 million people died of TB, new cases were estimated at 8.6 million, and the number of total TB cases worldwide is about 14 million.

1.1.1 Mortality

The global TB mortality rate dropped 45% between 1990 and 2012. In 2012, 1.3 million people died from TB, including almost one million deaths among HIV-negative individuals and 320,000 among people who were HIV-positive. TB is one of the top killers among women, with 250,000 deaths in HIV-negative women population and 160 000 deaths among HIV-positive women in 2012. An estimated 530,000 children were infected with TB and 74,000 children who were HIV-negative died of TB in 2012. Although globally the numbers of HIV-associated TB deaths were similar among men and women, there are regional variations. In the African Region, more deaths occurred among women than men, while in other regions more deaths were estimated to occur among men. The male:female ratio of HIV-associated TB deaths ranged from 0.83 in the African Region to 3.1 in the Western Pacific Region.

1.1.2 Incidence

In 2012, there were an estimated 8.6 million new cases of TB globally, equivalent to 122 cases per 100,000 population (Fig. 64). Most of the estimated number of cases in 2012 occurred in Asia (58%) and Africa (27%); smaller proportions of cases occurred in the Eastern Mediterranean Region (8%), the European Region (4%) and the South America, Central America and North America (3%).

The five countries with the largest number of incident cases in 2012 were India (2.0 million–2.4 million), China (0.9 million–1.1 million), South Africa (0.4 million–0.6 million), Indonesia (0.4 million–0.5 million) and Pakistan (0.3 million–0.5 million). India and China alone accounted for 26% and 12% of global cases, respectively.

Of the 8.6 million new cases in 2012, 1.0 million– 1.2 million (12–14%) were among people infected with HIV.

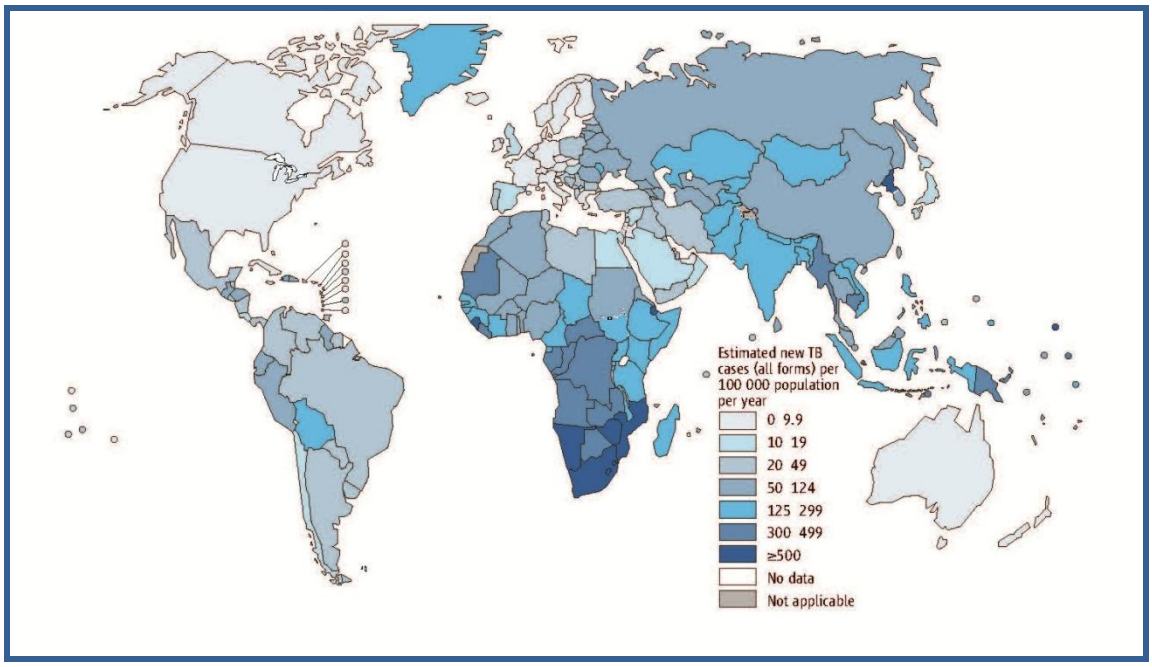

Fig. 64 Estimated TB incident rates, 2012 (WHO, 2013)

1.1.3 Prevalence

There were estimated 12 million prevalent cases (range, 10 million–13 million) of TB in 2012, equivalent to 169 cases per 100,000 population. The prevalence rate has fallen by 37% globally since 1990.

Geographically, most of the TB cases occur in Southeast Asia's most populous countries, with the highest number in China and India with 1.3 million and 1.2 million new cases respectively (almost 40% of the world's TB cases), followed by Indonesia. The heaviest TB burden is observed in Sub-Saharan Africa, with South Africa, Zimbabwe and DR Congo showing prevalence rates higher than 500 cases/100,000 population (Fig. 65). About 60% of cases are in the South-East Asia and Western Pacific regions.

Conversely, the TB prevalence in Western countries is dramatically lower, ranging from 10 to 50 cases per 100,000 populations, and it has been estimated that in Western European countries half of the TB cases occur in foreign-born citizens who migrated from countries with high TB prevalence.

India, the Russian Federation and South Africa have more than half of the world's cases of MDR-TB. The highest proportions of TB patients with MDR-TB are in eastern European countries.

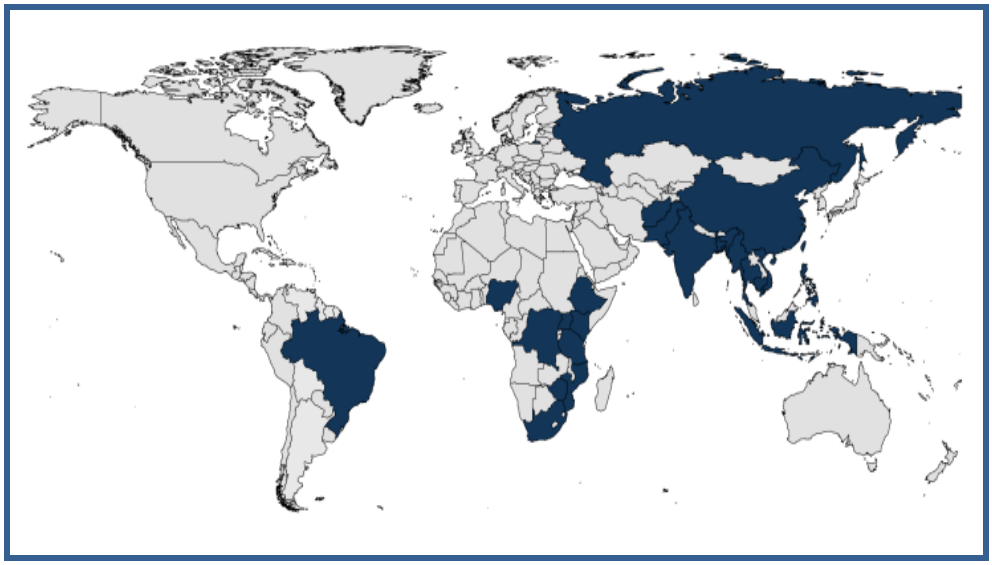

Fig. 65 The 22 high burden TB countries. Source: Kaiser Family Foundation, based on WHO Global Tuberculosis Report; 2013 (www.GlobalHealthFacts.org).

1.1.4 Tuberculosis and HIV

HIV infection is the most potent risk factor for the development of TB disease. Following acquisition of HIV-1 infection (the most common and pathogenic strain of the virus), the risk of TB in individuals with *Mtb* infection increases from an approximately 10% lifetime risk to over 10% each year (Corbett *et al.*, 2003). The risk in those living with HIV depends on the degree of immunodeficiency, the prevailing socioeconomic conditions, and the TB infection pressure in the community. HIV leads to disease as a result of the depletion of CD4+ T4 helper cells and the consequent inability to fight opportunistic infections. T4 cells are the major cell type that is infected by the virus. Infected CD4+ T4 helper cells become targets for HIV-specific CD8+ killer cells. Furthermore, the HIV virus has the ability to make a copy of itself which can integrate with the DNA of the T4 helper cell and result in a latent infection (Schlossberg 1983, Lawn *et al.*, 2010).

In addition, the risk of TB disease continues to rise as CD4+ cell counts decrease (Badri *et al.*, 2002, Holmes *et al.*, 2006) The velocity with which risk increases

following HIV seroconversion is striking, rising 2-3-fold within the first 2 years of infection (Sonnenberg *et al.*, 2005, Glynn *et al.*, 2008).

A major step forward is the development by the World Health Organization and the Centers for Disease Control and Prevention of a high sensitivity symptom screening tool for use in HIV-infected patients (Getahun *et al.*, 2010). In contrast to the existing strategy of screening for cough of 2-3 weeks duration, this new screening tool identifies any HIV-infected patient with cough (any duration), fever, night sweats, or weight loss, and such patients should be further evaluated for TB disease.

In 2012, 1.1 million (13%) of the 8.6 million people who developed TB worldwide were HIV-positive; 75% of these HIV-positive TB cases were in the African Region (WHO 2013) (Fig. 66).

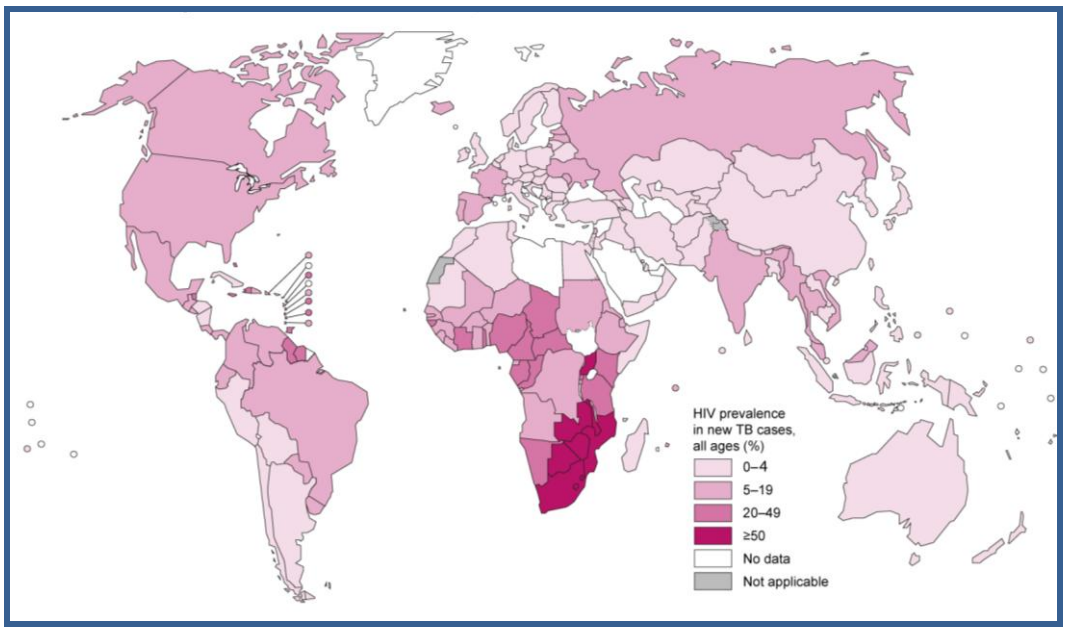

Fig. 66 Estimated HIV prevalence in new TB cases, 2012 (WHO, 2013).

1.2 Pathogenesis

The immune mechanisms that protect the individual against tuberculosis are extremely complex. Infection occurs when a person inhales droplet nuclei containing tubercle bacilli that reach terminal alveoli in the lungs.

The first step is the recognition of mycobacteria as invading pathogens, followed by activation of innate host defense responses. Cell-mediated immunity is usually

developed within approximately two to eight weeks from the initial infection, followed by initiation of adaptive immune responses.

The activated T lymphocytes, macrophages, and other immune cells form granulomas that wall off the growing necrotic tissue limiting further replication and spread of the tubercle bacilli.

Granulomatous inflammation is a distinctive pattern of chronic inflammation and adaptive immunity, and the granuloma is the hallmark of many human diseases among which tuberculosis is embraced (Thurlbeck *et al.,* 1995; Algood *et al.,* 2003). Its formation is firmly linked to the type IV (delayed type) hypersensitivity reaction (DTH), which is a form of adaptive cell- mediated immunity that is mediated by activated T lymphocytes and their products, called cytokines (Boyd 1995). Activated immune mechanisms lead to destruction of the bacilli and disease progression is arrested (Ahmad *et al*., 2011).

If the infection proceeds, bacilli begin to multiply rapidly and cause TB. This process can occur in different parts in the body. The infection starts with phagocytosis of the bacilli by phagocytic antigen-presenting cells in the lung including alveolar macrophages and dendritic cells.

Macrophages are central in chronic inflammation because of the vast number of substances they produce (Beutler, 2004) and different mechanisms through which they can eliminate mycobacteria, such as production of reactive oxygen and nitrogen (VanCrevel *et al.,* 2002). Autophagy, a cellular process through which cytoplasmic components, including organelles and intracellular pathogens, are detached in a double-membrane-bound autophagosome and delivered to the lysosome for degradation, also determines the fate of intracellular mycobacteria (Kundu *et al.,* 2008).

Dendritic cells play an important role in antigen capture and the induction of T cell responses, especially in naïve T cells (Hart 1997).

M. tuberculosis is recognized by the host through Toll-like receptors (TLRs), nucleotide-binding oligomerization domain- (NOD-) like receptors (NLRs), and C-type lectins (Jo *et al*., 1998; Harding *et al*., 2010).

The mycobacterial structures, such as lipoproteins and glycolipids, associated with a subset of immune receptors initiating phagocytosis and mediating specific host cell

responses, interact with TLRs. Signaling cascades are triggered with the significant role of adaptor molecule myeloid differentiation primary response protein 88 (MyD88) (Underhill *et al.,* 1999). Later, IL-1 receptor-associated kinases (IRAK), TNF receptor-associated factor 6 (TRAF6), TGFβ-activated protein kinase 1 (TAK1), and mitogen-activated protein (MAP) kinase are enrolled in a signaling pathways with the consequence of activation and nuclear translocation of transcription factors such as the nuclear transcription factor (NF)-κB (Takeda *et al.,* 2004). This introduces transcription of genes engaged in the activation of the innate host defense, mainly the production of proinflammatory cytokines as TNF, IL1β, and IL-12 and nitric oxide (Akira *et al.,* 2003).

NOD2 is an intracellular receptor, mediating stimulation of proinflammatory cytokine production by *Mtb*. It is a receptor for bacterial peptidoglycans (Girardin *et al.,* 2003) and plays role in the recognition of mycobacteria (Ferwerda *et al.,* 2005, 2007).

The mannose receptor (MR), belonging to the C-type lectins family, is involved in the recognition of polysaccharide structures of pathogen and is highly expressed on alveolar macrophages (Gordon *et al.,* 2003). Mycobacterial stimulation through MR leads to production of IL- 4 and IL-13, inhibition of IL-12 production, and failure to activate oxidative responses (Nigou *et al.,* 2001; Geijtenbeek *et al.,* 2003).

Produced inflammatory cytokines and chemokines serve as a signal for infection and are involved in many crucial outcomes.

The CD4+ T cells control infection in the granuloma through several functions, such as apoptosis of infected macrophages, production of other cytokines (*e. g.* IL-2 and TNF-α), induction of other immune cells (macrophages or dendritic cells) to produce other immunoregulatory cytokines such as IL-10, IL-12, and IL- 15, and activation of macrophages through direct contact via CD40 ligand (Chan and Flynn *et al.,* 2004, Cooper *et al*., 2009, Oddo *et al*., 1998).

The IFN-γ is the key cytokine in the defence against mycobacteria, as individuals revealing a genetic defect in IFNγ production or receptors, develop severe systemic infection (Frucht *et al.,* 1996; Dorman *et al.,* 1998).

Introduction of *M. tuberculosis* into the lungs leads to infection of the respiratory system; however, bacilli may reach any part of the body or spread from lungs to

other organs, such as the lymph nodes, pleura, bones/joints, or meninges, and cause extrapulmonary tuberculosis. Systemic (also called military) TB occurs when bacilli is being carried to all parts of body, through bloodstream.

1.3 Clinical symptoms

Mycobacterium tuberculosis mainly infects the lungs and causes a bad coughing. The clinical manifestations of tuberculosis can vary depending on the stage of tuberculosis, which include latency, primary disease, primary progressive (active) disease, and extrapulmonary disease.

Latency, which is minutely described in Chapter 3, does not display any signs or symptoms of the disease. Individuals do not feel sick and are not infectious.

Primary pulmonary tuberculosis is also often asymptomatic; however some self-limiting findings might be noticed in an assessment. Associated paratracheal lymphadenopathy may occur due to bacilli spread from the lungs through the lymphatic system. If the primary lesion enlarges, pleural effusion is a distinguishing finding. Whilst the bacilli infiltrate the pleural space from an adjacent area, the effusion develops and it may remain small and resolve spontaneously, or it may become large enough to induce indications such as fever, pleuritic chest pain, and dyspnea. Dyspnea is a consequence of faint gas exchange in the areas of affected lung tissue.

Active tuberculosis, which develops in 5% to 10% of persons infected with *Mtb,* produces nonspecific symptoms at early period. Manifestations often include progressive fatigue, malaise, weight loss, and a low-grade fever accompanied by chills and night sweats. Loss of weight, a classic feature of tuberculosis, is provoked by lack of appetite and the altered metabolism associated with the inflammatory and immune responses. It involves the loss of both fat and lean tissue, which leads to the fatigue as an effect of the decreased muscle mass (Paton *et al.,* 2004) and subsequently together with the weakness to the anemia. Finger clubbing, a late sign of poor oxygenation, may occur; however, it does not indicate the extent of disease (Ddungu *et al.,* 2006). A cough eventually develops in most patients and, although initially nonproductive, it advances to a productive cough of purulent

sputum with or without blood streak. Hemoptysis can be the result of a dilated vessel in a cavity, or the formation of an aspergilloma in an old cavity. Pleuritic chest pain may occur due to the inflamed parenchyma. Dyspnea or orthopnea are the consequences of the extensive disease when the increased interstitial volume leads to a decrease in lung diffusion capacity.

Due to the immune response to the infection and subsequently large increase of leukocytes, leukocytosis may also occur.

Although lungs are the most common location for tuberculosis, extrapulmonary disease is diagnosed in more than 20% of immunocompetent patients, indicating the increasing risk with immunosuppression. The most dangerous location is the central nervous system, where infection may result in or space occupying tuberculomas or meningitis, fatal if not treated (Frieden *et al.,* 2003). Clinical manifestations that should prompt consideration of this disease would be headache and change in mental status after possible exposure to TB or in high risk groups. Disseminated or miliary tuberculosis, where mycobacteria reaches bloodstram, is another fatal form of TB and can spread throughout the body, leading to multiorgan involvement (Wang *et al.,* 2007). This type of disease progresses rapidly and its systemic and nonspecific signs and symptoms, such as fever, weight loss, and weakness make it difficult to diagnose. Lymphatic tuberculosis is the most common extrapulmonary tuberculosis, in which cervical adenopathy occurs most often. Further possible locations of the infection extend include bones, joints, pleura, and genitourinary system (CDC).

1.4 Transmission

Tuberculosis is primarily transmitted through air and spread by small airborne droplets, called droplet nuclei. Individuals with pulmonary or laryngeal disease aerosolize droplet nuclei when coughin or sneezing tubercle bacilli which may be inhaled by others. Individuals at high risk of infection include those who are frequently exposed for long period of times to infectious individuals. The minuscule droplets can remain airborne for minutes to hours after expectoration.

There are four factors that determine the probability of transmission of *Mtb*: i) susceptibility (immune status) of the exposed individual; ii) infectiousness of the person with TB disease, which is directly proportional to the number of sprayed bacilli; iii) environmental factors that affect the concentration of *M. tuberculosis* organisms; and iv) exposure of the susceptible individual, measured in proximity, frequency, and duration.

Mathematical models of TB transmission classify individuals as either susceptible, exposed, infectious, recovered or vaccinated (Castillo-Chavez *et al.,* 2004). Since the first model, built for the transmission dynamics of TB (Waaler *et al.,* 1962), many others have been proposed. They consider diverse constituents, such as multiple strains of TB (Blower *et al.,* 1996; Castillo-Chavez *et al.,* 1997, 1998), density dependent demography (Levin *et al.,* 1981; Lin *et al.,* 1993; Lowell *et al.,* 1969), co-infection with HIV (Kirschner *et al.,* 1999; Schmitz *et al.,* 2000), and multiple levels of macrophages (Herrera *et al.,* 1996).

Two vaccine models, preexposure and postexposure (Lietman *et al.,* 2000) and one that examines both multiple strains and variable latent period have been described (Feng *et al.,* 2002).

1.5 Diagnosis

The most frequent method for diagnosing TB worldwide is sputum smear microscopy (Hopewell *et al.,* 2006). This test is relatively simple and rapid to perform, but it is not specific for tuberculosis as other mycobacteria give the same results. However, it does provide a quick method to determine if prevention should be taken while more definitive testing is performed.

For the test, sputum is smeared on a slide, stained, dried, and then treated with alcohol. Any bacilli that are present will remain red because they will not destain (Fig. 67). Results of sputum smears should be available within 24 hours of the sample collection.

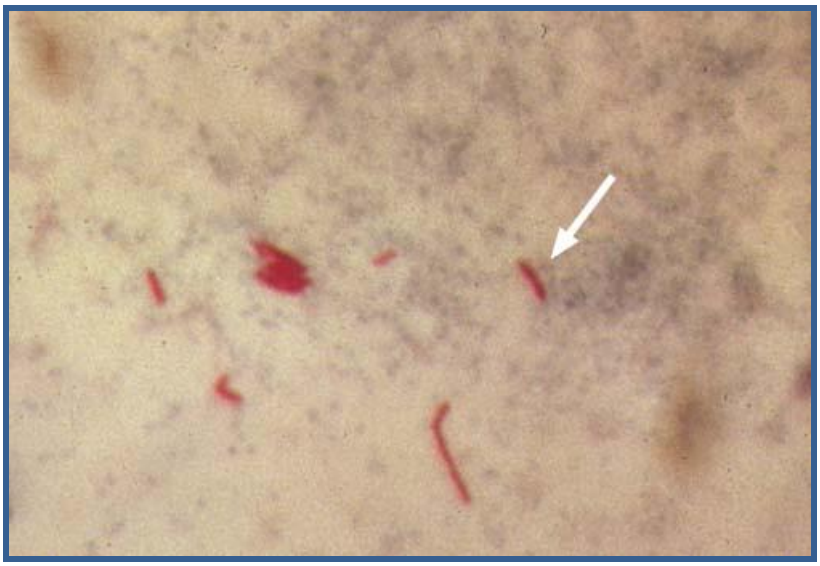

Fig. 67 *Mycobacterium tuberculosis.* Acid-fast stain, extracted from http://textbookofbacteriology.net/tuberculosis.html. The arrow indicates *Mtb* smear, stained with carbol-fuchsin.

Beside sputum samples, cerebrospinal fluids are required for the diagnosis of meningitis. Blood culture has become more important in the diagnosis of disseminated mycobacterial infections following the HIV epidemic.

Other material that can be used for TB diagnosis contains: gastric aspirate, effusion fluids, early-morning urine specimens, pus, faeces, fine-needle lymph-node aspirate, bronchoalveolar lavage (BAL) specimen, lymph-node biopsy, liver biopsy, pleural biopsy, uterine curettings, biopsy of affected skin, bone marrow (Bannister *et al.*, 2006).

Purified tuberculin protein derivative is used in tuberculin skin test (TST, Mantoux test). When injected intracutaneously into hypersensitive individuals, tuberculin evokes an intense inflammatory reaction (delayed hypersensitivity) at the site of injection. The degree of induration at the site of injection is an indication of the individual´s present or past association with the TB bacillus. The test is considered positive if the diameter of the resulting lesion, which is characterized by erythema (redness) and swelling, is 10 mm or bigger. 90% of people that have a lesion of 10-15mm are currently infected with *Mtb* or have been previously exposed to bacteria. Each invidual that has a lesion of ≥15 mm is actually infected with *Mtb* or has been previously exposed to *Mtb*.

To counteract some of the problems with the TST, such as false positives due to the prior BCG vaccination (Pouchot *et al.*, 1997), a new group of tests, the interferon-gamma release assays (IGRAs), have been developed. There are currently two commercially available tests: the QuantiFERON®-TB Gold In-Tube (Cellestis Limited, Chadstone, Australia) and the T-SPOT®.TB (Oxford Immunotec, Limited, Abingdon, UK). Both are whole-blood assays that measure interferon-gamma levels after *in vitro* exposure to TB-specific antigens (Norton *et al.*, 2012). They have been shown to predict TB at least as well (Bakir *et al.*, 2008) or better (Diel *et al.*, 2008,Leung *et al.*, 2010) than the TST, with much greater specificity in patients previously immunized with BCG (Pai *et al.*, 2008).

Several molecular typing methods, including a standard Southern blotting protocol based on insertion sequence IS 6110, are used internationally to investigate possible outbreaks and track the spread of strains of *Mtb*. Other important *Mtb* typing methods include spoligotyping, MIRU typing and variable tandem repeat (VNTR) (Inglis *et al.*, 2008). Spacer oligonucleotide typing (spoligotyping) is an amplification-based method for genotyping *Mtb* isolates that detects variability in the direct repeat region in the DNA of *Mtb*. The traditional spoligotyping method detects the presence or absence of 43 different spacer sequences. The test is often used as a first-line genotyping method due to its low cost, rate and robustness.

1.6 Current prevention and treatment of TB

1.6.1 Vaccination

Bacille Calmette-Guerin is an avirulent strain of *Mycobacterium bovis* that was attenuated by serial passages in potato slices imbibed with glycerol for 13 years (Calmette *et al.*, 1927).

BCG vaccines are the oldest of the vaccines currently used throughout the world (Starke *et al.*, 1991). BCG vaccination does not prevent infection with *Mtb* but may prevent dissemination of disease (Plotkin *et al.*, 2004). They have been given to 4 billion people and have been used routinely since the 1960s in almost all countries of the world, with the exception of few industrialized countries. The USA and

Netherlands are the only countries that have never routinely recommended BCG vaccination (Lugosi *et al.*, 1992).

The success of BCG is principally due to its efficacy in preventing TB meningitis in children (Colditz *et al.,* 1995), which is frequent in TB-endemic areas, where BCG immunization is mandatory nowadays. As BCG is live attenuated vaccine, it might lead to disseminated TB disease in people living with HIV and further immunosuppressive conditions (Colditz *et al.,* 1994).

New vaccination strategies against TB include:

• Prime: BCG replacement with either live recombinant BCG (rBCG) that may be more effective than the parental strains or genetically attenuated *Mtb* mutants.

Since BCG lacks many genes found in *Mtb* (>120 genes), it has been proposed that a live attenuated strain which contains a more complete antigen repertoire may be more protective than BCG.

• Prime-boost: enhance the limited immunity transmitted by BCG (or boost specific antigens presented by recombinant BCG or attenuated *Mtb*) adapting either viral-vectored or adjuvanted subunit vaccines.

The rationale for the development of a subunit-based vaccine against TB is linked with the induction by immunization of a Th-1 type immune response against *Mtb* antigens. Antigents secreted and abundant in the early steps of infection results in a more rapid and more effective mobilization of T cells at the site of bacteria multiplication. This would contain the infection and reduce the risk of developing active TB (Delogu *et al*., 2009). This type vaccine would be administered as boosters to a BCG prime to infants or in adolescents when BCG's protection begins to disappear.

• Immunotherapeutic: The therapeutic vaccines might associate with chemotherapy resulting in shorten treatment for TB. Those under development include whole-cell and fragmented mycobacteria, although several of these candidates also demonstrate prophylactic potential.

New TB vaccines are an urgent part of a comprehensive plan to control and ulimately eliminate TB. Over the past decade, researchers have made significant progress in TB vaccine development. Out of current 14 vaccine candidates

undergoing or preparing to enter human clinical trials, 4 have reached phase I trials to demonstrate safety, and eight have reached phase II trials to evaluate their safety and immunogenicity. *M. vaccae*, the whole-cell mycobacteria vaccine candidate, has successfully completed phase III trials (Table 10).

Table 10 The development pipeline for new vaccines (The TB Vaccines Pipeline, Mike Frick, July 2013).

Agent	Strategy	Type	Sponsors	Status
M. vaccae	Immunotherapeutic	Whole-cell *M. vaccae*	AnHui Longcom	Phase III
MVA85A/ AERAS-485	Prime-boost	Viral vector	Oxford University, Aeras	Phase IIb
M72 + AS01	Prime-boost	Adjuvanted subunit	GSK, Aeras	Phase IIb
Crucell Ad35/ AERAS-402	Prime-boost	Viral vector	Crucell, Aeras	Phase II (formerly phase IIb)
VPM1002	Prime	Live recombinant rBCG	Vakzine Projekt Management GmbH, Max Planck Institute for Infection Biology, TuBerculosis Vaccine Initiative (TBVI), Serum Institute of India	Phase IIa
RUTI	Immunotherapeutic	Fragmented *Mtb*	Archivel Farma	Phase IIa
Hybrid 1 + IC31	Prime-boost	Adjuvanted subunit	Statens Serum Institut (SSI), TBVI, Intercell, European & Developing Countries Clinical Trials Partnership	Phase IIa
Hybrid 56 + IC31	Prime-boost	Adjuvanted subunit	SSI, Aeras	Phase IIa
Hybrid 4 + IC31/ AERAS-404	Prime-boost	Adjuvanted subunit	Aeras, Sanofi Pasteur	Phase IIa
ID93 + GLA-SE	Prime-boost	Adjuvanted subunit	Infectious Disease Research Institute, Aeras	Phase I
Ad5Ag85A	Prime-boost	Viral vector	McMaster University, CanSino	Phase I
MTBVAC	Prime	Live genetically attenuated *Mtb*	University of Zaragoza, Biofabri, TBVI	Phase I

Dar-901	Prime-boost	Whole-cell *M. vaccae*	Geisel School of Medicine at Dartmouth University	Phase I pending

Note: For each candidate under the prime-boost strategy, trials are evaluating the experimental vaccine in the left-hand column given as a boost to a BCG prime.

1.6.2 Pharmacological treatment

Antitubercular drugs can be divided into first-line drugs, those that generally have the greatest bactericidal activity when used for TB treatment, the second-line therapeutic-drugs, which are less effective, more expensive and have higher toxicities, and experimental drugs. First-line drugs include isoniazid, rifampin, pyrazinamide, ethambutol, and streptomycin. Second-line drugs contain p-aminosalicylicacid, ethionamide, cycloserine, kanamycin, capreomycin, amikacin, ciproflaxin, ofloxacin and viomycin.

1.6.2.1 First line drugs

- Isoniazid (INH) (CAS 54-85-3) was first introduced as a therapy against *Mtb* in the 1950s and was first recommended in US guidelines for LTBI treatment in 1965. INH interferes with mycolic acid synthesis, resulting in disruption of the bacterial cell wall (Takayama et al., 1972, Winder et al., 1970) (Fig. 68). INH is a prodrug and is converted to an active form by catalase peroxidase (KatG) (Peloquin *et al.,* 2002; Zhan *et al.,* 1992). Activated INH inhibits the action of enoyl-acyl carrier protein reductase (InhA), which is an important enzyme component of the fatty acid synthetase II (FAS-II) complex. FAS-II is involved in the synthesis of long-chain mycolic acids. It is bactericidal against rapidly dividing bacteria, but has limited activity against slow growing populations (Budha *et al.,* 2009).

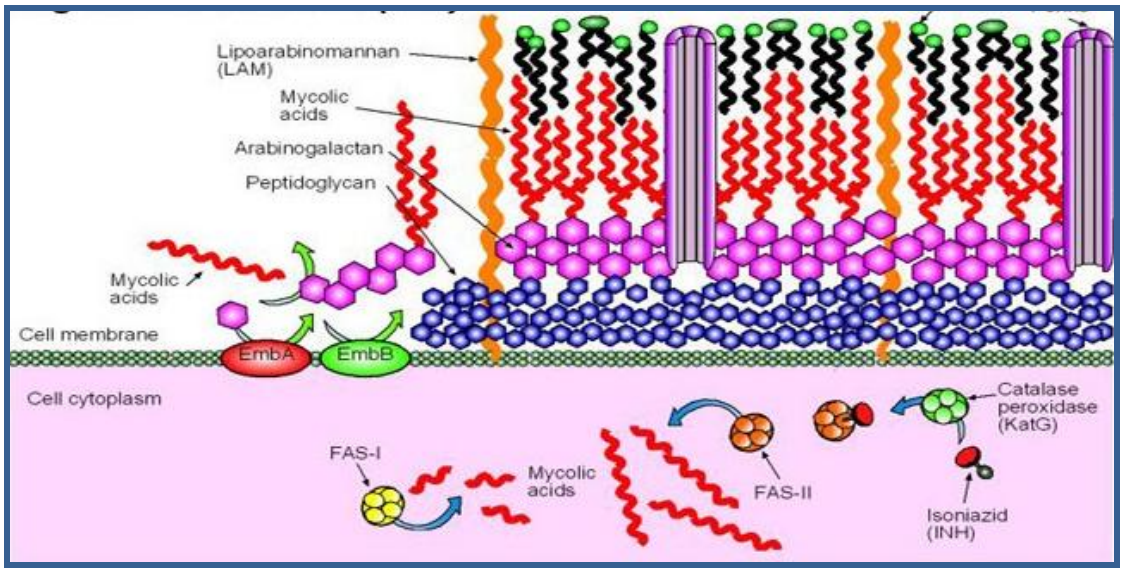

Fig. 68 Site of action of isoniazid. Extracted from www.immunopaedia.org

- Rifampin (RIF) (CAS 13292-46-1), a product of *Streptomyces sp.*, is the mainstay of current antituberculosis therapy. RIF inhibits bacterial DNA-dependent RNA polymerase by binding to its β-subunit (Norton *et al.*, 2012) (Fig. 69). Preventive treatment with rifampin-pyrazinamide causes severe hepatotoxicity more often than does preventive treatment with isoniazid or curative treatment for tuberculosis (van Hest *et al.*, 2004), which limits rifampin usage for long-term therapy.

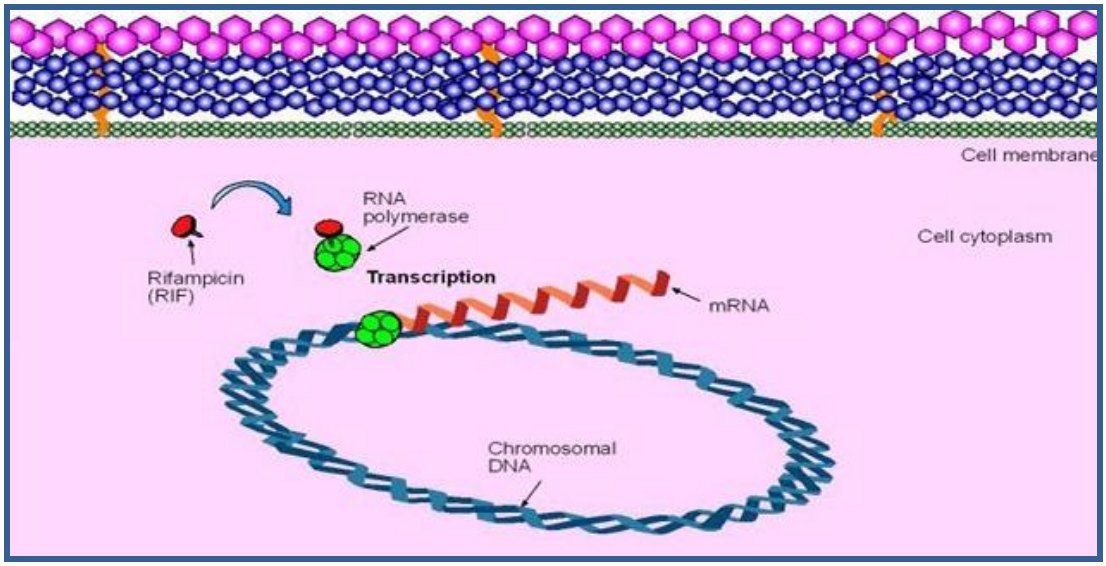

Fig. 69 Site of action of rifampicin. Extracted from www.immunopaedia.org

- Pyrazinamide (PZA) (CAS 98-96-4) is uniquely effective in eliminating potential persisters and is used during the first 2 months of chemotherapy to reduce the total length of therapy. PZN is a prodrug and is converted to active form (pyrazinoic acid) by a nicotinamidase-peroxidase enzyme known as pyrazinamidase mycolic acids (Fig. 70). PZA does not show any activity against mycobacteria under normal culture conditions at neutral pH but shows *in vitro* activity in acidic cultures (Wade *et al.*, 2004, Zhang *et al.*, 2002) and demonstrates high *in vivo* sterilizing activity (Tarshis *et al.*, 1953). Being effective at acidic pH makes it ideal drug for killing tuberculosis residing in acidic phagosomes within infected macrophages (Mandell *et al.*, 1996).

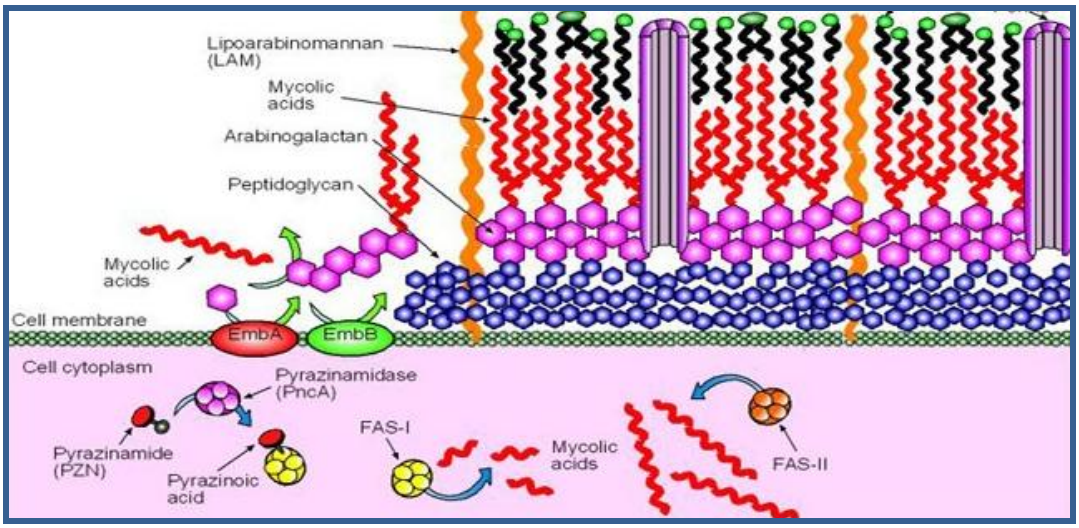

Fig. 70 Site of action of pyrazinamide. Extracted from www.immunopaedia.org

- Streptomycin (STR) (CAS 3810-74-0), first introduced by Waksman (Waksman *et al.*, 1946), was the first clinically effective antibiotic available for the treatment of TB. STR is an aminoglycoside that interferes with translation of messenger RNA transcripts in *Mtb*. STR binds to a ribosome protein (S12) that is a component of the 30S subunit of the ribosome complex and inhibits the synthesis of mycobacterial proteins (Fig. 71). Streptomycin is effective only against actively growing extracellular organisms and because of high rates of resistance sometimes it is not considered as a first line drug.

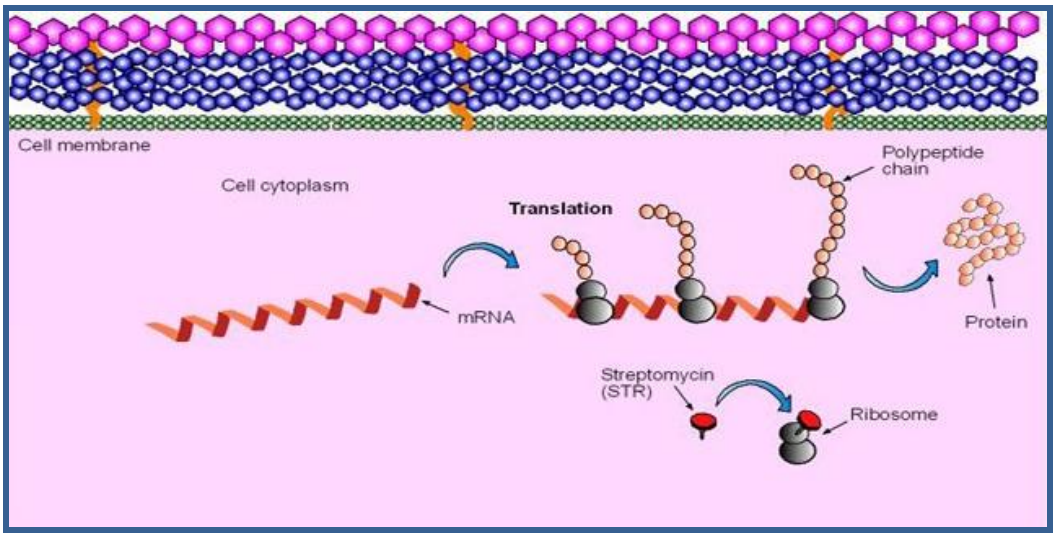

Fig. 71 Site of action of streptomycin. Extracted from www.immunopaedia.org

- Ethambutol (EMB) (CAS 74-55-5) interferes with cell wall biosynthesis in *Mtb* (Fig. 72). EMB inhibits the action of arabinosyl transferase (EmbB), which is a membrane-associated enzyme involved in the synthesis of arabinogalactan (Takayama *et al.*, 1989).

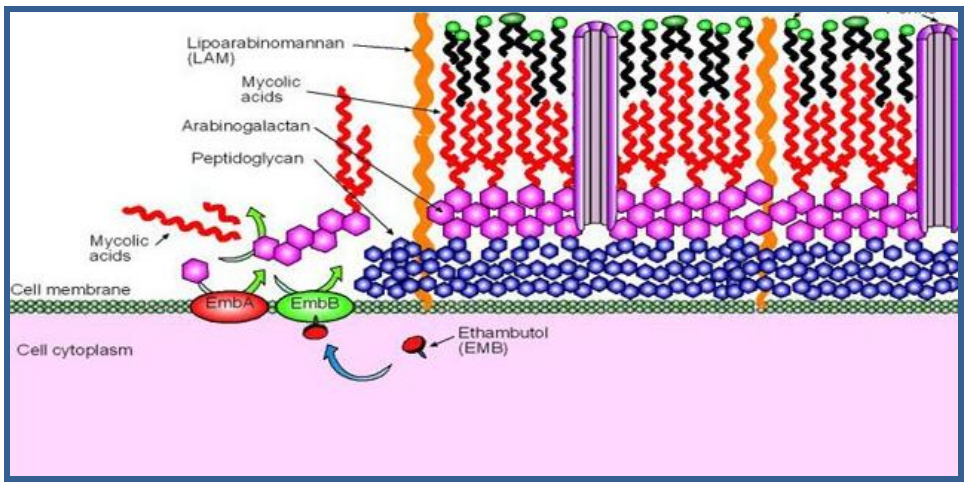

Fig. 72 Site of action of ethambutol. Extracted from www.immunopaedia.org

1.6.2.2 Second line drugs

The targets of second-line drugs against *Mtb* are cell wall biosynthesis, DNA supercoiling and protein synthesis.

Ethionamide (CAS 536-33-4) and cycloserine (CAS 68-41-7) interfere with cell wall biosynthesis by inhibiting mycolic acid synthesis and peptidoglycan synthesis, respectively.

Ciproflaxin (CAS 85721-33-1) and ofloxacin (CAS 82419-36-1) are fluoroquinolone drugs that inhibit DNA supercoiling by inhibiting the DNA gyrase enzyme.

Kanamycin (CAS 8063-07-8) and amikacin (CAS 37517-28-5) are aminoglycoside drugs that interfere with protein synthesis by inhibiting the action of ribosomes.

Similarly, viomycin (CAS 32988-50-4) and capreomycin (CAS 11003-38-6) are peptide drugs that also inhibit the action of ribosomes.

1.6.2.3 Experimental drugs

Existing therapy against tuberculosis is cumbersome, due to its length of ~6 months and often leads to prior patient compliance. There is an urgent need for more effective and tolerable treatment of drug-susceptible and drug-resistant disease, latent TB infection, and dosing strategies for children.

New drugs are required to shorten and simplify treatment, to improve the efficacy and tolerability of treatment for resistant strains of *Mtb* and to improve the treatment of TB among people living with HIV.

The status of the pipeline for new anti-TB drugs is shown in Table 11.

Table 11 The development pipeline for new TB drugs. Source: Stop TB Partnership Working Group on New TB Drugs; WHO, 2013. GLP: Good labolatory practice.

Lead optimization	Preclinical development	GLP toxicity	Phase I	Phase II	Phase III
Diarylquinoline					
DprE Inhibitors					
GyrB inhibitors				AZD-5847	
InhA Inhibitors				Bedaquiline	
LeuRS Inhibitors				(TMC-207)	
MGyrX1 inhibitors	CPZEN-45			Linezolid	Delamanid
Mycobacterial Gyrase	DC-159a			Novel Regimens	(OPC-67683)
Inhibitors	Q-201	BTZ-043			Gatifloxacin
Pyrazinamide Analogs	SQ-609	TBA-354		PA-824	Moxifloxacin
Riminophenazines	SQ-641			Rifapentine	Rifapentine
Ruthenium (II)	SPR-10199			SQ-109	
complexes				Sutezolid (PNU-	
Spectinamides				100480)	
Translocase-1 Inhibitors					

Chemical classes: **fluoroquinolone**, **rifamycin**, **oxazolidinone**, **nitroimidazole**, **diarylquinoline**, **benzothiazinone**

1.7 MDR-TB and XDR-TB

Multi-drug resistant tuberculosis (MDR-TB) is defined as resistance to the first-line drugs isoniazid and rifampin.

Extensively drug resistant TB (XDR-TB) is defined as MDR-TB plus resistance to a fluoroquinolone, and at least one of three injectable second-line drugs. Treating XDR-TB is difficult and requires tailored individual care.

Drug-resistant TB disease can develop in two different ways, called primary and secondary resistance. Primary resistance occurs in people who are initially infected with resistant organisms. Secondary resistance, or acquired resistance, develops during TB therapy, either because the patient was treated with an inadequate regimen, did not take the prescribed regimen appropriately, or because of other conditions such as drug malabsorption or drug-drug interactions that led to low serum levels.

Regimens for MDR-TB treatment currently recommended by WHO imply 20 months of treatment with second-line drugs for most patients, and are associated with multiple side-effects and lower cure rates (Who 2013).

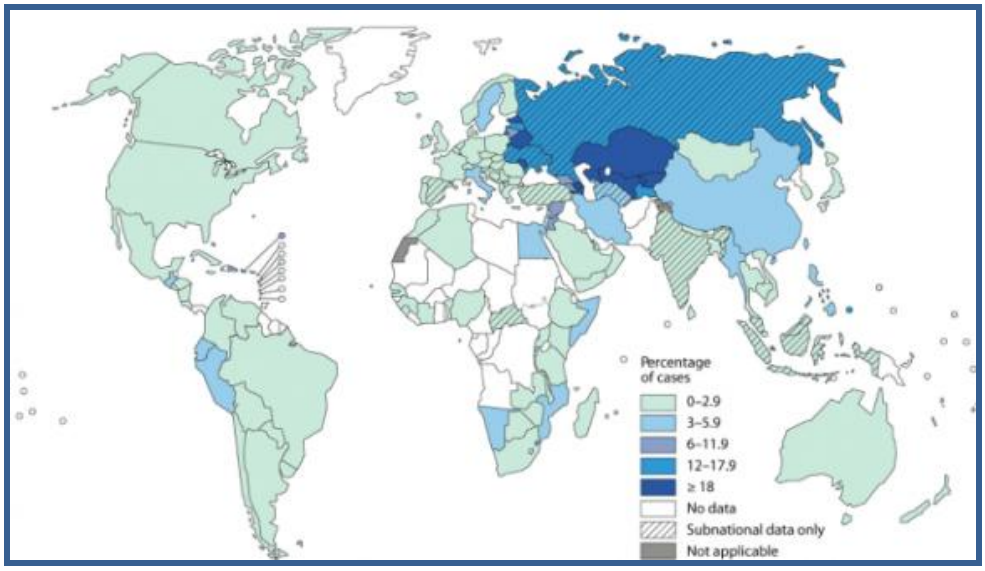

Fig. 73 Percentage of new tuberculosis cases with MDR-TB (WHO, 2013).

1.8 TB global initiatives

There are many government, multi-lateral and also non-governmental organizations focused on TB. Their role is to accelerate progress on access to TB diagnosis and treatment, research and development for new TB diagnostics, drugs and vaccines, and tackling drug resistant- and HIV-associated.

World Health Organization carries global leadership on matters critical to TB by monitoring TB situation in the world, including new strategies and standard implementation and measuring progress in TB care, control, and financing. WHO shapes the TB research agenda and stimulates the generation, translation and dissemination of valuable knowledge.

STOP TB PARTENRSHIP is a collection of nearly 1000 partners that is transforming the fight against TB in more than 100 countries. They include international and technical organizations, government programmes, research and funding agencies, foundations, non-governmental organizations, civil society and community groups and the private sector.

There are many non-profit organization dedicated to the discovery and development of new, globally accessible and affordable tuberculosis medicines, such as TB Alliance, Bill & Melinda Gates Foundation, Aeras and TuBerculosis Vaccine Initiative (TBVI).

Main target that unites all TB organizations is The Millennium Development Goal (MDG) under which by 2015 the global burden of TB disease (deaths and prevalence) will be reduced by 50% relative to 1990 levels, and further, by 2050, the global incidence of TB disease will be less than 1 per million population. By 2012, the prevalence rate fell 37% globally since 1990. Current forecasts suggest that the Stop TB Partnership target of halving TB prevalence by 2015 compared with a baseline of 1990 will not be met worldwide (WHO 2013).

Annex 2

Comparison of the annotated *Mycobacterium tuberculosis* H37Ra genome sequence with that of H37Rv (GenBank accession no. **AL123456**) did not reveal any differences in DosR, DosS, DosT aminoacid sequences (Fig. 74, Fig. 75, Fig. 76). For this reason, the Mtb DosRST proteins were cloned using H37Ra genomic DNA as template.

Score	Expect	Method	Identities	Positives	Gaps
425 bits(1092)	8e-157	Compositional matrix adjust.	217/217(100%)	217/217(100%)	0/217(0%)

```
Query  1    MVKVFLVDDHEVVRRGLVDLLGADPELDVVGEAGSVAEAMARVPAARPDVAVLDVRLPDG  60
            MVKVFLVDDHEVVRRGLVDLLGADPELDVVGEAGSVAEAMARVPAARPDVAVLDVRLPDG
Sbjct  1    MVKVFLVDDHEVVRRGLVDLLGADPELDVVGEAGSVAEAMARVPAARPDVAVLDVRLPDG  60

Query  61   NGIELCRDLLSRMPDLRCLILTSYTSDEAMLDAILAGASGYVVKDIKGMELARAVKDVGA  120
            NGIELCRDLLSRMPDLRCLILTSYTSDEAMLDAILAGASGYVVKDIKGMELARAVKDVGA
Sbjct  61   NGIELCRDLLSRMPDLRCLILTSYTSDEAMLDAILAGASGYVVKDIKGMELARAVKDVGA  120

Query  121  GRSLLDNRAAAALMAKLRGAAEKQDPLSGLTDQERTLLGLLSEGLTNKQIADRMFLAEKT  180
            GRSLLDNRAAAALMAKLRGAAEKQDPLSGLTDQERTLLGLLSEGLTNKQIADRMFLAEKT
Sbjct  121  GRSLLDNRAAAALMAKLRGAAEKQDPLSGLTDQERTLLGLLSEGLTNKQIADRMFLAEKT  180

Query  181  VKNYVSRLLAKLGMERRTQAAVFATELKRSRPPGDGP  217
            VKNYVSRLLAKLGMERRTQAAVFATELKRSRPPGDGP
Sbjct  181  VKNYVSRLLAKLGMERRTQAAVFATELKRSRPPGDGP  217
```

Fig. 74 Sequence alignment of two-component transcriptional regulatory protein DosR [*Mycobacterium tuberculosis* H37Rv] (NCBI Reference Sequence:NP_217649.1) (query) with two-component transcriptional regulatory protein DosR [*Mycobacterium tuberculosis* H37Ra] (NCBI Reference Sequence: YP_001284510.1) (Sbjct).

Score	Expect	Method	Identities	Positives	Gaps
1139 bits(2947)	0.0	Compositional matrix adjust.	578/578(100%)	578/578(100%)	0/578(0%)

```
Query  1    MTTGGLVDENDGAAMRPLRHTLSQLRLHELLVEVQDRVEQIVEGRDRLDGLVEAMLVVTA  60
            MTTGGLVDENDGAAMRPLRHTLSQLRLHELLVEVQDRVEQIVEGRDRLDGLVEAMLVVTA
Sbjct  1    MTTGGLVDENDGAAMRPLRHTLSQLRLHELLVEVQDRVEQIVEGRDRLDGLVEAMLVVTA  60

Query  61   GLDLEATLRAIVHSATSLVDARYGAMEVHDRQHRVLHFVYEGIDEETVRRIGHLPKGLGV  120
            GLDLEATLRAIVHSATSLVDARYGAMEVHDRQHRVLHFVYEGIDEETVRRIGHLPKGLGV
Sbjct  61   GLDLEATLRAIVHSATSLVDARYGAMEVHDRQHRVLHFVYEGIDEETVRRIGHLPKGLGV  120

Query  121  IGLLIEDPKPLRLDDVSAHPASIGFPPYHPPMRTFLGVPVRVRDESFGTLYLTDKTNGQP  180
            IGLLIEDPKPLRLDDVSAHPASIGFPPYHPPMRTFLGVPVRVRDESFGTLYLTDKTNGQP
Sbjct  121  IGLLIEDPKPLRLDDVSAHPASIGFPPYHPPMRTFLGVPVRVRDESFGTLYLTDKTNGQP  180

Query  181  FSDDDEVLVQALAAAAGIAVANARLYQQAKARQSWIEATRDIATELLSGTEPATVFRLVA  240
            FSDDDEVLVQALAAAAGIAVANARLYQQAKARQSWIEATRDIATELLSGTEPATVFRLVA
Sbjct  181  FSDDDEVLVQALAAAAGIAVANARLYQQAKARQSWIEATRDIATELLSGTEPATVFRLVA  240

Query  241  AEALKLTAADAALVAVPVDEDMPAADVGELLVIETVGSAVASIVGRTIPVAGAVLREVFV  300
            AEALKLTAADAALVAVPVDEDMPAADVGELLVIETVGSAVASIVGRTIPVAGAVLREVFV
Sbjct  241  AEALKLTAADAALVAVPVDEDMPAADVGELLVIETVGSAVASIVGRTIPVAGAVLREVFV  300

Query  301  NGIPRRVDRVDLEGLDELADAGPALLLPLRARGTVAGVVVVLSQGGPGAFTDEQLEMMAA  360
            NGIPRRVDRVDLEGLDELADAGPALLLPLRARGTVAGVVVVLSQGGPGAFTDEQLEMMAA
Sbjct  301  NGIPRRVDRVDLEGLDELADAGPALLLPLRARGTVAGVVVVLSQGGPGAFTDEQLEMMAA  360

Query  361  FADQAALAWQLATSQRRMRELDVLTDRDRIARDLHDHVIQRLFAIGLALQGAVPHERNPE  420
            FADQAALAWQLATSQRRMRELDVLTDRDRIARDLHDHVIQRLFAIGLALQGAVPHERNPE
Sbjct  361  FADQAALAWQLATSQRRMRELDVLTDRDRIARDLHDHVIQRLFAIGLALQGAVPHERNPE  420

Query  421  VQQRLSDVVDDLQDVIQEIRTTIYDLHGASQGITRLRQRIDAAVAQFADSGLRISVQFVG  480
            VQQRLSDVVDDLQDVIQEIRTTIYDLHGASQGITRLRQRIDAAVAQFADSGLRISVQFVG
Sbjct  421  VQQRLSDVVDDLQDVIQEIRTTIYDLHGASQGITRLRQRIDAAVAQFADSGLRISVQFVG  480

Query  481  PLSVVDSALADQAEAVVREAVSNAVRHAKASTLTVRVKVDDDLCIEVTDNGRGLPDEFTG  540
            PLSVVDSALADQAEAVVREAVSNAVRHAKASTLTVRVKVDDDLCIEVTDNGRGLPDEFTG
Sbjct  481  PLSVVDSALADQAEAVVREAVSNAVRHAKASTLTVRVKVDDDLCIEVTDNGRGLPDEFTG  540

Query  541  SGLTNLRQRAEQAGGEFTLASVPGASGTVLRWSAPLSQ  578
            SGLTNLRQRAEQAGGEFTLASVPGASGTVLRWSAPLSQ
Sbjct  541  SGLTNLRQRAEQAGGEFTLASVPGASGTVLRWSAPLSQ  578
```

Fig. 75 Sequence alignment of two-component sensor histidine kinase DevS [*Mycobacterium tuberculosis* H37Rv] (NCBI Reference Sequence: NP_217648.1) (query) with two-component sensor histidine kinase DevS [*Mycobacterium tuberculosis* H37Ra] (NCBI Reference Sequence: YP_001284509.1) (Sbjct).

Score	Expect	Method	Identities	Positives	Gaps
1130 bits(2923)	0.0	Compositional matrix adjust.	573/573(100%)	573/573(100%)	0/573(0%)

```
Query  1    MTHPDRANVNPGSPPLRETLSQLRLRELLLEVQDRIEQIVEGRDRLDGLIDAILAITSGL  60
            MTHPDRANVNPGSPPLRETLSQLRLRELLLEVQDRIEQIVEGRDRLDGLIDAILAITSGL
Sbjct  1    MTHPDRANVNPGSPPLRETLSQLRLRELLLEVQDRIEQIVEGRDRLDGLIDAILAITSGL  60

Query  61   KLDATLRAIVHTAAELVDARYGALGVRGYDHRLVEFVYEGIDEETRHLIGSLPEGRGVLG  120
            KLDATLRAIVHTAAELVDARYGALGVRGYDHRLVEFVYEGIDEETRHLIGSLPEGRGVLG
Sbjct  61   KLDATLRAIVHTAAELVDARYGALGVRGYDHRLVEFVYEGIDEETRHLIGSLPEGRGVLG  120

Query  121  ALIEEPKPIRLDDISRHPASVGFPLHHPPMRTFLGVPVRIRDEVFGNLYLTEKADGQPFS  180
            ALIEEPKPIRLDDISRHPASVGFPLHHPPMRTFLGVPVRIRDEVFGNLYLTEKADGQPFS
Sbjct  121  ALIEEPKPIRLDDISRHPASVGFPLHHPPMRTFLGVPVRIRDEVFGNLYLTEKADGQPFS  180

Query  181  DDDEVLVQALAAAAGIAVDNARLFEESRTREAWIEATRDIGTQMLAGADPAMVFRLIAEE  240
            DDDEVLVQALAAAAGIAVDNARLFEESRTREAWIEATRDIGTQMLAGADPAMVFRLIAEE
Sbjct  181  DDDEVLVQALAAAAGIAVDNARLFEESRTREAWIEATRDIGTQMLAGADPAMVFRLIAEE  240

Query  241  ALTLMAGAATLVAVPLDDEAPACEVDDLVIVEVAGEISPAVKQMTVAVSGTSIGGVFHDR  300
            ALTLMAGAATLVAVPLDDEAPACEVDDLVIVEVAGEISPAVKQMTVAVSGTSIGGVFHDR
Sbjct  241  ALTLMAGAATLVAVPLDDEAPACEVDDLVIVEVAGEISPAVKQMTVAVSGTSIGGVFHDR  300

Query  301  TPRRFDRLDLAVDGPVEPGPALVLPLRAADTVAGVLVALRSADEQPFSDKQLDMMAAFAD  360
            TPRRFDRLDLAVDGPVEPGPALVLPLRAADTVAGVLVALRSADEQPFSDKQLDMMAAFAD
Sbjct  301  TPRRFDRLDLAVDGPVEPGPALVLPLRAADTVAGVLVALRSADEQPFSDKQLDMMAAFAD  360

Query  361  QAALAWRLATAQRQMREVEILTDRDRIARDLHDHVIQRLFAVGLTLQGAAPRARVPAVRE  420
            QAALAWRLATAQRQMREVEILTDRDRIARDLHDHVIQRLFAVGLTLQGAAPRARVPAVRE
Sbjct  361  QAALAWRLATAQRQMREVEILTDRDRIARDLHDHVIQRLFAVGLTLQGAAPRARVPAVRE  420

Query  421  SIYSSIDDLQEIIQEIRSAIFDLHAGPSRATGLRHRLDKVIDQLAIPALHTTVQYTGPLS  480
            SIYSSIDDLQEIIQEIRSAIFDLHAGPSRATGLRHRLDKVIDQLAIPALHTTVQYTGPLS
Sbjct  421  SIYSSIDDLQEIIQEIRSAIFDLHAGPSRATGLRHRLDKVIDQLAIPALHTTVQYTGPLS  480

Query  481  VVDTVLANHAEAVLREAVSNAVRHANATSLAINVSVEDDVRVEVVDDGVGISGDITESGL  540
            VVDTVLANHAEAVLREAVSNAVRHANATSLAINVSVEDDVRVEVVDDGVGISGDITESGL
Sbjct  481  VVDTVLANHAEAVLREAVSNAVRHANATSLAINVSVEDDVRVEVVDDGVGISGDITESGL  540

Query  541  RNLRQRADDAGGEFTVENMPTGGTLLRWSAPLR  573
            RNLRQRADDAGGEFTVENMPTGGTLLRWSAPLR
Sbjct  541  RNLRQRADDAGGEFTVENMPTGGTLLRWSAPLR  573
```

Fig. 76 Sequence alignment of two-component system sensor histidine kinase DosT [*Mycobacterium tuberculosis* H37Rv] (NCBI Reference Sequence: YP_006515439.1) (Query) with histidine kinase response regulator [*Mycobacterium tuberculosis* H37Ra] (NCBI Reference Sequence: YP_001283364.1) (Sbjct).

Annex 3

Table 12 Cross-references for most important proteins in this thesis.

Protein	1. TubercuList	2. UniProt	4. Pfam	5. TB Database
DosR	Rv3133c.	P9WMF9	PF00072 PF00196	Rv3133c
DosS	Rv3132c.	P9WGK3	PF01590	Rv3132c
DosT	Rv2027c.	P9WGK1	PF02518 PF07730	Rv2027c
PknH	Rv1266c.	P9WI71	PF00069	Rv1266c

1. http://genolist.pasteur.fr/TubercuList/genome.cgi
2. http://www.uniprot.org/
3. http://pfam.xfam.org/
4. http://www.tbdb.org/